

S**ENGINEERING CHANGE NOTICE**Page 1 of 2**661804**Proj.
ECN 03/28/01

2. ECN Category (mark one) Supplemental <input type="checkbox"/> Direct Revision <input checked="" type="checkbox"/> Change ECN <input type="checkbox"/> Temporary <input type="checkbox"/> Standby <input type="checkbox"/> Supersedure <input type="checkbox"/> Cancel/Void <input type="checkbox"/>	3. Originator's Name, Organization. MSIN , and Telephone No. J.M. Grigsby, NS&L, R1-44, 376-1907		4. USQ Required? <input checked="" type="checkbox"/> Yes <input checked="" type="checkbox"/> No	5. Date <i>gjd</i>
	6. Project Title/No./Work Order No. RPP		7. Bldg./Sys./Fac. No. RPE	8. Approval Designator N/A
	9. Document Numbers Changed by this ECN (includes sheet no. and rev.) RFP-6213, Revision 0		10. Related ECN No(s). N/A	11. Related PO No. N/A
	12a. Modification Work <input type="checkbox"/> Yes (fill out Blk. 12b) <input checked="" type="checkbox"/> No (NA Blks. 12b, 12c, 12d)		12b. Work Package No. N/A	12c. Modification Work Completed N/A
		Design Authority/Co. Engineer Signature & Date		12d. Restored to Original Condition (Temp. or Standby ECNs only) N/A
		Design Authority/Co. Engineer Signature & Date		

waste storage tanks and related descriptions and conclusions based on these criteria.

Calculated revised heat up rates following a loss of cooling event based on updated decay heat loads in limiting tank 241-AZ-101.

Revised Chapter 7 to assess the control strategy of monitoring waste temperatures on a periodic basis with required recovery actions to restore cooling (i.e., primary tank ventilation).

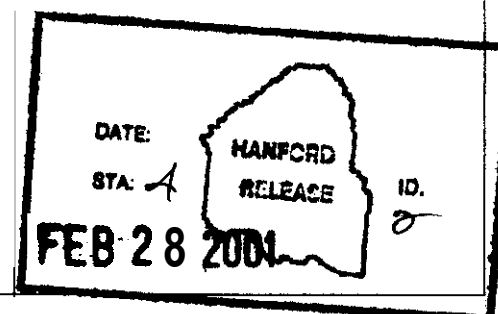
Added Appendix K to provide an updated decay heat load in Tank 241-AZ-101.

Added Appendix L to assess the temperature measurement uncertainty in DSTs

14a. Justification (mark one) Criteria Change <input checked="" type="checkbox"/> Design Improvement <input type="checkbox"/> Environmental <input type="checkbox"/> Facility Deactivation <input type="checkbox"/> As-Found <input type="checkbox"/> Facilitate Const. <input type="checkbox"/> Const. Error/Omission <input type="checkbox"/> Design Error/Omission <input type="checkbox"/>	14b. Justification Details Changes were made to support Office of River Protection (ORP) approval of Authorization Basis Amendments related to the FSAR tank bump accident and post-sluicing hazards in Tanks 241-AZ-102 and 241-C-106.
--	--

5. Distribution (include name, MSIN and no. of copies)

RELEASE STAMP



ENGINEERING CHANGE NOTICE

Page 2 of 2

1. ECN (use no. from pg. 1)

661804

6. Design Verification Required

☐ Yes
☒ No

17. Cost Impact

ENGINEERING

Additional ☐ \$ N/A
Savings ☐ \$ N/A

CONSTRUCTION

Additional ☐ \$ N/A
Savings ☐ \$ N/A

18. Schedule Impact (days)

Improvement ☐ N/A
Delay ☐ N/A

SDD/DD	<input type="checkbox"/>	Seismic/Stress Analysis	<input type="checkbox"/>	Tank Calibration Manual	<input type="checkbox"/>
Functional Design Criteria	<input type="checkbox"/>	Stress/Design Report	<input type="checkbox"/>	Health Physics Procedure	<input type="checkbox"/>
Operating Specification	<input type="checkbox"/>	Interface Control Drawing	<input type="checkbox"/>	Spares Multiple Unit Listing	<input type="checkbox"/>
Criticality Specification	<input type="checkbox"/>	Calibration Procedure	<input type="checkbox"/>	Test Procedures/Specification	<input type="checkbox"/>
Conceptual Design Report	<input type="checkbox"/>	Installation Procedure	<input type="checkbox"/>	Component Index	<input type="checkbox"/>
Equipment Spec.	<input type="checkbox"/>	Maintenance Procedure	<input type="checkbox"/>	ASME Coded Item	<input type="checkbox"/>
Const. Spec.	<input type="checkbox"/>	Engineering Procedure	<input type="checkbox"/>	Human Factor Consideration	<input type="checkbox"/>
Procurement Spec.	<input type="checkbox"/>	Operating Instruction	<input type="checkbox"/>	Computer Software	<input type="checkbox"/>
Vendor Information	<input type="checkbox"/>	Operating Procedure	<input type="checkbox"/>	Electric Circuit Schedule	<input type="checkbox"/>
OM Manual	<input type="checkbox"/>	Operational Safety Requirement	<input type="checkbox"/>	ICRS Procedure	<input type="checkbox"/>
FSAR/SAR	<input checked="" type="checkbox"/>	IEFD Drawing	<input type="checkbox"/>	Process Control Manual/Plan	<input type="checkbox"/>
Safety Equipment List	<input type="checkbox"/>	Cell Arrangement Drawing	<input type="checkbox"/>	Process Flow Chart	<input type="checkbox"/>
Radiation Work Permit	<input type="checkbox"/>	Essential Material Specification	<input type="checkbox"/>	Purchase Requisition	<input type="checkbox"/>
Environmental Impact Statement	<input type="checkbox"/>	Fac. Proc. Samp. Schedule	<input type="checkbox"/>	Tickler File	<input type="checkbox"/>
Environmental Report	<input type="checkbox"/>	Inspection Plan	<input type="checkbox"/>		<input type="checkbox"/>
Environmental Permit	<input type="checkbox"/>	Inventory Adjustment Request	<input type="checkbox"/>		<input type="checkbox"/>

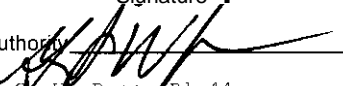
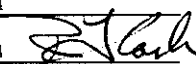
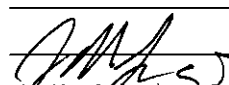


0. Other Affected Documents: (NOTE: Documents listed below will not be revised by this ECN.) Signatures below indicate that the signing organization has been notified of other affected documents listed below.

Document Number/Revision

Document Number/Revision

Document Number/Revision

1. Approvals

Signature	Date
Design Authority 	
Cog. Eng. G. W. Ryan RI-44	2/27/01
Cog. Mgr. R. J. Cash RI-44 	2/27/01
QA	
Safety	
Environ.	
Other M. G. Gigsby, G&PCI RI-44 	2/27/01
M. G. Gigsby, G&PCI RI-44 	2/27/01
B. Mainovic, Ebasco and Assoc. 	2/27/01

Signature	Date
Design Agent	
PE	
CIA	
Safety	
Design	
Environ	
Other	

DEPARTMENT OF ENERGY

Signature or a Control Number that tracks the Approval Signature

ADDITIONAL

[illegible]

Hanford Waste Tank Bump Accident and Consequence Analysis

J. M. Grigsby, G&PCI B. Malinovic, Fauske and Assoc., Inc
CH2M HILL Hanford Group, Inc.
Richland, WA 99352
U.S. Department of Energy Contract DE-AC²⁷06-99RL14047


EDT/ECN: 661804 UC: N/A
Cost Center: 7B300 Charge Code: 101961
B&R Code: N/A Total Pages: 194 232 2-28-01

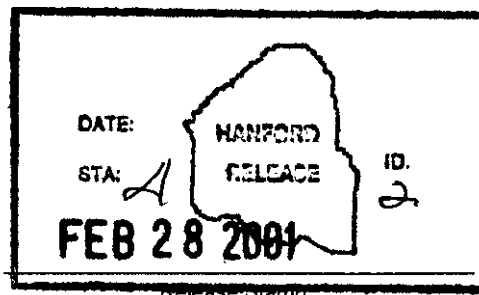
Keywords: tank bump accident, Single-Shell Tanks, Double-Shell Tanks, Authorization Basis.

Abstract: This report provides a new evaluation of the Hanford tank bump accident for incorporation into the Authorization Basis. The analysis scope is for the safe storage of waste in its current configuration in Single-Shell and Double-Shell tanks.

TRADEMARK DISCLAIMER. Reference herein to any specific commercial product process, or service by trade name, trademark, manufacturer, or otherwise, does not necessarily constitute or imply its endorsement, recommendation, or favoring by the United States Government or any agency thereof or its contractors or subcontractors.

Printed in the United States of America. To obtain copies of this document, contact: Document Control Services, P.O. Box 950, Mailstop H6-08, Richland WA 99352, Phone (509) 372-2420; Fax (509) 376-4989.

 2/28/01
Release Approval Date



Approved For Public Release

Hanford Waste Tank Bump Accident and Consequence Analysis

Prepared for the U.S. Department of Energy
Assistant Secretary for Environmental Management

CH2MHILL
Hanford Group, Inc.

Richland, Washington

Contractor for the U.S. Department of Energy
Office of River Protection under Contract DE-AC27-99RL14047

Approved for public release; further dissemination unlimited

LEGAL DISCLAIMER

This report was prepared as an account of work sponsored by an agency of the United States Government. Neither the United States Government nor any agency thereof, nor any of their employees, nor any of their contractors, subcontractors or their employees, makes any **warranty**, express or implied, or assumes any legal liability or responsibility for the accuracy, completeness, or any third party's use or the results of such use of any information, apparatus, product, or process disclosed, or represents that its use would not infringe privately owned rights. Reference herein to any specific **commercial** product, process, or service by trade name, trademark, manufacturer, or otherwise, does not necessarily constitute or imply its endorsement, recommendation, or favoring by the United States Government or any agency thereof or its contractors or subcontractors. The views and opinions of authors expressed herein do not necessarily state or reflect those of the United States Government or any agency thereof.

This report has been reproduced from the best available copy. Available in paper copy and microfiche.

Available electronically at
<http://www.doe.gov/bridge>. Available for a processing fee to the U.S. Department of Energy and its contractors, in paper, from:
U.S. Department of Energy
Office of Scientific and Technical Information
P.O. Box 62
Oak Ridge, TN 37831-0062
phone: 865-576-8401
fax: 865-576-5728
email: reports@adonis.osti.gov(423) 576-8401

Available for sale to the public, in paper, from:
U.S. Department of Commerce
National Technical Information Service
5285 Port Royal Road
Springfield, VA 22161
Phone: 800-553-6847
fax: 703-605-6900
email: orders@ntis.fedworld.gov
online ordering:
<http://www.ntis.gov/ordering.htm>

Printed in the United States of America

Hanford Waste Tank Bump Accident and Consequence Analysis

Prepared by:
J. M. Grigsby
G&P Consulting, Inc.

B. Malinovic
Fauske and Assoc., Inc.

Date Published
February 2001

Prepared for the U.S. Department of Energy
Assistant Secretary for Environmental Management

CH2MHILL
Hanford Group, Inc.

P. O. Box 1500
Richland, Washington

Contractor for the U.S. Department of Energy
Office of River Protection under Contract DE-AC27-99RL14047

Approved for public release; further dissemination unlimited

This **page** intentionally left **blank**.

CONTENTS

1.0	PURPOSE AND SCOPE.....	1-1
2.0	SUMMARY OF FINDINGS	2-1
3.0	HISTORICAL AND PRESENT EVALUATION DATA	3-1
3.1	HISTORICAL EVENTS.....	3-1
3.2	PREVIOUS ANALYSIS	3-3
3.2.1	Fauske and Associates, Inc., 1989.....	3-4
3.2.2	Tank 241-C-106 Steam Bump Evaluation	3-7
3.2.3	GOTH Analyses	3-7
3.2.4	Tank Bump Potential During In-Tank Washing Operations Proposed for the AZ Tanks	3-14
3.3	CHARACTERIZATION DATA	3-16
3.4	TANK CONFIGURATION DATA	3-19
4.0	TANK BUMP PHYSICAL MODELS AND CRITERIA	4-1
4.1	STEAM BUMPS BY GAS INJECTION	4-4
4.2	STEAM BUMP BY BUOYANT DISPLACEMENT	4-10
5.0	DESCRIPTION OF STEAM BUMP AND LIQUID WASTE RELEASE MODELS	5-1
5.1	STEAM BUMP SEQUENCE OF EVENTS	5-1
5.2	BUBBLE AND WASTE ASCENT MODEL	5-1
5.3	AEROSOL RELEASE MODEL.....	5-5
5.4	EXAMPLE CALCULATION	5-7
5.5	NUMERICAL EVALUATION NOTE	5-7
6.0	BUMP CRITERIA MODEL APPLICATION.....	6-1
6.1	APPLICATION OF TANK BUMP CRITERIA TO CURRENT TANK WASTE	6-1
6.2	41-AY-102 HAS A 40,700 W TOTAL APPLICATION OF TANK BUMP CRITERIA TO WASTE AT LIMITING CONDITIONS FOR OPERATION CONDITIONS	6-7
6.3	APPLICATION TO HISTORIC EVENTS	6-8
7.0	CONTROL STRATEGY EVALUATION	7-1
7.1	FAILURE TO RECOVER PROBABILITY	7-1
7.2	RESULTS FOR LIMITING CONDITIONS FOR OPERATION CONDITIONS	7-7
8.0	CONSEQUENCE EVALUATION.....	8-1
8.1	THE HADCRT CODE.....	8-1
8.2	HADCRT INPUT FOR 241-AZ-102 CASE.....	8-2
8.3	241-AZ-102 TANK BUMP CONSEQUENCE PHYSICAL RESULTS	8-4

8.4	241-AZ-102 TANK BUMP RADIOLOGICAL AND TOXIC CHEMICAL CONSEQUENCES	8-7
9.0	SUMMARY AND DISCUSSION OF ASSUMPTIONS AND APPROXIMATIONS	9-1
9.1	TANK BUMP PHYSICAL MODELS	9-1
9.2	TANK BUMP CONSEQUENCE EVALUATION	9-2
10.0	REFERENCES	10-1

APPENDICES

A	TANK WASTE CHARACTERIZATION DATA	A-i
B	POSTULATED BUMP SCENARIOS DEEMED NOT PLAUSIBLE	B-i
C	RISE DISTANCE TO YIELDING OF VOID-BEARING PARCEL	C-i
D	BUBBLE GROWTH MODEL AND INPUT	D-i
E	CLUSTER ENTRAINMENT MODEL AND INPUT	E-i
F	HADCRT CHANGES AND INPUT	F-i
G	SPREADSHEETS FOR BUMP CRITERIA	G-i
H	RESERVED FOR FUTURE USE	H-i
I	QUALITY ASSURANCE DOCUMENTS	I-i
J	CHECKLIST FOR TECHNICAL PEER REVIEW	J-i
K	DECAY HEAT LOAD FOR TANK 241-AZ-101 BASED ON THE BEST BASIS INVENTORY AND DECAYED TO JANUARY 31, 2001	K-i
L	THERMOCOUPLE ACCURACY (MEMO 7KN00-TCO-001)	L-i

FIGURES

Figure 3-1.	Surface Heat Removal	3-5
Figure 3-2.	Cavity Expansion During Rise in a Constant Temperature Pool.	3-6

Figure 3-3. Best-Estimate Initial Temperature Profile for 11 ft of Consolidated Non-Convective Waste.....	3-10
Figure 3-4. Conservative Initial Temperature Profile for 11 ft of Consolidated Non-Convective Waste.	3-10
Figure 3-5. Gas Volume Fraction Contours for GOTH Run With 18 in. Non-Convective Layer and No Condensation.	3-12
Figure 3-6. Dimensional HEATING7 Model.	3-15
Figure 3-7. Single-Shell Tank Instrumentation Configuration.	3-20
Figure 3-8. Double-Shell Tank Instrumentation Configuration.	3-21
Figure 4-1. Steam Bump By Gas Injection.	4-2
Figure 4-2. Steam Bump During a Buoyant Displacement.....	4-3
Figure 4-3. Bubble Expansion Ratio Versus Depth of Supematant Pool; Pool Temperature T_{λ} as a Parameter. Dashed curves refer to zero mass transfer resistance.....	4-8
Figure 4-4. Bubble Expansion Ratio Versus Depth of Supematant Pool; Initial Bubble Diameter as a Parameter. Dashed curve refers to zero mass transfer resistance.....	4-9
Figure 4-5. Bubble Expansion Ratio Versus Convective Layer Temperature (<100 °C) or Buoyant Parcel Temperature T_{bc} During Buoyant Displacement. Dashed curve refers to zero mass transfer resistance.	4-12
Figure 5-1. Sequence of Events in Model of Steam Bump and Liquid Waste Release.	5-2
Figure 5-2. Temperature History of Buoyant Parcel Compared With its Boiling Temperature; Open Headspace.	5-8
Figure 5-3. Temperature History of Buoyant Parcel Compared With its Boiling Temperature; Sealed Headspace	5-9
Figure 7-1. Probability of Recovering Ventilation as a Function of Days Available.	7-7
Figure 7-2. Probability of Not Recovering the Ventilation System as a Function of Available Time.	7-8
Figure 8-1. 241-AZ-102 Tank Bump Short-Term Results.....	8-5
Figure 8-2. 241-AZ-102 Tank Bump Long-Term Results.....	8-6

TABLES

Table 3-1. History of Events.....	3-1
Table 3-2. Waste Properties for GOTH Analysis	3-8
Table 3-3. GOTH Runs Flow Path Descriptions	3-9
Table 3-4. GOTH Run Summary	3-13
Table 3-5. Single-Shell Tanks With Liquid Inventory >400 kL	3-17
Table 3-6. Double-Shell Tank Waste Properties	3-18
Table 4-1. Gas and Steam Generation Rates in the Non-Convective Layer.....	4-14
Table 4-2. Buoyant Displacement Model (equation (4-16)) Predictions for the High-Power Double-Shell Tanks.....	4-14
Table 6-1. Double-Shell Tanks With Negligible Non-Convective Layer.....	6-2
Table 6-2. Single-Shell Tanks and Double-Shell Tanks With Small Heat Load and/or Small Supernatant Depth	6-2
Table 6-3. Time to Saturated Conditions for Double-Shell Tanks With Significant Supernatant Depth and Heat Load.....	6-5
Table 6-4. Heat-up Rates for AZ Double-Shell Tanks.....	6-7
Table 7-1. Critical Items List for the High-Level Waste Transfer RAM B, Ranked by the Contribution of System Type to Expected Schedule.....	7-2
Table 7-2. Component Types and Recovery Conditions	7-3
Table 7-3. Summary of Corrective Maintenance Requirements (Clock Hours and Effort)	7-5
Table 7-4. Corrective Maintenance Activity Clock Time Distributions.....	7-6
Table 8-1. Parameter Values for Consequence Analysis Example for Tank 241-AZ-102	8-3
Table 8-2. Radiological Consequence Factors.....	8-7
Table 8-3. Sum-of-Fraction of Risk Guidelines for a Unit Release of Chemicals	8-9
Table 8-4. Toxic Consequence Evaluation Results	8-10

TERMS

ALC	air lift circulator
HEPA	high-efficiency particulate air (filter)
HVAC	heating, ventilation, and air conditioning
DST	double-shell tank
LCO	Limiting Condition for Operation
RAM	reliability, availability, and maintainability
SST	single-shell tank

This **page** intentionally left **blank**.

1.0 PURPOSE AND SCOPE

This report provides a new evaluation of the Hanford tank bump accident analysis (HNF-SD-WM-SAR-067 2001). The purpose of the new evaluation is to consider new information and to support new recommendations for final safety controls. This evaluation considers historical data, industrial failure modes, plausible accident scenarios, and system responses.

A tank bump is a postulated event in which gases, consisting mostly of water vapor, are suddenly emitted from the waste and cause tank headspace pressurization. A tank bump is distinguished from a gas release event in two respects: First, the physical mechanism for release involves vaporization of locally superheated liquid, and second, gases emitted to the head space are not flammable. For this reason, a tank bump is often called a steam bump. In this report, even though non-condensable gases may be considered in bump models, flammability and combustion of emitted gases are not.

The analysis scope is safe storage of waste in its current configuration in single-shell tanks (SSTs) and double-shell tanks (DSTs). The analysis considers physical mechanisms for tank bump to formulate criteria for bump potential, application of the criteria to the tanks, and consequence analysis of bump scenarios. The result of consequence analysis is the mass of waste released from tanks for specific scenarios where bumps are credible; conversion to health consequences is performed using standard Hanford methods (Cowley et al. 2000; and WHC-SD-WM-SARR-011 1996). The analysis forms a baseline for future extension to consider waste retrieval.

This page intentionally left **blank**.

2.0 SUMMARY OF FINDINGS

Postulated physical scenarios leading to tank bumps are comprehensively examined here. We conclude that a combination of a substantial supernatant layer depth, supernatant temperatures close to saturation, and commensurate sludge temperatures are required for a tank bump to occur. We have ruled out scenarios postulated at various times for sludge layers lacking substantial supernatant, such as superheat within the layer and fumarole formation leading to a bump.

A graded set of criteria is presented to screen tanks for bump potential. These screening criteria may be applied as tank waste inventories are changed. Bump scenarios and criteria can explain observations of historical bump events and show the difference in tank bump potential earlier in tank life compared to the present day, essentially due to high historical tank power and in some cases gas injection.

Applying criteria for non-negligible supernatant layers and non-negligible non-convective layers, all but four SSTs in their present state may be considered immune to a tank bump, as can some DSTs. Simple screening for tank power removes the remaining **SSTs** and many DSTs from consideration.

Extended loss of cooling is required to develop initial conditions sufficient for a tank bump during safe storage. Tank 241-AZ-101 has the highest heat load and therefore the fastest heat-up rate during a loss of cooling event. Based on a heat load of 61 kW (conditions as of January 31, 2001), the calculated heat-up rate for 241-AZ-101 is 0.34 °C/day [0.61 °F/day].

Although Tank 241-AZ-101 has the fastest heat-up rate during a loss of cooling event, tank bump consequences are influenced by other waste conditions, notably the settled solids or non-convective layer depth. A consequence evaluation for a hypothetical tank bump in Tank 241-AZ-102 is therefore presented. Consequences are evaluated using a best-estimate model approach with an experimental basis for separate phenomena, including models for the amount of material released, consideration of successive releases, and mixing of formerly non-convective material with supernatant. Successive bumps are estimated to occur over approximately half-hour intervals with about 1/12 the non-convective layer released per bump. An average aerosol release to headspace of about 1.8 kg per bump is calculated, and long-term release of about 5.2 kg is predicted, with about 16.2 kg retained in the tank.

The mass of entrained material was converted to dose following the method of Cowley et al. (2000). An onsite dose of 0.05 Sv was calculated for worker exposure at 100 m during an 8-hour shift. An offsite dose of 1.2×10^{-4} Sv was calculated for an 8-hour event. Toxic chemical consequences are all acceptable.

This **page** intentionally left blank.

3.0 HISTORICAL AND PRESENT EVALUATION DATA

3.1 HISTORICAL EVENTS

Since the early 1950's, aging waste has been stored in underground storage tanks at the Hanford site. In the mid-1950's, a tank bump was first observed, which led to installation of air lift circulators (ALC) that provide liquid agitation and solid suspension. Air lift circulators, also referred to as air lift pumps, have successfully prevented bumps, and the few bumps that have occurred since the mid-1950's were initiated by ALC shutdown and restart. Discussion below presents a brief history of the documented events, which are listed in Table 3-1.

Table 3-1. History of Events.

Tank, 241-	Date	Heat Rate (Kw)	Waste Temp. at Bottom	Dome Pressure	Duration	No. of Documented	ALC	Initiator	Contamination	Vent System	Ref.
S-104	10/53-5/54	200	> 240	< 1.6	8 to 42	Many	0	None	Yes	No	[1]
S-101	10/54-8/54	200	> 240	< 1.6	8 to 42	Many	0	None	Yes	No	[1]
SX-101	2/55-4/55	400	300	0.7 - 1.8	3 to 13	> 40	Auger	None	Unknown	No	[1]
SX-104	7/55	600	290	Unknown	70	2	Proto-	ALC shutdown/restart	Unknown	No	[2]
SX-114	8/58	650	357	2.6	Unknown	4	4	ALC shutdown/restart	Yes	Yes	[3]
A-105	1/65	2300	310	1.8	30	1	4	Bottom of tank bulged	Yes	Yes	-
AX-101	1968-1969	2300	260	Unknown	20	1	22	ALC shutdown/restart	No	Yes	[1]

[1] Indixsen, R. B., 1989, *History of Tank Bumps in Aging Waste Tanks*, Letter report to A. Clapp.

[2] Kuhn, W. L., 1988, *Independent Review of Aging Waste-Tank "Bump" Analyses*, Final letter report from Pacific Northwest Laboratory, Richland, Washington, found within WHC-SD-WM-TI-406, Rev. 0.

[3] Jones, B. L., 1988, *Aging Waste Tank Bump Sensitivity to Thermal Conductivity and Heat Capacity, Incorporating the Assumption of N-Reactor Shutdown* (Internal Memo to L. A. Mihalik), Westinghouse Hanford Company, found within WHC-SD-WM-TI-406, Rev. 0.

In a passage describing waste tank operations history, Jo (1990) states that prior to August of 1952, conduction to underlying soil prevented boiling. In addition, air cooled heat exchangers for the S tanks were installed above ground. During August of 1952, Tank 241-S-110 boiled and water was sprayed on the air condensers, which was sufficient to condense vapor. In 1953,

Tank 241-S-107 also boiled, but because water spray could not keep up with the boiling rate, a water jacket was installed on the air condenser. In both cases, contamination was not found.

According to Tomlinson (1955), "In July, 1953, Tank 241-S-104 was filled and its contents started boiling at a rate which exceeded the heat exchange capacity of the water-jacketed air condenser." Despite installation of auxiliary water cooled condensers on Tanks 241-S-104 and 241-S-101 circa August 1953, occasional mild eruptions were observed, followed by increased evaporation rates and contamination. Eruptions were preceded by disturbing the waste in some cases, and in other cases by no observed cause. In January of 1954, "bumping" eruptions, in the form of a series of 5 to 25 abrupt pressure surges at roughly 100 second intervals, first took place in Tank 241-S-101. Bump initiation was concomitant with a temperature at the bottom of the tank greater than 240°F – the recorder temperature limit. The same phenomena were observed in Tank 241-S-104, including the greater than 240 °F temperature at the tank bottom. Tank overpressure never exceeded 1.6 psig. The two tanks were boiled down to approximately half-volume and refilled, which suggests the tanks were nearly full when the bumps first started. Bumps continued for another eight months and then gradually diminished to a simmer.

From May 1954 to February 1955, Redox waste (excepting coating waste) filled the 241-SX-101-102-103 cascade. In February 1955, bumping was observed in Tank 241-SX-101. It consisted of 5 to 25 abrupt pressure surges at intervals of about 30 seconds, with maximum pressures of 0.7 psig to 1.8 psig. These pressure surges occurred about once per day naturally, but could be initiated two or three times daily by starting an auger installed in the tank. Tank liquid level fell from 30 ft to 25 ft during the next two months, even though no waste was added.

In June of 1955, Tank 241-SX-104 was boiling but no bumps occurred. Boiling can be distinguished from a tank bump because boiling is gentle by comparison and involves only the supernatant rather than the settled solids. To prevent bumps, the prototype ALC was installed. Initial ALC operation increased the condensate flow rate from the normal 3 gpm to 7 gpm, but only for about six hours. On July 14, 1955, the ALC became inoperative because of a failed gasket (Hanson 1955). Upon ALC restart on July 15, 1955, a bump occurred, resulting in an instantaneous increase in the condensate flow rate from 0.8 gpm to 17.2 gpm; the bump lasted for about 70 minutes and released heat at a rate of 4.7×10^6 Btu/hr, or 1.38 MW. The bumping was attributed to the interruption in ALC operation (Hanson 1955).

Tank 241-SX-114 bumped four times during August of 1958. During the week of August 18, 1958, 241-SX-114 tank temperature gradually increased, despite the operation of four ALC at 10 cfm each. On August 22, operators shut off air and ran 2 cfm of water through each of the ALC. By this time, waste temperature was 357 °F. The tank bumped three times during the next couple of days, and once on August 25. In Harmon (1958), the bumps are attributed to turning off the ALC in Tank 241-SX-114. Contamination was extensive both inside and outside the tank farm, although no site employees were exposed (Harmon 1958). Bumps in Tank 241-SX-114 ejected "contaminated vapors" out of the Tank 241-SX-113 pump pit. Contamination within the tank farm spread over about 15,000 ft, with a maximum dose rate of 5 Rads/hr.

The most publicized event occurred in January of 1965, in Tank 241-A-105. This bump is attributed to evaporation of water trapped in between the liner and concrete floor. Waste

temperature was high enough that the vapor pressure just underneath the liner exceeded the hydrostatic head of the waste. In effect, the liner bulge was responsible for the bump, which means that this event is not applicable to the current analysis.

In an internal memorandum, Bendixsen (1989) reports that Tank 241-AX-101 bumped once between 1968 and 1969. The event was never recorded because there was no finding of any contamination near the tank. Waste temperature was estimated to be 260 °F. ALC shutdown and restart was identified as the event initiator.

These events led to three historically postulated scenarios for bump initiation (Jo 1990): (1) an organic crust, (2) liner bulge, and (3) ALC restart. In the first scenario, an organic crust forms over the supernatant and causes pressurization and super-heating. When the pressure is large enough to crack the crust, the supernatant is released until it depressurizes and the boiling point returns to normal. Single-shell liner instability was known prior to the 241-A-105 event (Brownell 1958). In several of the events described above, ALC restart after a long period resulted in vapor generation by heat released from the superheated waste. The organic crust and liner bulge scenarios are of historical interest only, and for current operations, only the ALC restart scenario has been retained.

Given current aging waste tank operations, the following tank bump scenario was accepted in 1990 as the only credible one (Jo 1990):

- Initiator: the initiator is an equipment failure that allows particle settling or loss of heat removal
- Heat build-up: a temperature rise in the solid and/or liquid phase caused by decay heat
- Heat release: ALC or mixer pumps agitate superheated solids and/or liquid, thereby releasing stored heat
- Vapor generation: superheated liquid rises and rapidly generates vapor
 - Environmental release: vapor generation is rapid enough to overwhelm the tank ventilation system, pressurize the tank, and release vapor and particles to the environment through unfiltered pathways.

Discussion below proceeds with this scenario in mind.

3.2 PREVIOUS ANALYSIS

Previous analyses consist of the Fauske and Associates, Inc. reports of 1989 (FAI 1989) and 1999 (Epstein et al. 1999; and Waters et al. 1991), and the GOTH analyses carried out by Westinghouse Hanford Company (Sathyanarayana 1996). The 1989 Fauske and Associates, Inc. document (FAI 1989) presents conclusions inferred from the documented events and supported by relatively straightforward hand calculations for the several bump heat transfer phenomena. As part of the technical basis for safe storage after sluicing and cessation of water addition, Epstein's et al. (1999) report considers the steam bump potential in **Tank** 241-C-106, although

the conclusions drawn in it can be applied generally. Using HEATING7, Waters et al. (1991) performed a series of parametric calculations to determine tank bump potential during-in-tank washing operation proposed for the **AZ** tanks. HEATING7 is a multi-dimensional code for finite difference solutions of the conduction equation in cylindrical, spherical, or rectangular coordinate systems. The Westinghouse Hanford Company report (Sathyanarayana 1996) contains parametric calculations based on the GOTH code, which was derived from EPRI's GOTHIC code. GOTH is a finite volume program that solves the transient equations expressing mass, momentum, and energy conservation for multi-component, multiphase fluid flow. The FAI (1989) report is considered first, as it provides a succinct overview of tank bump phenomenology.

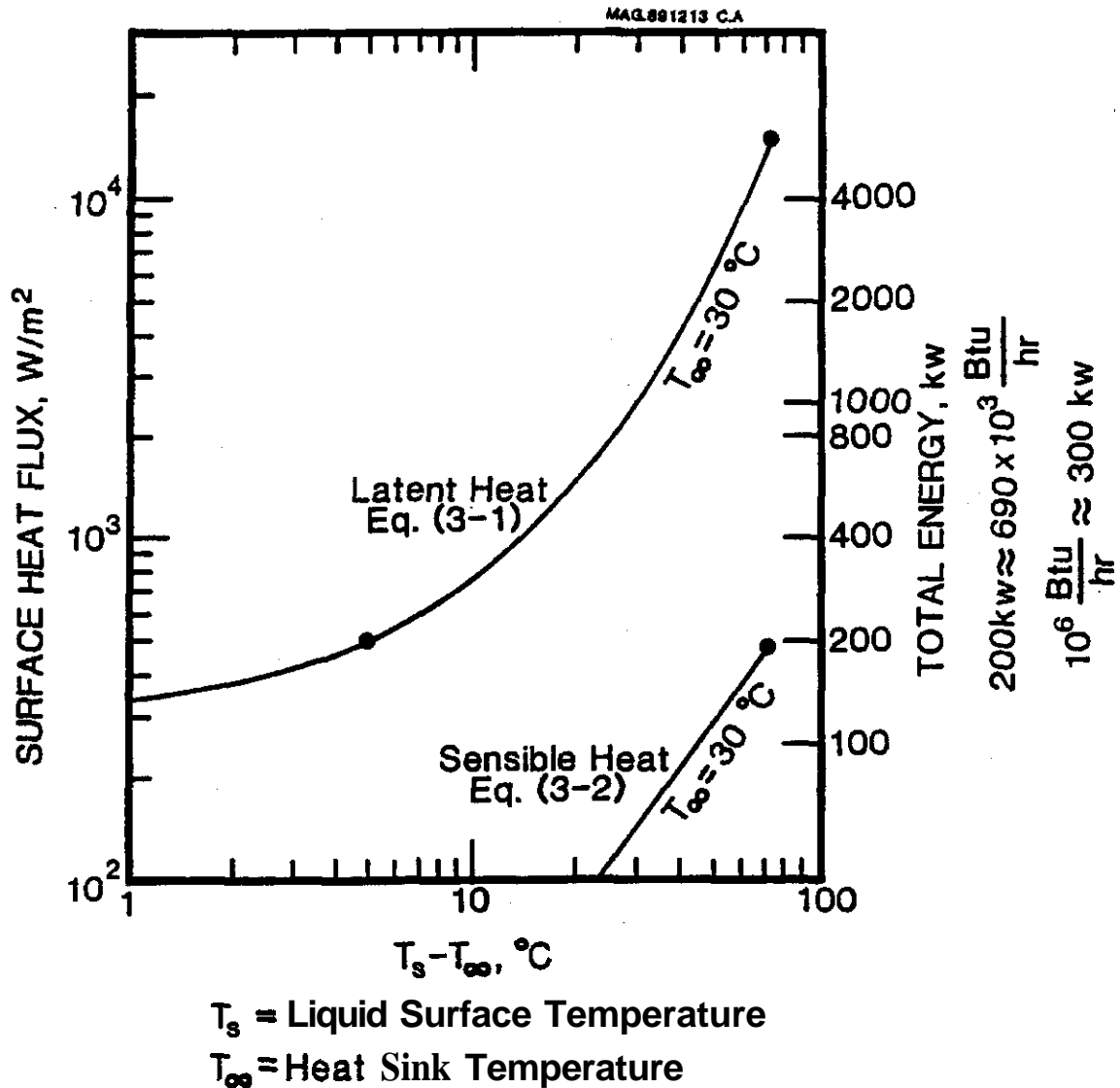
3.2.1 Fauske and Associates, Inc., 1989

In December of 1989, Fauske and Associates, Inc. issued an *Independent Review of Aging Waste Tank "Bump" Phenomena*, which considered the background material on tank bumps and presented new observations regarding bump heat transfer mechanisms (FAI 1989). Some of the conclusions stated in the report could be inferred from the documented events, but hand calculations were presented to characterize several bump heat transfer mechanisms. The report's conclusions are as follows:

- Tank bumps require that the pool surface reach the boiling temperature
- Tank dome ventilation should be sufficient to keep pool surface temperature below the boiling temperature
- Setting aside ALC restart, it is likely that the waste depth must exceed some minimum value for the tank bump to occur
- There is probably some minimum tank power level below which tank bumps cannot naturally occur, regardless of pool surface temperature.

To augment the basis for these conclusions, phenomena considered by hand calculation include surface evaporation, pool circulation, dryout in settled beds, and gas injection on restart of ALC. A surface evaporation calculation was used to show tank ventilation should be sufficient to keep pool surface temperature below the boiling temperature. By the evaporation heat transfer analogy of Epstein (1988), latent and sensible heat transfer from the pool to some sink temperature were computed as a function of pool surface temperature, T_s , assuming that water mass fraction at infinity was zero and the water mass fraction at the surface was related to vapor pressure at T_s . The results shown in Figure 3-1 indicate that surface evaporation can remove a pool heat rate of 200 kW at a surface temperature of only 35 to 40 °C, if the dome has low relative humidity.

Figure 3-1. Surface Heat Removal.



To demonstrate that convective motion in the pool is virtually certain, the Rayleigh number was calculated as follows:

$$Ra = \frac{g d^4 \beta \Delta T}{h \nu \alpha} \quad (3-1)$$

where g is the acceleration of gravity, d is the pool diameter (23 m), β is the thermal expansion coefficient for water ($6 \times 10^{-4} \text{ K}^{-1}$), h is the height of the pool (10 m), ν is the liquid kinematic viscosity ($3 \times 10^{-5} \text{ m}^2/\text{s}$), and α is the liquid thermal diffusivity ($3 \times 10^{-5} \text{ m}^2/\text{s}$). If the temperature difference is only 1°C , $Ra = 10^{15}$. This is orders of magnitude higher than the Rayleigh number required for the onset of convection, which is somewhere between 100 and 10,000, depending on the thermal boundary conditions. The report then goes on to conclude that

natural convection should suffice to keep the pool isothermal and that dome relative humidity determines bulk pool temperature. This conclusion means that a submerged air supply is not absolutely necessary.

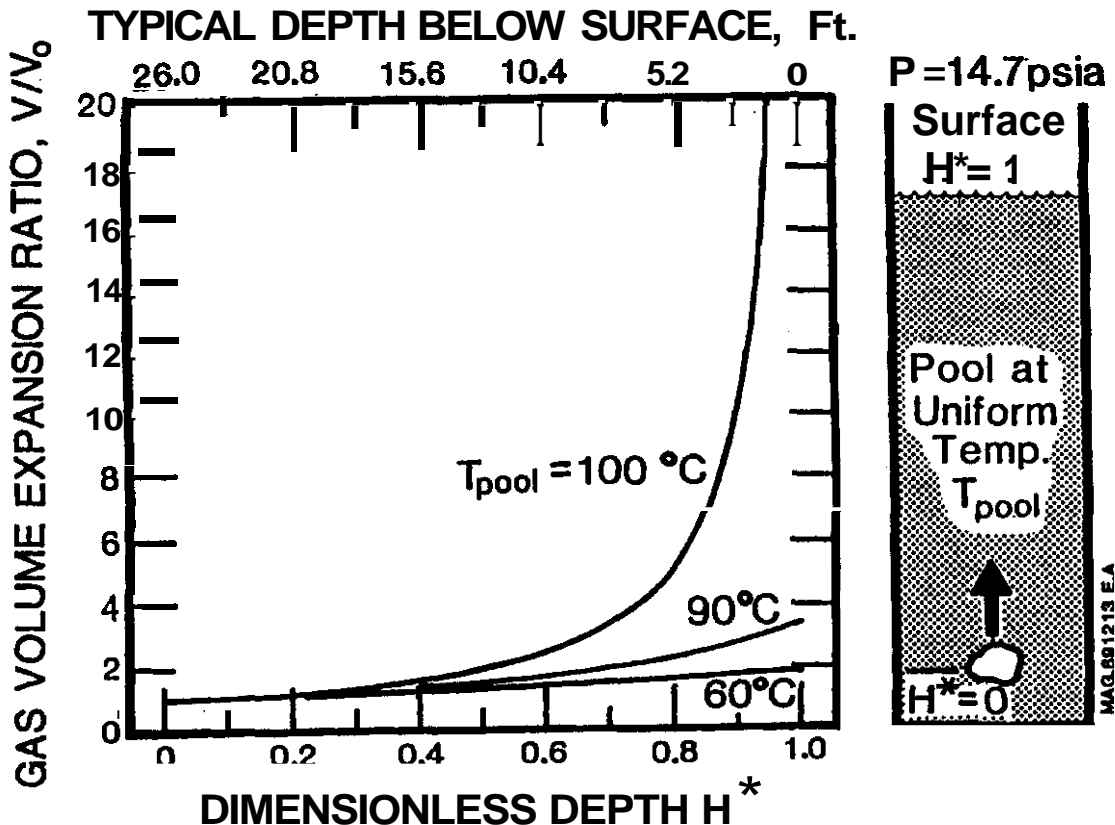
Phenomena relating to gas injection on restart of ALC were considered in both FAI (1989) and Epstein et al. (1999). Consider the ascent of a cavity volume in an isothermal pool.

A relationship for the relative volume (local volume divided by initial cavity volume, V/V_0) as a function of height is:

$$\frac{V}{V_0} = \frac{\beta + 1}{\beta + (1 - H^*)} \quad (3-2)$$

where $H^* = 1 - H/H_0$ is the dimensionless height, H_0 is the pool depth, and the term $\beta = [P_{\text{surf}} - P_{\text{sat}}(T_0)] / \alpha H_0$ represents the difference between the pool surface pressure and the vapor pressure of the liquid at temperature T_0 , divided by pressure increase at the depth of gas release. Evaluation is shown in Figure 3-2, assuming $\alpha = 0.41$ psi/ft and $H_0 = 26$ ft. Figure 3-2 illustrates that tank bump events are doubtful if the pool surface temperature is just 10°C below the boiling point. This expression also demonstrates that in the limit of a shallow pool ($\beta \rightarrow \infty$), $V/V_0 \rightarrow 1$. In other words, there is no expansion for a shallow pool and a tank bump cannot occur.

Figure 3-2. Cavity Expansion During Rise in a Constant Temperature Pool



3.2.2 Tank 241-C-106 Steam Bump Evaluation, (Epstein et al. 1999)

In this document, Epstein et al. (1999) give numerical examples to show that tank bumps cannot occur for shallow pools. If liquid temperature is 99°C ($P_{\text{sat}} = 97,780 \text{ Pa}$) and pool depth is 1.0 m, V/V_o is 3.7 at most, assuming the pool surface pressure is one atmosphere. If the pool depth is increased to 10.0 m but other assumptions remain unchanged, the maximum expansion ratio is 28. If liquid temperature is 95 °C ($P_{\text{sat}} = 84,550 \text{ Pa}$) and pool depth is 1.0 m, maximum expansion ratio is 1.6, assuming other assumptions remain unchanged. A pool depth of 1.0 m is most relevant because the 241-C-106 waste will be sluiced to this depth, more or less. In regard to Tank 241-C-106, tank humps by inert gas injection are impossible because the supernatant is only a few inches deep.

3.2.3 GOTH Analyses (Sathyanarayana 1996)

The purpose of the Westinghouse Hanford Company calculations using GOTH was to provide a technical basis **for** tank bumps and estimates of the consequences (releases of steam and solid particles) of tank bump events. The document begins by stressing that although current tank conditions preclude a tank bump event if normal ventilation is operating, loss of ventilation combined with increased non-convective layer thicknesses and heat load might lead to favorable conditions for a bump. Without dome ventilation, local non-convective layer temperature can increase to saturation temperature. Two types of non-convective layer vertical temperature distributions are envisioned by the report: “best-estimate” and “conservative”. A best-estimate temperature distribution is defined as the vertical temperature distribution just when the first piece of non-convective waste reaches the local saturation temperature. This temperature distribution is said to exist for the first plume release only. Repeated bumps are expected because without dome ventilation the heat load continues. After the first bump, hot non-convective waste mixes with cooler waste until it is everywhere near the local saturation temperature; this is referred to as the conservative temperature distribution.

Sathyanarayana (1996) lists the following parameters and assumptions as critical to the magnitude of the bump and mass of airborne aerosol:

- Thickness: larger non-convective layer thicknesses produce larger bumps and releases. GOTH analyses assumed three thicknesses: 18 and 48 in. thicknesses with Tank 241-AZ-101 solid and liquid waste properties (see Table 3-2) for each, and a thickness of 11 ft with composite properties of Tank 241-C-106 and 241-AY-102 wastes (see Table 3-2).
- Initial Temperature Distribution: the two assumed distributions – best-estimate and conservative – have been described above. The strength of the bump is proportional to the fraction of waste that is near the saturation temperature.
- Ventilation and Flow Paths: simulations were performed with three assumed flow areas, as shown in Table 3-3. In addition, preliminary calculations were made using the AZ tank farm 702-A ventilation system.

Table 3-2. Waste Properties for GOTH Analysis.

	241-AZ-101	241-AY-102/ 241-C-1066
Primary Tank Dia., ft (m)	75 (22.9)	75 (22.9)
Secondary Tank Dia., ft (m)	80 (24.4)	80 (24.4)
Solids Density, lbm/ft ³ (kg/m ³)	243.4 (3898.9)	113.9 (1822.4)
Aqueous Solution Density, lbm/ft ³ (kg/m ³)	75.5 (1209.4)	75.5 (1209.4)
Sludge (Mixture) Density, lbm/ft ³ (kg/m ³)	104.0 (1665.9)	81.2 (1299.2)
Total Waste Depth, ft (m)	30 (9.14)	30 (9.14)
Supernatant Depth, ft (m)	28.5/26 (8.7/7.9)	19 (5.8)
AY-102 Heat Load, Btu/hr (W)		33,000 (9671)
Total Heat Load, Btu/hr (W)		125,000 (36634)
Supernatant		
Thermal Conductivity, Btu/hr-ft-F (W/m-K)	0.35 (0.61)	0.35 (0.61)
Heat Generation Rate, Btu/hr-lbm (J/s-kg)	0.019 (0.0123)	0.0 (0.0)
Insoluble Solids		
Thermal Conductivity, Btu/hr-ft-F (W/m-K)	5.0 (8.5)	5.0 (8.5)
Heat Generation, unwashed, Btu/hr-lbm (J/s-kg)	0.37 (0.2391)	0.14 (0.09)
Volume Fraction of Solids, unwashed, %	17	16
Particle Size, washed	1 - 10 microns, 5 micron average	1 - 10 microns, 5 micron average

Source:

Sathyanarayana, K., 1996, *Evaluation of Potential and Consequences of Steam Bump in High Heat Waste Tanks and Assessment and Validation of GOTH Computer Code*, WHC-SD-WM-CN-022, Rev. 0-B, Westinghouse Hanford Company, Richland, Washington.

Table 3-3. GOTH Runs Flow Path Descriptions

Dome Flow Path Assumptions		
Riser Flanges, Cover Block Open	Five 4 in. Diameter Inleakage Paths	One 6 in. Diameter Inleakage
1. 42 in. dia. Pump Pit Path	Five 4 in. dia. Inleakage Paths	6 in. dia. Inleakage Path
2. 20 in. dia. Vent Path	20 in. dia. Vent Path	20 in. dia. Vent Path
3. Four 42 in. dia. Sluice Pits Path		

- Aerosol Deposition: the only deposition in the system is settling in the tank waste following release.
- Supernatant Depth: deeper pools result in higher tank bottom pressures and correspondingly higher saturation temperatures, which means that the bump will be more energetic when it finally happens. No attempt was made to study the effect pool depth. The total waste depth was 30 ft for all simulations.
- Non-Convective Layer Viscosity: 8,000 lbm/ft-s (12,000 kg/m-s) was assumed for all cases. Viscosity partially determines the ability to trap steam bubbles.
- Non-Convective Waste Yield Strength: the assumption is that yield strength is zero, for the sake of conservatism. High yield strength would hold some waste in place and prevent it from participating in the rollover.
- Supernatant Temperature: pool sub-cooling has a dramatic effect on the strength of a bump. Various sub-cooled temperatures were considered.

Thermal hydraulic simulations were performed with the GOTH code.

Initial conditions were generated by a set of one-dimensional GOTH runs to find the vertical temperature distribution in the waste when the peak temperature (at the bottom) exceeds the local saturation temperature. Prior to GOTH simulation for a bump, a preliminary run was needed to find conditions that would initiate the bump. These preliminary runs simulated the transient heat up of the waste assuming normal ventilation is replaced by an air inlet flow at **53.3°F**, which is the Hanford annual average temperature. For example, a GOTH calculation resulted in the best-estimate initial conditions for 11 ft of consolidated non-convective layer from Tanks 241-AY-102 and 241-C-106, as shown in Figure 3-3. The conservative temperature profile shown in Figure 3-4 results from assuming that at each point, the waste temperature corresponds to saturation. These calculations were repeated for the 18 and 48 in. depths, although only the 11 ft temperature profile is shown here because the temperature distribution is more apparent.

Figure 3-3. Best-Estimate Initial Temperature Profile for 11 ft of Consolidated Non-Convective Waste.

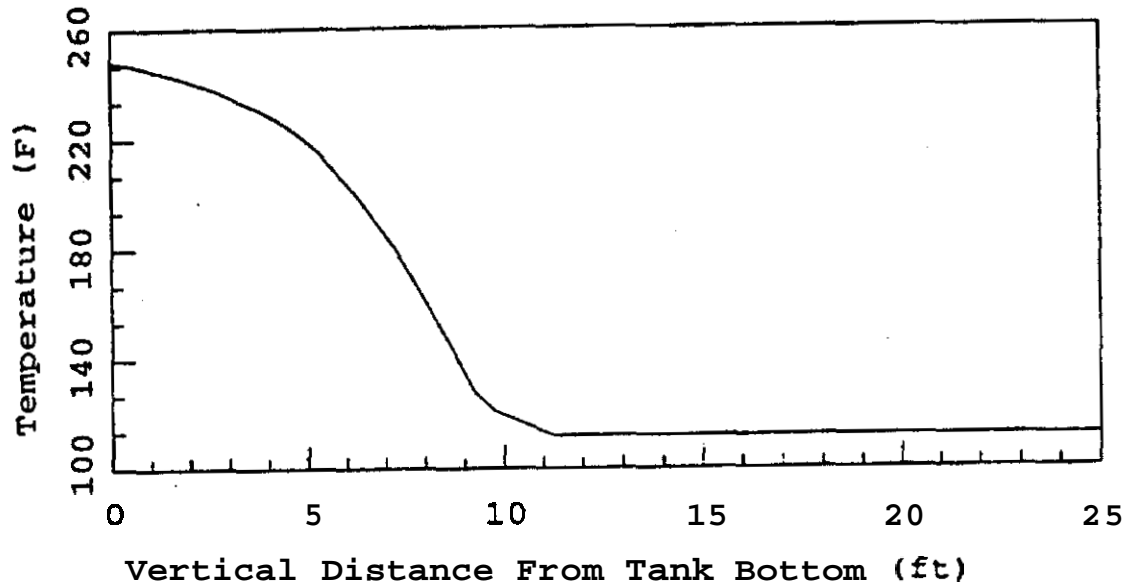
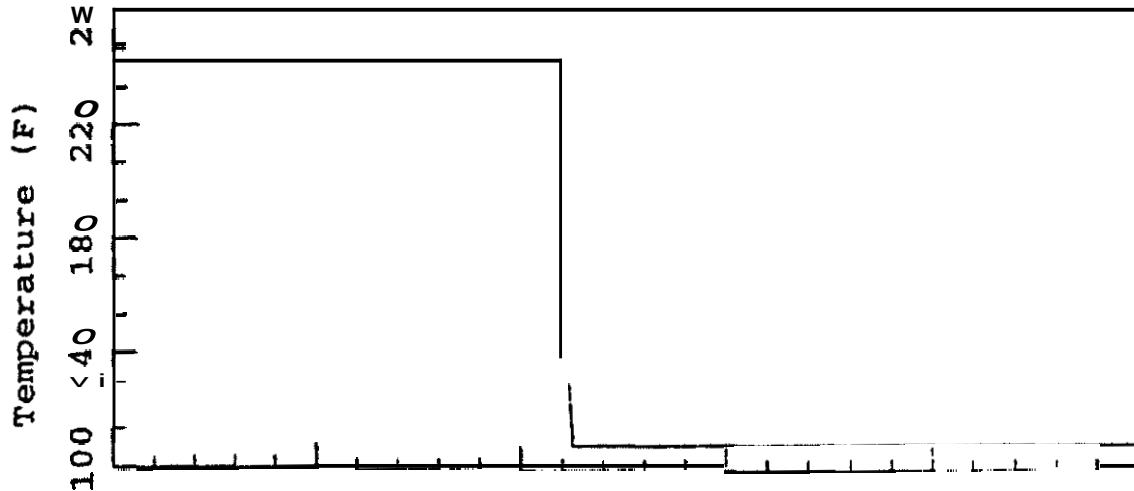


Figure 3-4. Conservative Initial Temperature Profile for 11 ft of Consolidated Non-Convective Waste.



The results of a GOTH run for the 18-in. non-convective layer with no condensation are shown in Figure 3-5, which represents the development of steam concentration contours in the waste. The figure shows gas volume fraction contour snapshots at four different times. Starting with the top left-hand corner, the frames show the start of the steam bump and development of hydrodynamic instability in the waste. In this figure, the maximum void fraction plotted is 0.9 and the minimum is 0.1. The top left-hand frame shows that 40 seconds into the run, the void fraction at the height of the original non-convective layer is about 0.1. Hydrodynamic instabilities start about five seconds later, as shown by the top right-hand frame, with a superheated plume identifiable at 50 seconds. Contours at 70 seconds show a plume breaking the waste surface and dispersing liquid droplets and solid particles to the dome space. Although not shown here, Sathyanarayana (1996) plots both liquid droplet and solid particle flowrate through the respective tank vent paths as a function of time. Results are also reported as integrated, total releases of liquid and particle mass. The report also goes on to state that humps will repeat until ventilation is restored.

The matrix of GOTH runs and a brief description of results are shown in Table 3-4. Important results culled from the table are as follows:

- For the conservative temperature profile with no condensation, dome pressurization is significant and particle releases can be enormous. Release quantity depends on the size and location of flow paths, but as a general trend releases are largest for “Riser Flanges, Cover Blocks Open” cases, which have the largest flow area. Releases for “One 6” Dia. Inleakage Path” cases are much smaller, although still significant. GOTH calculations are multi-dimensional, which means that the location of the bump with respect to the openings is important for determining releases.
- For 18 and 48-in. non-convective thicknesses, best-estimate cases do not result in humps, regardless of assumptions about condensation.
- For the 11 ft thickness, no hump occurs in the best-estimate case with condensation.
- Comparing Run 13 (peak pressure = 25.0 psia, release = 2,100 lbm) with Run 22 (peak pressure = 22.2 psia, release = 450 lbm) shows that a simple model provides a conservative estimate with respect to a complete ventilation model that considers all four tanks in the farm and other ventilation equipment.

In cases where bumps occur, the severity of predicted releases can be traced to the conservative assumptions made for the analyses. Total waste depth is 30 ft in all cases, which means that the small dome free volume cannot accommodate a large bump and that liquid slugs or droplets are pushed out dome flow paths. With a non-convective waste shear yield strength of zero, all of the waste participates in the bump event, which means that the void created is much larger than if only a small portion participated.

Figure 3-5. Gas Volume Fraction Contours for GOTH Run With 18in Non-Convective Layer and No Condensation.

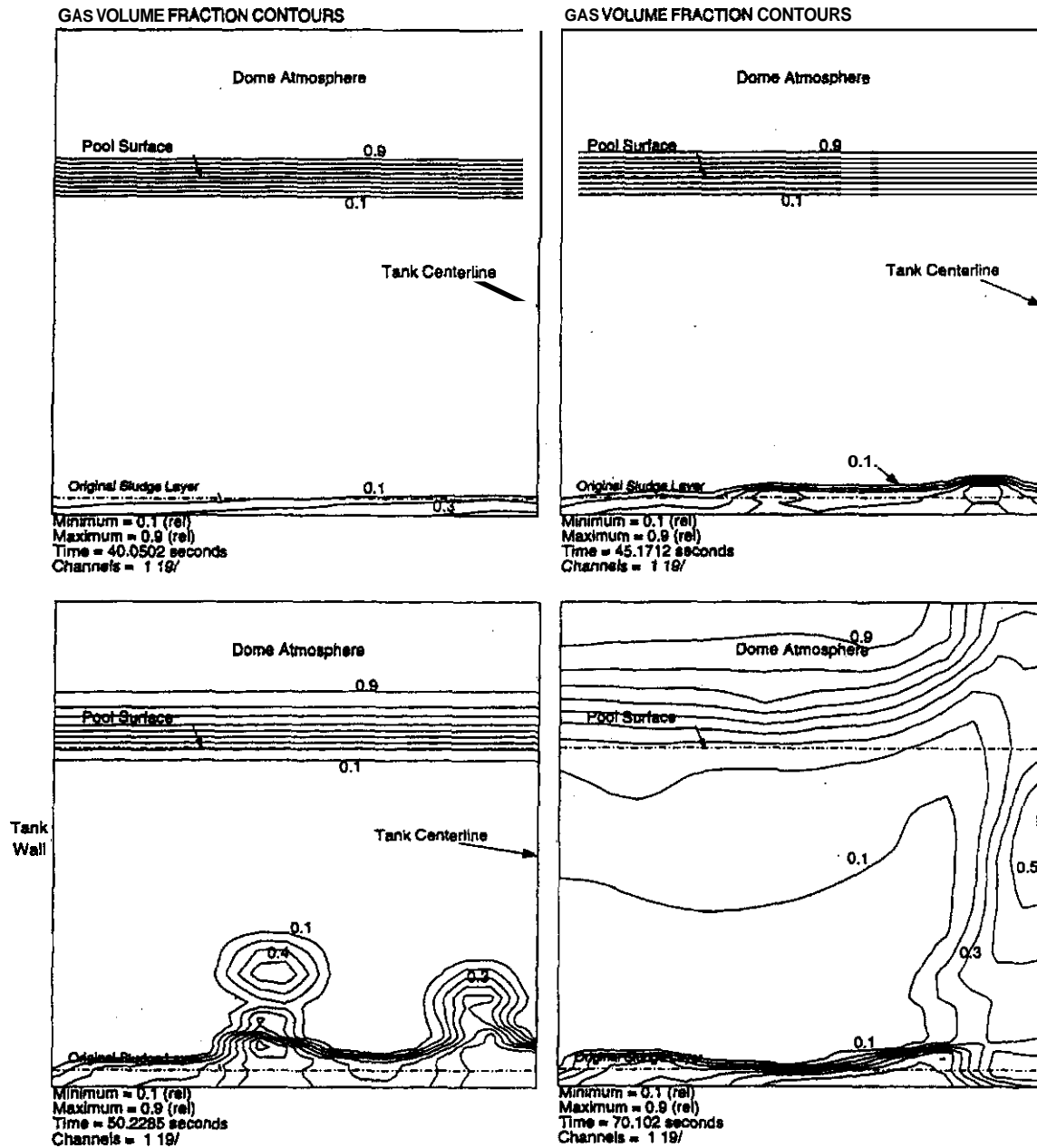


Table 3-4. GOTH Run Summary.

Run	Sludge Depth (ft)	Waste Properties	Temperature I.C.	Condensation	Flow Area ⁽¹⁾	Peak Dome Pressure (psia)	Particle Release (lbm)
1	1.5	241-AZ-101	Conservative	No	Riser Flanges, Cover Blocks Open	15.0	150
2	1.5	241-AZ-101	Conservative	No	Five 4 in. Dia. Inleakage Paths	15.7	1.3
3	1.5	241-AZ-101	Conservative	No	One 6 in. Dia. Inleakage Path	15.5	7
4	1.5	241-AZ-101	Conservative	Yes	No bump	No bump	No bump
5	1.5	241-AZ-101	Best-Estimate	No	Riser Flanges, Cover Blocks Open	No bump	No bump
6	4	241-AZ-101	Conservative	No	Riser Flanges, Cover Blocks Open	22.5	6,300
7	4	241-AZ-101	Conservative	No	Five 4 in. Dia. Inleakage Paths	17.3	85
8	4	241-AZ-101	Conservative	No	One 6 in. Dia. Inleakage Path	19.5	165
9	4	241-AZ-101	Conservative	Yes - 164°F Supernatant			
10	4	241-AZ-101	Best-Estimate	No	Riser Flanges, Cover Blocks Open	-	Minimal
11	4	241-AZ-101	Best-Estimate	Yes	Riser Flanges, Cover Blocks Open	No bump	No bump
12	11	241-C-106 / 241-AY-102	Conservative	No	Riser Flanges, Cover Blocks Open	27.0	97,000
13	11	241-C-106 / 241-AY-102	Conservative	No	Five 4 in. Dia. Inleakage Paths	25.0	2,100
14	11	241-C-106 / 241-AY-102	Conservative	No	One 6 in. Dia. Inleakage Path	25.0	1,050
15	11	241-C-106 / 241-AY-102	Conservative	Yes	Riser Flanges, Cover Blocks Open	28.0	6,200
16	11	241-C-106 / 241-AY-102	Conservative	Yes	Five 4 in. Dia. Inleakage Paths	30.0	260
17	11	241-C-106 / 241-AY-102	Conservative	Yes	One 6 in. Dia. Inleakage Path	32.0	2.5
18	11	241-C-106 / 241-AY-102	Best-Estimate	No	Riser Flanges, Cover Blocks Open	18.8	90
19	11	241-C-106 / 241-AY-102	Best-Estimate	No	Five 4 in. Dia. Inleakage Paths	19.2	78
20	11	241-C-106 / 241-AY-102	Best-Estimate	No	One 6 in. Dia. Inleakage Path	19.7	32
21	11	241-C-106 / 241-AY-102	Best-Estimate	Yes - 112 °F Supernatant	Riser Flanges, Cover Blocks Open	No bump	No bump
22	11	241-AZ-101	Conservative	No	AZ/AY Vent Farm Model	22.2	450

⁽¹⁾See Table 3-3 for details.

3.2.4 Tank Bump Potential During In-Tank Washing Operations Proposed for the AZ Tanks (Waters et al. 1991)

Waters et al. (1991) prepared this work to support "in-tank sludge washing" in DSTs 241-AZ-101 and -102. The report identified the physical conditions needed for a bump as follows:

1. Supernatant temperature must be near the boiling point
2. There must be a heat generating non-convective layer
3. Non-convective layer temperature must exceed saturation at the local hydrostatic pressure
4. Radiolytic heat load must be greater than 300 kW (1 Mbtu/hr)
5. Steaming rate must exceed the capacity of the vent line, which is about $4.43 \text{ m}^3/\text{s}$ ($9,400 \text{ ft}^3/\text{min}$)
6. Superheat with respect to the supernatant atmosphere boiling point must be $2.1 \times 10^{10} \text{ J}$ (20 Mbtu).

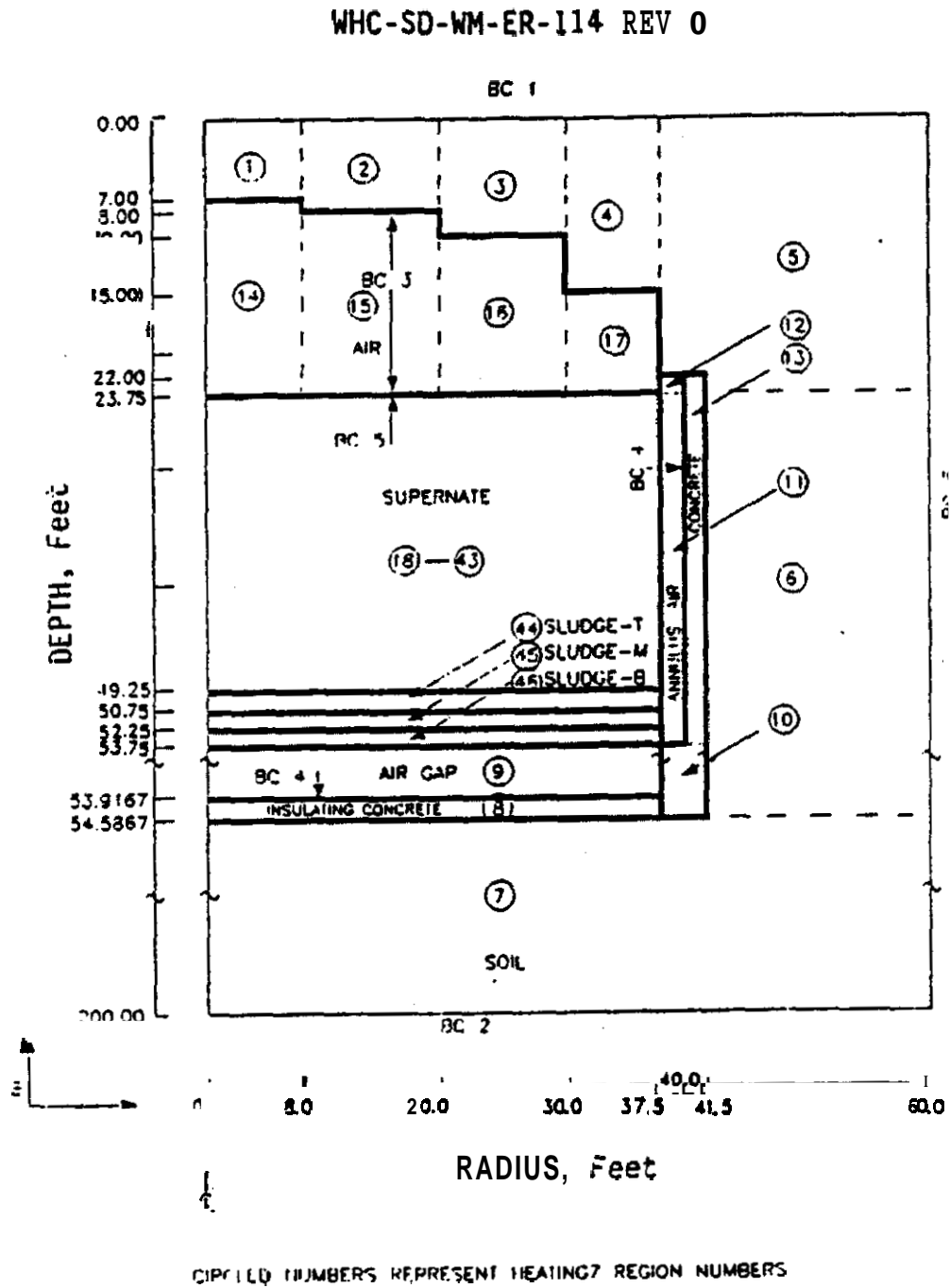
The first three items are essentially the same as the conclusions in the FAI report of 1991, while the remaining three items are based on historical tank bump events. At the time of the report, Tank 241-AZ-101 heat generation rate was projected to be 83.2 kW for April of 1993 and 73 kW for October of 1997.

Motivation for the report was the in-tank sludge washing procedure that used four mixer pumps dissipating a total of 800 kW ($2.73 \times 10^6 \text{ Btu/hr}$ or 1073 hp). Waters et al. (1991) used HEATING7 (Childs 1991) to determine if normal and off-normal sludge washing conditions lead to tank bump conditions. The first simulation performed was to determine if the waste temperatures will remain below saturated conditions under normal ventilation and prolonged input of 800 kW. Subsequent runs postulated power outages of various duration that begin after prolonged mixer pump operation has increased waste temperatures. And finally, a run was made with initial conditions prior to mixing and a 100-day outage of the airlift circulators and normal ventilation systems.

The HEATING7 model for transient thermal analysis in the three-dimensional cylindrical coordinate system is shown here as Figure 3-6. Six boundary conditions are required. The first (BC1 in Figure 3-6) is forced convection from the soil to the Hanford environment, assuming a heat transfer coefficient of $11.4 \text{ W/m}^2\text{-K}$ and average site temperature of 12.8°C (55°F). The second boundary condition (BC2) is a constant temperature of 12.8°C at the water table. Boundary condition 3 represents the radiative heat transfer and natural convection processes at the supernatant-dome interface, Boundary condition 4 approximates heat removal from the steel primary tank by the annulus ventilation system. Boundary condition 5 incorporates evaporative cooling as explained below, and heat transfer to bubbles rising through the supernatant by way of

ALC operation. Boundary condition 6 is an adiabatic condition to simulate an array of tanks with a 120-ft center-to-center spacing.

Figure 3-6. Dimensional **HEATING7** Model (Waters et al. 1991).



Evaporative cooling was included in the model based on the following relationship from Perry (1950):

$$W = 0.0138 (P_{\text{svp}} - P_p)^{1.20} \quad (3-3)$$

where W is the evaporation rate in lb/hr-ft^2 , P_{svp} is the vapor pressure of the waste liquid at the surface in mm Hg, and P_p is the partial pressure of water vapor in the airspace above the surface. Waters et al (1991) was able to reconcile this equation with the results shown in Figure 3-1. Flow rates were 634 scfm for normal primary ventilation and 500 scfm for annulus flow, with inlet temperature and relative humidity of 70 °F and 50%, respectively. Airlift circulators flow rate was 154 scfm before and during mixer operation. In outage scenarios, all flow rates were set to zero.

Results of the HEATING7 runs show the following:

1. Primary ventilation controls the equilibrium waste temperature by evaporative cooling,
2. Given ventilation system operation, waste temperatures remain below saturation, even with prolonged 800 kW power input,
3. Bump conditions do not result from a 72 hr power outage that begins after mixer pump operation has increased waste temperature,
4. Bump conditions do not arise after a 100 day outage that begins prior to mixer pump operation, and
5. A permanent outage could result in tank bump conditions under certain circumstances

Waters et al. (1991) did not specify what circumstances lead to tank bump conditions

3.3 CHARACTERIZATION DATA

The brief survey above suggests that the following waste parameters are needed for analysis of tank bump potential: non-convective layer depth, supernatant depth, and total waste volume. Tank-specific values for these parameters, along with many of the basic inputs that will be needed in the calculations to follow, are found in Hu et al. (2000) and Barton and Bingham (1999).

The analyses surveyed in the previous section show that only tanks with a deep supernatant layer are relevant. SSTs with appreciable amounts of liquid are listed in Table 3-5; a value of 400 kL (about 110 kgal) is the criterion here because this amount of liquid would result in a 1.0 m deep supernatant layer, assuming that the waste in these tanks is separated into distinct non-convective and supernatant layers. Core samples suggest that for the SSTs listed here, this is not really the case. For example, 241-A-I01 and 241-AX-I01 were found to have solids floating on the free liquid (Stewart et al. 1996). These SSTs are nevertheless considered in Section 6.0, where tank inventories and heat loads will be compared against bump criteria to develop a short list of tank

that are susceptible to bumps. DST supernatant depths are generally significant for tank bump phenomenology. Supernatant layer depths range from 20 cm to 10.3 m, and non-convective layer depths range from 0 m to 5.4 m. A few DSTs have deep supernatant layers but trivial non-convective layer depths; e.g., 241-AP-102 has 10 m of supernatant but no non-convective waste. Parts of Hu et al. (2000) are included here as Appendix A. In Section 6.0, supernatant and non-convective layer depths will be compared against bump criteria to develop a list of tanks potentially susceptible to tank bumps.

Table 3-5. Single-Shell Tanks With Liquid Inventory >400 kL.

Tank	Liquid Volume (kL)	Waste Volume (kL)
241-A-101*	1,923	3,608
214-Ax-101*	1,461	2,831
214-S-111	420	2,044
241-SX-102	507	1,946

*Solids atop liquid

Waste properties are also key to evaluation of tank bump potential and consequences, in particular the thermophysical properties of heat capacity, viscosity, thermal conductivity, density, and heat generation rate. Thermophysical properties are highly uncertain, and vary from tank to tank, as well as at different locations within the same tank. The mechanical property of shear yield strength, also referred to as shear strength or simply yield strength; is an input to predictive models for the size of the “gob” released from the non-convective layer. A summary of the available property data is presented below.

Using an analysis of variance tool, Willingham (1994) compiled a statistical analysis of waste properties and listed the total variability of several key properties. Source data came from characterizations for individual tanks. Data were available from only 33 of the 177 tanks and were not grouped into SST and DST categories; i.e., the statistical summary includes data from both tank types to calculate mean, standard deviation, etc. Sources of variability include tank-to-tank variation, core-to-core (radial difference) variation, segment-to-segment (axial difference) variation, and measurement error. Willingham’s (1994) compilation is presented here for completeness, but it is difficult to apply here because it does not distinguish between DSTs and SSTs, and has been obviated.

Since by and large only the double-shell tanks have significant supernatant depths, discussion can be narrowed to a survey of DST waste properties. Based on ball rheometer and void fraction instrument measurements taken between December 1994 and May 1996, Meyer et al. (1997) reported DST waste properties pertinent to gas retention and release behavior: density, yield stress, and viscosity. Meyer et al. (1997) list supernatant and non-convective densities based on data for five DSTs on the flammable tank watch list (241-SY-103, 241-AN-103, 241-AN-104, 214-AN-105, and 241-AW-101). These five salt cake tanks exhibit episodic gas releases that are typically less than 30 m³, although there have been episodes of releases as large as 100 m³ in 241-SY-101, the sixth tank on the list. Supernatant densities are in the range between

1,430kg/m³ and 1,600kg/m³, with an uncertainty of roughly $\pm 2\%$ about any one value. Non-convective layer densities are in the range 1,570kg/m³ and 1,730kg/m³, with an uncertainty of $\pm 6\%$ or so about any one value.

Meyer et al. (1997) also list non-convective layer yield strength (referred to as shear strength by Willingham [1994]) as a function of depth for the same five tanks. The non-convective layer is a viscoplastic material with a finite yield strength and shear rate dependency that can be measured by a ball rheometer. Yield strength is largest near the bottom; maximum yield stress is somewhere between 200 and 325 Pa, depending on the tank.

Another compilation of DST waste property data is given in Barton and Bingham (1999). Descriptive statistics were developed from this compilation, with the six salt cake DSTs differentiated from the other (sludge) DSTs. For the six salt cake DSTs, the mean and standard deviation of the convective layer density are 1.48 and 0.06 g/ml, respectively; mean and standard deviation of the non-convective layer density are 1.62 and 0.08 g/ml, respectively. For the remaining twenty-two DSTs, mean and standard deviation for the convective layer density are 1.13 and 0.12 g/ml, respectively. Mean and standard deviation for non-convective layer are 1.51 and 0.09 g/ml, respectively. Only fourteen DSTs were used for non-convective layer averaging because eight of the DSTs have only a trivial amount of settled solids. Waste yield strength is listed for many of the tanks, but in other instances a probability density function is used. This function is a truncated normal distribution with mean equal to 120 Pa, standard deviation equal to 30 Pa, minimum equal to 50 Pa, and maximum equal to 200 Pa. Tank-specific yield strengths listed range from **81** to 225 Pa.

To conclude, Table 3-6 provides a summary of DST waste property data. Table 3-6 shows values obtained from averaging over the salt cake DSTs and sludge DSTs. Both the Hu et al. (2000) database and the pedigreed database were considered and found to be in reasonable agreement. The differences between values for the salt cake DSTs and values for the other DSTs should be noted. Mean non-convective layer and supernatant densities in the salt cake DSTs are higher, and the difference between non-convective layer density and supernatant density (e.g., 1.63 minus 1.50 g/ml) is smaller than the corresponding difference for a sludge DST (e.g., 1.51 minus 1.13 g/ml). The table therefore illustrates an important difference between salt cake and sludge tanks: the sludge tanks have a higher neutral buoyancy void fraction.

Table 3-6. Double-Shell Tank Waste Properties. (2 sheets)

Property	Units	Source	Mean	Uncertainty
	g/ml	Six Salt Cake DSTs ²	1.60	Stand. Dev. = 0.07
		Five Salt Cake DSTs ¹	1.63	$\pm 6\%$
		Six Salt Cake DSTs ¹	1.62	Stand. Dev. = 0.08
Supernatant Density	g/ml	Fifteen Sludge DSTs ²	1.47	Stand. Dev. = 0.12
		Six Salt Cake DSTs ²	1.43	Stand. Dev. = 0.04
		Five Salt Cake DSTs ³	1.50	$\pm 2\%$
		Six Salt Cake DSTs ¹	1.48	Stand. Dev. = 0.06

Table 3-6. Double-Shell Tank Waste Properties. (2 sheets)

Property	Units	Source	Mean	Uncertainty
Shear Strength	Pa	Twenty-Two Sludge DSTs ¹	1.13	Stand. Dev. = 0.12
		Twenty-Two Sludge DSTs ²	1.19	Stand. Dev. = 0.12
		Five Salt Cake DSTs ³	263 (Max. Value)	±62
			120	Truncated Normal: Stand. Dev. = 30, Min. = 50, Max. = 200
Liquid Heat Capacity	J/kg-°C	Refer to Table 3-2 ⁴	3349	
Solid Heat Capacity	J/kg-°C	Refer to Table 3-2 ⁴	837	

¹Barton, W. B., and J. D. Bingham, 1999, *Gas Release Event Safety Analysis Tool Ped* ze Database for Hanford Tanks, HNF-SD-WM-TI-806, Rev. 2-A, Lockheed Martin Hanford Corporation, Richland, Washington.

²Hu, T. A., S. A. Barker, J. D. Bingham, and M. A. Kufahl, 2000, Steady State Flammable Gas *Release Rate* Calculation and **Lower Flammability Level** Evaluation for Hanford Tank Waste, RPP-5926, Rev. 0, CH2M HILL Hanford Group, Inc., Richland, Washington.

³Meyer, P. A., M. E. Brewster, S. A. Bryan, G. Chen, L. R. Pederson, C. W. Stewart, and G. Terrones, 1997, *Gas Retention and Release Behavior in Hanford Double-Shell Waste Tanks*, PNNL-11536, Rev. 1, Pacific Northwest National Laboratory, Richland, Washington.

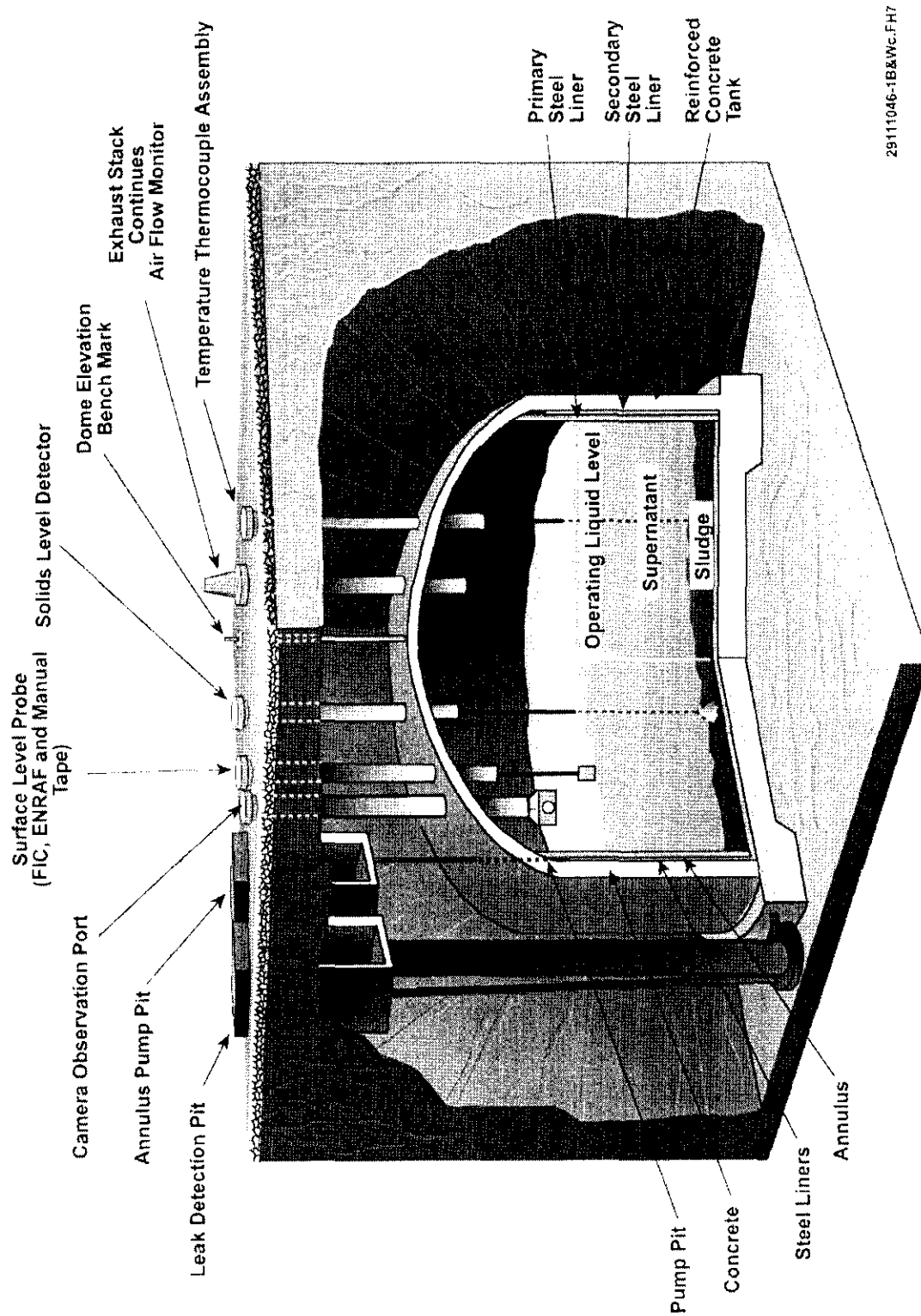
⁴Sathyanarayana, K., 1996, *Evaluation of Potential and Consequences of Steam Bump in High Heat Waste Tanks and Assessment and Validation of GOTH Computer Code*, WHC-SD-WM-CN-022, Rev. 0-B, Westinghouse Hanford Company, Richland, Washington.

DST = double-shell tank.

3.4 TANK CONFIGURATION DATA

SST and DST configurations are pictured here in Figures 3-7 and 3-8, respectively. Tank configuration data are important to consequences of the tank bump. These data include the headspace volume, headspace flowpaths, and decontamination factors for flowpaths from the headspace. For a given tank bump magnitude, the headspace volume obviously has a first-order effect on consequences by determining the peak overpressure. Headspace free volume is known by subtracting the waste volume, which is listed in Appendix A, from the total tank volume, which can be obtained from the Barton and Bingham (1999) database; the total tank volume as listed in the Barton and Bingham (1999) database includes the dome space and is not the designed waste capacity. This calculation gives the total free volume available in the headspace.

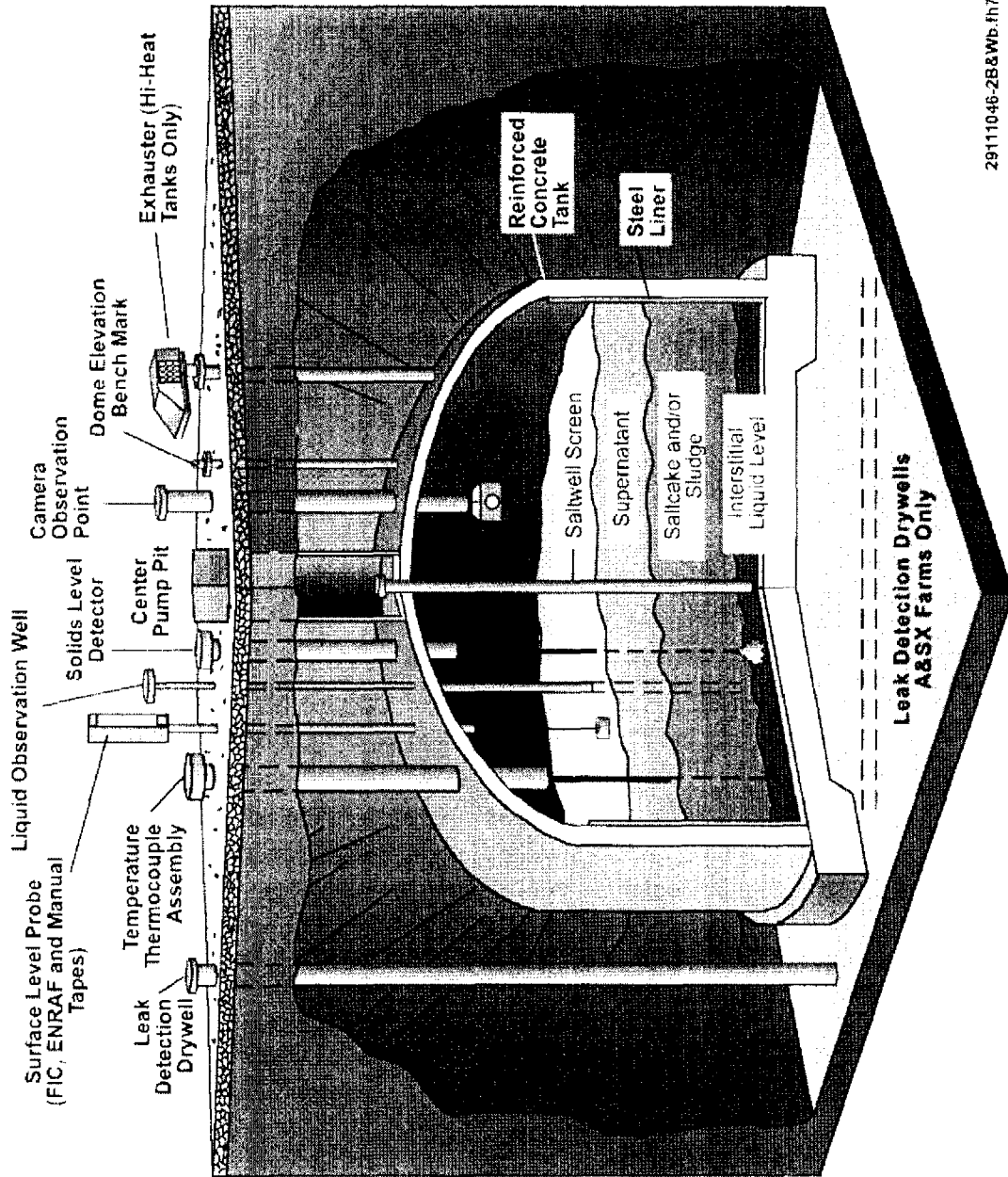
Figure 3-8. Double-Shell Tank Instrumentation Configuration.



29111046-1B&Wc.FH7

FIGURE D-2. DOUBLE-SHELL TANK INSTRUMENTATION CONFIGURATION

Figure 3-7. Single-Shell Tank Instrumentation Configuration



29111046-2B&WB.th7

FIGURE D-3. SINGLE-SHELL TANK INSTRUMENTATION CONFIGURATION

The size and nature of flowpaths from the tank headspace determine the final overpressure and magnitude of releases. These flowpaths are in the form of ventilation ducts, risers, cascade lines, pit cover, flanges, etc., as described in the rise configuration document (Alstad 1993).

Ventilation flowrate and duct diameter are listed in the Barton and Bingham (1999) database. Consequences depend on the flow resistance and decontamination factor provided by a riser high-efficiency particulate air (HEPA) filter. Releases are greatly mitigated if the HEPA filter remains intact. For the DST, the Barton and Bingham (1999) database lists 5 psig as the HEPA filter failure pressure and 99.96% as the efficiency.

Some tank-specific information for 241-AZ-101 and 214-AZ-102 are mentioned here because it will be used later. Units are presented in British or **SI** as obtained from the original reference, for clarity in tracing. Pit and riser information is obtained from drawings (H-2-68304, H-2-68305, H-2-68423, and H-Unknown-1), and from Barton and Bingham (1999).

Normal flowpaths between tank headspace and ambient are the filtered 8 in. diameter inlet and 20 in. diameter outlet. Unfiltered release paths from Barton and Bingham (1999) do not apply due to pit riser configuration details, as follows.

Each of the four sluice pits and the center pump pit contain a 42 in. riser for sluicing and a drain riser of 3 in. diameter in sluice pits and 4 in. diameter in the pump pit. The 42 in. risers terminate close to the tank dome and communicate with the headspace, while the drain risers extend to within 5 ft of the tank bottom and are immersed in waste. The 42 in. risers have concrete and steel shield plugs that are 5 ft thick and weigh 8,500 lb or 3,864 kg.

Steel flanges on these 42 in. risers and shield plugs have 16 bolt holes of 7/8 in. diameter for sealing, but the sealing status of these risers is not known. If unsecured, a pressure difference of about $(3,864 \text{ kg}) (9.81 \text{ m/s}^2) / (0.89 \text{ m}^2) = 42.5 \text{ kPa}$ from tank to ambient will cause the plugs to lift.

Sluice pits measure about 6.5 ft wide x 8 ft long x 7 ft deep with pit covers of 2.0 ft thickness in place. So open volume in sluice pits is about 10 m^3 and the pressure to lift a pit cover is about 13.8 kPa (using a concrete density of $2,300 \text{ kg/m}^3$). Pump pits have dimensions of about 8.5 ft wide x 12 ft long x 7 ft deep with pit covers of 2.5 ft in place, so open volume is about 20 m^3 and cover lift pressure is about 17 kPa.

Following the Barton and Bingham (1999) assumption of 1/64 in. gap around unsealed risers, the leakage area for a single such riser is $\pi (42 \times 0.0254) (0.0254 / 64) = 1.33 \times 10^{-3} \text{ m}^2$, which is the equivalent of a 1.6 in. diameter hole. The reference pit leakage gap is 1/4 in., which applied to a sluice pit (perimeter = 29 ft) yields $87 \text{ in}^2 = 0.056 \text{ m}^2$ and to a pump pit (perimeter = 41 ft) yields $123 \text{ in}^2 = 0.079 \text{ m}^2$.

4.0 TANK BUMP PHYSICAL MODELS AND CRITERIA

Tank bumps are related to rapid steam generation in the waste liquid and the release of energy when the steam, in the form of a large bubble (or numerous bubbles), passes through the waste surface. These eruptions are not sufficient to threaten the mechanical integrity of the tank, but may lead to undesirable discharge of radioactive contaminants.

It is difficult to imagine a tank bump event in the absence of a deep layer of supernatant at a temperature approaching 100°C overlying a heat-producing normally non-convective waste layer. This concept will be developed and proven here in this section. Two physical scenarios for tank bump are deemed plausible and are investigated here:

In Section 4.1, we will demonstrate that tanks lacking a fairly deep, nearly saturated supernatant layer cannot have a significant tank bump. The scenario developed here is for gas injection from a (normally) non-convective lower waste layer into an overlying supernatant layer, Figure 4-1. The gas injection may be natural release of radiolytically and thermally generated non-condensable gases, such as hydrogen, or it may be gas injection due to some operation in the tank. A bump criterion for this scenario is the combination of significant gas injection, deep supernatant layer, and nearly saturated supernatant layer.

In Section 4.2, we will demonstrate that a buoyant displacement event (Figure 4-2) is a mechanism that can result in a significant steam bump providing that the non-convective layer is capable of self-heating to nearly its boiling point at the local static pressure and providing that non-condensable gas generation can bring the non-convective layer to a buoyant state.

Two additional physical scenarios for tank bump postulated over the years are deemed not plausible based on analysis presented in Appendix B:

In Appendix B.1 we investigate a hypothetical scenario for steam bump due to interstitial liquid super heating in stationary sludge, Figure B-1. The purpose of this investigation is to prove that significant sudden release of vapor cannot occur from a stationary sludge layer alone.

In Appendix B.2 we examine steam bubble growth due to local convection in an otherwise non-convective layer, Figure B-3. This scenario corresponds to concerns raised at one time for Tank 241-C-106, when an increase in waste temperature was observed following a process test. Local convection, or fumaroles as the phenomenon was called at the time, are shown not to be a source for a significant steam bump.

Figure 4-1. Steam Bump By Gas Injection

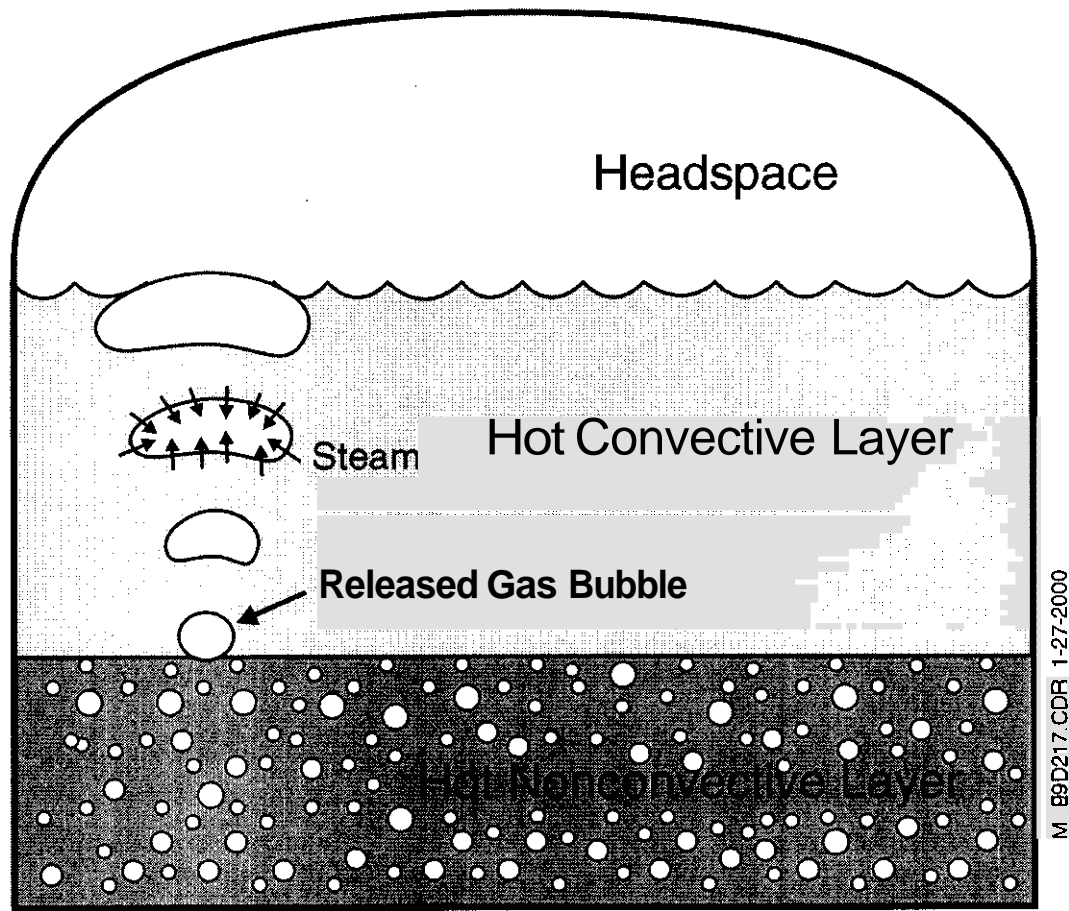
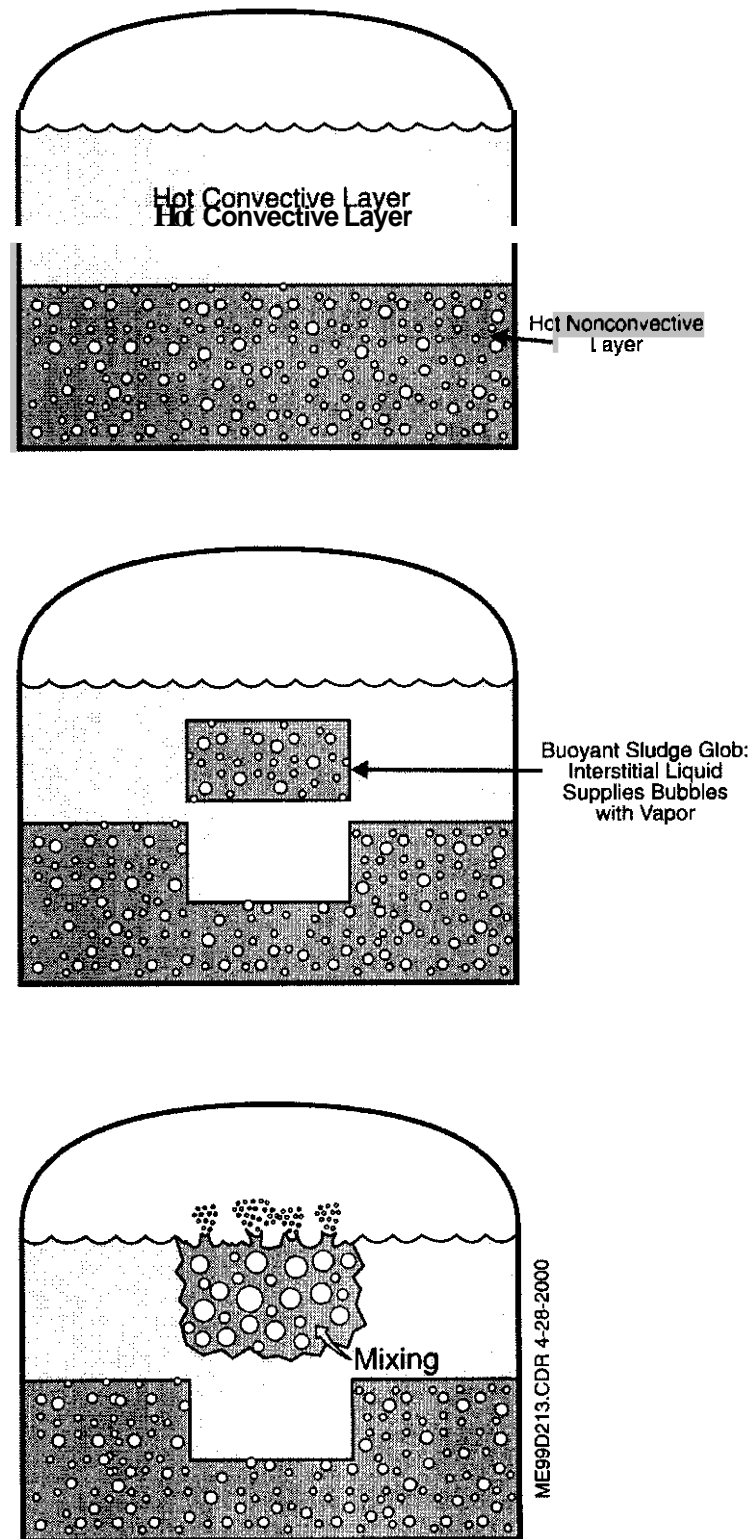


Figure 4-2. Steam Bump During a Buoyant Displacement.



4.1 STEAM BUMPS BY GAS INJECTION

Consider the growth of a gas cavity of volume $V_b(0)$ that suddenly appears at the bottom of a supernatant layer of depth H and uniform temperature T_ℓ , Figure 4-1. The cavity is filled with the vapor of the surrounding water and by the non-condensable gas generated in the underlying non-convective layer. It is well known that natural convection currents within the water layer are more than sufficient to maintain the liquid at a nearly isothermal condition. The magnitude of the cavity expansion during its ascent through the liquid layer is a measure of the severity of the tank bump event and this is the problem treated below.

In keeping with our objectives, we consider the transient growth of a spherical cavity (bubble), initially containing the gas and water vapor (steam) it gradually accumulated before it was released at the bottom of the supernatant layer. The initial partial pressure of steam in the bubble, $P_{eq}(T_\ell)$, is specified by demanding thermodynamic equilibrium between steam and liquid at the bubble surface. As the bubble rises into regions of lower hydrostatic pressure, due to the presence of non-condensable gas (hereafter referred to as "gas"), the bubble expands and the steam partial pressure in the interior of the bubble falls below the equilibrium steam partial pressure at the bubble surface. This results in a concentration gradient within the bubble and steam transport from the surface of the bubble to its interior. In turn, water must evaporate and pass from the supernatant and into the bubble. The evaporation process tends to cool the liquid so that its temperature decreases from T_ℓ in the immediate vicinity of the bubble surface and a thermal boundary layer develops on the liquid side of the bubble. Thus the growth of the bubble is controlled by heat and mass transport; it is limited by the rate at which latent heat can be supplied by liquid convection at the bubble surface and by the rate at which steam can diffuse (convect) into the bubble from its surface. The bubble growth problem is obviously complicated.

To simplify matters and still retain a conservative approach, it is assumed that bubble growth is limited by steam transport within the bubble. The resistance to growth imposed by the thermal boundary layer on the liquid side is ignored. From this assumption it follows that the steam partial pressure at the bubble surface equals $P_{eq}(T_\ell)$ throughout its motion. Thus, the rate at which steam enters the bubble is given by a mass transport law of the form

$$\frac{d m_v}{dt} = 4 \pi r^2 h_m \rho_{mix} \ln \left[1 + \frac{\rho_{eq}(T_\ell) - \rho_v}{\rho_{mix} - \rho_{eq}(T_\ell)} \right] \quad (4-1)$$

where m_v is the instantaneous mass of steam within the bubble at time t , r is the bubble radius, ρ_v is the bulk steam density within the bubble, ρ_{mix} is the bulk gas/vapor mixture density within the bubble, $\rho_{eq}(T_\ell)$ is the equilibrium density of steam at the inside surface of the bubble evaluated at the supernatant temperature T_ℓ , and h_m is the coefficient for steam transport from the bubble surface into its interior.

A maximum rate of bubble-gas side mass transfer can be predicted by postulating a model in which the bubble interior ~~is~~ well mixed and the entire resistance to mass transfer restricted to a thin gas/steam boundary layer at the bubble surface. Such a model was analyzed by

Ruckenstein et al. (1971). A Hill's vortex bubble flow field was linearized near the bubble surface and the final expression for h_m was found to be

$$h_m = \left(\frac{2 U_b D}{\pi r} \right)^{1/2} \quad (4-2)$$

where U_b is the bubble rise velocity relative to the surrounding liquid and D is the binary diffusion coefficient for the bubble mixture (steam + gas).

The mass of vapor in the bubble in equation (4-1) can be expressed as the product of the bulk (bubble-interior) steam density and bubble volume V_b

$$m_v = \rho_v V_b \quad (4-3)$$

Assuming that steam behaves as an ideal gas, we may write

$$\rho_{eq}(T_\ell) = \frac{P_{eq}(T_\ell)}{R T_\ell} \quad ; \quad \rho_{mix} = \frac{P_{mix}}{R T_\ell} \quad (4-4)$$

$$\rho_v = \frac{P_v}{R T_\ell} \quad (4-5)$$

where R is the ideal gas constant for steam, P_{mix} is the total bulk pressure within the bubble, and P_v is the steam partial pressure in the well-mixed bubble interior. The second relation in equation (4-4) is based on the justifiable assumption that the steam contribution to the value of the bubble mixture molecular weight far exceeds that due to the inert gas. The bubble is assumed to rise through the supernatant as part of an ensemble (cluster) of bubbles. A constant "terminal" speed of the cluster is assumed and denoted by the symbol U . Thus time may be replaced by vertical distance traversed by the bubble as follows:

$$t = \frac{z}{U} \quad (4-6)$$

where z is measured from the bottom of the supernatant pool. The constant U assumption will be relaxed later on when a more complete steam bump model is constructed. Combining equations (4-1) to (4-6) gives

$$\frac{d(P_v V_b)}{dz} = \left(\frac{24 D U_b}{U^2} \cdot V_b \right)^{1/2} P_{mix} \ln \left[1 + \frac{P_{eq}(T_\ell) - P_v}{P_{mix} - P_{eq}(T_\ell)} \right] \quad (4-7)$$

To close the problem, we need a relationship between P_v and the bubble volume V_b . This relationship is obtained by the following liquid (supernatant) statics analysis. The gas partial pressure P , plus the steam pressure P_v within the bubble must equal the local hydrostatic pressure imposed by the supernatant; that is,

$$P_{\text{mix}} = P_v + P_g = P_{\text{hs}} + \rho_\ell g (H - z) \quad (4-8)$$

where P_{hs} is the pressure in the tank headspace, g is the gravitational constant, and ρ_ℓ and H are, respectively, the density and depth of the supernatant layer. The mass of inert gas in the bubble remains constant so that by virtue of the ideal gas law

$$P_g(0) V_b(0) = P_g V_b \quad (4-9)$$

where $P_g(0)$ and $V_b(0)$ denote the values of P , and V_b at the bottom of the supernatant layer (i.e., at $z = 0$). Evaluating equation (4-8) at $z = 0$ and making the reasonable assumption that the bubble emerges from the non-convective layer with an equilibrium concentration of steam throughout its volume, so that,

$$P_v(0) = P_{\text{eq}}(T_\ell) \quad (4-10)$$

yields

$$P_{\text{eq}}(T_\ell) + P_g(0) = P_{\text{hs}} + \rho_\ell g H \quad (4-11)$$

Eliminating P , between equations (4-8) and (4-9) and inserting $P_g(0)$ from equation (4-11) into the result gives

$$\frac{V_b}{V_b(0)} = \frac{P_{\text{hs}} + \rho_\ell g H - P_{\text{eq}}(T_\ell)}{P_{\text{hs}} + \rho_\ell g (H - z) - P_v} \quad (4-12)$$

Equations (4-7) and (4-12) are sufficient to solve for the unknowns V_b and P_v as a function of elevation z . Unfortunately, the system cannot be integrated in closed form; a numerical solution of equation (4-7) is required. Note, however, that in the limit of no mass transfer resistance to bubble growth, equation (4-12) alone can be used to calculate the bubble volume as a function of vertical distance. This is accomplished by replacing P_v on the right-hand side of equation (4-12) with $P_{\text{eq}}(T_\ell)$. Note also that P_{hs} in equation (4-12) is not constant during a steam bump but increases in response to the rising and expanding bubble cluster within the supernatant. For the purpose of illustrating the conditions required for a strong steam bump due to gas injection, it is convenient to first ignore the coupling between the bubble cluster and the headspace atmosphere and assume that P_{hs} remains at its near-atmospheric value.

The various property values used in the illustrative calculations are: $P_{\text{hs}} = 0.1013 \text{ MPa}$, $\rho_\ell = 1,100 \text{ kg m}^{-3}$, $D = 9.2 \times 10^{-5} \text{ m}^2 \text{ s}^{-1}$, and $U = 1.0 \text{ m s}^{-1}$. The diffusion coefficient D for mass transfer within the bubble was estimated for a hydrogen gas/steam mixture at 373 K and

0.14 MPa pressure by the method outlined in Reid and Sherwood (1966) for polar/non-polar gas pairs. The maximum possible bubble velocity relative to the cluster liquid is the terminal rise velocity of an isolated bubble in a quiescent liquid. The terminal rise velocity of an isolated bubble is typically about $U_b = 0.2 \text{ ms}^{-1}$. The rise velocity of a collection of bubbles can be estimated from the formula

$$U = 0.68 (g D_{\text{eff}})^{1/2} \quad (4-13)$$

where D_{eff} is the diameter of a large, fictitious bubble having the same volume as the total volume of the bubble ensemble (Moody 1986). The formula implies a bubble ensemble rise velocity of at least $U = 1.0 \text{ m s}^{-1}$ for gas injections capable of producing a steam bump. Finally, the equilibrium vapor pressure of steam $P_{\text{eq}}(T_\ell)$ was estimated as a function of supernatant temperature T_ℓ by using steam table values.

Figures 4-3 and 4-4 illustrate the results of the numerical calculations. Computational details are shown in Appendix D. In both figures, the bubble volume $V_b(H)$ at the end of the bubble's ascent through the supernatant layer divided by its initial volume $V_b(0)$ at the bottom of the layer is plotted against the depth H of the layer. Figure 4-3 shows the effect of supernatant temperature on bubble expansion while Figure 4-4 shows the effect of initial bubble size (diameter d_0) on bubble expansion. Mass transfer resistance becomes important as the supernatant temperature T_ℓ approaches its boiling point (100 °C). Clearly, the bubble expansion ratio is sensitive to the initial bubble size. Observations of retained gas in simulants and actual wastes indicate that the average bubble diameter is approximately 1.0 mm and that the upper end of the size range of retained round gas bubbles in waste is about 5.0 mm (Gauglitz et al. 1996). The larger bubbles should serve as the sites from which the bubbles grow during a spontaneous gas release event or waste disturbing operation as the free energy required to initiate bubble growth decreases by an amount proportional to the volume of the embryo bubble. It follows that conservative estimates of the bubble expansion ratio may be based on the choice $d_0 = 1.0 \text{ mm}$. It should be mentioned that during a spontaneous gas release event there will be a significant reduction in the bubble size (and in total release void volume) due to vapor condensation as the bubbles are transported from the non-convective layer to the relatively cooler supernatant.

Regardless of the dimensions of the bubbles, it is clear from Figures 4-3 and 4-4 that a significant tank bump event by gas injection requires a deep supernatant layer whose temperature approaches the boiling point.

In the preceding example, the ambient temperature was assumed to be a standard atmosphere. **Also**, the effect of salt in solution to increase the boiling point was neglected. These simplifications do not change conclusions when values pertinent to a given tank and ambient pressure are used.

Figure 4-3. Bubble Expansion Ratio Versus Depth of Supernatant Pool;
Pool Temperature T_λ as a Parameter. Dashed curves
refer to zero mass transfer resistance.

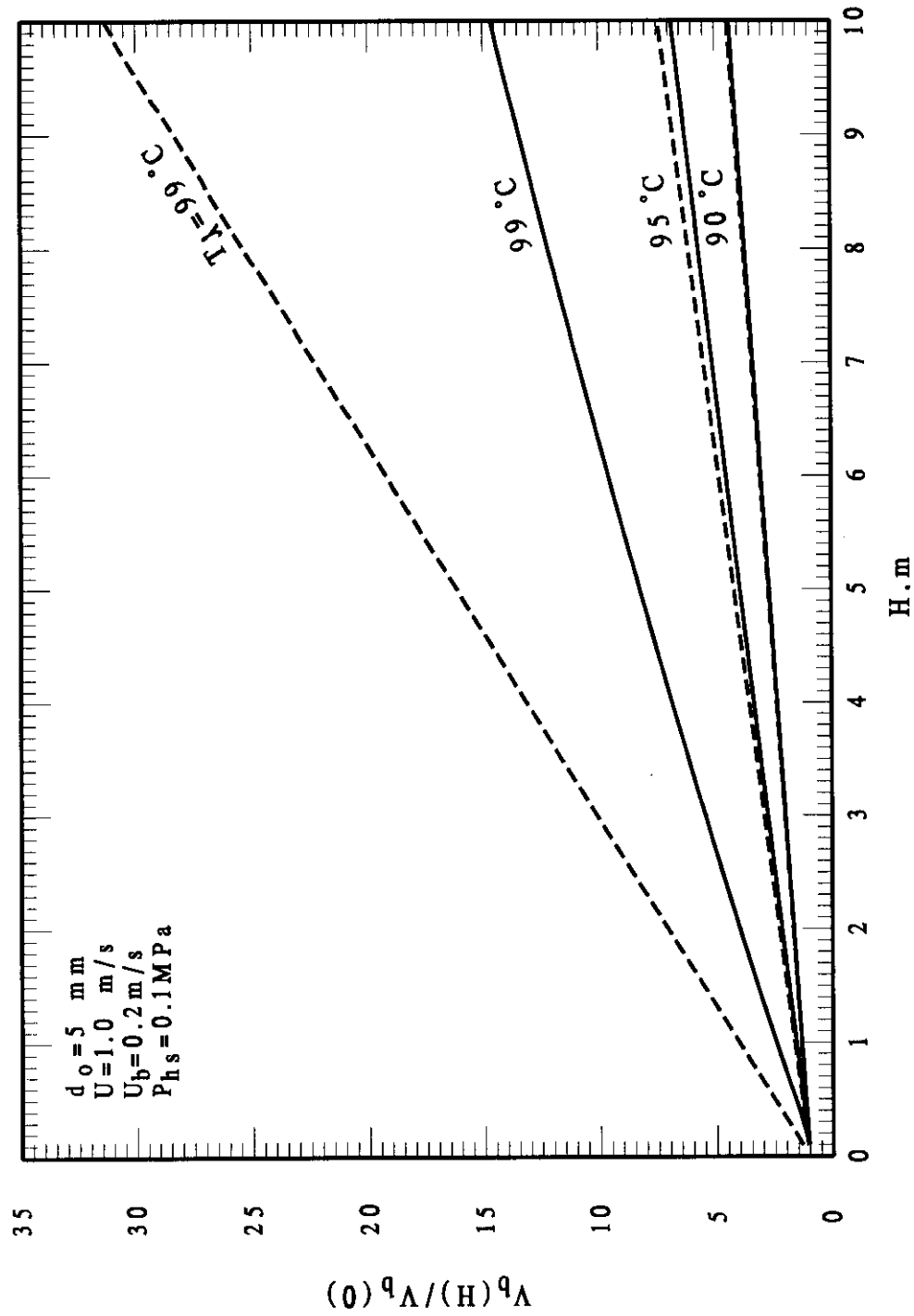
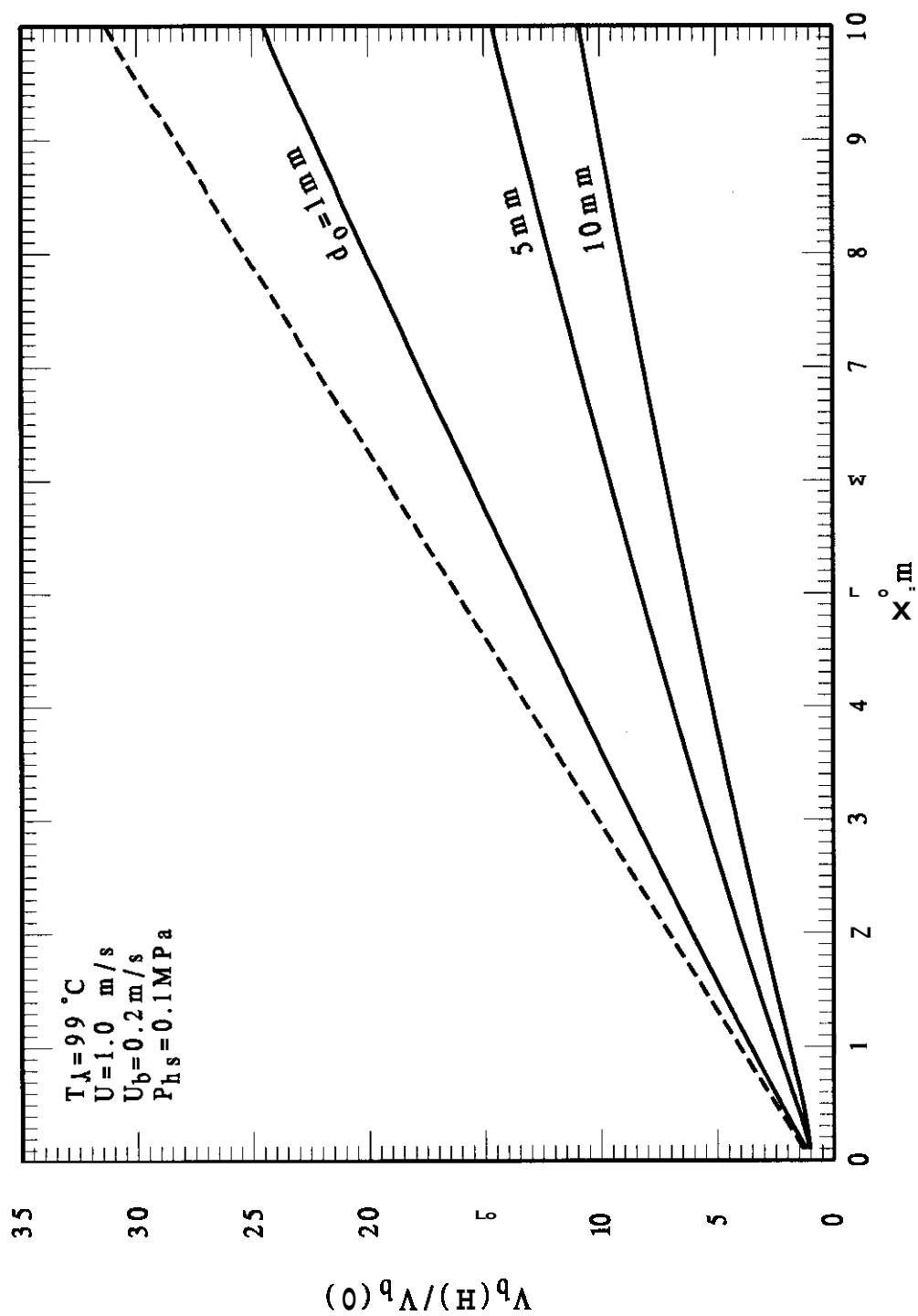


Figure 4-4. Bubble Expansion Ratio Versus Depth of Supernatant Pool;
Initial Bubble Diameter as a Parameter. Dashed curve
refers to zero mass transfer resistance.



While the volume expansion ratio $V_b(H) / V_b(0)$ results given in Figures 4-3 and 4-4 were obtained for a single bubble in a bubble ensemble, the results are also applicable for the bubble ensemble itself providing that bubble coalescence is ignored and an effective mean bubble size is specified. For the bubble ensemble case, $V_b(0)$ and $V_b(H)$ in the volume expansion ratio refer respectively to the total volume of the bubble ensemble at the bottom of the supernatant and the total volume of the bubble ensemble upon its arrival at the waste surface. Therefore, to calculate the absolute bubble volume produced as a result of a gas injection and bubble ascent, we must estimate $V_b(0)$. The application of the bubble growth theory presented in the foregoing to the behavior of a cluster of bubbles is postponed until Section 5.0 where a tank bump consequence model is described and exercised.

An underlying assumption in the calculation is that the supernatant temperature is uniform; this is typically taken as obvious as mentioned above and in the discussion of Section 3.1. The point is proven here to illustrate how rigid the requirement is for the entire supernatant layer to be nearly saturated. For turbulent natural convection in a liquid layer with a free upper surface, the relationship between heat flux and core to surface temperature difference is (Katsaros et al. 1977):

$$Nu = 0.156 Ra^{0.33} \quad (4-14)$$

where $Nu = h L / k$, and

$$Ra = g \beta \Delta T L^3 / \alpha \nu.$$

Heat flux is given by the product $h AT$, and is equal to the amount of tank power Q_u lost upward divided by area A ,

$$\frac{Q_u}{A} = k \left(\frac{g \beta}{\alpha \nu} \right)^{\frac{1}{3}} (\Delta T)^{4/3} \quad (4-15)$$

For a representative (and high) power of 10 kW, and typical values as follows, $A = 411 \text{ m}^2$, $k = 0.68 \text{ W/m/K}$, $g = 9.81 \text{ m/s}^2$, $\beta = 6 \times 10^{-4} \text{ K}^{-1}$, $\alpha = 3 \times 10^{-5} \text{ m}^2/\text{s}$, $\nu = 3 \times 10^{-5} \text{ m}^2/\text{s}$, the temperature difference is only $\Delta T = 0.29 \text{ K}$. The total temperature difference between the bottom of the layer and the top of the layer would double this value, or about 0.6 K. For higher upward heat flux, typically required for the supernatant layer to be nearly saturated, the temperature difference would be even lower.

4.2 STEAM BUMP BY BUOYANT DISPLACEMENT

A buoyant displacement occurs when a gas (vapor)-generating and gas (vapor)-trapping non-convective layer is covered by a relatively thick layer of initially less dense supernatant. Eventually, gas (vapor) generation in the lower layer leads to a density inversion and the buoyant displacement event. The temperature T_{nc} in the non-convective layer usually exceeds the

temperature T_ℓ in the overlying supernatant. Using the physical properties of water it is possible for the non-convective layer to reach a temperature of 120 °C at a depth 10m below the free surface of the waste. Owing to natural convection the supernatant temperature cannot exceed its boiling point of 100 °C at atmospheric pressure. During a buoyant displacement in a "hot tank", the bubbles trapped in the rising, hot non-convective layer material grow by converting the hot interstitial liquid (>100 °C) into steam while a bubble injected into the supernatant grows by accumulating vapor from the relatively low temperature supernatant (<100 °C). The model derived in the previous sub-section can be used to illustrate the effect of the temperature of the host liquid (supernatant or non-convective buoyant material) on the bubble volume expansion ratio $V_b(H) / V_b(0)$. The results are shown in Figure 4-5 where we see that the severity of a tank bump event increases dramatically once the non-convective layer temperature exceeds the maximum supernatant temperature $T_{nc} = 100$ °C.

The results in Figure 4-5 pertain only to representative cluster-bubble behavior beneath a constant pressure headspace. It will be seen later on that owing to the pressurization of the tank headspace and mixing between the buoyant parcel of initially non-convective material and the surrounding supernatant, the bubble volume expansion ratios achieved within the buoyant parcel during a tank bump are much smaller than those presented in Figure 4-5.

Most of the Hanford site tanks have little potential for a tank bump because either their heat loads are too low to heat the waste to its boiling point or the time required to self-heat to the boiling point is very long compared with the time required to repair the equipment failure. Possible exceptions are Tanks 241-AZ-101, 241-AZ-102, and 241-AY-102, which have rather large non-convective layer heat generation rates. The question remains as to whether these tanks will exhibit a buoyant displacement after their non-convective layer is heated to the boiling temperature.

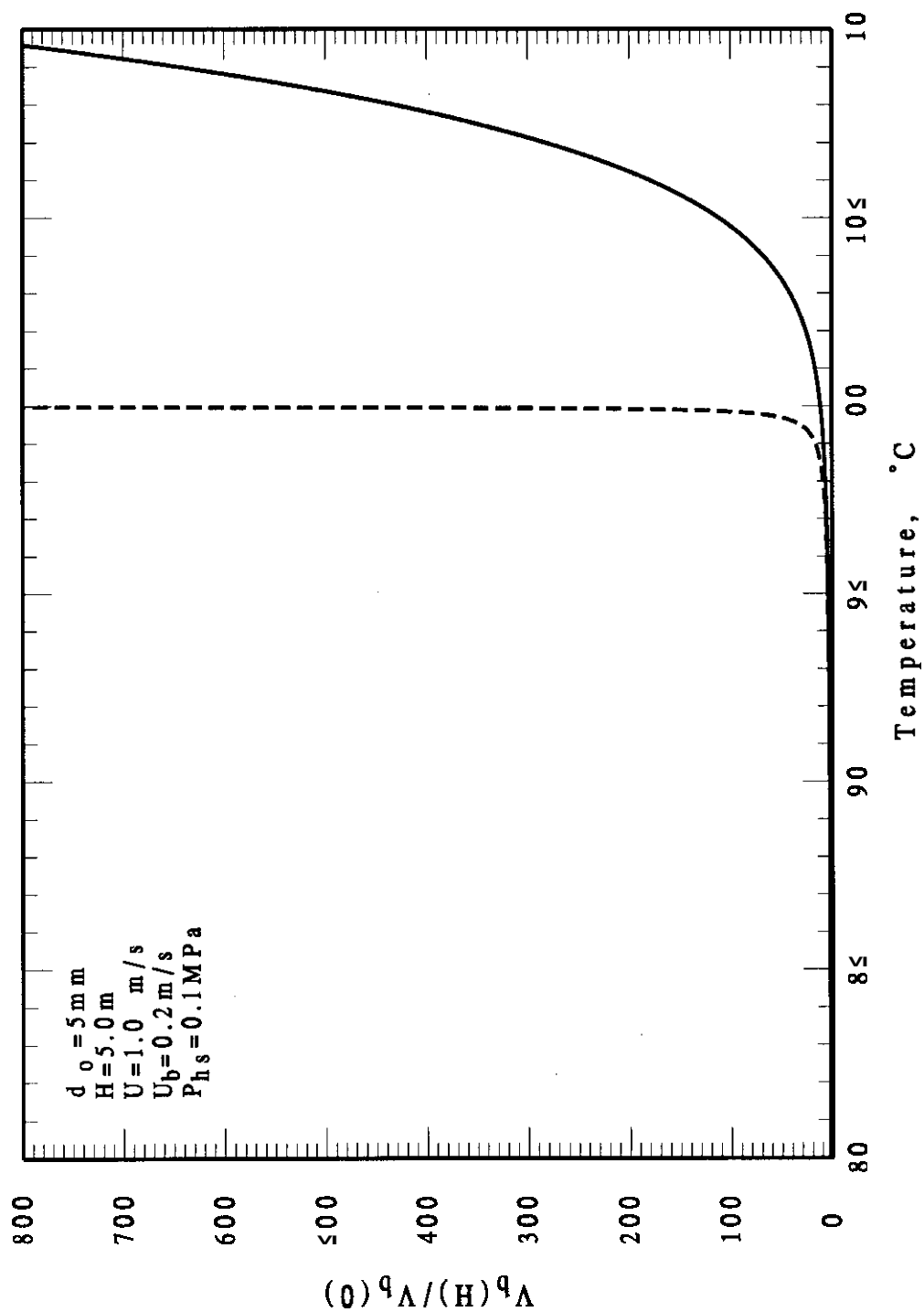
Meyer and Wells (2000) derived models that give criteria that must be satisfied in order for buoyant displacements to occur. Briefly, they developed an equation for the vertical void fraction profile within the non-convective layer based on a balance between internal gas generation and the rate at which gas is released at the top of the layer. The integrated average of this void fraction profile is compared with the neutral buoyant void fraction to determine whether a buoyant displacement may occur at some point during the transient (quasi-steady) void growth period. Two limiting case solutions were found for the void fraction profile and the corresponding criteria for a buoyant displacement are

$$\frac{C_1 h_{NCL}^2}{\rho_{NCL} - \rho_{CL}} \left(\frac{G T}{P_{NCL}} \right)^{1/3} > 1 \quad (4-16)$$

for a uniform bubble nucleation rate and a zero initial void fraction, and

$$\frac{C_2}{\rho_{NCL} - \rho_{CL}} \left(\frac{\rho_{NCL}^2 h_{NCL}^2 G T}{P_{NCL}} \right)^{1/3} > 1 \quad (4-17)$$

Figure 4-5. Bubble Expansion Ratio **Versus** Convective Layer Temperature ($<100^{\circ}\text{C}$) or Buoyant Parcel Temperature T_{hc} During Buoyant Displacement.
Dashed curve refers to zero mass transfer resistance.



for an assumed bubble flux at the lower boundary and zero internal nucleation rate. In equations (4-16) and (4-17), ρ_{NCL} and ρ_{CL} are the density of the non-convective layer and the density of the convective layer (kg m^{-3}), respectively, G is the molar gas generation rate per unit volume of non-convective layer ($\text{g-mole m}^{-3} \text{ day}^{-1}$), T is the average temperature of the non-convective layer (K), P_{NCL} is the average pressure of the non-convective layer (atm), and h_{NCL} is the depth of the non-convective layer (m). The constants C_1 and C_2 , each with dimensional units, are empirically adjusted so that all the double-shell tanks with observed buoyant displacements obey the criteria given by equations (4-16) and (4-17). Equation (4-17) provides much more conservative results than equation (4-16). However, equation (4-16) yields a better representation of double-shell tank buoyant displacement behavior (Stewart 2000) and is chosen here for application to Tanks 241-AZ-101, 241-AZ-102, and 241-AY-102. The value of the constant in equation (4-16) based on the most recent tank data is $C_1 = 18.5$ (Stewart 2000).

The gas generation rate originally used in equation (4-16) is non-condensable gas generation by radiolysis and thermal decomposition. It is of interest to evaluate equation (4-16) when G is based on steam generation only, and then, when G is based on non-condensable gas generation only. In both evaluations, the non-convective layer is presumed to be at its boiling temperature at the local static pressure. The steam production rate G_v may be approximated by

$$G_v = \frac{\dot{Q}_{\text{NCL}}'''}{h_{\text{fv}} M_v} \quad (4-18)$$

where \dot{Q}_{NCL}''' is the heat generation rate per unit volume of non-convective layer, h_{fv} is the latent heat of evaporation of water, and M_v is the molecular weight of water. The non-condensable gas generation rate at the boiling point T_{bp} (evaluated at the mid-plane of the non-convective layer) is obtained by using the Arrhenius equation to extrapolate the known gas generation rate at the prevailing non-convective layer temperature T_o to its value at T_{bp} :

$$G_g(T_{\text{bp}}) = G_g(T_o) \exp \quad (4-19)$$

where the activation temperature $T_{\text{act}} (= E / R)$ is 1.074×10^4 (Hu 1999).

Table 4-1 lists the predicted values of G_v and G_g for Tanks 241-AZ-101, 241-AZ-102, and 241-AY-102. It is obvious from the table that the steam production rate is much larger than the non-condensable gas generation rate. While the boiling temperature may be increased by a few degrees due to dissolved salt, this has only a minor effect.

Tank, 241-	Prevailing Temp. T_o (K)	Boiling Temp. T_{bp} (K)	\dot{Q}_{wcl}''' (W/m³)	G_g (T_o) $\left(\frac{\text{g-mole}}{\text{m}^3 \text{ day}}\right)$	G_g (T_{bp}) $\left(\frac{\text{g-mole}}{\text{m}^3 \text{ day}}\right)$	G_v $\left(\frac{\text{g-mole}}{\text{m}^3 \text{ day}}\right)$
AZ-101	345	392	260	6.12 x 10 ⁻³	0.26	567
Az-102	355	390	99	1.26 x 10 ⁻²	0.19	216
AY-102	350	384	31	1.80 x 10 ⁻²	0.27	68

The results of the buoyant displacement criterion calculations from equation (4-16) are listed in Table 4-2.

Table 4-2. Buoyant Displacement Model (equation (4-16))
Predictions for the High-Power Double-Shell Tanks.

Tank	ρ_{NCL} (kg m⁻³)	ρ_{CL} (kg m⁻³)	h_{NCL} (m)	P_{NCL} (atm)	LHS* Equation (4-16): G = G_v	LHS* Equation (4-16): G = G_g
241-AZ-101	1,690	1,190	0.43	1.91	0.33	0.026
241-AZ-102	1,490	1,100	0.96	1.79	1.60	0.15
241-AY-102	1,480	1,080	1.72	1.50	3.55	0.56

An examination of the last column of Table 4-2 indicates that even in the presence of steam generation 241-AZ-101 fails to satisfy the buoyant displacement criterion, owing to its shallow non-convective layer. It is recognized that the Meyer and Wells (2000) criterion is valid at non-convective layer boiling conditions only if the gas retention and gas migration properties of the non-convective layer remain the same during boiling of the layer. The criterion is probably valid during the period when the layer is heated from its initial, steady-state temperature to its boiling temperature and non-condensable gas generation is the dominant mode of void production. The last two columns of Table 4-2 show that buoyant displacements in the subject tanks can only occur by steam generation. Non-condensable gas generation alone cannot bring the non-convective layer to a buoyant condition. However, steam condensation brought on by mixing of the supernatant with the buoyant materials (see below) will prevent the buoyant displacement from developing into a steam bump.

A postulated buoyant displacement in Tanks 241-AZ-101, 241-AZ-102, or 241-AY-102 implies a weak (low yield strength) non-convective layer. In these tanks, the density difference between the non-convective layer and the overlying supernatant is large owing to the absence of

significant quantities of dissolved salt. Consequently, the neutral buoyancy void fraction is high (~ 0.3). The experimental evidence (Gaughlitz et al. 1996) suggests that if the waste has a high yield strength, the gas bubbles will connect and form a continuous path at void fractions below the neutral buoyancy void fraction. If the waste in Tanks 241-AZ-101, 241-AZ-102, or 241-AY-102 is stiff, these tanks do not pose a buoyant-displacement-steam bump concern. Thus, a prerequisite for a steam bump, due to a non-condensable gas buoyant displacement gas release event, is a low non-convective-layer yield strength of the order of the known yield strengths of the non-convective layers in the six DSTs that exhibit buoyant displacement, say $\tau_y \approx 100\text{Pa}$. The available buoyant energy is more than sufficient to overcome the 100Pa yield strength and rapidly transform the non-convective material in the rising parcel into a Newtonian fluid (Meyer et al. 1997). This transformation is immediately followed by the mixing of the buoyant parcel material with the surrounding sub-cooled supernatant.

Intense mixing of the structurally weak, steam-void containing buoyant parcel with the surrounding supernatant will begin just as the parcel rises from the non-convective layer (*see* Appendix C). Mixing is caused by a vertical buoyancy-dominated, turbulent diffusion mechanism (Epstein and Burelbach 2000a). The density difference between the buoyant parcel and the surrounding supernatant, combined with the very low initial momentum of the buoyant release, causes the inward flow of supernatant so that an unstable density gradient persists above the release area. Consequently, a density-gradient driven vertical mixing zone is quickly established between the rising parcel of previously non-convective material and the overlying supernatant. It is pertinent to note here that the top 10 to 50 cm of the parcel is sub-cooled and has a low void fraction. This parcel “cover” is non-buoyant and stiff with respect to the convective layer. However, it is reasonable to believe that the cover will move some distance to the side to allow the underlying, buoyant, and flowing portion of the parcel to rise into the supernatant. Thus, vertical mixing between the steam-bearing material and supernatant will still occur, although over an area that is smaller than the horizontal extent of the parcel.

The temperature at the top of the mixing layer T_{mix} as a function of the supernatant temperature T_{CL} and the temperature T_{bp} of the non-convective layer may be determined from Epstein and Burelbach's (2000b) formula for mixing above a circular source of buoyancy. For the miscible liquid-liquid (**supernatant-non-convective** layer) system of interest here, their formula takes the form

$$\frac{T_{\text{CL}} - T_{\text{mix}}}{T_{\text{NCL}} - T_{\text{CL}}} = 2.8 \left[\frac{v_0^2 \left(\frac{\rho_{\text{CL}}}{\rho'_{\text{NCL}}} \right)^2}{g \left(\frac{\rho_{\text{CL}}}{\rho'_{\text{NCL}}} - 1 \right) R_0} \right]^{1/3} \quad (4-20)$$

where ρ'_{NCL} is the two-phase density of the void-containing non-convective layer ($\rho_{\text{CL}} > \rho'_{\text{NCL}}$), R_0 is the effective horizontal extent of the mixing zone, and v_0 is the velocity (initial) of the buoyant parcel as it rises from and passes by the “surface” of the non-convective layer. Equation (4-20) is based on theoretical analysis and experimental data obtained specifically to address

fluid mixing in Hanford waste tanks (Epstein and Burelbach 1998), and it is currently applied in the flammable gas safety basis (Slezak et al. 1998).

The rise velocity v_0 of the buoyant parcel is proportional to the density difference $\rho_{CL} - \rho'_{NCL}$. The parcel cannot rise from the non-convective layer faster than the supernatant can flow into the region (cavity) vacated by the departing buoyant parcel. Thus, the velocity v_0 in equation (4-20) is less than or equal to the so-called exchange flow velocity v_0 across an opening of radius R_0 ; namely (see Brown [1962] or Epstein [1988]),

$$v_0 = 0.1 \left[R_0 g \left(\frac{\rho_{CL}}{\rho'_{NCL}} - 1 \right) \right]^{1/2} \quad (4-21)$$

Eliminating v_0 between equations (4-20) and (4-21) and assuming $\rho_{CL} > \rho'_{NCL}$ in the numerator of equation (4-20), gives the following simple result for the temperature of the mixing zone above the buoyant release area:

$$T_{mix} = T_{CL} + 0.6 (T_{NCL} - T_{CL}) \quad (4-22)$$

Inserting the typical values $T_{NCL} = 118^\circ\text{C}$ and $T_{CL} = 100^\circ\text{C}$ for the high self-heat tanks, gives $T_{mix} = 111^\circ\text{C}$ or $T_{NCL} - T_{mix} = 7^\circ\text{C}$. Such a large and sudden drop in temperature will collapse the steam voids within the initially buoyant parcel. The void collapse results in the withdrawal of the released material's buoyancy and the material settles back into the non-convective layer.

As the parcel slumps and spreads out over the top of the non-convective layer, its residual energy relative to the surrounding supernatant is transported upward through the supernatant to the surface where it is "absorbed" by surface evaporation (boiling). It is of interest to estimate the pressure rise in the headspace due to the upward energy flux from the spreading and cooling parcel. Heat flows from the parcel by turbulent natural convection in accord with equation (4-15):

$$Q_u = k A \left(\frac{g \beta}{\alpha \nu} \right)^{1/3} (\Delta T)^{4/3} \quad (4-23)$$

where Q_u is the upward total heat flow, A is the heat transfer area, and ΔT is the temperature difference between the parcel and the overlying supernatant. The maximum possible upward heat flow occurs from a parcel that spreads out over the entire non-convective layer, i.e., to the tank wall, so that $A = 411 \text{ m}^2$. The mixing calculation presented in the foregoing indicates that $\Delta T \approx 10^\circ\text{C}$. Inserting these estimates into equation (4-23), together with the physical properties of water given below equation (4-15), yields a maximum upward heat flow $Q_u = 1.12 \text{ MW}$. The volumetric flow of steam \dot{V}_v at the surface of the supernatant in response to the upward heat flow is

$$\dot{V}_v = \frac{Q_u}{\rho_v h_{fv}} \quad (4-24)$$

where ρ_v is the density of saturated steam at one atmosphere (**0.6 kg m⁻³**). Assuming that the major resistance to steam flow from the tank headspace is exerted by the HEPA filters, the headspace pressure rise ΔP above ambient required to accommodate the heat flow from the aborted steam bump is

$$\Delta P = R \dot{V}_v = \frac{R Q_u}{\rho_v h_{fv}} \quad (4-25)$$

where R is an empirical (filter) resistance coefficient equal to $2.34 \times 10^3 \text{ Pa s m}^{-3}$. The predicted pressure rise is $\Delta P = 2 \text{ kPa}$ (0.29 psi), which is negligible in comparison with the filter failure pressure of 36 kPa.

In summary, the buoyant displacement cannot be completed if the buoyant condition arises as a result of buildup of condensable vapor within the non-convective layer. A steam bump requires a sustained buoyant displacement, and this can only occur if non-condensable gas lifts a portion of the non-convective layer. Since non-condensable gas is not capable of performing this task in Tanks 241-AZ-101, 241-AZ-102, and 241-AY-102, these tanks are not susceptible to steam bumps caused by this mechanism.

With regard to the historical bumping events, it is clear that the events occurred in tanks with deep supernatant layers and with sufficient powers to bring the non-convective layers to a boil and the supernatant layers up to their one-atmosphere boiling point. Many of the events were initiated by shutdown and restart of air lift circulators and may be classified as steam bumps by gas injection, as discussed in Section 4.1. Some of the events occurred naturally and periodically, most likely in tanks subject to episodic buoyant displacements driven by non-condensable gas generation.

This page intentionally left blank.

5.0 DESCRIPTION OF STEAM BUMP AND LIQUID WASTE RELEASE MODELS

5.1 STEAM BUMP SEQUENCE OF EVENTS

In this section, we consider a hypothetical tank with a non-convective layer that is capable of self-heating to its boiling point and within which non-condensable gas generation may lead to a buoyant displacement event. The major assumption underlying the models presented in this section is that the near-boiling buoyant displacement parcel becomes fluid as soon as it starts to move. In Appendix C, the Meyer et al. (1997) energy criterion is used to justify this assumption.

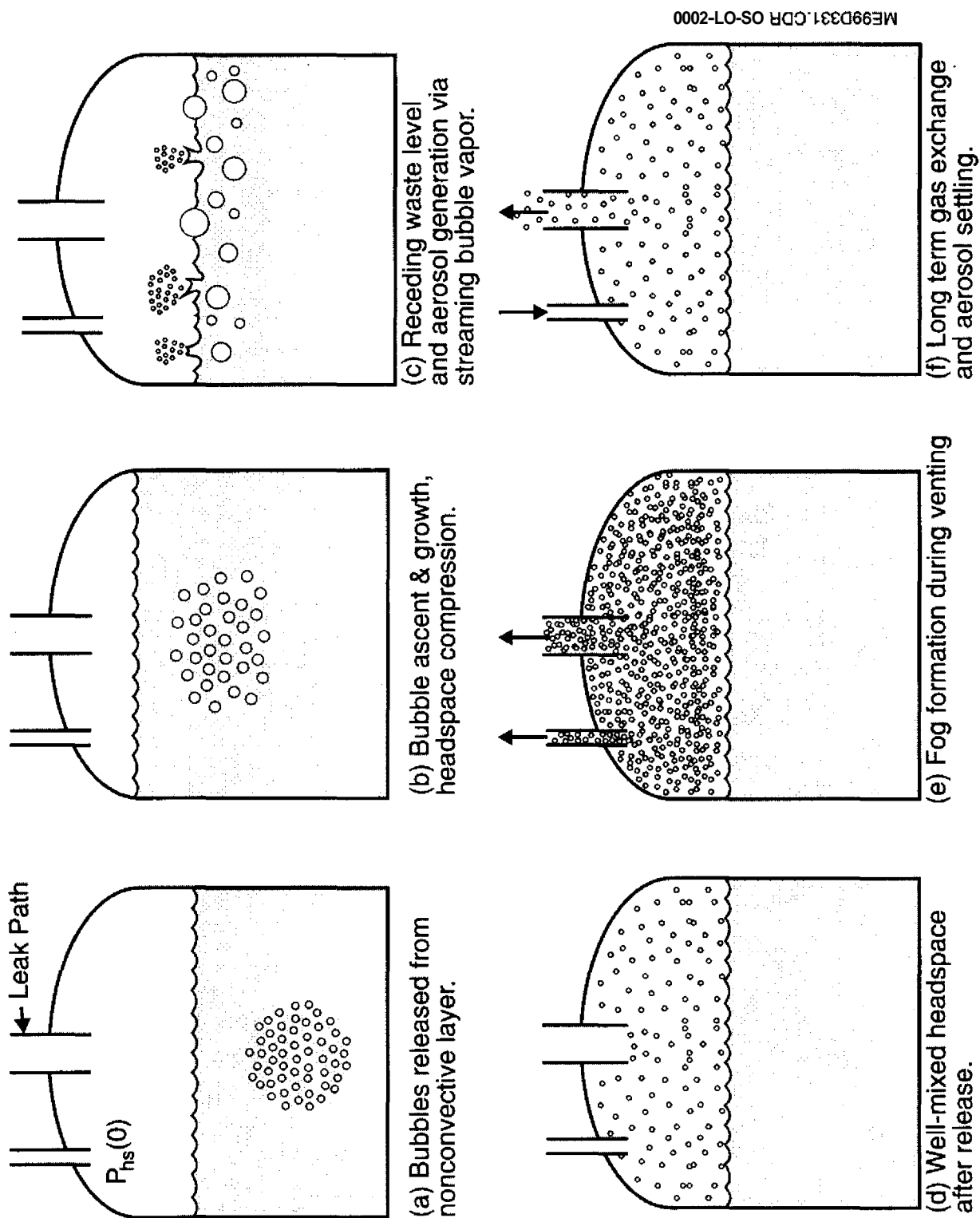
The envisioned sequence of events that result in liquid waste release from a tank during a steam bump is illustrated in Figure 5-1. Gas released from the non-convective layer forms a cluster of fine bubbles at the bottom of the convective layer or supernatant (Figure 5-1a). The cluster rises and grows due to the growth of the numerous individual bubbles that comprise the cluster. The bubbles' demand for volume causes the liquid surface to rise and the headspace gas to compress (Figure 5-1b). If the waste surface rises above the location of an open vent, the combination of a high waste level relative to the elevation of the vent opening and a pressurized headspace causes liquid to flow from the tank to the outside. Steam bump model results show that this mode of waste release to the outside does not occur because the vent openings are located close to the tank dome. Ultimately, the bubbles reach the surface of the waste. As the bubbles break through the surface, the release of bubble gas and vapor to the headspace is accompanied by the ejection of a spray of liquid waste [Figure 5-1c). Simultaneous bubble breakthrough and aerosol generation are assumed to occur instantaneously at the waste surface and result in a spatially uniform aerosol concentration within the headspace [Figure 5-1d). Finally, the venting pressurized headspace gas carries waste aerosol to the vent where it is released to the outside [Figure 5-1e). The addition of steam to the headspace via bubble breakthrough causes the headspace to expand to a saturated state before the depressurization process is over. Consequently, fog formation occurs during depressurization which contributes to the aerosol loading within the headspace. Subsequent aerosol transport to the outside may occur via natural ventilation flow over a relatively long time scale compared with the duration of the depressurization stage of the steam bump (Figure 5-1e).

5.2 BUBBLE AND WASTE ASCENT MODEL

The heart of the steam bump model are the equations for the rate at which the gas bubbles grow as they rise through the convective layer. Recall that equations (4-7) and (4-12) describe the bubble-interior diffusion-limited growth of a representative bubble. They are rewritten below in terms of the bubble volume normalized by the initial bubble volume and time t ; that is,

$$\frac{d[P_v V_b / V_b(0)]}{dt} = \left[\frac{24 D U_b}{V_b(0)} \cdot \frac{V_b}{V_b(0)} \right]^{1/2} P_{\text{mix}} \ln \left[1 + \frac{P_{\text{eq}}(T_\ell) - P_v}{P_{\text{mix}} - P_{\text{eq}}(T_\ell)} \right] \quad (5-1)$$

Figure 5-1. Sequence of Events in Model of Steam Bump and Liquid Waste Release



$$\frac{V_b}{V_b(0)} = \frac{P_{hs} + \rho_\ell g H - P_{eq}(T_\ell)}{P_{mix} - P_v} \quad (5-2)$$

$$\text{where } P_{mix} = P_{hs} + \rho_\ell g (H - z_{bc}) \quad (5-3)$$

The symbol $V_b(0)$ in the group $24DU / V_b(0)$ is the volume of a representative bubble. As already mentioned, equations (5-1) and (5-2) are valid for both an isolated bubble and a cluster of bubbles, i.e., $V_{bc}(z) / V_{bc}(0) = V_b(z) / V_b(0)$ where V_{bc} is the bubble cluster volume and $V_{bc}(z) / V_{bc}(0)$ represents the volume expansion ratio of the bubble cluster at time t or at location z above the bottom of the convective layer (at $z = 0$). The instantaneous location z_{bc} of the center of the bubble cluster is related to time by the differential equation

$$\frac{dz_{bc}}{dt} = U \quad (5-4)$$

where U is given by equation (4-13) for the rise velocity of a bubble cluster. In terms of the total volume of the bubbles in the cluster, this equation becomes:

$$U = 0.76 (g^3 V_{bc})^{1/6} \quad (5-5)$$

The value of $P_{eq}(T_\ell)$ in equations (5-1) and (5-2) depends on whether the bubbles are surrounded by supernatant liquid or, in the event of a buoyant displacement, by buoyant sludge (non-convective) interstitial liquid. In the former case, T_ℓ is limited by the boiling point of the supernatant at essentially atmospheric pressure; while in the latter case, T_ℓ may exceed this limit. For the buoyant displacement case, T_ℓ is a time-varying function which is determined by the mixing process which takes place between the buoyant parcel and the surrounding supernatant. This mixing process is different than the mixing process discussed at the end of Section 4.2, which occurs via a vertical buoyancy-dominated turbulent diffusion mechanism just as the parcel tries to emerge from the non-convective layer. In what follows, the mixing process is driven by the momentum carried by the buoyant parcel after it separates completely from the non-convective layer and while it rises to the surface of the waste.

To calculate the rate of mixing of the buoyant parcel with the supernatant, we adopt the now-classical entrainment assumption (Morton et al. 1956) which states that the mean supernatant inflow (entrainment) velocity v_{en} across the edge of the parcel is proportional to the instantaneous rise velocity U of the parcel; that is,

$$v_{en} = E_o U \quad (5-6)$$

where E_o is the so-called entrainment coefficient with an experimentally determined value of approximately 0.1. Equation (5-6) has proved enormously successful as an effective way of quantifying gas-phase and liquid-phase mixing problems involving jets, plumes, or buoyant puffs over a very wide range of scales (see, e.g., Briggs [1969] and Turner [1973]).

The instantaneous liquid mass m_ℓ within the buoyant parcel may be determined from the continuity equation

$$\frac{d m_\ell}{dt} = \rho_\ell v_{en} A_{bp} - \dot{m}_v \quad (5-7)$$

where ρ_ℓ is the liquid density, \dot{m}_v is the mass rate at which liquid is converted to vapor by bubble growth within the buoyant parcel, and A_{bp} is the instantaneous area of the boundary through which supernatant is entrained by the buoyant parcel:

$$A_{bp} = 4.84 \left(V_b + \frac{m_\ell}{\rho_\ell} \right)^{2/3} \quad (5-8)$$

The instantaneous mean temperature T_ℓ of the liquid mass within the buoyant parcel is predicted with the energy equation

$$m_\ell c_\ell \frac{dT_\ell}{dt} = -\rho_\ell v_{en} A_{bp} c_\ell (T_\ell - T_{CL}) - \dot{m}_v h_{fv} \quad (5-9)$$

where T_{CL} is the constant temperature of the non-convective layer and c_ℓ is the specific heat of the liquid. Note that in integrating equations (5-7) and (5-9), the mass of the solid component of the material released from the non-convective layer is included in the initial volume of m_ℓ . For the sake of simplicity, the differences between the liquid and solid densities and specific heats are not included in equations (5-8) and (5-9).

The important initial conditions for the numerical simulation of a buoyant displacement-induced steam bump are the total volume $V_b(0)$ of the bubbles and the mass $m_\ell(0)$ of liquid that participates in the buoyant displacement. Meyer et al. (1997) recommend the following formula for the volume of gas released to the headspace during a buoyant displacement:

$$V_b(0) = 750 \frac{\alpha_{NB} h_{NCL} \tau_y}{P_{NCL} \rho_{CL}} \quad (5-10)$$

where τ_y is the yield stress of the non-convective material in Pa and α_{NB} is the neutral buoyant void fraction. Equation (5-10) is an approximate result that Meyer et al. (1997) derived from a more cumbersome set of equations; it is a dimensional equation that requires the units h_{NCL} in m, ρ_{CL} in kg m^{-3} , and P_{NCL} in atm. Actually equation (5-10) is the Meyer et al. (1997) expression divided by $(P_{NCL} - 1)P_{NCL}$, since it is the volume of the gas in the just released buoyant parcel that is of interest here rather than the volume of gas released to the headspace. The leading coefficient in equation (5-10) was chosen to best match the gas release volumes from the tank buoyant displacement data. Equation (5-10) is applicable only to the relatively weak non-convective layers in the double-shell tanks for which $\tau_y = 100 \text{ Pa}$. Once $V_b(0)$ is determined from equation (5-10), the initial void-free mass of the buoyant parcel is estimated using

$$m_\ell(0) = \rho_{\text{NCL}} V_b(0) \left(\frac{1}{\alpha_{\text{NB}}} - 1 \right) \quad (5-11)$$

Another parameter of interest to tank bump consequence analysis is the frequency of a buoyant displacement event. The average time t_{BD} between any two buoyant displacement events can be shown to be (Meyer et al. 1997):

$$t_{\text{BD}} = \frac{V_b(0)}{G_g A_T h_{\text{NCL}}} \quad (5-12)$$

where A_T is the tank cross-sectional area. Equation (5-12) is based on the Meyer et al. (1997) formulation for a right circular cylindrical displacement parcel; it may be derived as follows. Referring to the equation numbers in the Meyer et al. (1997) report, divide equation (4.5.11) by equation (4.5.3) and use equation (4.5.5) to eliminate the waste level rise rate dh/dt from the result. Regardless of whether or not the non-convective layer is at its boiling point, G_g in equation (5-12) is the volume of non-condensable gas generated per unit volume of non-convective material per unit time, since the non-condensable gas is responsible for the buoyant displacement (*see* Section 4.2).

The headspace pressure P_{hs} in equation (5-2) is as yet an unknown quantity. Early on, the dynamic interaction between cluster bubble growth and the simultaneous compression of the headspace atmosphere determines the instantaneous value of P_{hs} . Later, fog formation and open ventilation paths determine the value of P_{hs} . The steam bump simulations are carried out by inserting equations (5-1) to (5-9) into the HADCRT waste tank source term computer model. The HADCRT model has been described by Malinovic et al. (2000) and will not be belabored here. Suffice it to say that the model is capable of tracking in-leakage and vent-path flows, simultaneous fog formation and deposition within the headspace, waste aerosol released from the headspace to the outside, and waste aerosol that enters the headspace from below. With respect to waste aerosol that enters the headspace from below, it remains to write the equations that describe the rate of generation of liquid aerosol by gas bubble breakthrough.

5.3 AEROSOL RELEASE MODEL

To simplify the calculation of droplet generation by the mechanism of gas bubble breakthrough at the liquid surface, all the bubbles are assumed to pass through the surface simultaneously and, correspondingly, the supernatant pool suddenly collapses to its initial depth $H(0)$. The volume of liquid waste aerosol V_a that enters the headspace air (hereafter referred to as entrained liquid) is given by the definition of the entrainment coefficient E (*see* e.g., Ginsberg [1983]; or Kataoka and Ishii [1984]):

$$V_a = E \left(\frac{\rho_{\text{hs}}}{\rho_\ell} \right) V_b(H) \quad (5-13)$$

where ρ_{hs} is the density of the compressed headspace air and $V_b(H)$ is the volume of the bubble cluster, both evaluated at the instant the cluster arrives at the liquid surface, that is when $z_{bc} = H$. The mass m_a of aerosol entrained is

$$m_a = V_a \rho_l = E \rho_{hs} V_b(H) \quad (5-14)$$

The droplets produced just above the waste surface will not all be carried off into the core of the headspace atmosphere. Only those droplets whose terminal velocities are less than the gas velocity generated by bubble break through will be carried off. Kataoka and Ishii (1984) have developed the following correlation of the data of Golub (1970) and Gamer *et al.* (1954) for the efficiency of stable aerosol production above a liquid pool with gas sparging:

$$E = 7.13 \times 10^{-4} \left[\frac{\mu_g^4 \rho_g^2 (\rho_l - \rho_g)^3}{\sigma^9 g^5} \right]^{1/8} j_g^3 \quad (5-15)$$

where j_g is the superficial velocity of the sparging gas, μ_g and ρ_g are the viscosity and density of the bubble gas, respectively, and σ is the interfacial tension of the waste liquid. For the present application, j_g must be related to the velocity $U(H)$ of the bubble cluster when it arrives at the waste surface. The void fraction α of bubble clusters, estimated from slow motion photography (Marble 1983), appears to be about 0.5. Moody (1986) opines that a better estimate is $\alpha = 2/3$, a value which is more consistent with bubble cluster rise velocities. It follows that

$$j_g = \alpha U(H) = \frac{2}{3} U(H) \quad (5-16)$$

Once the bubble cluster velocity $U(H)$ at the waste surface is calculated, the mass of the entrained liquid can be determined from equations (5-14) to (5-16). This is the theoretical maximum quantity that can enter the environment.

A portion of the entrained liquid (aerosol) will escape from the tank early on by flow of pressurized headspace air through vents and leakage paths. Subsequently, over a much longer time span, a portion of the remaining aerosol may be released by free-convection-driven exchange flow between the outside and the tank headspace. If unfiltered leak paths are small or have high flow resistance, substantial aerosol release can only occur if the headspace pressure exceeds the HEPA filter failure pressure. The major results of the steam bump simulations are postponed until Section 8.0. However, it is useful at this point to discuss the predicted buoyant parcel temperature versus time trends because of their potential importance to aerosol production at the waste surface.

5.4 EXAMPLE CALCULATION

Due to the mixing of the buoyant parcel with the supernatant, the liquid component of the parcel is predicted to remain sub-cooled during its rise to the surface of the waste. Figure 5-2 shows the calculated temperature history (solid curve) of the parcel for a buoyant release of initial liquid mass 4,000 kg, initial void volume 32 m^3 , and initial near-saturation temperature 391.5 K into an 8.0-m deep supernatant at 373 K and density $1,210 \text{ kg m}^{-3}$. See Appendix E for computational details and other inputs. The headspace pressure is constant and equal to atmospheric pressure. That is, the tank is assumed to be wide open to the outside. The dashed curve in Figure 5-2 represents the boiling point of the liquid in the buoyant parcel at the instantaneous location of the parcel. Clearly, since the boiling point always exceeds the parcel temperature, the only mechanism of vapor generation is evaporation at the surface of the bubbles that were originally trapped in the non-convective layer.

Suppose that the vessel remains effectively sealed during the period of buoyant parcel rise, and the temperature of the supernatant is assumed to be at its one-atmosphere boiling point. In this case, the liquid component of the parcel is predicted to be slightly superheated by several degrees relative to the atmospheric boiling point 373 K when the parcel reaches the surface, but sub-cooled relative to the boiling point at the peak tank pressure (see Figure 5-3). As the tank gradually depressurizes, the warm parcel liquid will spread out beneath the surface and ultimately it will begin to boil and produce steam at a rate dictated by the depressurization rate of the tank. Additional mixing may occur between the parcel liquid and the supernatant as the parcel spreads. Even if no credit is given for the additional mixing and an adiabatic evaporation process is assumed for the stratified parcel liquid, the steam **flux** across the waste surface is found to be small ($< 0.1 \text{ ms}^{-1}$). Thus, the liquid aerosol above the waste surface is created by the busting of bubbles and the volume of the aerosol is found to be small compared with that of the aerosol produced earlier by the breakthrough of the bubbles transported to the free surface within the buoyant parcel.

5.5 NUMERICAL EVALUATION NOTE

To couple integration of bubble volume and vapor pressure with other quantities, the P_v term of equation (5-1) is expanded as follows. State variables describing bubble rise are the bubble cluster volume expansion ratio $v = V_{bc}(z) / V_{bc}(0)$ and vapor pressure in the bubble P_v which appear in equations (5-1) and (5-2), are recast as:

$$P_v \frac{dv}{dt} + v \frac{dP_v}{dt} = \sqrt{\frac{24 D U_b v}{V_{b0}}} P_{\text{mix}} \ln \left[1 + \frac{P_{\text{eq}}(T_\ell) - P_v}{P_{\text{mix}} - P_{\text{eq}}(T_\ell)} \right] \quad (5-17)$$

$$\frac{dv}{dt} = \frac{d}{dt} \left[\frac{P_{\text{hs}} + \rho_\ell g H - P_{\text{eq}}}{P_{\text{hs}} + \rho_\ell g (H - z) - P_v} \right] \quad (5-18a)$$

$$\frac{dv}{dt} = \left(\frac{1-v}{\Delta P_g} \right) \frac{dP_{\text{hs}}}{dt} + \rho_\ell g \left(\frac{1-v}{\Delta P_g} \right) \frac{dH}{dt} + \frac{\rho_\ell g v U}{\Delta P_g} + \frac{v}{\Delta P_g} \frac{dP_v}{dt} \quad (5-18b)$$

Figure 5-2. Temperature History of Buoyant Parcel Compared With its Boiling Temperature; Open Headspace.

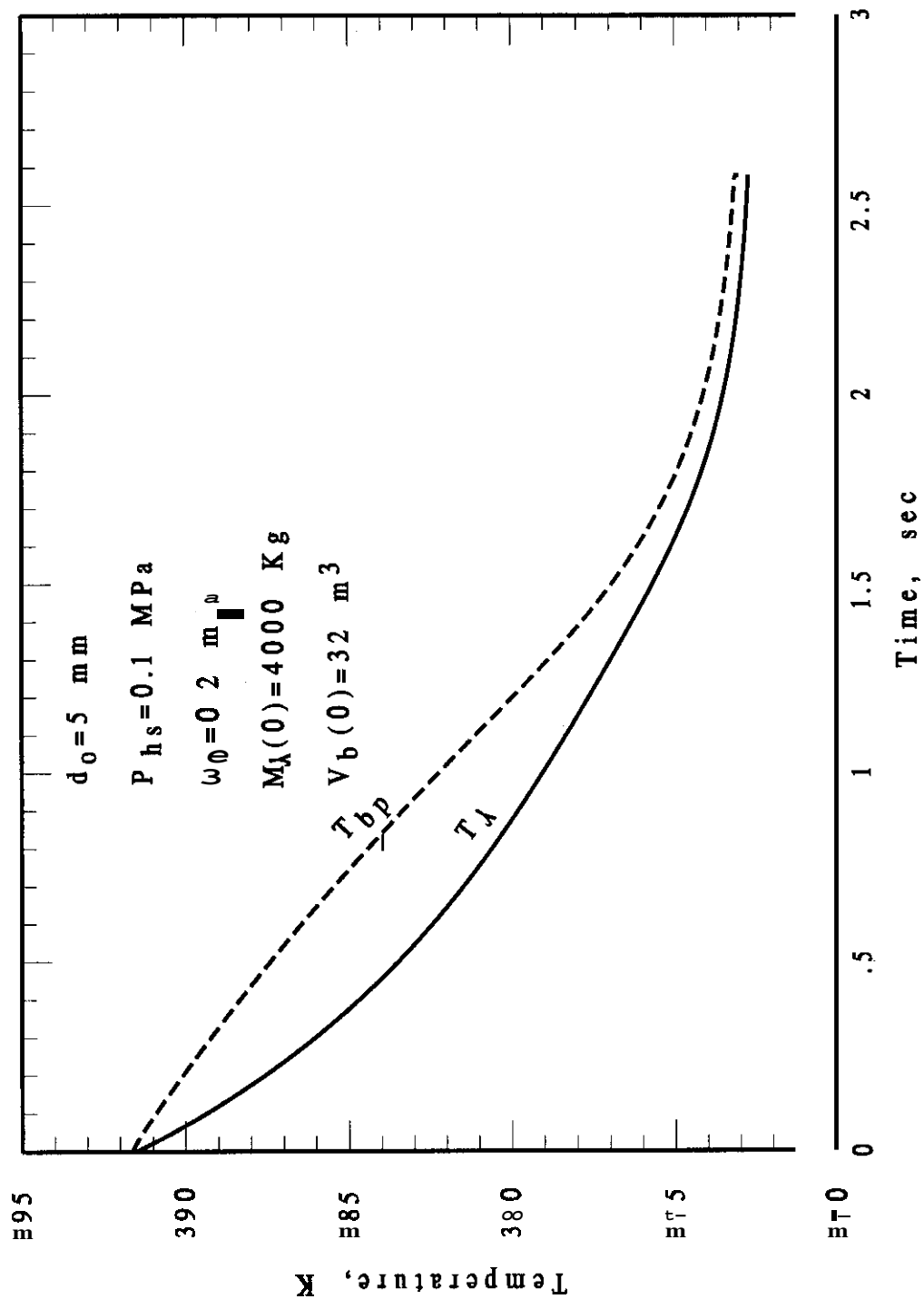
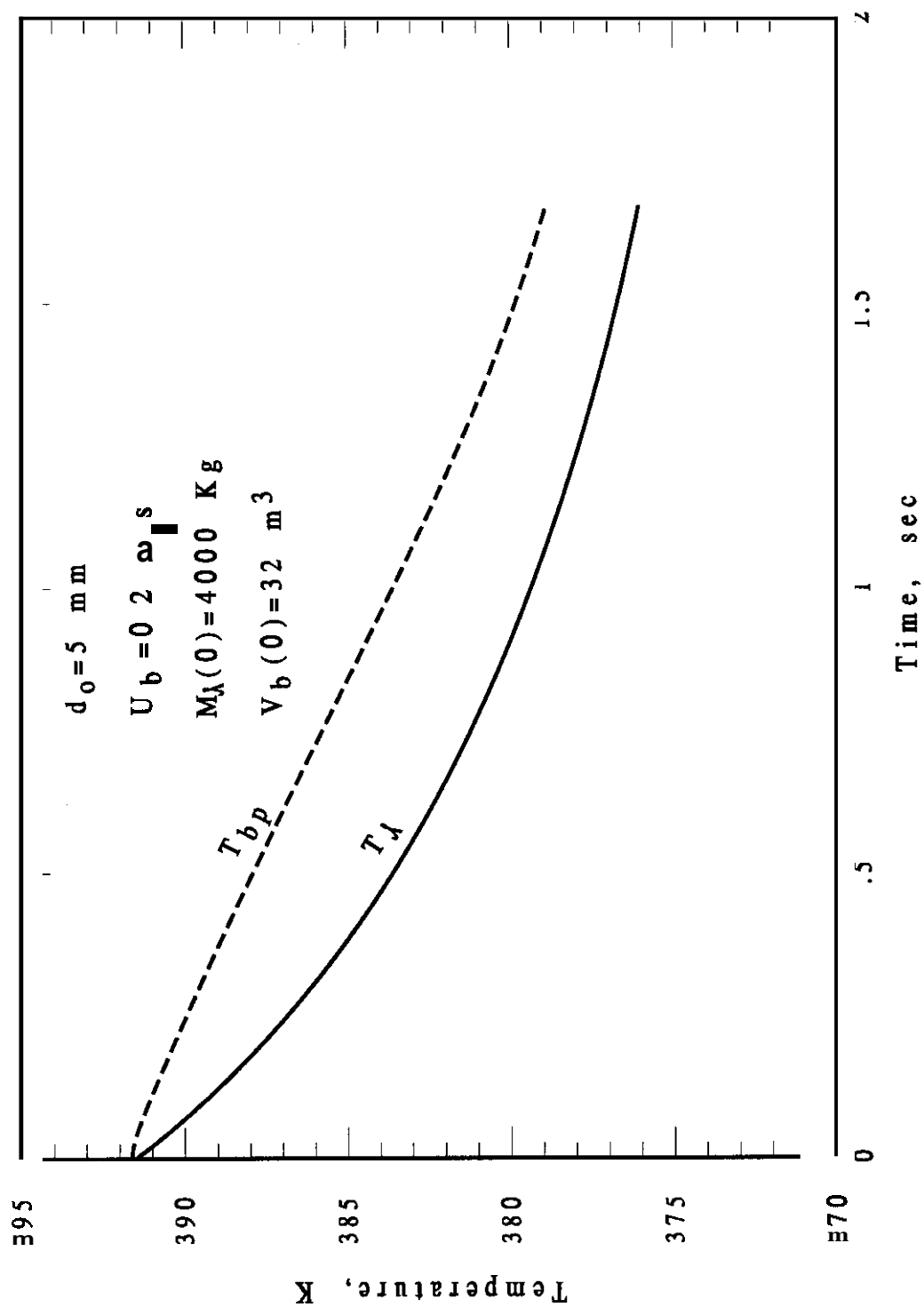


Figure 5-3. Temperature History of Buoyant Parcel Compared With its Boiling Temperature; Sealed Headspace.



$$\text{where } \Delta P_g = P_{hs} + \rho_\ell g (H - z) - P_v \quad (5-18)c$$

$$\text{and } P_{mix} = P_{hs} + \rho_\ell g (H - z) \quad (5-18)d$$

Derivatives other than dP_v / dt in equation (5-18) may be eliminated through auxiliary relations as follows. The headspace pressure derivative is given by

$$\frac{d P_{hs}}{dt} = \frac{P_{hs}}{m_{hs}} \frac{d m_{hs}}{dt} - \frac{P_{hs}}{V_{hs}} \frac{d V_{hs}}{dt} + \frac{P_{hs}}{T_{hs}} \frac{d T_{hs}}{dt} \quad (5-19)$$

The mass flowrate leaving the headspace is comprised of **HEPA** and leakage flow paths that can be quantified later:

$$\frac{d m_{hs}}{dt} = - W_{hs} \quad (5-20)a$$

$$W_{hs} = W_{HEPA} + W_{leak} \quad (5-20)b$$

$$W_{HEPA} = \rho_{hs} \left(\frac{P_{hs} - P_{amb}}{R_{HEPA}} \right) \quad (5-20)c$$

The **HEPA** flowrate is directly proportional to pressure difference, and the standard compressible flow relation is used for leakage paths or in case of **HEPA** failure. The headspace volume derivative is simply

$$\frac{d V_{hs}}{dt} = - V_{bco} \frac{d v}{dt} \quad (5-21)$$

The headspace temperature derivative is found from the energy equation

$$m_{hs} c_{vhs} \frac{d T_{hs}}{dt} = - W_{hs} (c_{Phs} - c_{vhs}) T_{hs} + P_{hs} V_{bco} \frac{d v}{dt} \quad (5-22)a$$

$$\frac{d T_{hs}}{dt} = - (\gamma - 1) T_{hs} \frac{W_{hs}}{m_{hs}} + (\gamma - 1) T_{hs} \frac{d v}{dt} \quad (5-22)b$$

which allows the pressure derivative to be recast as

$$\frac{d P_{hs}}{dt} = - \frac{\gamma W_{hs} P_{hs}}{m_{hs}} + \frac{\gamma P_{hs} V_{bco}}{V_{hs}} \frac{d v}{dt} \quad (5-22)c$$

Remaining derivatives required by equation (5-18) are

$$\frac{dz}{dt} = U \quad (5-23)$$

$$\frac{dH}{dt} = H_o \frac{V_{bco}}{V_\ell + V_{bco}} \frac{dv}{dt} \quad (5-24)$$

when equations (5-18) through (5-24) are combined, this yields an equation of the form

$$A_{12} \frac{dv}{dt} - \frac{v}{\Delta P_g} \frac{dP_v}{dt} = b_2 \quad (5-25)a$$

$$A_{12} = 1 - \frac{\gamma_{hs}}{\gamma_{hs} + \frac{\rho_\ell g H_o}{V_\ell + V_{bco}}} \quad (5-25)b$$

$$b_2 = \frac{\rho_\ell g U v}{\Delta P_g} - \left(\frac{1-v}{\Delta P_g} \right) \gamma_{hs} P_{hs} \frac{W_{hs}}{M_{hs}} \quad (5-25)c$$

so that equations (5-17) and (5-25) may be solved simultaneously to calculate bubble cluster rise.

This page intentionally left blank.

6.0 BUMP CRITERIA MODEL APPLICATION

Current safe-storage conditions are first considered to find a short list of tanks that would be susceptible to bumps after a prolonged duration without active heat removal. In practice, this means that initial conditions for waste temperature are the Limiting Condition for Operation (LCO) rather than the current waste temperatures. The criteria developed in the previous sections are then applied to rationalize historic events shown in Table 3-1. Note that the criteria may be continually re-applied when reference tank conditions change.

6.1 APPLICATION OF TANK BUMP CRITERIA TO CURRENT TANK WASTE

This section applies the criteria developed in Section 4.0 to the Hanford SSTs and DSTs under a safe-storage off-normal scenario. This scenario assumes that the waste is undisturbed but there is no active system (ALCs, primary system ventilation or annular ventilation system) for heat removal.

Criteria are presented and ordered to create a graded approach from the easiest to most difficult to apply, and to leave successively fewer remaining tanks to screen. Individual tanks are excluded from further consideration if any of the following are true:

1. There is an insignificant¹ non-convective layer
2. Supernatant depth does not exceed 1 m
3. Total tank heat load can be removed by steady-state conduction through the soil overburden (total tank heat load is less than 8,500 W)

The first two criteria are obvious from the discussion in Sections 3.0 and 4.0. The third criterion is derived from the one-dimensional, steady-state conduction equation:

$$Q = \frac{k A \Delta T}{\delta} \quad (6-1)$$

where Q is the total heat removal in W, k is the soil thermal conductivity (1.0 W/m-K), A is the heat transfer area (411 m²), ΔT is the difference between the maximum allowable tank dome temperature and the Hanford environment average temperature, and δ is the soil overburden, which has a nominal thickness of 4.0 m (Kummerer 1994). Assuming that the supernatant temperature and dome temperature are the same, the maximum allowable temperature is just a few degrees below the boiling point. With a site average temperature of 14 °C (Kummerer 1994), $\Delta T \approx 80$ °C is justifiable. These assumptions result in $\dot{Q} = 8,500$ W after

¹ Tanks with non-convective layers of less than 0.16 m are eliminated according to this criterion (see Table 6-2).

rounding down. This calculation conservatively ignores downward or sideways conduction, and yields an easily applied screening criterion.

Considering SSTs, all but the four tanks listed in Table 3-5 fail Criterion #2, and are excluded on that basis. Table 6-1 lists DSTs with trivial non-convective layer depths, while Table 6-2 lists tanks that are excluded from further consideration based on a small heat load (<8,500 W) and/or a small supernatant depth.

Table 6-1. Double-Shell Tanks With Negligible Non-Convective Layer.

241-AP-101
241-AP-102
241-AP-103
241-AP-104
241-AP-106
241-AP-107
241-AP-108

Source:

Hu, T. A., S. A. Barker, J. D. Bingham, and M. A. Kufahl, 2000, *Steady State Flammable Gas Release Rate Calculation and Lower Flammability Level Evaluation for Hanford Tank Waste*, RPP-5926, Rev. 0, CH2M HILL Hanford Group, Inc., Richland, Washington.

Tank	Waste Depth (m)	Non-Convective Layer Depth (m)	Supernatant Depth (m)	Heat Load (W)
241-A-101	8.78	4.10	4.67	7,340
241-AX-101	6.90	3.34	3.56	5,890
241-S-111	4.98	3.96	1.02	6,990
241-SX-102	4.74	3.51	1.24	5,020
241-AN-101	1.48	0.30	1.17	2,790
241-AN-106	0.36	0.16	0.20	138
241-AP-105	7.06	0.82	6.24	2,780
241-AW-102	0.74	0.37	0.37	1,530

Table 6-2. Single-Shell Tanks and Double-Shell Tanks With Small Heat Load and/or Small Supernatant Depth. (2 sheets)

Tank	Waste Depth (m)	Non-Convective Layer Depth (m)	Supernatant Depth (m)	Heat Load (W)
241-AW-103	4.70	3.21	1.49	674
241-AW-104	10.32	2.13	8.19	2,530
241-AW-106	4.36	2.10	2.26	2,800
241-AY-101	1.42	1.00	0.42	14,400
241-SY-102	5.64	0.81	4.83	1,580
241-SY-103	6.86	3.34	3.53	4,760

A fourth criterion has been proposed based on the analytical insights described in Section 4.0. This criterion is that a steam bump from quiescent storage conditions may not be possible without an initiating non-condensable gas, buoyant-displacement gas release event. This criterion is not applied at this time, however, because of uncertainties regarding its validity.

Note that Tanks 241-AN-I06 and 241-AW-102 fail on account of supernatant depth and total heat load (Criterion #3). From an operational standpoint, these DSTs can be excluded on the basis of total tank power alone, which means that a variable supernatant level is not a concern.

DSTs not appearing in either Table 6-1 or Table 6-2 are considered in further detail by estimating the time to reach saturated conditions. These calculations will determine which DST should be considered for control strategy evaluation and source term analysis. Many of the DSTs that fail the screening criteria (do not appear in Table 6-1 or Table 6-2) have a very long time to saturated conditions, relative to the amount of time needed to restore cooling, and do not present a realistic tank bump potential.

The time to saturated conditions can be estimated using a lumped capacitance solution for the transient waste temperature:

$$\left(V_{nc} \rho_{nc} c_{nc} + V_{cl} \rho_{cl} c_{cl} \right) \frac{dT}{dt} = \dot{Q} - \frac{k_s A (T - T_\infty)}{\delta} - \frac{k_s A (T - T_\infty)}{R} \quad (6-2)$$

where V , ρ , and c are volume, density and specific heat, respectively, subscript nc denotes the non-convective layer, subscript cl denotes convective layer, T is the waste average temperature, \dot{Q} is the tank heat load, k_s is soil thermal conductivity (1.0 W/m-K), A is the tank heat transfer area (411 m²), δ is the soil thickness (4 m), R is the tank radius (11 m), and T_∞ is the average ambient temperature of 14°C. Solving this first-order, linear differential equation gives the time to saturated conditions, t_{bp} , subject to the initial condition that $T = T_o$:

$$\left[\frac{T_{\infty} + \dot{q} / K - T_0}{T_{\infty} + \dot{q} / K - T_{bp}} \right] \quad (6-3)$$

where

$$\dot{q} = \frac{\dot{Q}}{V_{nc} \rho_{nc} c_{nc} + V_{cl} \rho_{cl} c_{cl}} \quad (6-4)$$

and

$$K = \frac{k_s A \left(\frac{1}{\delta} + \frac{1}{R} \right)}{V_{nc} \rho_{nc} c_{nc} + V_{cl} \rho_{cl} c_{cl}} \quad (6-5)$$

Initial temperature T_0 is assumed to be the peak non-convective layer temperature, which conservatively overstates the initial waste average temperature. Final temperature, T_{bp} , is the supernatant boiling point, accounting for vapor suppression by dissolved salts. Tank-specific data is not available for supernatant boiling point, but a convenient expression stating that the supernatant vapor pressure is 85% of the vapor pressure of pure water is used instead (Crea et al. 2000). Supernatant boiling point is then 104°C.

The method described here updates Kummerer's (1994) calculation by using recent tank-specific data and incorporating approximate expressions for conduction losses. The approximate expression for heat loss through the soil overburden is simply the steady-state expression for one-dimensional conduction through a planar slab held at the average waste temperature, T , on one side, and the average ambient air temperature, T_{∞} , on the other side. The expression for heat loss to underlying soil is the steady-state solution to the conduction equation for a circular region of radius R , at temperature T , in contact with a semi-infinite medium at temperature, T . The closed form solution assumes that the average air temperature and soil temperature are equal, when they actually differ by a degree C or so. A quasi-steady state formulation is an excellent approximation for times greater than the time constant for conduction, which is 106 days ($R^2 / \pi \alpha = 10^8$ seconds) for the underlying soil.

Table 6-3 shows the results of this calculation for DSTs that have not been screened already (i.e., not appearing in Tables 6-1 nor 6-2), but excluding the AZ / AY tank **farm**. Computational details are provided in Appendix G. In Table 6-3, initial temperature and one set of tank heat load inputs are from the Barton and Bingham (1999) database; the other set of tank heat load inputs is from Hu et al. (2000). Excluding the AZ and AY DSTs, the tank heat loads shown in Hu et al. (2000) are smaller than those in the Barton and Bingham (1999) database. Clearly, the calculated DST time to saturated condition values greatly exceed any conceivable corrective maintenance times.

Table 6-3. Time to Saturated Conditions for Double-Shell Tanks
With Significant Supersaturation Depth and Heat Load.

DST, 241-	CL ⁽¹⁾ Density, (kg/m ³)	NCL ⁽²⁾ Density, (kg/m ³)	T ₀ ⁽³⁾ , (K)	CL Volume, (m ³)	NCL Volume, (m ³)	Barton and Bingham Tank Heat Load, (W)	Hu et al. Tank Heat Load, (W)	Barton and Bingham Time ⁽⁴⁾ , (days)	Hu et al. Time ⁽⁵⁾ , (days)
SY-101	1,390	1,610	323	2,286	2,214	16,100	10,600	2,028	Inf. ⁽⁵⁾
AN-IO3	1,490	1,710	314	2,074	1,552	18,700	12,100	1,334	Inf. ⁽⁵⁾
AN-IO4	1,400	1,590	317	2,286	1,700	19,700	13,700	1,196	3,312
AN-105	1,420	1,580	313	2,411	1,851	13,400	9,340	4,137	Inf. ⁽⁵⁾
AW-IO1	1,400	1,630	314	3,104	1,158	15,200	10,300	2,361	Inf. ⁽⁵⁾
AN-102	1,410	1,500	320	3,676	337	11,500	9,340	Inf. ⁽⁵⁾	Inf. ⁽⁵⁾
AN-IO7	1,370	1,560	308	3,017	935	13,700	11,700	3,256	Inf. ⁽⁵⁾

⁽¹⁾Convective layer density and volume from Hu et al. (2000).

⁽²⁾Non-convective layer density and volume from Hu et al. (2000).

⁽³⁾Initial temperature is the current NCL peak temperature.

⁽⁴⁾Calculations assume final temperature = 104 °C, soil conductivity = 1.0 W/m-K, heat transfer area = 411 m², tank radius = 11.0 m, CL specific heat = 3,300 J/kg, and NCL specific heat = 3,000 J/kg. Inf. = 104 °C never reached.

⁽⁵⁾An "Inf." entry means that the DST reaches a steady-state condition below T_{bp}.

Hu, T. A., S. A. Barker, J. D. Bingham, and M. A. Kufahl, M. A., 2000, *Steady State Flammable Gas Release Rate Calculation and Lower Flammability Level Evaluation for Hanford Tank Waste*, RPP-5926, Rev. 0, CH2M HILL Hanford Group, Inc., Richland, Washington.

CL = convective layer.

DST = double-shell tank.

NCL = non-convective layer.

AZ and **AY** DSTs require a more detailed calculation because there is a significant temperature difference between the convective and non-convective layers. An energy balance can be written for each layer:

$$\rho_{CL} V_{CL} c_{CL} \frac{dT_{CL}}{dt} = \dot{Q}_{CL} - \frac{k_s A}{R} (T_{CL} - T_{\infty}) + h_{ex} A (T_{NCL} - T_{CL}) \quad (6-6)$$

$$\rho_{NCL} V_{NCL} c_{NCL} \frac{dT_{NCL}}{dt} = \dot{Q}_{NCL} - \frac{k_s A}{R} (T_{NCL} - T_s) - h_{ex} A (T_{NCL} - T_{CL}) \quad (6-7)$$

where symbols and subscripts are defined as above. A heat transfer coefficient, h_{ex} , is defined for exchange between the two layers. This heat transfer coefficient is sized so that in the quasi-steady approximation,

$$\frac{dT_{CL}}{dt} = \frac{dT_{NCL}}{dt} \quad (6-8)$$

For DSTs 241-AZ-101 and -102, this system of equations was integrated under the initial condition that the supernatant temperature is the same as the headspace temperature, which is available from the Barton and Bingham (1999) database. Initial temperature, T_{NCL} , was assumed to be the peak non-convective layer temperature. Total heat loads are based on the Bingham and Barton (1999) database and the heat load split between convective and non-convective layers is defined (Crea et al. 2000). Bump conditions exist when the supernatant reaches the boiling point (104 °C, as described above) or the non-convective layer reaches saturated conditions at the non-convective layer mid-height. Accounting for vapor suppression by dissolved salts, boiling point at the non-convective layer mid-height would be 398 and 396 K, respectively, for Tanks 241-AZ-101 and 241-AZ-102.

For Tanks 241-AZ-101 and 241-AZ-102, calculation inputs and the temperature rates of change are listed in Table 6-4. Calculational details are provided in Appendix G. Table 6-4 differs from the previous tables in that it lists heat-up rate rather than time to saturated conditions. This keeps the solution of equations (6-6) and (6-7) general and applicable for various combinations of total heat load and initial conditions. A parametric study for temperature rise as a function of heat load is performed to find heat-up rate (see Appendix G), considering Tank 241-AZ-101 first. Nominal total tank heat load used is 77.3 kW (Barton and Bingham 1999), with 60% of the heat load in the non-convective layer (Crea et al. 2000), and the resulting heat-up rate (dT/dt) is 0.44 °C/day. This calculation was repeated with total heat load values of 50 kW, 60 kW, 90 kW, and 100 kW; in each case, 60% of the total load was placed in the non-convective layer. The following equation describes the heat-up rate as a function of total power, Q , in units of kW:

$$dT/dt = 0.0068 Q - 0.071 \text{ °C/day}$$

Knowing the heat-up rate, it is simply a matter of determining initial temperatures and bump condition temperatures (saturated conditions) to determine the time to bump conditions. With the quasi-steady approximation, the two layers have the same heat-up rate.

The process can be repeated for Tank 241-AZ-102 and the resulting heat-up rate equation is found to be $0.0066 Q - 0.075 \text{ °C/day}$, where Q is in kW (see Appendix G).

As an example of time to bump calculation, consider the heat loads from (Barton and Bingham 2000), which are 77.3 kW for Tank 241-AZ-101 and 63.0 kW for Tank 241-AZ-102 and are conservatively high for these tanks compared to heat load estimates based on the "Best Basis Inventory" decayed to January 2001 (see Appendix K). Assume that the bump condition is a supernatant temperature of 104 °C. Using the heat-up rate listed in Table 6-4 for Tank 241-AZ-101, and starting at the typical waste temperatures listed in Table 6-4, the supernatant temperature reaches 104 °C in 111 days. At that time, the non-convective layer is approaching 125 °C [398 K]. For Tank 241-AZ-102, the non-convective layer reaches the limiting temperature of 123 °C [396 K] at 120 days, at which time the supernatant temperature is still well below 104 °C.

Table 6-4. Heat-up Rates for AZ Double-Shell Tanks.

DST	CL ⁽¹⁾ Density, (kg/m ³)	NCL ⁽²⁾ Density, (kg/m ³)	T _{NCL} ⁽³⁾ , (K)	T _{CL} ⁽⁴⁾ , (K)	CL Volume, (m ³)	NCL Volume, (m ³)	NCL Heat Load, (W) (Crea et al. 2000)	Heat-up Rate ⁽⁵⁾ , (°C/day)
241-AZ-101	1,190	1,670	345	327	3,021	178	45,949	0.0068 Q - 0.077
241-AZ-102	1,100	1,490	355	321	3,131	394	38,894	0.0066 Q - 0.075

⁽²⁾Non-convective layer density and volume from Hu et al. (2000).

⁽³⁾Initial temperature is the current NCL peak temperature.

⁽⁴⁾Initial temperature is the current headspace temperature.

⁽⁵⁾Calculations assume Q (total heat load) is in kW, soil conductivity = 1.0 W/m-K, heat transfer area = 411 m², tank radius = 11.0 m, CL specific heat = 3,300 J/kg, and NCL specific heat = 3,000 J/kg.

Crea, B. A., K. Sathyanarayana, and D. M. Ogden, 2000, *Parametric Analyses of Heat Removal from High-Level Waste Tanks*, RPP-5637, Rev. 0, CH2M HILL Hanford Group, Inc., Richland, Washington.

Hu, T. A., S. A. Barker, J. D. Bingham, and M. A. Kufahl, 2000, *Steady State Flammable Gas Release Rate Calculation and Lower Flammability Level Evaluation for Hanford Tank Waste*, RPP-5926, Rev. 0, CH2M HILL Hanford Group, Inc., Richland, Washington.

CL = convective layer.

DST = double-shell tank.

NCL = non-convective layer

Tank 241-AY-102 has a 40,700 W total tank heat load (after the waste transfer from Tank 241-C-106), and initial peak non-convective layer temperature of 77 °C [350 K]. The heat-up rate for Tank 241-AY-102 is therefore roughly 33% smaller than the heat-up rate for either Tank 241-AZ-101 or Tank 241-AZ-102.

6.2 41-AY-102 HAS A 40,700 W TOTAL APPLICATION OF TANK BUMP CRITERIA TO WASTE AT LIMITING CONDITIONS FOR OPERATION CONDITIONS

In this section, the transient time to waste saturated conditions is calculated for Tank 241-AZ-101 (the highest heat-up rate waste), assuming that the initial conditions are the LCO rather than typical conditions. LCO conditions are stated in the DST and AWF Tank Waste Temperature Controls LCS/LCO 3.3.2:

The WASTE temperature shall be either:

- a. $\leq 195^{\circ}\text{F}$ in all levels of the WASTE,

OR

- b. $\leq 195^{\circ}\text{F}$ in the top 15 ft of the WASTE

AND

 $\leq 215^{\circ}\text{F}$ in the WASTE below 15 ft.

The LCO basis also accounts for temperature measurement uncertainty. That is, it assumes that the actual waste temperature could be higher than the measured temperature because of measurement errors. A 5.6°C (10°F) uncertainty is used and is appropriate based on Appendix L.

The best basis heat load is 61 kW (see Appendix K) decayed to January 31, 2001. Using the heat-up rate equation for Tank 241-AZ-101 from Table 6-4 and a 61 kW heat load, the heat-up rate is:

$$0.0068 (61) - 0.077 = 0.34^{\circ}\text{C/day} (0.61^{\circ}\text{F/day})$$

Assuming saturated conditions are 104°C (220°F) in the supernatant and 125°C (257°F) for the non-convective layer, the time to saturation in the supernatant is:

$$[220^{\circ}\text{F} - (195^{\circ}\text{F} + 10^{\circ}\text{F})]/0.61^{\circ}\text{F/day} = 25 \text{ days}$$

and for the non-convective layer is:

$$[257^{\circ}\text{F} - (215^{\circ}\text{F} + 10^{\circ}\text{F})]/0.61^{\circ}\text{F/day} = 52 \text{ days.}$$

6.3 APPLICATION TO HISTORIC EVENTS

The historic events shown in Table 3-1 can be better understood in light of the discussion in this section. The most important aspect of Table 3-1 is that the tank heat rates greatly exceed even the highest current tank heat loads. For the historic tanks, the time to bump conditions would have been much less than the 100 days or so predicted for the present AZ DSTs, and without a sufficient ventilation flowrate, bumping could have been expected shortly after the tank was filled, even without an initiator. For example, Tank 241-S-104 was filled in July 1953, and began bumping in October of 1953, despite the installation of auxiliary water-cooled condensers (Tomlinson 1955). In Tank 241-S-101, bumping began in January 1954. In both cases, the waste temperature at the bottom probably exceeded the saturation temperature at the bottom hydrostatic pressure. This was definitely the case in the other events, where the temperature at the bottom was anywhere between 260°F and 357°F . This can be compared to the value used in this section as the bump criterion for, say, Tank 241-AZ-101, which is 398 K, or 257°F .

Finally, we note that a number of later bump events were initiated by ALC restart after shutdown, and observed behavior is in qualitative accordance with expectations based on Section 4.1.

7.0 CONTROL STRATEGY EVALUATION

A tank bump requires loss of active waste cooling functions for an extended period, given the requisite conditions of waste volumetric heat generation, supernatant depth, etc., described in the previous section. The control strategy is to monitor waste temperature and require actions to restore cooling when the temperature exceeds a specified limit. This control strategy works if there is sufficient time available to discover the increasing temperature event and restore cooling prior to the waste reaching accident conditions (i.e., saturation temperature). The results of Section 6.0 show that the main active waste cooling function of interest is the AZ/AY ventilation system. The evaluation is therefore focused on finding the probability that the ventilation system cooling function can be recovered, as a function of the available time.

In a study that presents the probability of schedule delays for delivery of high-level waste feed batches, the reliabilities of the primary heating, ventilation, and air conditioning (HVAC) system, the annulus HVAC system, ancillary HVAC systems, the ALCs, and miscellaneous support systems have been considered for Tank 241-AZ-101 waste transfer operations (Carlson 1999a and 1999b). Schedule delays were estimated by creating individual reliability, availability, and maintainability (RAM) models for each of the following contributors: primary HVAC, annulus HVAC, service air, transfer system, monitoring system, recirculation condenser, human errors, ventilation condenser system, and external events. In the RAM, the ALC system is modeled within the service air system. The primary HVAC system consists of individual air inlets, filters, an exhaust condenser, a high-efficiency mist eliminator, redundant exhaust fans and filter banks, and an exhaust stack with radiological sampling equipment. Individual RAM models were built for the annulus HVAC, ventilation condenser cooling, and recirculation condenser cooling.

By using 10,000 simulated waste transfer operations, Carlson's (1999b) studies found the number of "off-normal" events that occurred and the delay due to each event. In summary, out of 10,000 simulated batch transfer events, 8 delay events can be expected on average, with a mean delay per event of 43 hours. The breakdown by system contribution is shown in Table 7-1. The results of this study will be adapted to find recovery times for loss of ventilation under LCO conditions. A key assumption is that the individual recovery times for restoration and/or corrective maintenance as determined by the waste feed delivery RAM can be applied to the safe storage scenario.

7.1 FAILURE TO RECOVER PROBABILITY

Failure to recover probability consists of two components: failure to restore ventilation within the available time and failure to enact corrective maintenance within the available time. Restoration considers that ventilation system functions can be recovered without repair in many instances by manual switchover for functions with redundant hardware. This was recognized and accounted for in the waste transfer RAM by developing probability density functions for restoration times and determining whether recovery from an off-normal event required a restoration function or a corrective maintenance function. A key assumption was that if the first component failed, the backup component would run with negligible failure rate until the main component could be repaired. For the most part, restoration functions inside a tank farm fence required an expected value (mode) of one day, with a maximum time of one week.

Table 7-1. Critical Items List for the High-Level Waste Transfer RAM B, Ranked by the Contribution of System Type to Expected Schedule.

System Type	Expected No. of Delay Events	Expected Delay per Event (hrs)	Total Expected Delay Time (hrs)	Percent Contribution to No. of Events	Percent Contribution to Total Delay
Total	8.0	43	341	100%	100%
HVAC Primary	2.32	37	85	29.0%	25.0%
HVAC Annulus	1.22	52	64	15.3%	18.7%
Transfer	2.23	28	62	28.0%	18.2%
Service Air	0.61	88	54	7.7%	15.9%
Monitoring	0.22	167	37	2.8%	10.9%
Vent Cond. Cooling Svstem	0.38	27	10	4.8%	3.0%
Raw Water	0.10	31	3	1.2%	0.9%
Dilution/Flush	0.01	168	2	0.1%	0.6%
Nitrogen	0.00	1006	2	0.02%	0.6%
Instrument Air	0.06	30	2	0.7%	0.5%
Process Air	0.04	29	1	0.5%	0.4%
Service Water	0.003	131	0.4	0.04%	0.1%
Instrumentation	0.01	34	0.3	0.1%	0.1%
Electric Power	0.01	6	0.03	0.1%	0.01%

Source:

Carlson, A. B., 1999b, *Waste Feed Delivery System Phase I Preliminary Reliability, Availability, Maintainability Analysis*, HNF-2863, Rev. 1, Numatec Hanford Corporation, Richland, Washington.

HVAC = heating, ventilation, and air conditioning.

From Table 7-1, it is clear that most, but not all, recoveries involved restoration actions rather than corrective maintenance actions. This is because expected delays were on the order of two days, which is much less than the expected corrective maintenance times. A description of corrective maintenance activities is given in Table 7-2, and log-normal distributions (low = 5th percentile and high = 95th percentile) for clock hours to complete these activities are shown in Table 7-3. From Table 7-2, activities requiring tank farm radiological access are considered to estimate corrective maintenance times; in response to ventilation system failures, activities requiring pit or tanks access are not expected, as are activities not requiring radiological access. Activities requiring tank farm radiological access have identifiers TRISA, TRIEL, TCIEL, TCNSA, and TCNEL. For these activities, 200 hours is representative of a mean time for corrective maintenance. An estimate of the fraction of recovery activities that are restoration functions rather than corrective maintenance activities is calculated using the following expression:

$$t_d = x_{rs} t_{rs} + (1 - x_{rs}) t_{CM} \quad (7-1)$$

where t_d is the mean delay time, x_{rs} is the fraction of events that requires restoration rather than corrective maintenance, t_{rs} is the mean restoration time, and t_{CM} is the mean corrective maintenance time. Assuming the mean delay time is 37 hours, the mean restoration time is 24 hours and the mean corrective maintenance time is 200 hours, x_{rs} equals 93%. Assuming the mean restoration time is very small, but the mean corrective maintenance time is still 200 hours, x_{rs} equals 82%. In application, x_{rs} is taken to be 85% as a point-estimate.

Table 7-2. Component Types and Recovery Conditions. (2 sheets)

Recovery ID	Basic Description	Component Repair Effort Category								
		1	2	3	4	5	6	7	8	9
PRIML	Definition: Pit or Tank Access, Remote Handled, Moderate Planning, Long Lead Spares. Examples: new or a replacement jumper, initial installation of a mixer pump.					X				
PRIEL	Definition: Pit or Tank Access, Remote Handled, Extensive Planning, Long Lead Spares. Examples: Pump removal replacement, thermocouple tree removal/replacement.	X				X			X	
PCIML	Definition: Pit or Tank Access, Contact Handled, Moderate Planning, Long Lead Spares. Example: Replace valve/piping components (waste contacted surfaces) on an existing jumper that has been removed and is intended to be reinstalled.					X			X	
PCIEL	Definition: Pit Access Only (no tank access), Contact Handled, Extensive Planning, Long Lead Spares. Examples. This includes, for example, the investigation and repair of frozen or non-rotating pump impellers, the replacement of valve actuator components.	X		X		X			X	
TRISA	Definition: Tank Farm Rad area access, Remote Handled /Intrusive, Simple Planning, Spares Available. Examples: pre-approved maintenance procedure, semi-routine actions.									
TRIEL	Definition: Tank Farm Rad area access, Remote Handled, Moderator to Extensive Planning, Long Lead Spares. Examples: Removal/replacement of vent system de-entrainer or mist eliminator elements.					X				
TCISA	Definition: Tank Farm Rad area access, Contact Handled /Intrusive, Simple Planning, Spares Available. Examples: Routine removal/replacement of consumable components, process instrument (pressure, temperature, and flow device) calibrations.	X				X	X			

Table 7-2. Component Types and Recovery Conditions. (2 sheets)

Recovery ID	Basic Description	Component Repair Effort Category								
		1	2	3	4	5	6	7	8	9
TCIEL	Definition: Tank Farm Rad area access, Contact Handled/Intrusive, Mod to Extensive Planning, Long Lead Spares. Examples: Removal/replace ENRAF, contaminated piping/ducting weld repairs, primary vent heater element replacement.			X		X				
TCNSA	Definition: Tank Farm Rad area access, Non-intrusive (non-Contact), Simple Planning, Spares Available. Examples: replacing roughing (pre) filters, CAM vacuum pump replacement	X	X	X		X	X	X		X
TCNEL	Definition: Tank Farm Rad area access, Non-intrusive, Mod to Extensive Planning, Long Lead Spares. Examples: Non-routine maintenance on electrical feeds/motor control centers, primary vent system fan wheel replacement.	X	X	X		X				
NCNNA	Definition: Non-Radiological area access, Minimum Planning, Spares Available. Examples: Infrastructure repairs, site utility, and Refrigeration and Equipment Services (RES) team support.	X	X	X	X	X	X			X
NCNEL	Definition: Non-Radiological area access, Moderate to Extensive Planning, Long Lead Spares. Examples: major component rebuilds/replacements.	X		X	X	X		X		

Source:

Carlson, A. B., 1999a, *Waste Feed Delivery Technical Basis, Volume IV: Waste Feed Delivery Operations and Maintenance Concept*, HNF-1939-Vol. IV, Rev. 0, Numatec Hanford Corporation, Richland, Washington.

Component Repair Effort Categories:

1 = I&C General

2 = I&C Special

3 = Electrical Onsite

4 = Electrical Offsite

5 = Mechanical General

6 = HVAC Special

7 = Computer

8 = Mechanical Major

9 = Support Facilities

Table 7-3. Summary of Corrective Maintenance Requirements
(Clock Hours and Effort). (2 sheets)

Recovery Time Description	Recovery Time ID	Range Factor	Clock Hours Required to Complete a Corrective Maintenance		
			Low	Mean	High
I&C COMP, NCNEL	1NCNEL	2	44	96	176
I&C COMP, NCNNA	1NCNNA	1.5	23	36	52
I&C COMP, PCIEL	1PCIEL	3.5	185	865	2,266
I&C COMP, PRIEL	1PRIEL	3	158	592	1,422
I&C COMP, TCISA	1TCISA	2	46	101	184
I&C COMP, TCNEL	1TCNEL	2.5	54	158	338
I&C COMP, TCNSA	1TCNSA	2	31	68	124
I&C SPECIAL, NCNNA	2NCNNA	1.5	26	40	59
I&C SPECIAL, TCNEL	2TCNEL	2.5	56	163	350
I&C SPECIAL, TCNSA	2TCNSA	2	34	74	136
ELEC ONSITE, NCNEL	3NCNEL	2	52	114	208
ELEC ONSITE, NCNNA	3NCNNA	1.5	25	39	56
ELEC ONSITE, PCIEL	3PCIEL	3.5	155	725	1,899
ELEC ONSITE, TCIEL	3TCIEL	2.5	123	359	769
ELEC ONSITE, TCNEL	3TCNEL	2.5	64	187	400
ELEC ONSITE, TCNSA	3TCNSA	2	30	66	120
ELEC OFFSITE, NCNEL	4NCNEL	2	8	17	32
ELEC OFFSITE, NCNNA	4NCNNA	1.5	6	9	14
MECH COMP, NCNEL	5NCNEL	2	41	90	164
MECH COMP, NCNNA	5NCNNA	1.5	26	40	59
MECH COMP, PCIEL	5PCIEL	3.5	223	1,043	2,732
MECH COMP, PCIML	5PCIML	3.5	212	992	2,597
MECH COMP, PRIEL	5PRIEL	3	207	776	1,863
MECH COMP, PRIML	5PRIML	3	186	697	1,674
MECH COMP, TCIEL	5TCIEL	2.5	102	298	638
MECH COMP, TCISA	5TCISA	2	71	155	284
MECH COMP, TCNEL	5TCNEL	2.5	53	155	331
MECH COMP, TCNSA	5TCNSA	2	30	66	120
MECH COMP, TRIEL	5TRIEL	2	74	162	296
HVAC SPECIAL, NCNNA	6NCNNA	1.5	28	43	63
HVAC SPECIAL, TCISA	6TCISA	2	45	98	180
HVAC SPECIAL, TCNSA	6TCNSA	2	35	76	140
COMPUTER, NCNEL	7NCNEL	2	47	103	188
COMPUTER, TNTSA	7TCNSA	2	38	83	152
MECH MAJOR, PCIEL	8PCIEL	3.5	660	3,087	8,085

Table 7-3. Summary of Corrective Maintenance Requirements
(Clock Hours and Effort). (2 sheets)

Recovery Time Description	Recovery Time ID	Range Factor	Clock Hours Required to Complete a Corrective Maintenance		
			Low	Mean	High
MECH MAJOR. PCIML	8PCIML	3.5	441	2,063	5,402
MECH MAJOR, PRIEL	EPRIEL	3	532	1,995	4,788
SUP FACILITY, NCNNA	9NCNNA	1.5	16	25	36
SUP FACILITY, TCNSA	9TCNSA	2	33	72	132

Carlson, A. B., 1999a, *Waste Feed Delivery Technical Basis, Volume IV: Waste Feed Delivery Operations and Maintenance Concept*, HNF-1939-Vol. IV, Rev. 0, Numatec Hanford Corporation, Richland, Washington.

The probability that ventilation is not recovered in the available time is then:

$$P_{nrR} = (1 - x_{rs}) \sum_{n=1}^N x_n \left[1 - \log\text{-normal}(t_a, \alpha_n, \beta_n) \right] \quad (7-2)$$

where N is the number of corrective maintenance activities, x is the fraction of all corrective maintenance activities for the n^{th} corrective maintenance activity (the relative frequency such that the sum of all x_n values is equal to one), log-normal is the cumulative log-normal distribution function evaluated at the available time, t_a , for the log-mean α_n and log-standard deviation, β_n , of the n^{th} corrective maintenance activity. This expression assumes that restoration activities succeed during the available time, which is a crude approximation made justifiable because timeframes on the order of a day are unimportant. This expression states that the probability that corrective maintenance fails is the sum of the probabilities that individual corrective maintenance activities fail. The probability that an individual corrective maintenance activity will fail in the available time is just the exceedance probability for the lognormal distribution of repair time. Exceedance probability for each individual corrective maintenance activity is weighted by the relative frequency of each corrective maintenance activity.

Based on Table H-6 of the Carlson (1999a) reference, only the 3TCNEL, STCISA, and 5TCIEL corrective maintenance activities are relevant and log-normal distribution for these repair times have the following input values (see Table 7-4).

Corrective Maintenance Activity	Relative Frequency (Mean Value) (x_n)	Log-Mean α	Log-S. D. β	5 th Percentile (hrs)	95 th Percentile (hrs)
3TCNEL (n = 1)	48.5%	5.08	0.56	64	400
5TCISA (n = 2)	48.5%	4.89	0.56	71	284
5TCIEL (n = 3)	3%	5.56	0.56	102	638

7.2 RESULTS FOR LIMITING CONDITIONS FOR OPERATION CONDITIONS

Equation (7-2) is evaluated with the following input:

- The relative frequency of the corrective maintenance activity 5TCIEL is 3.0 % and the other two corrective maintenance activities **are** equally likely
- Available time varies between 1 day and 30 days
- The fraction of events that require corrective maintenance rather than restoration is 15%.

Figures 7-1 and 7-2 illustrate results. Figure 7-1 expresses results in terms of the probability of recovering the ventilation system. To make results clear as time available approaches 30 days, Figure 7-2 shows the failure probability, which is just one minus the success probability, on a log scale. Figure 7-1 starts at 85% because the assumption is that restoration actions take one day and 85% of recovery actions are restoration actions. This assumption is not important, however, because we would never expect such a small available time. In a similar vein, the calculation ends at a probability of failure of just under 0.1% at 30 days.

Figure 7-1. Probability of Recovering Ventilation as a Function of Days Available.

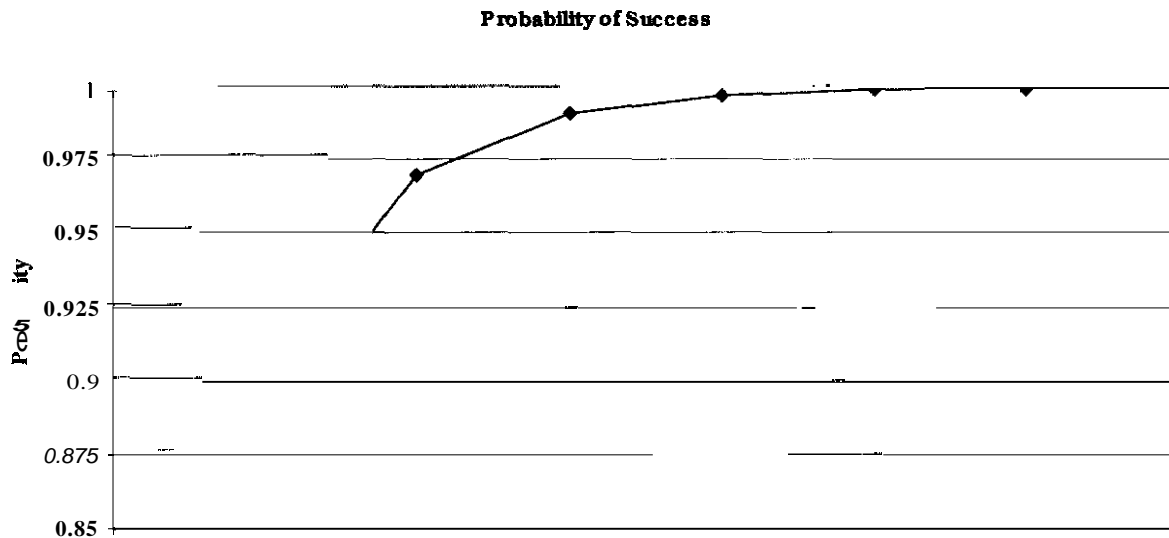
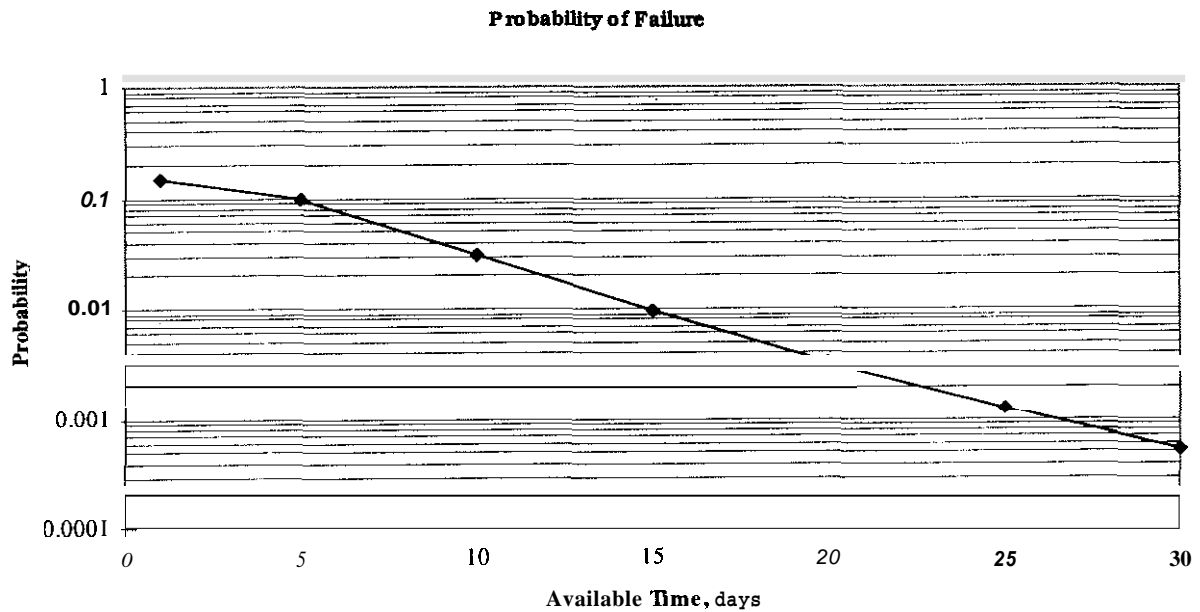


Figure 7-2. Probability of Not Recovering the Ventilation System as a Function of Available Time.



Conclusions

Figure 7-1 or 7-2 show that there is high confidence that ventilation cooling can be restored in less than about 1 **week**. One week is short compared to the time available to reach waste saturation temperatures. Therefore, the strategy of monitoring waste temperature and requiring restoration actions is viable.

8.0 CONSEQUENCE EVALUATION

Here we consider consequences of a tank bump that occurs during off-normal conditions of storage, i.e., without retrieval actions. Due to the long time for waste heat-up after loss of power in such circumstances, such events are evaluated against evaluation criteria for accidents with an “unlikely” frequency.

The consequence model employed is essentially that of Section 5.0 with modification to consider gas flows from the tank headspace. This allows the conservative adiabatic headspace compression assumption to be relaxed, and ultimately allows attenuation in the headspace to be considered. Also, aerosol models are added, as are representations of pump and sluice pit regions. This is accomplished by incorporating the model from Section 5.0 into the HADCRT code, as described next.

A review of the consequence model described in Section 5.0 indicates that the non-convective layer (N_{CL}) depth is an important factor in determining the consequences of a tank bump. A deeper N_{CL} results in a larger initial bubble volume and a thus a larger bubble volume as it is released at the waste surface. Because the mass of aerosol released to the tank headspace is related to the released bubble volume, consequences are expected to be high for a high heat load waste that has a deeper N_{CL} . Therefore, although Tank 241-AZ-101 has a higher head load and a faster heat-up rate following a loss of cooling, consequence analysis is performed for Tank 241-AZ-102 which has a somewhat lower decay heat load but a deeper N_{CL} . Consequences for Tank 241-AZ-102 are therefore judged to be representative of the consequences for other tanks and waste conditions.

8.1 THE HADCRT CODE

The HADCRT code (Malinovic et al. 2000) is an integrated model for considering storage tank thermal-hydraulic and accident phenomena, such as deflagration, detonation, and the potential for fission product release. HADCRT accounts for generic phenomena such as gas and aerosol transport between regions, and heat transfer to structures, including evaporation/condensation. Generic phenomenological capabilities include:

- Multiple compartment representation
- Pressure-driven and counter-current gas flows
- Gas and aerosol transport between compartments
- Vapor-aerosol equilibrium
- Aerosol deposition due to gravitational sedimentation, impaction, etc.
- Heat transfer to structures.

Routines containing phenomenology specific to an accident *or* thermal-hydraulic scenario are used to provide rates-of-change for the generic routines listed above, for example, vapor-phase combustion followed by blowdown and entrainment of aerosols. Accident-specific routines provides sources of mass, such as products of combustion or entrained aerosols from liquid

surfaces and deposited solid particulate, or energy, as in the heat of reaction by hydrogen combustion.

The tank bump phenomena described in this section were coded and added to the HADCRT code. HADCRT integrates the rates-of-change over the course of the bubble cluster rise to obtain position, volume of gas and liquid, vapor pressure, and temperature as a function of time, as described in equations (5-1) through (5-9) and (5-17) and (5-25). Temperature and pressure in the headspace are tracked by generic models during bubble cluster rise, so as to capture the feedback between bubble cluster dynamics and the headspace conditions during compression.

Vapor and entrained aerosols passing through the top of the supernatant are a source of **mass** and energy to the headspace. When the bubble cluster center reaches the supernatant surface, which has swollen per equation (5-6), the aerosol release equations (5-12) through (5-14) define the mass of material released to the headspace. These sources are used in turn to determine pressure, temperature, and airborne aerosol mass as a function of time.

Effects of headspace inflow/outflows and heat transfer to structures during and after the bump Coding details are left for Appendix F.

8.2 HADCRT INPUT FOR 241-AZ-102 CASE

Best-estimate consequences of a series of tank bumps in 241-AZ-102 are considered here to exemplify consequences. The HADCRT model for this case contains four volumes or regions: the tank headspace, a region representing four sluice pits, the center pump pit, and the environment. Normal flowpaths between the environment and the headspace are the filtered 8 in. diameter inlet and the filtered 20 in. diameter. Tank configuration is given in Section 3.4. Sluice pit covers lift at a pressure differential of 13.8 kPa and pump pit covers lift at a pressure differential of 17 kPa. Other inputs are shown in Table 8-1.

For the tank bump model, 241-AZ-102 inputs are as follows: convective layer height = 7.0 m, non-convective waste temperature = 385 K, supernatant temperature = 100°C, and supernatant volume = 2,859 m³. Other parameters important to bump size are the volume of gas releases during the buoyant displacement, the initial mass of liquid in the buoyant parcel, the time between bumps, and the number of humps. The volume of gas for 241-AZ-102 is computed using equation (5-10), assuming $P_{NCL} = 1.8 \text{ atm}$, $\alpha_{NB} = 0.262$, $h_{NCL} = 96 \text{ cm}$, $\rho_{CL} = 1,100 \text{ kg/m}^3$, and $\tau_y = 100 \text{ Pa}$. This results in a gas volume of $V_b(0) = 8 \text{ m}^3$. With a non-convective layer density of $1,490 \text{ kg/m}^3$, the initial amount of liquid plus suspended solids in the buoyant parcel is 34,000 kg. Average time between bumps is given by equation (5-12):

$$t_{BD} = \frac{V_b(0)}{G_g A_T h_{NCL}} \quad (8-1)$$

Table 8-1. Parameter Values for Consequence Analysis Example for Tank 241-AZ-102

Waste and Headspace Parameters	
$V_b(0) = 6.54 \times 10^{-8} \text{ m}^3$	Initial volume of representative bubble based on 5.0 mm bubble diameter.
$V_b(0) = 8 \text{ m}^3$	Initial total volume of bubbles released from sludge and used in ratio $V_b / V_b(0)$, parameter variation. 8 m^3 is a best-estimate case.
$V_\ell = 2859 \text{ m}^3$	Volume of convective layer.
$V_{hs}(0) \approx 1800 \text{ m}^3$	Initial volume of headspace.
$H(0) = 7.0 \text{ m}$	Initial depth of convective layer.
$m_\ell(0) = 34,000 \text{ kg}$	Initial non-convective layer mass in parcel.
$T_\ell(0) \approx 115^\circ\text{C}$	Initial parcel temperature.
$P_{hs}(0) = 1.012 \times 10^5 \text{ Pa}$	Initial headspace pressure.
$T_{hs}(0) = 100^\circ\text{C}$	Headspace initial temperature.
$X_{st}(0) = 95\%$	Headspace steam mole fraction.
B. Flow Path Parameters	
$A_{in} = 0.03 \text{ m}^2$	8 in. inlet line.
$A_{out} = 0.20 \text{ m}^2$	20 in. outlet line,
$A_{leak} = 5 \times 0.00133 \text{ m}^2$	Leakage around 42 in. risers.
$\Delta P_{HEPA} = 35,600 \text{ Pa}$	HEPA failure AP, crediting vent path pressure losses.
$C_v = 0.5$	Flow coefficient for inlet and outlet paths.
$V_{pit} = 4 \times 10 \text{ m}^3$ $+ 1 \times 20 \text{ m}^3$	Sluice pit and center pit volumes.
$T_{nit}(0) = 75^\circ\text{C}$	Pit initial temperature.
$P_{nit}(0) = 1.012 \times 10^5 \text{ Pa}$	Pit initial pressure.
$\rho_\ell = 1100 \text{ kg m}^{-3}$	Density of convective layer.
$\mu_g = 1.2 \times 10^{-5} \text{ kg m}^{-1} \text{ s}^{-1}$	Viscosity of bubble gas (vapor).
$\rho_g = 0.6 \text{ kg m}^{-3}$	Density of bubble gas (vapor).
$D = 9.2 \times 10^{-5} \text{ m}^2 \text{ s}^{-1}$	Bubble gas/water vapor diffusion coefficient.

HEPA = high-efficiency particulate air (filter).

The volume of non-condensable gas generated per unit volume of non-convective material per unit time, G_g is given by:

$$\frac{G_g}{G_o} = \left(\frac{1}{0.15} \right)^3 \quad (8-2)$$

where the 0.15 value is the buoyant displacement model prediction in Table 4-2 and G_o is the value of T_{bp} from Table 4-1, $0.19 \text{ gmol/m}^3/\text{day}$. This results in $G_g = 1.02 \text{ m}^3/\text{m}^3/\text{day}$ after converting units. Substituting into the equation for average time between bumps gives 0.48 hours. Since there are about 100 m^3 ($\alpha_{NB} A, h_{NCL}$) of gas in the non-convective layer, there will be 12 bumps spaced at roughly half-hour intervals.

8.3 241-AZ-102 TANK BUMP CONSEQUENCE PHYSICAL RESULTS

Results of the 241-AZ-102 tank bump calculation are shown in Figures 8-1 and 8-2, which provide short- and long-term histories for headspace temperature and pressure, and the aerosol distribution. Looking at short-term results, the pressure attained during a bump is about 3 psig, which is sufficiently large to not credit the HEPA filters as assumed. Temperature and pressure decay immediately following a bump due to forced flow and natural circulation flow to the environment. The natural circulation flow path is down through the damaged inlet line and up through the damaged outlet line.

In the first bump, about 1.5 kg of aerosol are released, of which somewhat more than 10%, about 0.17 kg, is forced into the environment, so that 1.3 kg are retained. During the half-hour interval between bumps, sedimentation in the tank accounts for about 0.5 kg depletion from the headspace and natural circulation flow removes about 0.05 kg, so that about 0.75 kg aerosol remain when the second bump occurs. In the second and all successive bumps, about the same amount of aerosol is produced, but more aerosol is available in the headspace for release during short-term blowdown. Therefore, the cumulative release to the environment increases faster than linearly with the number of bumps, for this chosen bump interval of one-half hour. Also, as the aerosol concentration builds up, after each bump, the amount of sedimentation between bumps increases. Due to property variations, the average amount of aerosol released per bump is about 1.8 kg.

After 12 bumps in this calculation, the entire non-convective layer has undergone buoyant displacement. Immediately following this last bump, the aerosol inventory is as follows: about 13.5 kg are settled in the tank, 3 kg are airborne in the headspace, and 5 kg are released to the environment, from a total source of about 21.4 kg. Long-term natural circulation competes with settling, but only an additional 0.25 kg are released while the remainder of the 3 kg airborne settle. Overall, 5.2 kg are released to the environment and 16.2 kg are retained in the tank.

Figure 8-1. 241-AZ-102 Tank Bump Short-Term Results.

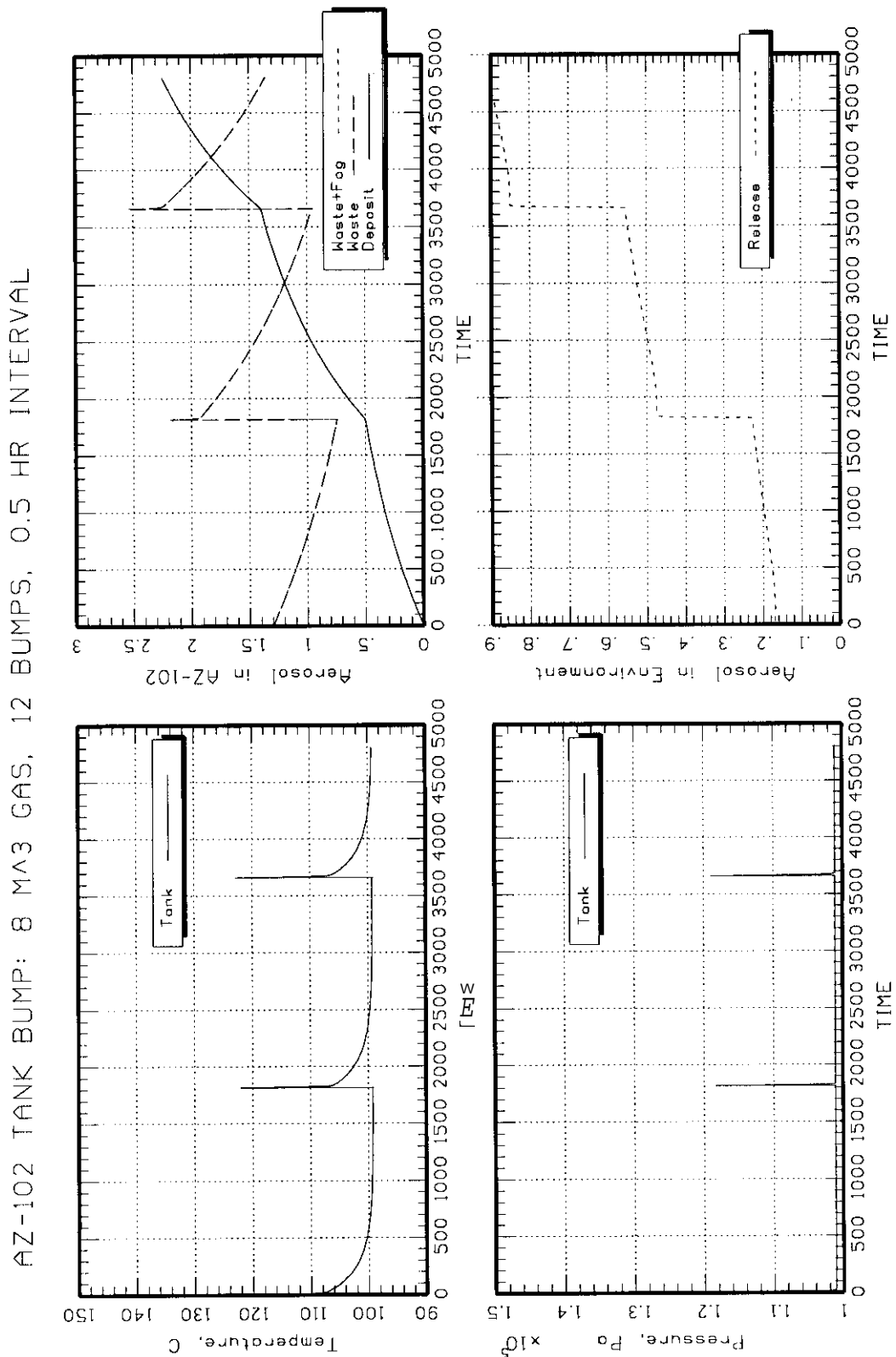
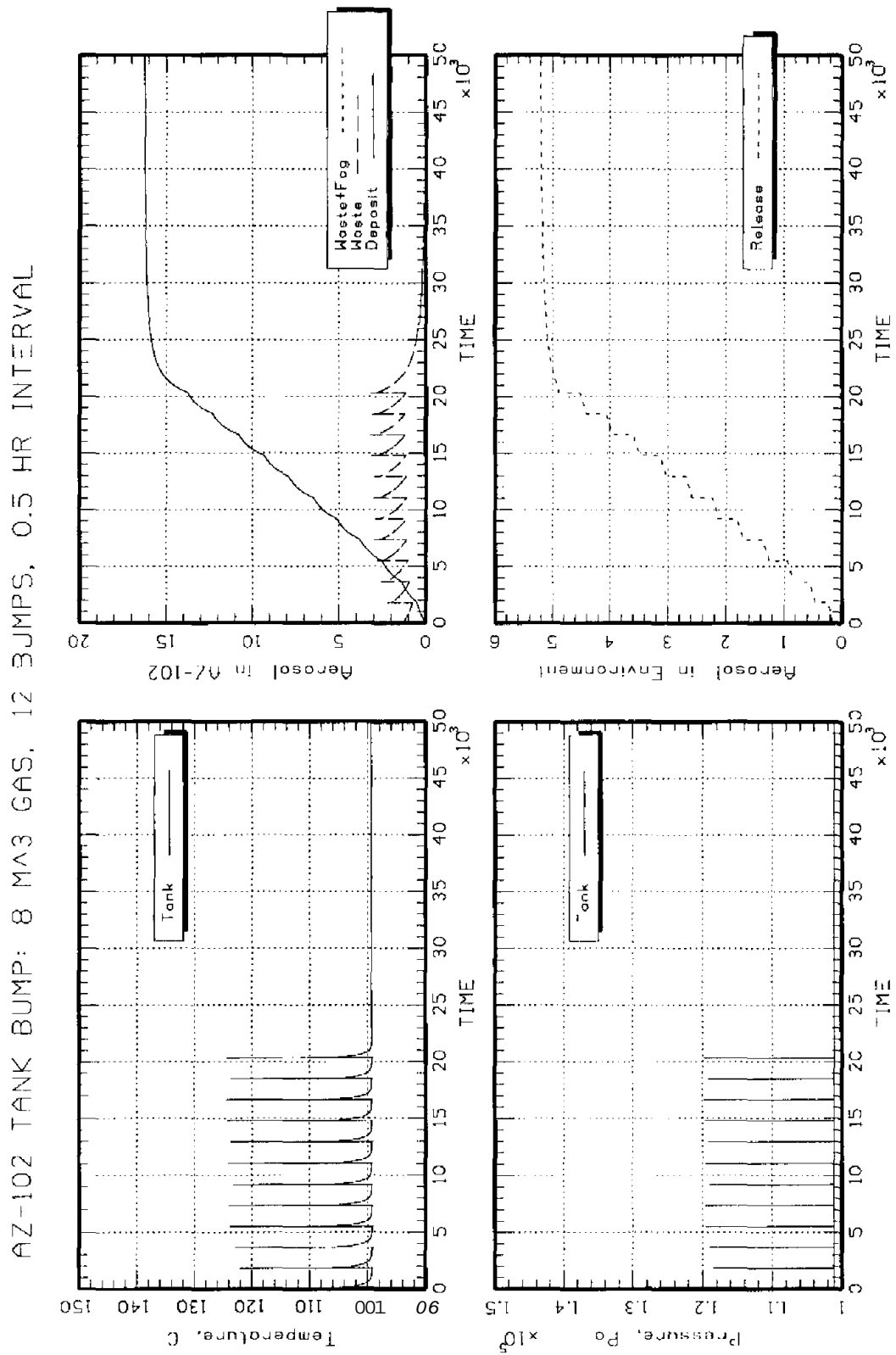


Figure 8-2. 241-AZ-102 Tank Bump Long-Term Results.



The present calculation considers one sequence of bumps that eventually displaces all non-convective material. Sedimentation, non-condensable gas retention, and attainment of neutral buoyancy are required for a subsequent bump sequence. Another sequence of successive bumps can therefore repeat later in time after neutral buoyancy is again achieved, on a timescale consistent with buoyant displacement events.

8.4 241-AZ-102 TANK BUMP RADIOLOGICAL AND TOXIC CHEMICAL CONSEQUENCES

Mass of entrained material is converted to dose using the following method from Cowley et al. (2000):

$$D = (Q)(ULD) \left(\frac{X}{Q} \right) (BR) \quad (8-3)$$

where D = Dose, Sv,

Q = Released quantity, L,

ULD = Unit Liter Dose, Sv/L,

X/Q = Atmospheric dispersion coefficient, s/m^3 , and

BR = Breathing rate, m^3/s .

The released mass, kg, calculated above can be converted into volume, L, for waste solids and liquids. Then, parameter values from Cowley et al. (2000) as summarized in Table 8-2 may be applied.

Table 8-2. Radiological Consequence Factors.

Factor	Onsite	Offsite
DST Solids	1.07×10^5	1.84×10^5
DST Liquids	7.97×10^2	8.45×10^2
$X/Q, sm^3$	5.58×10^{-3}	$8.0 \times 10^{-6} (1)$
$BR, m^3/s$	3.33×10^{-4}	3.33×10^{-4}

Source:

Cowley, W. L., K. R. Sandgren, and J. C. Van Keuren, 2000, *Radiological Source Terms for Tank Farm Safety Analysis*, RPP-5294, Rev. 0, CH2M HILL Hanford Group, Inc., Richland, Washington.

“Calculated in equation (8-4).

BR = breathing rate.

DST = double-shell tank.

ULD = unit liter dose.

For onsite dose, worker exposure at 100 m is taken for an 8-hour shift, so the X / Q value of $5.58 \times 10^{-3} \text{ s/m}^3$ from Section 5.2.3 of Cowley et al. (2000) applies. Similarly, the breathing rate is specified in Section 3.7 of the reference for light work.

For offsite dose, the methods of Section 5.2.3 of Cowley et al. (2000) are applied using values from Table 5-2 of the reference and approximating the release as an 8-hour event because 90% of the release occurs over a 6-hour interval. Performing this evaluation,

$$\frac{\log (1.74 \times 10^{-5}) - \log (X/Q \text{ 8 hrs.})}{\log (1.74 \times 10^{-5}) - \log (1.47 \times 10^{-7})} = \frac{\log (2 \text{ hrs.}) - \log (8 \text{ hrs.})}{\log (2 \text{ hrs.}) - \log (8,760 \text{ hrs.})} \quad (8-4)$$

yielding $X / Q = 8 \times 10^{-6} \text{ s/m}^3$. The light work breathing rate also applies offsite due to the short **release** duration.

Next, liters of solid and liquids released must be derived. In the first bump, non-convective solids are substantially diluted by supernatant: an initial release of 34,000 kg (liquid + solid) is increased to about 120,000 kg total in the rising parcel after entrainment (a calculation detail not plotted). But in later bumps, some solids now present in the supernatant are entrained as well, so that in the last bump of the series, the tank mixed-mean solid fraction applies. From Hu et al. (2000), waste properties are:

	Density (kg/l)	Volume (kL)	H ₂ O (wt. %)
Convective	1.10	3,131	84%
Non-Convective	1.49	394	56%

where dissolved salts are responsible for an $\text{H}_2\text{O}\% < 100\%$ in the convective layer. From Crea's et al. (2000) Table B3-1, the solids volume fraction in the non-convective layer is 17%. Thus, the overall mixed mean solids volume fraction is $(17)(394) / (394 + 3131) = 1.9\%$. Noting that the released non-convective volume is $34,000 \text{ kg} / 1.49 (\text{kg/L}) = 22.8 \text{ kL}$ and the entrained volume is $86,000 \text{ kg} / (1.1 \text{ kg/L}) = 78 \text{ kL}$, the maximum fraction of entrained solids at the final bump is approximately

$$\frac{(1.9)(78) + (17)(23)}{78 + 23} = 5.3\% \quad (8-5)$$

The average density of released material is simply $(34,000 + 86,000) / (22,800 + 78,000) = 1.19 \text{ kg/L}$. Therefore, the 5.2 kg release is equivalent to 4.37 L total, of which 5.3% or 0.23 L are solid, and 4.14 L are liquid. Note that exact volume fractions and densities could be derived for conversions above, but the amount of solids entrained varies with each bump, so a somewhat conservative approach was taken.

The overall $Q^* \text{ ULD}$ for waste is found by weighting Table 8-2 values by the volume released,

$$\text{Onsite} \quad Q^* \text{ ULD} = (1.07 \times 10^5) (0.23) + (797) (4.14) = 27,900 \text{ Sv}$$

$$\text{Offsite} \quad Q^* \text{ ULD} = (1.84 \times 10^5) (0.23) + (845) (4.14) = 45,800 \text{ Sv}$$

Therefore, total onsite worker dose is

$$\text{Onsite} \quad D = (27,900 \text{ Sv}) (5.58 \times 10^{-3} \text{ s/m}^3) (3.33 \times 10^{-4} \text{ m}^3/\text{s}) = 0.05 \text{ Sv}$$

and offsite receiver dose is:

$$\text{Offsite} \quad D = (45,800) (8 \times 10^{-6} \text{ s/m}^3) (3.33 \times 10^{-4} \text{ m}^3/\text{s}) = 1.2 \times 10^{-4} \text{ Sv}$$

Toxic chemical consequences are found using the methods of WHC-SD-WM-SARR-011 (1996). Table 3-8 of the reference provides the toxic limit sum-of-fractions for toxic chemical dose relative to allowed thresholds. Pertinent sum-of-fraction data from Table 3-8 of the reference are summarized in Table 8-3. Values are given for continuous release consistent with the radiological evaluation. When viewed as a continuous release, values in the table are applied to the released volumes of 0.23 L solid and 4.14 L liquid over a duration of 21,600 seconds. A puff evaluation is made for a single worst release which is 1/10th the total, with a duration of 60 seconds per Cowley et al. (2000). This means the puff release result is a factor of $1/10 \times 21,600/60 = 36$ times larger than the continuous release result. The puff evaluation is made because the release history for the tank bump accident presented earlier has aspects of both a continuous and a puff release, and because toxic chemical consequences are sensitive to peak concentration. **Also**, separate evaluations are made for frequency bins of $10^{-4}/\text{yr}$ to $10^{-6}/\text{yr}$, corresponding to current waste temperatures, and level from $10^{-2}/\text{yr}$ to $10^{-4}/\text{yr}$, corresponding to operation at LCO temperatures, given results from Section 6 above.

Table 8-3. Sum-of-Fraction of Risk Guidelines for a Unit Release of Chemicals.

Continuous Release, units s/L			
Waste Type	Receptor Location	Accident Frequency 1/yr.	
		10^{-2} to 10^{-4}	10^{-4} to 10^{-6}
DST Liquids	Onsite	750	210
DST Solids	Onsite	3,300	630
DST Liquids	Offsite	8.4	0.62
DST Solids	Offsite	15	2.8

A release duration of 21,600 s and volumes of 0.23 L solid and 4.14 L liquid are applied for the continuous release. The last bump event produces the largest puff which accounts for about 10% of the total release, hence, volumes of 0.023 L solid and 0.414 liquid are applied. The result of the evaluation is given in Table 8-4. Clearly, onsite puff release consequences are not within guidelines, while all other calculated consequences are within guidelines.

Table 8-4. Toxic Consequence Evaluation Results.

Receptor Location	Accident Frequency 1/yr.	
	10^{-2} to 10^{-4}	10^{-4} to 10^{-6}
Continuous Release		
Onsite	0.18	0.047
Offsite	0.0018	0.00015
Onsite	6.5	1.7
Offsite	0.07	0.005

Continuous release results are within guidelines, while puff release results are above guidelines.

9.0 SUMMARY AND DISCUSSION OF ASSUMPTIONS AND APPROXIMATIONS

9.1 TANK BUMP PHYSICAL MODELS

The steam bump model is subject to a number of simplifying, realistic, and conservative assumptions. The important assumptions are listed below together with their estimated degree of conservatism.

A1.1 Bubble growth is limited by steam transport within the bubble.

Degree of Conservatism: This assumption is believed to be moderately conservative in that the resistance to growth imposed by the thermal boundary layer on the liquid side of the bubble surface is at least as important as the diffusional resistance to growth on the vapor side.

A1.2 The flow field within the bubble is approximated by a Hill's vortex for the purpose of estimating the resistance to steam mass transfer within the bubble.

Degree of Conservatism: This assumption is regarded as realistic since it has been supported by bubble growth data available in the literature.

A1.3 The rise velocity of the buoyant parcel is estimated by appealing to an available correlation for the rise velocity of gas-bubble ensembles.

Degree of Conservatism: This assumption is realistic as the quasi-steady application of the correlation to growing, but essentially inertialess bubbles is valid.

A1.4 The mixing of the rising buoyant parcel with the surrounding supernatant is well described by the Morton-Taylor-Tumer entrainment equation.

Degree of Conservatism: This very realistic assumption is supported by numerous experiments on mixing of jets, plumes, or buoyant parcels with the ambient fluid.

A1.5 The mass of aerosol produced by steam bubble breakthrough is estimated with the Kataoka and Ishii (1984) correlation.

Degree of Conservatism: The use of this correlation is regarded as realistic since it is consistent with the available data in the high gas-flow regime.

A1.6 The Meyer et al. (1997) semi-empirical expressions are used to assess the total void volume and the total mass of non-convective material that are assumed to suddenly appear and participate in the buoyant displacement.

Degree of Conservatism: This assumption is probably very conservative for several reasons. The evidence from the six DSTs that exhibit buoyant displacements suggests that the buoyant release occurs gradually over time (– 1 min) as opposed to the sudden release of the single, large parcel assumed in the model. The tanks believed to be most susceptible to a bump and chosen for tank bump model evaluation are sludge tanks. It is doubtful that neutral buoyancy can be attained in the non-convective layers in these tanks through buildup of non-condensable gases. The Meyer et al. (1997) energy criterion for gas release indicates that non-condensable gas generation cannot bring the non-convective layers to a buoyant condition, even at their boiling points. Also, there are some reasons to believe that gas-solid or steam-solid attachment is difficult in sludge-like materials so that gas or vapor retention is limited in these materials (Kovach 2000).

9.2 TANK BUMP CONSEQUENCE EVALUATION

A2.1 Initially released gas volume and time between bumps are found using the Meyer et al. (1997) expressions.

Degree of Conservatism: These are best-estimate models for tanks observed to undergo buoyant displacements today, but per (A1.6) and (A3.1), this is conservative for application to Tank **241-AZ-102**.

A2.2 Leakage paths from the tank headspace are gaps around the 42 in. riser shield plugs, and inlet/outlet HEPA filters are assumed not present.

Degree of Conservatism: Leakage path values follow the Barton and Bingham (1999) methodology, and are best-estimate, although it is unclear whether or not other leakage paths may exist for any given tank. Neglect of HEPA filters is slightly conservative because the headspace pressure attained during a bump is at the threshold for failure, and this is a simplifying assumption. The actual effect of filters would be difficult to justify.

A2.3 Aerosol retention in sluice and pump pits is not credited.

Degree of Conservatism: This is somewhat conservative, but most aerosols are released via the normal inlet and outlet paths, so the contribution to release from the pits is small.

A2.4 Approximate solid fractions are used to convert released mass to solid and liquid volumes.

Degree of Conservatism: The mass of solids entrained per bump varies throughout the sequence of bumps, so a somewhat conservative approach was taken, whose impact is deemed small.

A2.5 Onsite and offsite doses assume an 8-hour release duration.

Degree of Conservatism: 90% of the waste is released over **6** hours (12 bumps at 30 minute intervals), so the worker shift assumption is reasonable, and the offsite conservatism is small.

A2.6 The effect of further bumps after settling of waste from the original sequence of bumps is not quantified.

Degree of Conservatism: Further sets of bumps would result in the same sources as predicted for the original sequence described here, and this is mentioned in Section 8.3. However, considerable time would elapse for sufficient non-condensable gas generation and accumulation to trigger a new set of bumps. Even though not considering further sets of bumps is non-conservative, this is judged to be an unlikely event following an originally unlikely event.

This page intentionally left **blank**.

10.0 REFERENCES

- Alstad, A. T., 1993, *Riser Configuration Document for Single-Shell Waste Tanks*, WHC-SD-RE-TI-053, Rev. 8, Westinghouse Hanford Company, Richland, Washington.
- Barton, W. B., and J. D. Bingham, 1999, *Gas Release Event Safety Analysis Tool Pedigree Database for Hanford Tanks*, HNF-SD-WM-TI-806, Rev. 2-A, Lockheed Martin Hanford Corp., Richland, Washington.
- Bendixsen, R. B., 1989, *History of Tank Bumps in Aging Waste Tanks*, Letter Report to D. A. Clapp.
- Briggs, G. A., 1969, *Plume Rise*, U.S. Atomic Energy Commission Critical Review Series, TID-25075, NTIS.
- Brown, W. G., 1962, "Natural Convection Through Rectangular Openings in Partitions-2. Horizontal Partitions," *Int'l. J. Heat Mass Transfer*, Vol. 5, pp. 869-878.
- Brownell, L. E., 1958, *Instability of Steel Bottoms in Waste Storage Tanks*, WHC-SD-WM-TI-406, Rev. 0, Doc. No. HW-57274, General Electric, Hanford Atomic Products Operation, Richland, Washington.
- Carlson, A. B., 1999a, *Waste Feed Delivery Technical Basis, Volume IV: Waste Feed Delivery Operations and Maintenance Concept*, HNF-1939-Vol. IV, Rev. 0, Numatec Hanford Corporation, Richland, Washington.
- Carlson, A. B., 1999b, *Waste Feed Delivery System Phase I Preliminary Reliability. Availability, Maintainability Analysis*, HNF-2863, Rev. 1, Numatec Hanford Corporation, Richland, Washington.
- Childs, K. W., 1991, *Heating 7.1 User's Manual*, K/CSD/TM-96, Draft, Martin Marietta, Oak Ridge, Tennessee.
- Cowley, W. L., K. R. Sandgren, and J. C. Van Keuren, 2000, *Radiological Source Terms for Tank Farm Safety Analysis*, RPP-5294, Rev. 0, CH2M HILL Hanford Group, Inc., Richland, Washington.
- Crea, B. A., K. Sathyanarayana, and D. M. Ogden, 2000, *Parametric Analyses of Heat Removal from High-Level Waste Tanks*, RPP-5637, Rev. 0, CH2M HILL Hanford Group, Inc., Richland, Washington.
- Epstein, M., 1988, *Surface Evaporation Model*, FAI Internal Memorandum, Fauske & Associates, Burr Ridge, Illinois.
- Epstein, M., and J. P. Burelbach, 1998, *Experimental and Theoretical Turbulent Diffusion Modeling of Light Gas Releases in a Tank Headspace: 2. Local Releases*, FAI/98-50, Fauske & Associates, Inc., Burr Ridge, Illinois.

- Epstein, M., and J. P. Burelbach, 2000a, "Transient Vertical Mixing by Natural Convection in a Wide Mixing Layer," *Int'l. J. Heat and Mass Transfer*, Vol. 43, pp. 321-325.
- Epstein, M., and J. P. Burelbach, 2000b, "Vertical Mixing Above a Steady Circular Source of Buoyancy," *Int'l. J. Heat and Mass Transfer* (in press).
- Epstein, M., H. K. Fauske, and M. G. Plys, 1999, *Hanford Tank 241-C-106 Temperature Limit & Steam Bump Evaluation*, FAI/99-18, Fauske & Associates, Inc., Burr Ridge, Illinois.
- FAI, 1989, *Independent Review of Aging Waste Tank "Bump" Phenomena*, FAI/89-94, Fauske & Associates, Inc., Burr Ridge, Illinois.
- Garner, F. H., S. R. M. Ellis, and J. A. Lacey, 1954, "The Size Distribution and Entrainment of Droplets," *Trans. Instr. Chem. Engrs.*, Vol. 32, pp. 222-324.
- Gauglitz, P. A., S. D. Rassat, P. R. Bredt, J. H. Konynenbelt, S. M. Tingey, and D. P. Mendoza, 1996, *Mechanisms of Gas Bubble Retention and Release: Results for Hanford Waste Tanks 241-S-102 and 241-SY-103 and Single-Shell Tank Simulants*, PNNL-11298, Pacific Northwest National Laboratory, Richland, Washington.
- Ginsberg, T., 1983, "Aerosol Generation from Sparging of Molten Pools of Corium by Gases Released During Core-Concrete Interactions," *Proc. Int'l Mtg. Light Water Reactor Severe Accident Evaluation*, Vol. 2, Cambridge, Massachusetts.
- Golub, S. I., 1970, *Investigation of Moisture Carryover and Separation in Evaporation Apparatus*, Candidates Dissertation, MEI (quoted from Kataoka and Ishii [1984]).
- H-2-68304, Rev. 4, *Structural Concrete Pump Pit Plans - Sections - Details Tank 241-AZ-102 and 101*.
- H-2-68305, Rev. 4, *Structural Concrete Sluice Pit Plans - Sections - Details Tank 241-AZ-102 and 101*.
- H-2-68423, Rev. 2, *Tank Riser and Airlift Circulator Details*.
- H-Unknown-1, *Air Lift Circulator and Riser Extension Details*, Bldg. 241-AZ.
- Hanson, G. L., 1955, *241-SX-Operation*, Internal Letter, General Electric Co.
- Harmon, M. K., 1958, *Radiation Occurrence*, Form found within WHC-SD-WM-TI-106, Rev. 0.
- HNF-SD-WM-SAR-067, 2001, *Tank Farms Final Safety Analysis Report*, Rev. 2-A, CH2M HILL Hanford Group, Inc., Richland, Washington.
- Hu, T. A., 1999, *Empirical Rate Equation Model and Rate Calculations of Hydrogen Generation for Hanford Tank Waste*, HNF-3851, Rev. 0, Lockheed Martin Hanford Corporation, Richland, Washington.

- Hu, T. A., S. A. Barker, J. D. Bingham, and M. A. Kufahl, 2000, *Steady State Flammable Gas Release Rate Calculation and Lower Flammability Level Evaluation for Hanford Tank Waste*, RPP-5926, Rev. 0, CH2M HILL Hanford Group, Inc., Richland, Washington.
- Jo, J., 1990, *The History and Existing Evaluations of the Tank Bump*, WHC-SD-WM-TI-406.
- Jones, B. L., 1988, *Aging Waste Tank Bump Sensitivity to Thermal Conductivity and Heat Capacity, Incorporating the Assumption of N-Reactor Shutdown*, (Internal Memo to L. A. Mihalik), Westinghouse Hanford Company, Richland, Washington (found within WHC-SD-WM-TI-406, Rev. 0).
- Kataoka, I., and M. Ishii, 1984, "Mechanistic Modeling of Pool Entrainment Phenomenon," *Int'l J. Heat Mass Transfer*, Vol. 27, pp. 1999-2014.
- Katsaros, K. B., W. T. Liu, J. A. Businger, and J. E. Tillman, 1977, "Heat Transport and Thermal Structure in the Interfacial Boundary Layer Measured in an Open Tank of Water in Turbulent Free Convection," *J. Fluid Mech.*, Vol. 83, pp. 311-355.
- Kovach, J. L., 2000, *Comments on Gas Solid Attachment in Liquid Phase*, Memorandum to SY-101 SubTAP.
- Kuhn, W. L., 1988, *Independent Review of Aging Waste Tank "Bump" Analyses*, Final letter report from Pacific Northwest Laboratory, Richland, Washington (found within WHC-SD-WM-TI-406, Rev. 0).
- Kummerer, M., 1994, *Topical Report on Heat Removal Characteristics of Waste Storage Tanks*, WHC-SD-WM-SARR-010, Rev. 0, Westinghouse Hanford Company, Richland, Washington.
- Malinovic, B., M. G. Plys, and M. Epstein, 2000, *Hanford Waste Tank Source Term Model HADCRT 1.1: User's Manual*, FAUOO-3, Fauske & Associates, Inc., Burr Ridge, Illinois.
- Marble, W. J., 1983, *Preliminary Report on the Fission Product Scrubbing Program*, General Electric Report, NEDO-30017.
- Meyer, P. A., M. E. Brewster, S. A. Bryan, G. Chen, L. R. Pederson, C. W. Stewart, and G. Terrones, 1997, *Gas Retention and Release Behavior in Hanford Double-Shell Waste Tanks*, PNNL-I 1536, Rev. 1, Pacific Northwest National Laboratory, Richland, Washington.
- Meyer, P., and B. Wells, 2000, "Understanding Gas Release Events in Hanford Double Shell Tanks," *WM'00 Proceedings of the Symposium on Waste Management*, Tucson, Arizona.
- Moody, F. J., 1986, "Dynamic and Thermal Behavior of Hot Gas Bubbles Discharged into Water," *Nuclear Engng. & Design*, Vol. 95, pp. 47-54.
- Morton, B. R., G. I. Taylor, and J. S. Turner, 1956, "Turbulent Gravitational Convection From Maintained and Instantaneous Sources," *Proc. R. Soc. Lond.*, Vol. A234, pp. 1-23.

- Perry, J. H., 1950, *Chemical Engineers' Handbook*, 3rd Edition, McGraw-Hill, New York, New York, p. 546.
- Reid, R. C., and T. K. Sherwood, 1966, *The Properties of Gases and Liquid, Their Estimation and Correlation*, 2nd ed., McGraw-Hill, New York, New York.
- Ruckenstein, E., V. D. Dang, and W. H. Gill, 1971, "Mass Transfer with Chemical Reaction from Spherical One- or Two-Component Bubbles or Drops," *Chem. Eng. Sci.*, Vol. 26, pp. 647-659.
- Sathyanarayana, K., 1996, *Evaluation of Potential and Consequences of Steam Bump in High Heat Waste Tanks and Assessment and Validation of GOTH Computer Code*, WHC-SD-WM-CN-022, Rev. 0-B, Westinghouse Hanford Company, Richland, Washington.
- Slezak**, S. E., D. C. Williams, W. Cheng, F. Gelbard, and D. R. Bratzel, 1998, *Refined Safety Analysis Methodology for Flammable Gas Risk Assessment in the Hanford Site Tanks*, Sandia National Laboratory, HNF-SD-WM-ES-410, Rev. 2, DE&S Hanford, Richland, Washington.
- Stewart, C. W., M. E. Brewster, P. A. Gauglitz, L. A. Mahoney, P. A. Meyer, K. P. Recknagle, and H. C. Reid, 1996, *Gas Retention and Release Behavior in Hanford Single-Shell Waste Tanks*, PNNL-11391, Pacific Northwest National Laboratory, Richland, Washington.
- Stewart, C. W., 2000, *personal communication*
- Tomlinson, R. E., 1955, *Storage of High Activity Wastes*, WHC-SD-WM-TI-406, Rev. 0, Westinghouse Hanford Company, Richland, Washington.
- Turner, J. S., 1973, *Buoyancy Effects in Fluids*, Cambridge University Press, Cambridge
- Waters, E. D., G. K. Allen, and D. E. Place, 1991, *Analysis of Tank Bump Potential During In-Tank Washing Operations Proposed for the 241-AZ Tanks*, WHC-SD-WM-ER-114, Rev. 0, Westinghouse Hanford Company, Richland, Washington.
- WHC-SD-WM-SARR-011, 1996, *Toxic Chemical Considerations for Tank Farm Releases*, Rev. 2., Westinghouse Hanford Company, Richland, Washington.
- Willingham, C. E., 1994, *Thermophysical Properties of Hanford High-Level Tank Wastes - A Preliminary Survey of Recent Data*, PNL-9419, Pacific Northwest Laboratory, Richland, Washington.

APPENDIX A

TANK WASTE CHARACTERIZATION DATA

This **page** intentionally left blank.

APPENDIX A

TANK WASTE CHARACTERIZATION DATA

A.1 E-MAIL CORRESPONDENCE

From: Blaine-A-Crea@RL.gov
Sent: Tuesday, April 04, 2000 6:38 PM
To: plys@Fauske.com
Cc: Thomas_G_Tom_Goetz@apimc01.rl.gov; David_R_Bratzel@apimc01.rl.gov
Subject: RE: DST Inlet Information Needs

The following explanation of the ventilation systems in the aging waste facility hopefully will clarify item 8 for you: I'll dig up appropriate reference material for you later.

There are four tanks in this facility. Two in AY tank farm (AY-101 and AY-102). Two in AZ tank farm (AZ-101 and AZ-102)

First each tank has both a primary (Dome space) and secondary (Annulus) ventilation system.

I'll discuss the annulus vent systems first. They are in general capable of drawing about 1000 CFM of air through the tank annulus when they're operating this is true for the current configuration of all the systems.

Each tank in the AY tank farm has a similar but totally separate annulus vent system. The two tanks in the AZ farm, however, share a common exhaust i.e. fans filters, stack, monitors.

All four tanks share elements of a common primary vent system. Each tank has, however, a separate recirculation cooling system. The included simplified sketch of the primary system may help to show the component arrangement.

The components in the lower right corner of the sketch are housed in a separate building outside of the farms. This provides tank vacuum and discharge cleanup. It also can provide some cooling, but the original design basis for the chiller driven condenser was to cool the off gas to slightly above 0 centigrade and so remove almost all the moisture and the associated tritium. It also is serviced by dedicated UPS's and a backup diesel generator with an automatic start/transfer switch.

The components of the recirculation modules shown next to each tank are designed to remove most of the heat over the long run. There is one of these recirculation modules with associated condensers, fans, cooling towers, coolant loops etc for each tank.

RPP-6213 REV 1

From: Sathyanarayana, K
Sent: Wednesday, April 05, 2000 4:36 PM
To: 'plys@fauske.com,' Bratzel, David R; Crea, Blaine A
Cc: Sathyanarayana, K
Subject: Pumps and Sluice Pits Information

Marty and Dave,

Blaine was looking for information on details of Pump and Sluice Pits for Tank 241-AZ-101. I donot have drawings but I could find the following information in old SAR document (SD-HS-SAR-010,Rev.1).

Above each of the 241-AZ tanks is a Pump Pit, located in the center of the tank, and two Sluice Pits located opposite to each other. The Pump Pits have approximate inside dimensions of 8 ft by 12 ft by 7 ft deep with 2.5 ft thick concrete cover blocks. The walls are 1 ft thick concrete. The Sluice Pits have approximate inside dimensions of 6 ft by 8 ft by 7 ft deep with 2 ft thick concrete cover blocks. The walls are 1 ft thick concrete.

The pump and sluice pit covers are purposely not air tight to permit some air leakage into the tank. The pits have drains and base plate openings for a pump or sluice nozzle, going directly into the vapor space of the tanks. Air can leak in through the cracks between cover blocks and the penetrations in the blocks (i.e., holes for mechanisms to operate the sluice nozzle, valves, etc.).

I hope this information is correct and represen present conditions. Hope this is the information that you are looking for and to make sure Blaine can verify this.

Thanks
Sathya

From: Blaine-A-Crea@RL.gov
Sent: Monday, April 10, 2000 9:44 AM
To: plys@Fauske.com
Cc: Thomas_G_Tom_Goetz@APIMC01.RL.GOV; David_R_Bratzel@APIMC01.RL.GOV
Subject: RE: DST Inlet Information Needs

The only information that I have been able to come up with on filter failure threshold is from ASME AGA-1. This is the standard that all HEPA filters must meet.

The performance test requires that they withstand a differential pressure of 10 inches of water while subjected to an air stream that contains 1 lbm water droplets /1000 cubic feet of air for an hour. The airflow rate during this test is adjusted to maintain the 10 inches of water differential pressure throughout the test.

The filter is a 500 SCFM rated filter. That means that it has an initial (clean) pressure drop of 1 inch of water at 500 SCFM. Since the pressurization of the dome will be a back flow it would seem reasonable that this would be the filter characteristic at the initiation of the backflow sequence.

RPP-62 13 REV I

From: K_Sathyanarayana@RL.gov
Sent: Monday, April 10, 2000 12:32 PM
To: plys@Fauske.com
Cc: David_R_Bratzel@apimc01.rl.gov; Blaine_A_Crea@apimc01.rl.gov;
K_Sathyanarayana@apimc01.rl.gov
Subject: RE: Pumps and Sluice Pits Information

Marty-

The primary Tank Ventilation System contains individual controlled air inlets and a common off-gas exhaust for the four AY and AZ Tank Farm waste tanks. The individual tank air inlet consists of a heater, pre-filter, high-efficiency particulate air (HEPA) filter, flow control valve and a vacuum relief valve.

Inlet Equipment: Heater, Pre-filter and HEPA filter

1. The outside air inlet has an electric 3-phase heater to protect the filters from excessive humidity or frost. Heaters are sized for an air flow of 100 to 500 cfm.

2. The pre-filter protects the HEPA filter from unnecessary particulate loading which would shorten its life. The pre-filter efficiency is about 25 to 30% per ASHRAE Standard 52-68. It is 12" by 24" by 2", UL Class 1, fiber glass media with nonflammable frame. The filter surface area is at least 8.5 ft².

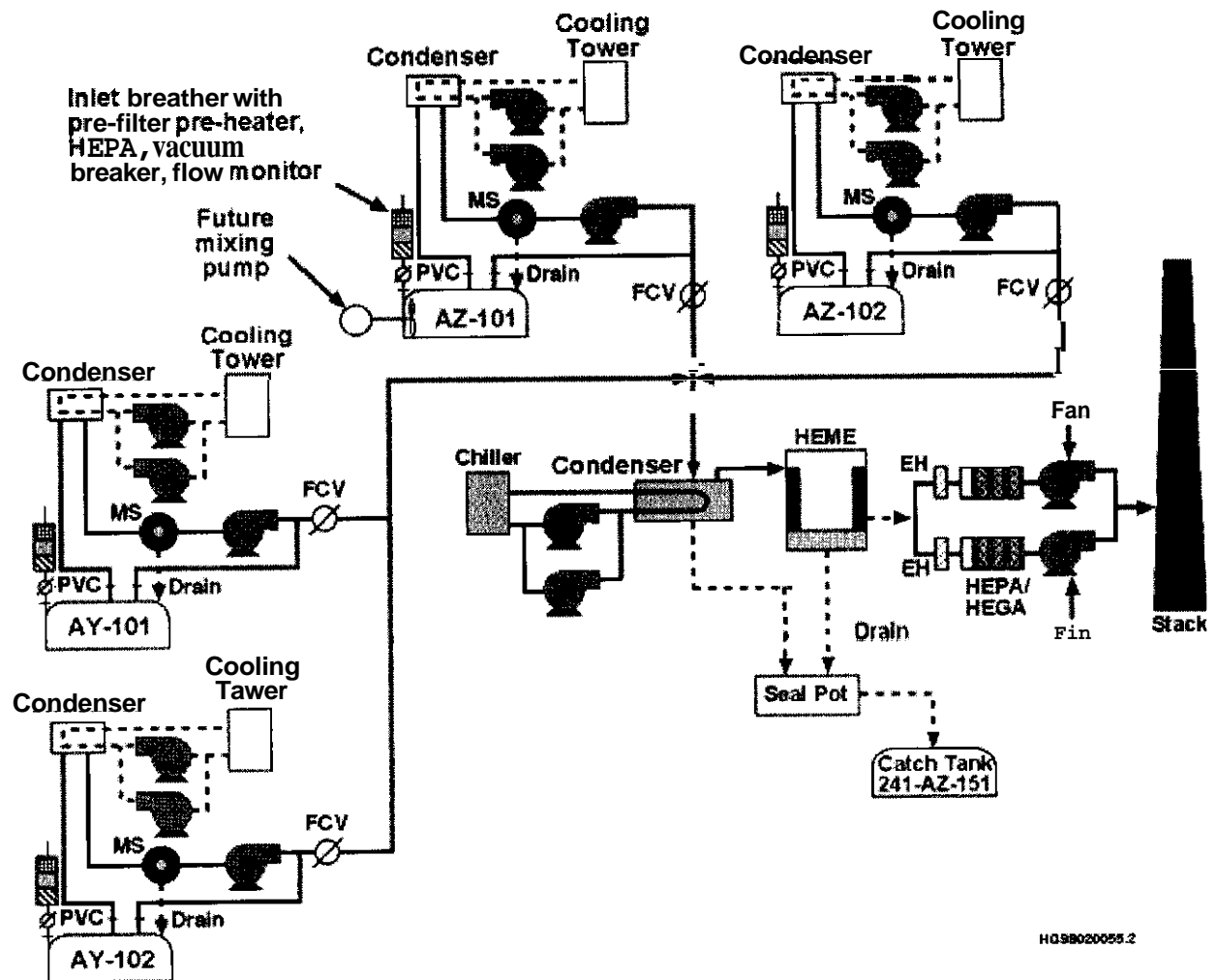
3. The HEPA filter is necessary to protect the environment against potential backflow from the waste tank inlet. The filter is nuclear grade, 12" by 24" by 1 1/2" with a nominal rating of 500 cfm. The operating pressure drop of 3" of water for the nominal flow rate. The maximum pressure for leak is 10" of water gauge (I need to get confirmation of this value).

The inlet pipe is 6 inches diameter schedule 40.

Thanks
Sathya

A.2 DRAWINGS

Figure A-1. System Schematic Diagram.



HQS8020055.2

Figure A-2. Structural Concrete Sluicing Pit Plans - Part 1 of 2.

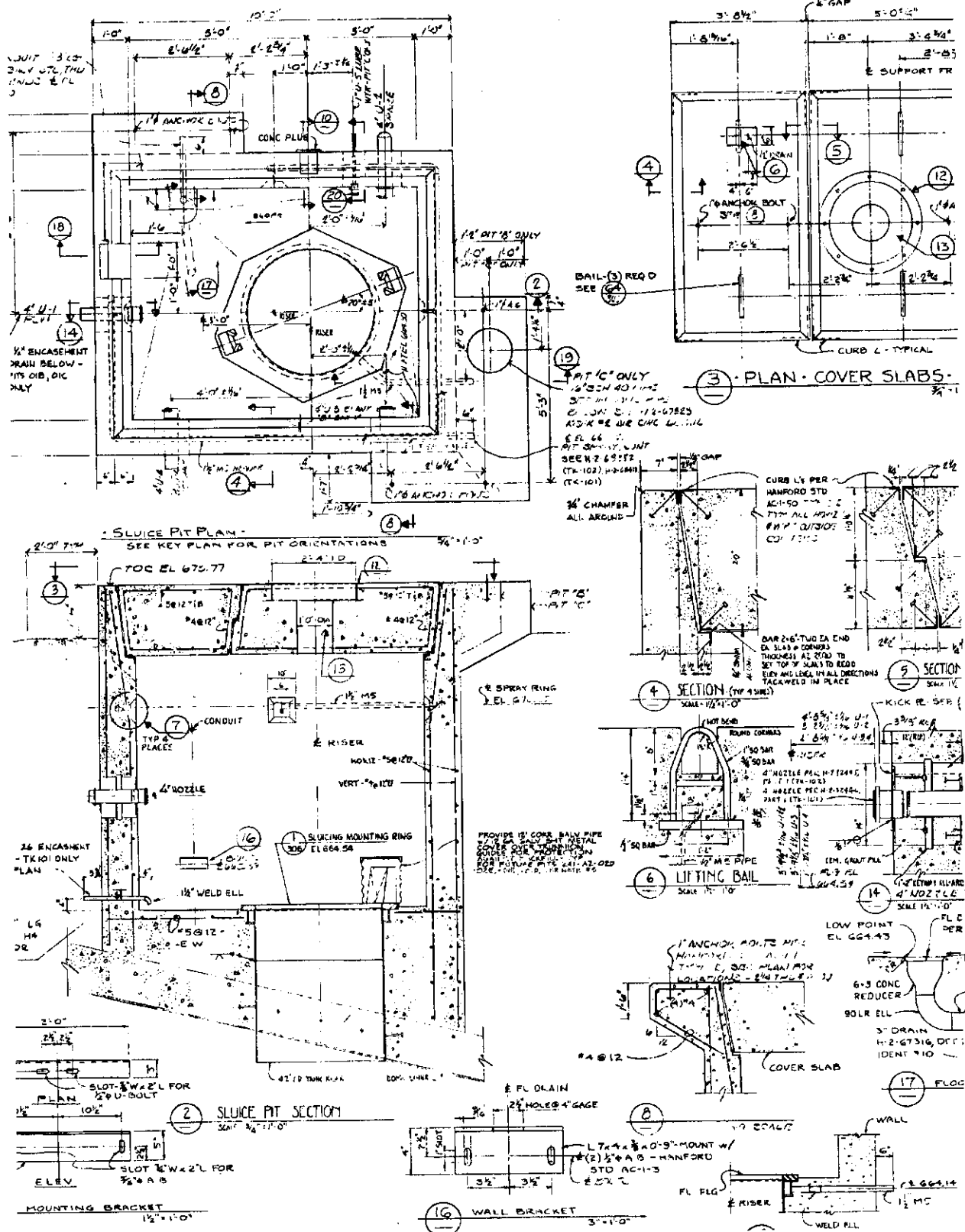


Figure A-3. Structural Concrete Sluicing Pit Plans - Part 2 of 2.

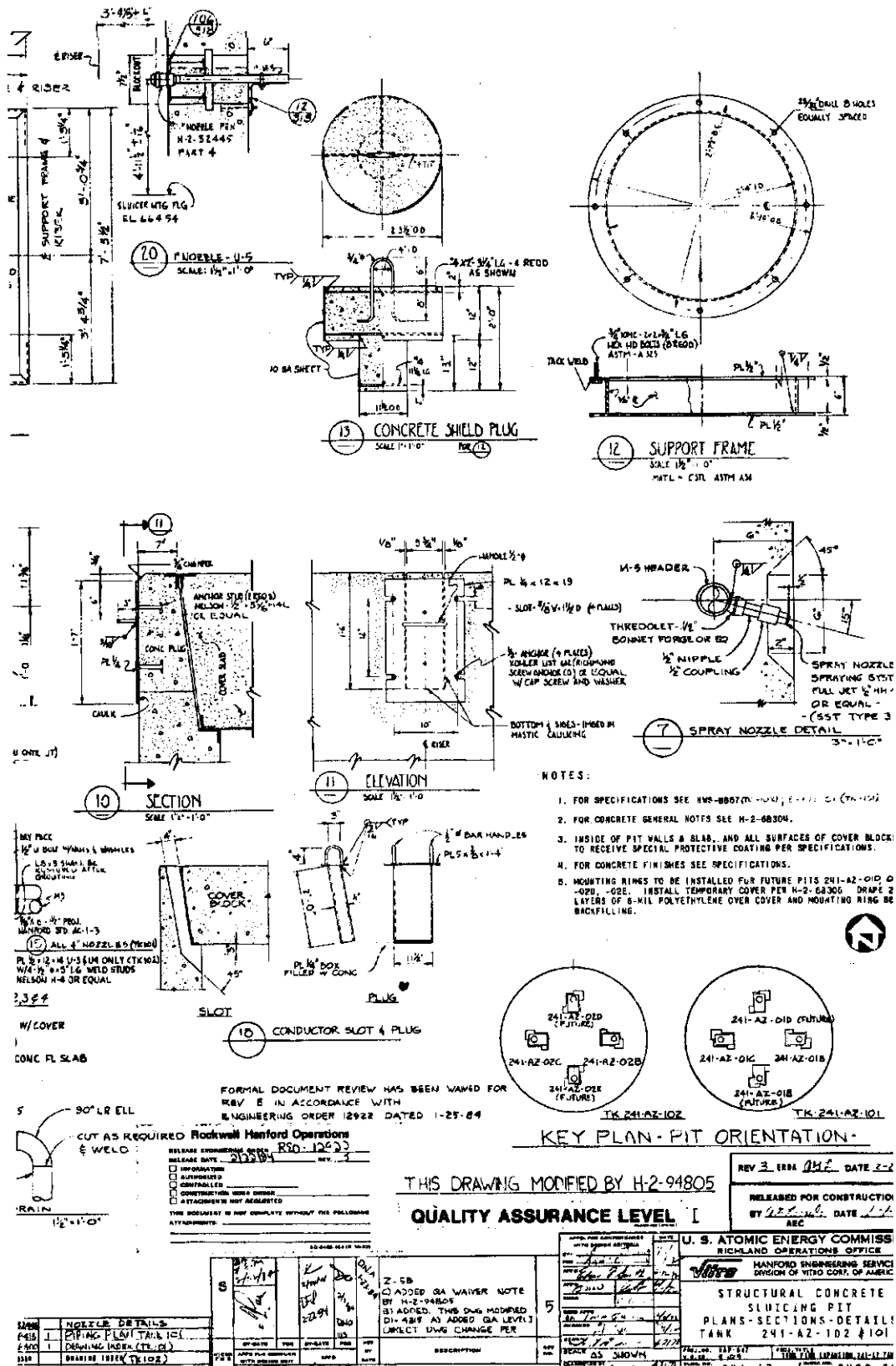


Figure A-4. Structural Concrete Pump Pit Plans - Part 1 of 2.

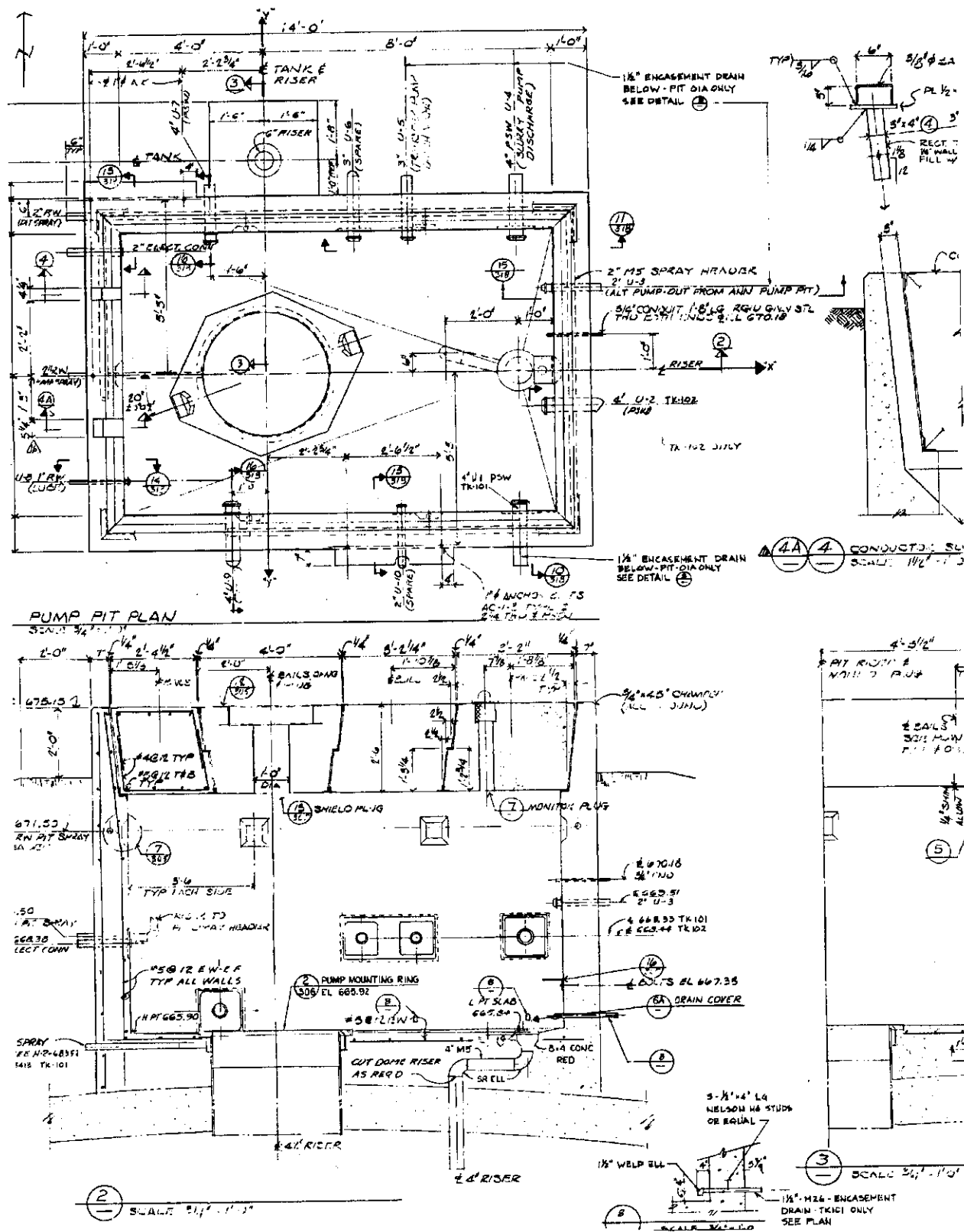


Figure A-5. Structural Concrete Pump Pit Plans - Part 2 of 2

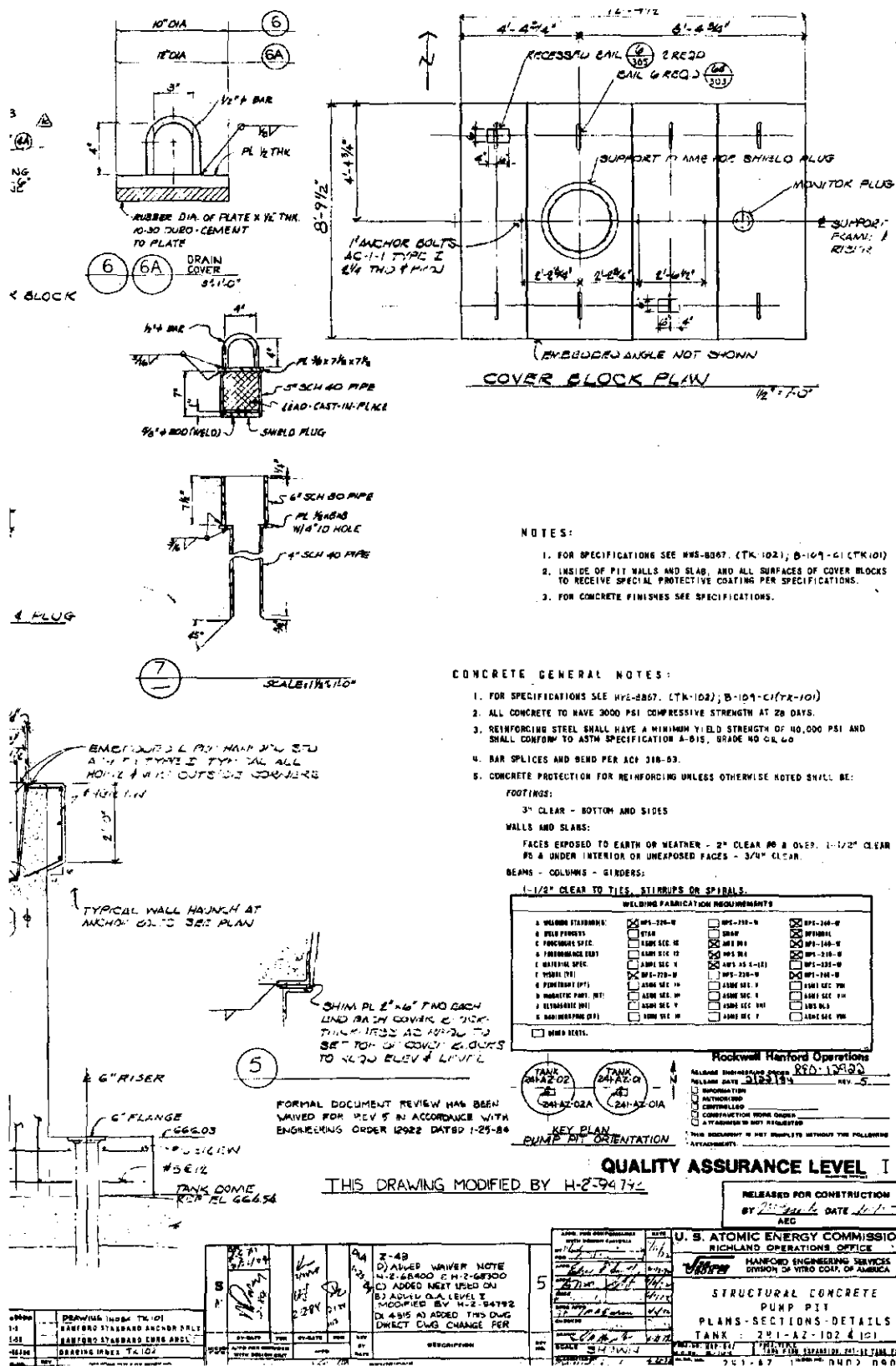
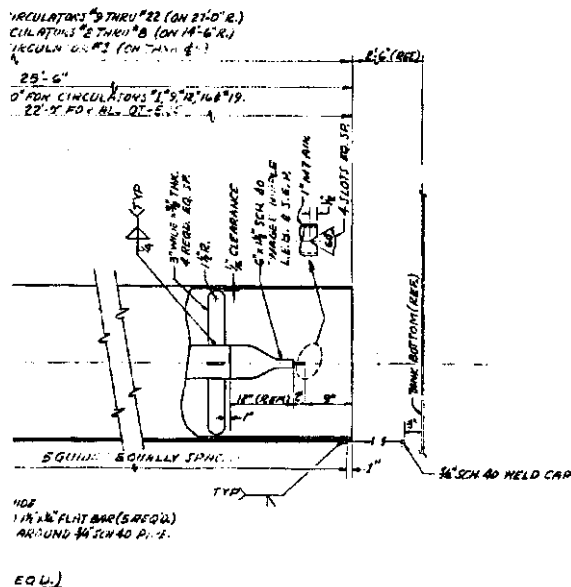


Figure A-7. Air Lift Circulator and Riser Extension Details - Part 2 of 2.



GENERAL NOTES:

1. NUMBER REQUIRED PER DETAIL IS FOR ONE TANK ONLY.
2. FOR CIRCULATOR NUMBERS, & LOCATION SEE DWG H-2-67314 FOR TK-10
H-2-67315 FOR TK-102.
3. PROPER SIZE STUDS, NUTS AND 1/16" THICK ASBESTOS GASKET SHALL
BE SUPPLIED FOR ALL TANK RISERS.
4. MATERIAL TO BE AS FOLLOWS UNLESS OTHERWISE NOTED:
 - a. PIPE AND PIPE FITTINGS: ASTM A53, C'STL (TYPE E OR G)
OR A-134
 - b. FLANGES: ASTM A184, GRADE 1, C'STL
DR B57H A30
 - c. PLATE AND FLATBAR: ASTM A36, C'STL
5. TOLERANCE: 1/8" UNLESS NOTED OTHERWISE.

SEE DWG. H-2-67316
DET. 1-8 FOR #3
DET. 2 FOR #10
DET. 4 FOR #9, #11 & #30

SCM 40 PIPE FOR #9, 11 & 30
SCM 40 PIPE FOR #10
SCM 40 PIPE FOR #3

TANK BOTTOM (P.D.)

VISCH. (1960)
URAIN (1962)
DRAIN (1962)
2.7 URAIN (1962)
URAIN (1962)

N-2-67816		PENETRATIONS OUTSIDE TUBES & JOINTS
N-2-67815		PLANT TUBING PENETRATIONS SCHEDULE
N-2-67814		PLANT TUBING PENETRATIONS SCHEDULE
N-2-67240		SEALING INDEX

NO		DATE		TIME		CHECKED FOR AS-BUILT ADDED DETAIL IN ENF-8	
BY DATE	FOR	BY DATE	FOR	BY DATE	DESCRIPTION		
ADD FOR DETAIL WITH DESIGN SET		ADD		DATE			

[illegible]

A.3 TRANSMITTED DATABASE SPREADSHEET

Tank Name	Grad (cfm) HGR from Radiolysis	Gtherm (cfm) HGR from Thermolysis	Gcorr (cfm) HGR from Corrosion	(Grad) % Percent HGR from Radiolysis	(Gtherm) % Percent HGR from Thermolysis	(Gcorr) % Percent HGR from Corrosion	Gmod (cfm) Total HGR from Model	Gmod (L/Day) Total HGR from Model	Sr-90 in Waste (uCi/g)	Cs137 in Waste (uCi/g)	Density (g/ml)	Waste Volume (kL)	Waste Volume (ft3)	H2O (wt%)	Power Load (watt)
241-AN-101 Convective	7.86E-05	5.07E-06	3.34E-04	18.8%	1.2%	80.0%	4.18E-04	17	5.04E+02	8.48E+01	1.22	606	21,389	67%	2.79E+03
Non-Convective	7.03E-06	4.02E-06	5.44E-05	10.7%	6.1%	83.1%	6.54E-05	3	3.84E-02	7.65E+01	1.16	481	16,978	70%	2.02E+02
	7.16E-05	1.05E-06	2.80E-04	20.3%	0.3%	79.4%	3.52E-04	14	2.04E+03	1.10E+02	1.46	125	4,412	56%	2.59E+03
241-AN-102 Convective Layer	4.05E-03	5.33E-03	7.19E-04	40.1%	52.8%	7.1%	1.01E-02	414	6.36E+01	2.58E+02	1.42	4,013	141,703	48%	9.34E+03
Non-Convective	3.62E-03	4.93E-03	4.16E-04	40.4%	55.0%	4.6%	8.97E-03	367	5.46E+01	2.57E+02	1.41	3,676	129,805	49%	8.19E+03
	4.29E-04	4.04E-04	3.03E-04	37.8%	35.6%	26.7%	1.14E-03	47	1.56E+02	2.63E+02	1.50	337	11,898	41%	1.15E+04
241-AN-103 Convective Layer	1.04E-03	1.43E-03	6.76E-04	32.8%	45.9%	21.4%	3.16E-03	130	1.33E+00	4.43E+02	1.58	3,626	128,067	41%	1.21E+04
Non-Convective	8.27E-04	9.25E-04	2.35E-04	41.6%	46.6%	11.8%	1.99E-03	81	1.50E-02	5.98E+02	1.49	2,074	73,258	49%	8.73E+03
	2.10E-04	5.26E-04	4.41E-04	17.8%	44.7%	37.5%	1.18E-03	48	2.86E+00	2.63E+02	1.71	1,552	54,810	32%	3.34E+03
241-AN-104 Convective Layer	7.64E-04	9.66E-04	2.59E-04	38.4%	48.6%	13.0%	1.99E-03	81	7.31E-02	5.38E+02	1.40	2,286	80,744	51%	8.13E+03
Non-Convective	4.70E-04	7.34E-04	4.58E-04	28.3%	44.2%	27.6%	1.66E-03	68	3.70E+01	3.83E+02	1.59	1,700	60,023	46%	5.56E+03
	1.25E-03	2.82E-03	7.48E-04	25.9%	58.6%	15.5%	4.81E-03	197	7.70E+00	3.01E+02	1.49	4,262	150,526	48%	9.34E+03
241-AN-105 Convective Layer	6.76E-04	1.61E-03	2.73E-04	26.4%	62.9%	10.7%	2.56E-03	105	3.11E-02	2.95E+02	1.42	2,411	85,155	50%	4.77E+03
Non-Convective	5.70E-04	1.21E-03	4.75E-04	25.3%	53.7%	21.1%	2.23E-03	92	1.67E+01	3.08E+02	1.58	1,851	65,371	44%	4.57E+03
	5.99E-06	3.43E-06	2.82E-04	2.1%	1.2%	96.8%	2.92E-04	12	2.12E+01	1.13E+02	1.39	148	5,214	52%	1.38E+02
241-AN-106 Convective Layer	1.89E-06	2.07E-06	9.42E-06	14.1%	15.5%	70.4%	1.34E-05	1	3.24E-02	6.55E+01	1.19	83	2,941	65%	3.06E+01
Non-Convective	4.10E-06	1.36E-06	2.73E-04	1.5%	0.5%	98.0%	2.78E-04	11	4.10E+01	1.58E+02	1.64	64	2,273	40%	1.08E+02
	6.96E-03	1.39E-03	7.13E-04	76.8%	15.4%	7.9%	9.07E-03	372	1.11E+02	2.87E+02	1.41	3,952	139,564	48%	1.17E+04
241-AN-107 Convective Layer	5.16E-03	1.09E-03	3.41E-04	78.3%	16.5%	5.2%	6.59E-03	270	8.50E+01	2.99E+02	1.37	3,017	106,545	50%	8.17E+03
Non-Convective	1.80E-03	3.07E-04	3.71E-04	72.7%	12.4%	15.0%	2.48E-03	102	1.87E+02	2.53E+02	1.56	935	33,019	40%	3.56E+03
	1.89E-04	1.44E-04	7.43E-04	17.6%	13.4%	69.0%	1.08E-03	44	1.09E-01	1.39E+02	1.27	4,221	149,055	58%	3.53E+03
241-AP-101 Convective Layer	1.89E-04	1.44E-04	7.43E-04	17.6%	13.4%	69.0%	1.08E-03	44	1.09E-01	1.39E+02	1.27	4,221	149,055	58%	3.53E+03
Non-Convective	not exist	not exist	not exist	not exist	not exist	not exist	not exist	not exist	0.00E+01	0.00E+01	0.00	0	0	0%	0.00E+01
	2.54E-04	1.74E-04	7.33E-04	21.9%	15.0%	63.1%	1.16E-03	48	1.19E+00	1.88E+02	1.20	4,134	145,981	75%	4.44E+03
241-AP-102 Convective Layer	2.54E-04	1.74E-04	7.33E-04	21.9%	15.0%	63.1%	1.16E-03	48	1.19E+00	1.88E+02	1.20	4,134	145,981	75%	4.44E+03
Non-Convective	not exist	not exist	not exist	not exist	not exist	not exist	not exist	not exist	0.00E+01	0.00E+01	0.00	0	0	0%	0.00E+01
	7.51E-05	2.68E-05	3.87E-04	15.3%	5.5%	79.2%	4.89E-04	20	2.93E-01	2.04E+02	1.38	1,079	38,099	98%	1.43E+03
241-AP-103 Convective Layer	7.51E-05	2.68E-05	3.87E-04	15.3%	5.5%	79.2%	4.89E-04	20	2.93E-01	2.04E+02	1.38	1,079	38,099	98%	1.43E+03
Non-Convective	not exist	not exist	not exist	not exist	not exist	not exist	not exist	not exist	0.00E+01	0.00E+01	0.00	0	0	0%	0.00E+01
	1.23E-06	8.32E-09	2.76E-04	0.4%	0.0%	99.6%	2.77E-04	11	8.23E-02	3.86E+00	1.00	91	3,208	97%	1.71E+00
241-AP-104 Convective Layer	1.23E-06	8.32E-09	2.76E-04	0.4%	0.0%	99.6%	2.77E-04	11	8.23E-02	3.86E+00	1.00	91	3,208	97%	1.71E+00
Non-Convective	not exist	not exist	not exist	not exist	not exist	not exist	not exist	not exist	0.00E+01	0.00E+01	0.00	0	0	0%	0.00E+01
	7.85E-05	8.19E-05	5.93E-04	13.6%	11.5%	74.9%	7.97E-04	32	3.48E+00	1.44E+02	1.37	2,896	102,267	60%	2.78E+03
241-AP-105 Convective Layer	7.85E-05	8.19E-05	5.93E-04	13.6%	11.5%	74.9%	7.97E-04	32	3.48E+00	1.44E+02	1.37	2,896	102,267	60%	2.78E+03
Non-Convective	2.93E-05	9.26E-06	3.03E-04	8.6%	18.2%	64.4%	4.50E-04	18	1.96E-01	1.13E+02	1.34	2,559	90,369	62%	1.84E+03
	4.25E-06	2.15E-06	3.05E-04	1.4%	0.7%	97.9%	3.12E-04	13	3.20E-01	6.61E+01	1.11	352	12,432	94%	1.23E+02
241-AP-106 Convective Layer	4.25E-06	2.15E-06	3.05E-04	1.4%	0.7%	97.9%	3.12E-04	13	3.20E-01	6.61E+01	1.11	352	12,432	94%	1.23E+02
Non-Convective	not exist	not exist	not exist	not exist	not exist	not exist	not exist	not exist	0.00E+01	0.00E+01	0.00	0	0	0%	0.00E+01
	4.18E-05	1.12E-05	6.83E-04	5.7%	1.5%	92.8%	7.36E-04	30	3.24E-01	7.06E+01	1.13	3,695	130,474	89%	1.40E+03
241-AP-107 Convective Layer	4.18E-05	1.12E-05	6.83E-04	5.7%	1.5%	92.8%	7.36E-04	30	3.24E-01	7.06E+01	1.13	3,695	130,474	89%	1.40E+03
Non-Convective	not exist	not exist	not exist	not exist	not exist	not exist	not exist	not exist	0.00E+01	0.00E+01	0.00	0	0	0%	0.00E+01

Tank Name	Grad (cfm) HGR from Radiolysis	Gtherm (cfm) HGR from Thermolysis	Gcorr (cfm) HGR from Corrosion	(Grad)% Percent HGR from Radiolysis	(Gtherm)% Percent HGR from Thermolysis	(Gcorr)% Percent HGR from Corrosion	Gmod (cfm) Total HGR from Model	Gmod (L/Day) Total HGR from Model	Sr90 in Waste (uCi/g)	Cs137 in Waste (uCi/g)	Density (g/ml)	Waste Volume (kl.)	Waste Volume (ft3)	H2O (wt%)	Power Load (watt)
241-AP-108	2.16E-05	9.77E-06	4.23E-04	4.7%	2.1%	93.1%	4.55E-04	19	8.44E-01	8.46E+01	1.14	1.397	49,329	84%	6.45E+02
Convective Layer	2.16E-05	9.77E-06	4.23E-04	4.7%	2.1%	93.1%	4.55E-04	19	8.44E-01	8.46E+01	1.14	1.397	49,329	84%	6.45E+02
Non-Convective	not exist	not exist	not exist	not exist	not exist	not exist	not exist	not exist	0.00E+01	0.00E+01	0.00	0	0	0%	0.00E+01
241-AW-101	1.16E-03	2.02E-03	7.48E-04	29.5%	51.5%	19.0%	3.93E-03	161	9.17E-00	3.36E+02	1.46	4.262	150,526	47%	1.03E+04
Convective Layer	8.59E-04	1.46E-03	3.51E-04	32.2%	54.7%	13.2%	2.67E-03	109	3.22E-02	3.58E+02	1.40	3.104	109,619	49%	7.34E+03
Non-Convective	3.02E-04	5.62E-04	3.96E-04	24.0%	44.6%	31.5%	1.26E-03	52	3.02E+01	2.84E+02	1.63	1.158	40,907	43%	2.92E+03
241-AW-102	2.35E-05	1.59E-06	3.00E-04	7.2%	0.5%	92.3%	3.25E-04	13	5.13E+02	1.01E+02	1.29	303	10,695	59%	1.53E+03
Convective Layer	2.03E-06	9.99E-07	1.71E-05	10.1%	5.0%	85.0%	2.02E-05	1	3.51E-01	7.77E+01	1.13	151	5,347	88%	6.29E+01
Non-Convective	2.14E-05	5.87E-07	2.83E-04	7.0%	0.2%	92.8%	3.05E-04	12	9.12E+02	1.19E+02	1.45	151	5,347	40%	1.46E+03
241-AW-103	1.92E-04	1.94E-06	4.84E-04	28.3%	0.3%	71.4%	6.77E-04	28	7.47E-00	5.09E+01	1.20	1,931	68,178	65%	6.74E+02
Convective Layer	2.80E-05	7.45E-07	6.94E-05	28.5%	0.8%	70.7%	9.81E-05	4	2.24E-04	2.10E+01	1.02	613	21,656	93%	6.19E+01
Non-Convective	1.64E-04	1.19E-06	4.14E-04	28.2%	0.2%	71.5%	5.79E-04	24	1.02E+01	6.19E+01	1.29	1,317	46,521	55%	6.12E+02
241-AW-104	1.62E-04	2.38E-04	7.45E-04	14.2%	20.8%	65.0%	1.14E-03	47	9.91E-00	8.35E+01	1.30	4,236	149,590	75%	2.53E+03
Convective Layer	1.62E-04	1.98E-04	3.80E-04	21.9%	26.8%	51.3%	7.41E-04	30	1.29E+01	1.09E+02	1.25	3,361	118,710	82%	2.52E+03
Non-Convective	1.12E-07	3.95E-05	3.64E-04	0.0%	9.8%	90.2%	4.04E-04	17	1.69E-01	2.00E-01	1.47	874	30,881	53%	2.67E-00
241-AW-105	2.63E-05	3.04E-06	4.49E-04	5.5%	0.6%	93.9%	4.78E-04	20	4.50E+01	2.55E+01	1.21	1,624	57,350	73%	8.27E+02
Convective Layer	2.81E-07	1.12E-06	6.38E-05	0.4%	1.7%	97.8%	6.52E-05	3	4.61E-02	2.25E-00	1.02	564	19,919	93%	6.28E-00
Non-Convective	2.60E-05	1.92E-06	3.85E-04	6.3%	0.5%	93.2%	4.13E-04	17	6.36E+01	3.51E+01	1.31	1,060	37,431	66%	8.21E+02
241-AW-106	2.31E-04	2.77E-04	4.68E-04	23.6%	28.4%	48.0%	9.70E-04	40	1.63E+01	2.06E+02	1.45	1,791	63,232	57%	2.80E+03
Convective Layer	1.16E-04	1.41E-04	1.05E-04	32.0%	39.0%	29.1%	3.61E-04	15	2.32E+01	2.26E+02	1.38	927	32,752	59%	1.36E+03
Non-Convective	1.15E-04	1.37E-04	3.63E-04	18.7%	22.2%	59.1%	6.15E-04	25	3.18E+01	1.86E+02	1.53	863	30,480	55%	1.44E+03
241-AY-101	1.62E-03	1.66E-05	3.31E-04	82.3%	0.8%	16.8%	1.97E-03	81	2.93E+03	9.80E+01	1.23	583	20,587	58%	1.44E+04
Convective Layer	1.33E-05	3.80E-06	1.97E-05	36.1%	10.3%	53.6%	3.68E-05	2	1.75E-00	1.01E+02	1.08	174	6,149	84%	9.18E+01
Non-Convective	1.61E-03	1.28E-05	3.12E-04	83.2%	0.7%	16.1%	1.93E-03	79	3.97E+03	9.70E+01	1.30	409	14,438	82%	1.43E+04
241-AY-102	1.34E-02	1.12E-04	5.32E-04	95.4%	0.8%	3.8%	1.40E-02	575	2.83E+03	1.20E+02	1.18	2,355	83,150	88%	5.42E+04
Convective Layer	1.08E-04	4.44E-05	1.76E-04	33.0%	13.5%	53.5%	3.29E-04	13	8.29E-01	3.18E+01	1.09	1,556	54,943	98%	2.64E+02
Non-Convective	1.33E-02	6.73E-05	3.56E-04	96.9%	0.5%	2.6%	1.37E-02	562	7.28E+03	2.58E+02	1.35	799	28,207	56%	5.40E+04
241-AZ-101	7.04E-03	1.12E-03	6.27E-04	80.1%	12.8%	7.1%	8.79E-03	360	2.55E+03	1.35E+03	1.22	3,199	112,961	72%	9.12E+04
Convective Layer	1.97E-03	1.03E-03	3.42E-04	58.9%	30.8%	10.2%	3.34E-03	137	1.01E-00	1.34E+03	1.19	3,021	106,678	73%	2.27E+04
Non-Convective	5.07E-03	8.99E-05	2.86E-04	93.1%	1.7%	5.2%	5.44E-03	223	3.34E+04	1.48E+03	1.67	178	6,283	56%	6.85E+04
241-AZ-102	8.72E-03	1.21E-03	6.64E-04	82.3%	11.4%	6.3%	1.06E-02	434	2.30E+03	9.31E+02	1.14	3,524	124,458	80%	7.98E+04
Convective Layer	1.44E-03	7.84E-04	3.54E-04	55.9%	30.4%	13.7%	2.58E-03	106	5.90E-00	9.46E+02	1.10	3,131	110,555	84%	1.55E+04
Non-Convective	7.28E-03	4.26E-04	3.10E-04	90.8%	5.3%	3.9%	8.01E-03	328	1.58E+04	8.43E+02	1.49	394	13,903	56%	6.43E+04
241-SY-101	4.05E-03	1.86E-02	7.75E-04	17.3%	79.4%	3.3%	2.35E-02	961	1.35E+01	3.14E+02	1.50	4,501	158,948	38%	1.06E+04
Convective Layer	1.96E-03	9.56E-03	2.59E-04	16.6%	81.2%	2.2%	1.18E-02	483	8.00E-00	3.01E+02	1.39	2,286	80,744	41%	4.69E+03
Non-Convective	2.09E-03	9.06E-03	5.16E-04	17.9%	77.6%	4.4%	1.17E-02	478	1.85E+01	3.26E+02	1.61	2,214	78,204	35%	5.92E+03
241-SY-102	6.20E-05	6.44E-05	5.27E-04	9.5%	9.8%	80.7%	6.54E-01	27	1.62E+01	9.54E+01	1.22	2,317	81,813	81%	1.58E+03
Convective Layer	5.31E-05	5.75E-05	2.24E-04	15.9%	17.2%	67.0%	3.35E-04	14	1.21E-00	1.09E+02	1.18	1,984	70,049	87%	1.23E+03
Non-Convective	8.91E-06	6.93E-06	3.03E-04	2.8%	2.2%	95.0%	3.19E-04	13	8.96E+01	2.77E+01	1.44	333	11,764	51%	3.50E+02
241-SY-103	7.28E-04	1.82E-03	5.84E-04	23.3%	58.0%	18.7%	3.13E-03	128	1.71E-00	2.38E+02	1.49	2,816	99,459	40%	4.76E+03
Convective Layer	5.11E-04	1.07E-03	1.64E-04	29.3%	61.4%	9.4%	1.75E-03	72	2.08E-00	2.95E+02	1.47	1,446	51,067	47%	2.99E+03
Non-Convective	2.17E-04	7.44E-04	4.20E-04	15.7%	53.9%	30.4%	1.38E-03	57	1.33E-00	1.80E+02	1.51	1,370	48,393	34%	1.78E+03
241-A-101	1.09E-03	1.23E-02	1.40E-03	7.4%	83.1%	9.5%	1.48E-02	605	2.72E+01	2.45E+02	1.52	3,608	127,399	45%	7.34E+03
Convective Layer	6.74E-04	8.40E-03	1.00E-03	6.7%	83.4%	9.9%	1.01E-02	413	5.73E-02	2.77E+02	1.40	1,923	67,910	53%	3.52E+03
Non-Convective	4.17E-04	3.87E-03	3.95E-04	8.9%	82.6%	8.4%	4.68E-03	192	5.34E+01	2.14E+02	1.66	1,685	59,489	37%	3.81E+03
241-A-102	1.13E-04	5.82E-05	5.79E-04	15.1%	7.8%	77.2%	7.50E-04	31	7.49E+02	1.31E+02	1.61	155	5481	36%	1.41E+03

Tank Name	Grad (cfm) HGR from Radiolysis	Gtherm (cfm) HGR from Thermolysis	Gcorr (cfm) HGR from Corrosion	(Grad)% Percent HGR from Radiolysis	(Gtherm)% Percent HGR from Thermolysis	(Gcorr)% Percent HGR from Corrosion	Gmod (cfm) Total HGR from Model	Gmod (L/Day) Total HGR from Model	Sr90 in Waste (uCi/g)	Cs137 in Waste (uCi/g)	Density (g/ml)	Waste Volume (kL)	Waste Volume (ft3)	H2O (wt%)	Power Load (watt)
Convective Layer	3.69E-06	7.53E-06	3.51E-06	25.0%	51.1%	23.8%	1.47E-05	1	4.00E-00	2.83E+02	1.40	15	535	55%	2.89E+01
Non-Convective	1.09E-04	5.06E-05	5.75E-04	14.9%	6.9%	78.2%	7.36E-04	30	8.18E+02	1.17E+02	1.63	140	4946	34%	1.38E+03
241-A-103	9.10E-03	6.87E-04	8.62E-04	85.5%	6.5%	8.1%	1.07E-02	436	8.21E+03	6.38E+02	1.30	1404	49596	44%	1.06E+05
A-103 liquid	4.49E-06	1.77E-05	4.35E-06	16.9%	66.7%	16.4%	2.66E-05	1	1.67E-00	2.30E+02	1.48	19	668	75%	3.07E+01
A-103 solid	9.10E-03	6.70E-04	8.58E-04	85.6%	6.3%	8.1%	1.06E-02	435	8.34E+03	6.44E+02	1.30	1385	48928	44%	1.06E+05
241-A-104	3.89E-03	4.67E-04	5.72E-04	78.9%	9.5%	11.6%	4.93E-03	202	1.69E+04	4.49E+02	1.64	106	3743	44%	2.00E+04
A-104 liquid	not exist	not exist	not exist	not exist	not exist	not exist	not exist	not exist	1.29E+01	1.09E+02	1.17	0	0	75%	0.00E+01
A-104 solid	3.89E-03	4.67E-04	5.72E-04	78.9%	9.5%	11.6%	4.93E-03	202	1.69E+04	4.49E+02	1.64	106	3743	44%	2.00E+04
241-A-105	na	na	na	na	na	na	na	na	na	na	na	na	na	na	na
A-105 liquid	not exist	not exist	not exist	not exist	not exist	not exist	not exist	not exist	not exist	not exist	not exist	not exist	not exist	not exist	not exist
A-105 solid	4.62E-04	3.13E-04	6.70E-04	32.0%	21.7%	46.4%	1.45E-03	59	9.73E+02	1.25E+02	1.55	473	16710	44%	5.21E+03
241-A-106	not exist	not exist	not exist	not exist	not exist	not exist	not exist	not exist	1.29E+01	1.09E+02	1.17	0	0	75%	0.00E+01
A-106 liquid	4.62E-04	3.13E-04	6.70E-04	32.0%	21.7%	46.4%	1.45E-03	59	9.73E+02	1.25E+02	1.55	473	16710	44%	5.21E+03
A-106 solid	5.66E-04	3.42E-03	1.19E-03	10.9%	66.1%	23.0%	5.17E-03	212	3.06E+01	2.37E+02	1.57	2831	99994	42%	5.89E+03
241-A-X-101	3.14E-04	1.91E-03	3.35E-04	12.2%	74.7%	13.1%	2.56E-03	105	1.80E+01	2.77E+02	1.48	1461	51601	48%	2.82E+03
AX-101 liquid	2.52E-04	1.51E-03	8.53E-04	9.7%	57.7%	32.7%	2.61E-03	107	5.93E+01	2.00E+02	1.67	1370	48393	36%	3.07E+03
AX-101 solid	1.06E-04	1.19E-05	5.55E-04	15.8%	1.8%	82.4%	6.73E-04	28	5.93E+03	2.67E+02	1.45	114	4010	34%	1.94E+03
AX-102 liquid	not exist	not exist	not exist	not exist	not exist	not exist	not exist	not exist	8.00E-00	3.01E+02	1.39	0	0	51%	0.00E+01
AX-102 solid	1.06E-04	1.19E-05	5.55E-04	15.8%	1.8%	82.4%	6.73E-04	28	5.93E+03	2.67E+02	1.45	114	4010	34%	1.94E+03
241-A-X-103	5.82E-04	4.05E-04	6.42E-04	35.7%	24.8%	39.4%	1.63E-03	67	7.41E+02	2.02E+02	1.62	424	14972	43%	4.07E+03
AX-103 liquid	not exist	not exist	not exist	not exist	not exist	not exist	not exist	not exist	8.00E-00	3.01E+02	1.39	0	0	51%	0.00E+01
AX-103 solid	5.82E-04	4.05E-04	6.42E-04	35.7%	24.8%	39.4%	1.63E-03	67	7.41E+02	2.02E+02	1.62	424	14972	43%	4.07E+03
241-A-X-104	1.13E-04	3.02E-07	5.48E-04	17.1%	0.0%	82.9%	6.61E-04	27	5.18E+04	1.24E+03	1.80	30	1069	7%	1.92E+04
AX-104 liquid	not exist	not exist	not exist	not exist	not exist	not exist	not exist	not exist	1.29E+01	1.09E+02	1.17	0	0	75%	0.00E+01
AX-104 solid	1.13E-04	3.02E-07	5.48E-04	17.1%	0.0%	82.9%	6.61E-04	27	5.18E+04	1.24E+03	1.80	30	1069	7%	1.92E+04
241-B-101	6.40E-05	2.55E-04	6.43E-04	6.6%	26.5%	66.9%	9.62E-04	39	4.10E+01	1.58E+02	1.48	428	15106	29%	6.46E+02
B-101 liquid	not exist	not exist	not exist	not exist	not exist	not exist	not exist	not exist	8.00E-00	3.01E+02	1.39	0	0	50%	0.00E+01
B-101 solid	6.40E-05	2.55E-04	6.43E-04	6.6%	26.5%	66.9%	9.62E-04	39	4.10E+01	1.58E+02	1.48	428	15106	29%	6.46E+02
241-B-102	2.51E-06	4.64E-06	5.46E-04	0.5%	0.8%	98.7%	5.53E-04	23	3.36E-00	4.86E+01	1.73	121	4278	21%	5.27E+01
B-102 liquid	2.01E-06	1.11E-06	3.35E-06	31.0%	17.1%	51.8%	6.47E-06	0	8.00E-00	3.01E+02	1.39	15	535	51%	3.10E+01
B-102 solid	5.00E-07	3.53E-06	5.43E-04	0.1%	0.6%	99.3%	5.47E-04	22	2.84E-00	2.04E+01	1.78	106	3743	18%	2.17E+01
241-B-103	1.70E-06	1.66E-05	5.67E-04	0.3%	2.8%	96.9%	5.85E-04	24	1.92E-00	1.38E+01	1.78	223	7887	45%	3.09E+01
B-103 liquid	not exist	not exist	not exist	not exist	not exist	not exist	not exist	not exist	8.00E-00	3.01E+02	1.39	0	0	51%	0.00E+01
B-103 solid	1.70E-06	1.66E-05	5.67E-04	0.3%	2.8%	96.9%	5.85E-04	24	1.92E-00	1.38E+01	1.78	223	7887	45%	3.09E+01
241-B-104	9.45E-04	2.23E-05	8.34E-04	52.5%	1.2%	46.3%	1.80E-03	74	2.04E+03	1.10E+02	1.22	1404	49596	47%	2.42E+04
B-104 liquid	1.15E-07	6.40E-08	8.42E-07	11.3%	6.3%	82.4%	1.02E-06	0	1.29E+01	1.09E+02	1.17	4	134	52%	2.66E-00
B-104 solid	9.45E-04	2.23E-05	8.34E-04	52.5%	1.2%	46.3%	1.80E-03	74	2.04E+03	1.10E+02	1.22	1401	49462	47%	2.42E+04
241-B-105	7.63E-05	2.27E-05	6.51E-04	10.2%	3.0%	86.8%	7.50E-04	31	3.08E+02	1.52E+02	1.64	598	21122	32%	2.73E+03
B-105 liquid	not exist	not exist	not exist	not exist	not exist	not exist	not exist	not exist	8.00E-00	3.01E+02	1.39	0	0	51%	0.00E+01
B-105 solid	7.63E-05	2.27E-05	6.51E-04	10.2%	3.0%	86.8%	7.50E-04	31	3.08E+02	1.52E+02	1.64	598	21122	32%	2.73E+03
241-B-106	3.28E-04	5.97E-06	6.18E-04	34.5%	0.6%	64.9%	9.53E-04	39	2.03E+03	1.10E+02	1.46	443	15641	60%	9.10E+03
B-106 liquid	1.08E-07	4.55E-08	8.39E-07	10.9%	4.6%	84.5%	9.93E-07	0	1.29E+01	1.09E+02	1.17	4	134	67%	2.66E-00
B-106 solid	3.28E-04	5.87E-06	6.17E-04	34.5%	0.6%	64.9%	9.53E-04	39	2.04E+03	1.10E+02	1.46	439	15507	60%	9.10E+03
241-B-107	2.14E-04	2.85E-05	6.51E-04	23.9%	3.2%	72.9%	8.93E-04	37	7.25E+02	1.30E+02	1.66	625	22058	36%	5.67E+03
B-107 liquid	4.36E-07	2.32E-07	8.29E-07	29.1%	15.5%	55.4%	1.50E-06	0	4.00E-00	2.83E+02	1.40	4	134	57%	7.22E-00
B-107 solid	2.13E-04	2.82E-05	6.50E-04	23.9%	3.2%	72.9%	8.91E-04	37	7.28E+02	1.30E+02	1.66	621	21924	36%	5.66E+03
241-B-108	3.17E-06	1.11E-05	5.96E-04	0.5%	1.8%	97.7%	6.10E-04	25	1.88E+01	2.13E+01	1.60	356	12566	31%	1.29E+02
B-108 liquid	not exist	not exist	not exist	not exist	not exist	not exist	not exist	not exist	4.00E-00	2.83E+02	1.40	0	0	79%	0.00E+01

Tank Name	Grad (cfm) HGR from Radiolysis	Gtherm (cfm) HGR from Thermolysis	Gcorr (cfm) HGR from Corrosion	(Grad)% Percent HGR from Radiolysis	(Gtherm)% Percent HGR from Thermolysis	(Gcorr)% Percent HGR from Corrosion	Gmod Total HGR from Model	Gmod (L/Day) Total HGR from Model	Sr-90 in Waste (uCi/g)	Cs-137 in Waste (uCi/g)	Density (g/ml)	Waste Volume (kL)	Waste Volume (ft3)	H2O (wt %)	Power Load (watt)
B-108 solid	3.17E-06	1.11E-05	5.96E-04	0.5%	1.8%	97.7%	6.10E-04	25	1.88E+01	2.13E+01	1.60	356	12566	31%	1.29E+02
241-B-109	2.19E-04	4.18E-05	6.27E-04	24.6%	4.7%	70.6%	8.88E-04	36	6.49E+02	1.32E+02	1.87	481	16978	40%	4.46E+03
B-109 liquid	not exist	not exist	not exist	not exist	not exist	not exist	not exist	not exist	4.00E-00	2.83E+02	1.40	0	0	55%	0.00E+01
B-109 solid	2.19E-04	4.18E-05	6.27E-04	24.6%	4.7%	70.6%	8.88E-04	36	6.49E+02	1.32E+02	1.87	481	16978	40%	4.46E+03
241-B-110	2.41E-05	1.24E-05	7.37E-04	3.1%	1.6%	95.3%	7.73E-04	32	9.87E+01	1.40E+01	1.36	931	32886	44%	9.19E+02
B-110 liquid	1.20E-07	7.46E-08	8.51E-07	11.5%	7.1%	81.4%	1.05E-06	0	1.29E+01	1.09E+02	1.17	4	134	75%	2.66E-00
B-110 solid	2.40E-05	1.24E-05	7.36E-04	3.1%	1.6%	95.3%	7.72E-04	32	9.90E+01	1.37E+01	1.36	927	32752	44%	9.17E+02
241-B-111	6.48E-05	1.15E-05	7.26E-04	8.1%	1.4%	90.5%	8.03E-04	33	2.47E+02	1.58E+02	1.19	897	31683	44%	2.56E+03
B-111 liquid	1.23E-07	8.67E-08	8.48E-07	11.7%	8.2%	80.1%	1.06E-06	0	1.29E+01	1.09E+02	1.17	4	134	75%	2.66E-00
B-111 solid	6.47E-05	1.14E-05	7.25E-04	8.1%	1.4%	90.5%	8.02E-04	33	2.48E+02	1.58E+02	1.19	893	31549	44%	2.56E+03
241-B-112	4.37E-06	1.50E-07	5.47E-04	0.8%	0.0%	99.2%	5.52E-04	23	1.65E+02	8.03E+01	1.27	125	4412	47%	2.35E+02
B-112 liquid	6.36E-07	2.19E-08	2.51E-06	20.0%	0.7%	79.3%	3.17E-06	0	1.65E+02	8.03E+01	1.27	11	401	75%	2.13E+01
B-112 solid	3.73E-06	1.28E-07	5.45E-04	0.7%	0.0%	99.3%	5.48E-04	22	1.65E+02	8.03E+01	1.27	114	4010	44%	2.13E+01
241-B-201	1.45E-07	4.79E-07	1.26E-04	0.1%	0.4%	99.5%	1.27E-04	5	3.82E-00	4.26E-02	1.25	110	3877	45%	4.90E-00
B-201 liquid	9.72E-08	2.58E-08	3.09E-06	3.0%	0.8%	96.2%	3.22E-06	0	1.29E+01	1.09E+02	1.17	4	134	75%	2.66E-00
B-201 solid	4.80E-08	4.53E-07	1.23E-04	0.0%	0.4%	99.6%	1.23E-04	5	1.99E-00	7.64E-01	1.25	106	3743	44%	2.24E-00
241-B-202	1.09E-07	8.97E-07	1.21E-04	0.1%	0.7%	99.2%	1.22E-04	5	3.82E-00	9.61E-02	1.30	102	3609	68%	3.45E-00
B-202 liquid	not exist	not exist	not exist	not exist	not exist	not exist	not exist	not exist	1.29E+01	1.09E+02	1.17	0	0	83%	0.00E+01
B-202 solid	1.09E-07	8.97E-07	1.21E-04	0.1%	0.7%	99.2%	1.22E-04	5	3.82E-00	9.61E-02	1.30	102	3609	68%	3.45E-00
241-B-203	1.05E-07	9.35E-07	1.93E-04	0.1%	0.5%	99.5%	1.94E-04	8	3.86E-01	2.26E-00	1.19	193	6818	76%	3.04E-00
B-203 liquid	9.41E-08	2.11E-08	3.08E-06	2.9%	0.7%	96.4%	3.19E-06	0	1.29E+01	1.09E+02	1.17	4	134	89%	2.66E-00
B-203 solid	1.14E-08	9.14E-07	1.90E-04	0.0%	0.5%	99.5%	1.91E-04	8	1.40E-01	1.59E-01	1.19	189	6684	76%	3.80E-01
241-B-204	5.86E-05	7.72E-07	1.91E-04	23.4%	0.3%	76.3%	2.50E-04	10	2.01E+03	1.10E+02	1.19	189	6684	45%	3.14E+03
B-204 liquid	9.03E-08	2.71E-08	3.09E-06	2.8%	0.8%	96.3%	3.21E-06	0	1.29E+01	1.09E+02	1.05	4	134	89%	2.39E-00
B-204 solid	5.85E-05	7.45E-07	1.88E-04	23.7%	0.3%	76.0%	2.47E-04	10	2.04E+03	1.10E+02	1.19	185	6550	44%	3.13E+03
241-BX-101	6.85E-06	1.64E-06	5.60E-04	1.2%	0.3%	98.5%	5.68E-04	23	2.17E+02	8.33E+01	1.72	163	5748	20%	5.16E+02
BX-101 liquid	1.06E-07	1.09E-07	8.44E-07	10.0%	10.3%	79.8%	1.06E-06	0	2.56E+00	8.36E+01	1.28	4	134	75%	2.00E-00
BX-101 solid	6.75E-06	1.53E-06	5.59E-04	1.2%	0.3%	98.5%	5.67E-04	23	2.20E+02	8.33E+01	1.73	159	5615	19%	5.14E+02
241-BX-102	4.41E-06	1.87E-06	5.99E-04	0.7%	0.3%	99.0%	6.06E-04	25	7.72E+01	3.07E+01	0.76	363	12833	44%	1.82E+02
BX-102 liquid	not exist	not exist	not exist	not exist	not exist	not exist	not exist	not exist	1.29E+01	1.09E+02	1.17	0	0	75%	0.00E+01
BX-102 solid	4.41E-06	1.87E-06	5.99E-04	0.7%	0.3%	99.0%	6.06E-04	25	7.72E+01	3.07E+01	0.76	363	12833	44%	1.82E+02
241-BX-103	1.37E-05	5.78E-06	5.81E-04	2.3%	1.0%	96.8%	6.00E-04	25	1.07E+02	5.07E+01	1.64	269	9491	50%	4.20E+02
BX-103 liquid	9.22E-07	8.68E-07	7.57E-06	9.8%	9.3%	80.9%	9.36E-06	0	2.56E+00	8.36E+01	1.28	34	1203	75%	1.80E+01
BX-103 solid	1.28E-05	4.91E-06	5.73E-04	2.2%	0.8%	97.0%	5.91E-04	24	1.18E+02	4.71E+01	1.69	235	8288	47%	4.02E+02
241-BX-104	4.00E-05	1.28E-05	6.15E-04	6.0%	1.9%	92.1%	6.68E-04	27	2.24E+02	8.13E+01	1.72	375	13235	45%	1.21E+03
BX-104 liquid	5.08E-07	4.91E-07	2.57E-06	14.2%	13.8%	72.0%	3.57E-06	0	1.78E+00	1.29E+02	1.29	11	401	75%	9.06E-00
BX-104 solid	3.94E-05	1.24E-05	6.13E-04	5.9%	1.9%	92.2%	6.65E-04	27	2.29E+02	8.02E+01	1.73	363	12833	44%	1.20E+03
241-BX-105	4.64E-06	2.61E-06	5.62E-04	0.8%	0.5%	98.7%	5.70E-04	23	1.10E+02	5.24E+01	1.65	193	6818	18%	3.13E+02
BX-105 liquid	1.03E-06	8.46E-07	4.19E-06	16.9%	14.0%	69.1%	6.07E-06	0	7.44E-00	1.16E+02	1.29	19	668	75%	1.46E+01
BX-105 solid	3.61E-06	1.76E-06	5.58E-04	0.6%	0.3%	99.0%	5.64E-04	23	1.18E+02	4.71E+01	1.69	174	6149	13%	2.98E+02
241-BX-106	5.26E-06	1.45E-06	5.52E-04	0.9%	0.3%	98.8%	5.58E-04	23	1.18E+02	4.71E+01	1.69	144	5080	39%	2.46E+02
BX-106 liquid	not exist	not exist	not exist	not exist	not exist	not exist	not exist	not exist	1.29E+01	1.09E+02	1.17	0	0	75%	0.00E+01
BX-106 solid	5.26E-06	1.45E-06	5.52E-04	0.9%	0.3%	98.8%	5.58E-04	23	1.18E+02	4.71E+01	1.69	144	5080	39%	2.46E+02
241-BX-107	7.85E-06	1.58E-05	8.10E-04	0.9%	1.9%	97.2%	8.33E-04	34	9.59E-00	1.71E+01	1.44	1306	46120	51%	2.72E+02
BX-107 liquid	1.12E-07	5.43E-08	8.39E-07	11.1%	5.4%	83.5%	1.01E-06	0	1.29E+01	1.09E+02	1.17	4	134	75%	2.66E-00
BX-107 solid	1.74E-06	1.57E-05	8.09E-04	0.9%	1.9%	97.2%	8.32E-04	34	9.58E-00	1.69E+01	1.44	1302	45987	51%	2.70E+02
241-BX-108	1.90E-06	5.80E-07	5.41E-04	0.4%	0.1%	99.5%	5.43E-04	22	1.18E+02	1.45E+01	1.46	98	3476	28%	1.23E+02
BX-108 liquid	not exist	not exist	not exist	not exist	not exist	not exist	not exist	not exist	1.29E+01	1.09E+02	1.17	0	0	75%	0.00E+01
BX-108 solid	1.90E-06	5.80E-07	5.41E-04	0.4%	0.1%	99.5%	5.43E-04	22	1.18E+02	1.45E+01	1.46	98	3476	28%	1.23E+02

Tank Name	Grad (cfm) HGR from Radiolysis	Gtherm (cfm) HGR from Thermolysis	Gcorr (cfm) HGR from Corrosion	(Grad) % Percent HGR from Radiolysis	(Gtherm) % Percent HGR from Thermolysis	(Gcorr) % Percent HGR from Corrosion	Gmod (cfm) Total HGR from Model	Gmod (L/Day) Total HGR from Model	Sr90 in Waste (uCi/g)	Cs137 in Waste (uCi/g)	Density (g/ml)	Waste Volume (kL)	Waste Volume (ft3)	H2O (wt%)	Power Load (watt)
241-BX-109	4.34E-05	1.20E-05	6.84E-04	5.9%	1.6%	92.5%	7.40E-04	30	1.84E+02	1.30E+01	1.48	731	25801	51%	1.40E+03
BX-109 liquid	not exist	not exist	not exist	not exist	not exist	not exist	not exist	not exist	1.29E+01	1.09E+02	1.17	0	0	72%	0.00E+01
BX-109 solid	4.34E-05	1.20E-05	6.84E-04	5.9%	1.6%	92.5%	7.40E-04	30	1.84E+02	1.30E+01	1.48	731	25801	51%	1.40E+03
241-BX-110	3.68E-05	3.00E-05	6.93E-04	4.8%	3.9%	91.2%	7.60E-04	31	2.86E+01	7.67E+01	1.83	784	27672	39%	7.46E+02
BX-110 liquid	4.52E-07	4.47E-07	2.52E-06	13.2%	13.1%	73.7%	3.42E-06	0	1.00E-02	9.05E+01	1.40	11	401	53%	6.79E+00
BX-110 solid	3.64E-05	2.95E-05	6.91E-04	4.8%	3.9%	91.3%	7.57E-04	31	2.38E+01	7.65E+01	1.84	772	27271	39%	7.39E+02
241-BX-111	2.85E-06	4.35E-06	6.54E-04	0.4%	0.7%	98.9%	6.61E-04	27	1.58E+01	7.79E+01	1.38	613	21656	20%	4.02E+02
BX-111 liquid	4.99E-07	2.74E-07	8.36E-07	31.0%	17.0%	52.0%	1.61E-06	0	8.00E-00	3.01E+02	1.39	4	134	51%	7.76E+00
BX-111 solid	2.35E-06	4.08E-06	6.53E-04	0.4%	0.6%	99.0%	6.59E-04	27	1.59E+01	7.65E+01	1.38	609	21523	20%	3.94E+02
241-BX-112	7.89E-06	1.09E-06	6.56E-04	1.2%	0.2%	98.6%	6.65E-04	27	6.09E-00	5.22E+01	1.31	625	22058	62%	2.35E+02
BX-112 liquid	1.08E-07	7.16E-09	8.36E-07	11.4%	0.8%	87.9%	9.52E-07	0	1.29E+01	1.09E+02	1.18	4	134	75%	2.68E+00
BX-112 solid	7.78E-06	1.08E-06	6.55E-04	1.2%	0.2%	98.7%	6.64E-04	27	6.05E+00	5.18E+01	1.31	621	21924	62%	2.32E+02
241-BY-101	6.71E-05	7.10E-05	8.51E-04	6.8%	7.2%	86.0%	9.89E-04	41	9.12E+01	1.17E+02	1.66	1465	51735	26%	2.83E+03
BY-101 liquid	not exist	not exist	not exist	not exist	not exist	not exist	not exist	not exist	8.00E-00	3.01E+02	1.39	0	0	51%	0.00E+01
BY-101 solid	6.71E-05	7.10E-05	8.51E-04	6.8%	7.2%	86.0%	9.89E-04	41	9.12E+01	1.17E+02	1.66	1465	51735	26%	2.83E+03
241-BY-102	9.90E-06	9.88E-06	7.62E-04	1.3%	1.3%	97.5%	7.82E-04	32	2.36E+01	8.70E+01	1.50	1049	37030	29%	8.94E+02
BY-102 liquid	not exist	not exist	not exist	not exist	not exist	not exist	not exist	not exist	8.00E-00	3.01E+02	1.44	0	0	51%	0.00E+01
BY-102 solid	9.90E-06	9.88E-06	7.62E-04	1.3%	1.3%	97.5%	7.82E-04	32	2.36E+01	8.70E+01	1.50	1049	37030	29%	8.94E+02
241-BY-103	5.11E-05	1.07E-04	8.63E-04	5.0%	10.5%	84.5%	1.02E-03	42	2.88E+01	8.78E+01	1.71	1514	53473	32%	1.57E+03
BY-103 liquid	not exist	not exist	not exist	not exist	not exist	not exist	not exist	not exist	8.00E-00	3.01E+02	1.39	0	0	59%	0.00E+01
BY-103 solid	5.11E-05	1.07E-04	8.63E-04	5.0%	10.5%	84.5%	1.02E-03	42	2.88E+01	8.78E+01	1.71	1514	53473	32%	1.57E+03
241-BY-104	5.28E-04	5.10E-04	8.11E-04	28.6%	27.6%	43.8%	1.85E-03	76	6.05E+02	1.34E+02	1.64	1234	43580	23%	9.45E+03
BY-104 liquid	not exist	not exist	not exist	not exist	not exist	not exist	not exist	not exist	4.00E-00	2.83E+02	1.40	0	0	49%	0.00E+01
BY-104 solid	5.28E-04	5.10E-04	8.11E-04	28.6%	27.6%	43.8%	1.85E-03	76	6.05E+02	1.34E+02	1.64	1234	43580	23%	9.45E+03
241-BY-105	4.43E-05	1.60E-04	9.61E-04	3.8%	13.7%	82.5%	1.16E-03	48	6.23E+01	5.26E+01	1.92	1904	67242	17%	2.43E+03
BY-105 liquid	not exist	not exist	not exist	not exist	not exist	not exist	not exist	not exist	8.56E-02	1.65E+02	1.44	0	0	52%	0.00E+01
BY-105 solid	4.43E-05	1.60E-04	9.61E-04	3.8%	13.7%	82.5%	1.16E-03	48	6.23E+01	5.26E+01	1.92	1904	67242	17%	2.43E+03
241-BY-106	4.35E-04	1.06E-03	1.01E-03	17.3%	42.3%	40.4%	2.51E-03	103	1.26E+02	1.75E+02	1.72	2127	75129	26%	6.11E+03
BY-106 liquid	not exist	not exist	not exist	not exist	not exist	not exist	not exist	not exist	8.00E-00	3.01E+02	1.39	0	0	59%	0.00E+01
BY-106 solid	4.35E-04	1.06E-03	1.01E-03	17.3%	42.3%	40.4%	2.51E-03	103	1.26E+02	1.75E+02	1.72	2127	75129	26%	6.11E+03
241-BY-107	5.01E-05	1.18E-04	7.57E-04	5.4%	12.7%	81.8%	9.25E-04	38	3.75E+01	1.55E+02	1.66	1007	35559	40%	1.64E+03
BY-107 liquid	not exist	not exist	not exist	not exist	not exist	not exist	not exist	not exist	8.00E-00	3.01E+02	1.46	0	0	49%	0.00E+01
BY-107 solid	5.01E-05	1.18E-04	7.57E-04	5.4%	12.7%	81.8%	9.25E-04	38	3.75E+01	1.55E+02	1.66	1007	35559	40%	1.64E+03
241-BY-108	6.83E-04	3.15E-04	7.32E-04	39.5%	18.2%	42.3%	1.73E-03	71	9.21E+02	1.60E+02	1.58	863	30480	29%	9.46E+03
BY-108 liquid	not exist	not exist	not exist	not exist	not exist	not exist	not exist	not exist	4.00E-00	2.83E+02	1.40	0	0	33%	0.00E+01
BY-108 solid	6.83E-04	3.15E-04	7.32E-04	39.5%	18.2%	42.3%	1.73E-03	71	9.21E+02	1.60E+02	1.58	863	30480	29%	9.46E+03
241-BY-109	2.95E-05	3.18E-05	7.60E-04	3.6%	3.9%	92.5%	8.21E-04	34	6.13E+01	7.87E+01	1.66	1098	38768	39%	1.43E+03
BY-109 liquid	not exist	not exist	not exist	not exist	not exist	not exist	not exist	not exist	8.00E-00	3.01E+02	1.39	0	0	53%	0.00E+01
BY-109 solid	2.95E-05	3.18E-05	7.60E-04	3.6%	3.9%	92.5%	8.21E-04	34	6.13E+01	7.87E+01	1.66	1098	38768	39%	1.43E+03
241-BY-110	1.03E-04	2.93E-04	8.68E-04	8.1%	23.2%	68.7%	1.26E-03	52	1.15E+02	8.53E+01	1.73	1507	53205	26%	3.05E+03
BY-110 liquid	not exist	not exist	not exist	not exist	not exist	not exist	not exist	not exist	8.00E-00	3.01E+02	1.39	0	0	41%	0.00E+01
BY-110 solid	1.03E-04	2.93E-04	8.68E-04	8.1%	23.2%	68.7%	1.26E-03	52	1.15E+02	8.53E+01	1.73	1507	53205	26%	3.05E+03
241-BY-111	2.00E-05	3.10E-05	9.13E-04	2.1%	3.2%	94.7%	9.64E-04	40	4.10E+01	1.58E+02	1.57	1738	61360	36%	2.78E+03
BY-111 liquid	not exist	not exist	not exist	not exist	not exist	not exist	not exist	not exist	8.00E-00	3.01E+02	1.39	0	0	54%	0.00E+01
BY-111 solid	2.00E-05	3.10E-05	9.13E-04	2.1%	3.2%	94.7%	9.64E-04	40	4.10E+01	1.58E+02	1.57	1738	61360	36%	2.78E+03
241-BY-112	1.96E-05	3.72E-05	7.73E-04	2.4%	4.5%	93.2%	8.30E-04	34	4.10E+01	1.58E+02	1.46	1102	38901	29%	1.64E+03
BY-112 liquid	not exist	not exist	not exist	not exist	not exist	not exist	not exist	not exist	8.00E-00	3.01E+02	1.39	0	0	49%	0.00E+01
BY-112 solid	1.96E-05	3.72E-05	7.73E-04	2.4%	4.5%	93.2%	8.30E-04	34	4.10E+01	1.58E+02	1.46	1102	38901	29%	1.64E+03
241-C-101	4.80E-05	1.14E-05	6.18E-04	7.1%	1.7%	91.2%	6.77E-04	28	5.33E+02	8.20E+01	1.54	333	11764	28%	2.03E+03

Tank Name	Grad (cfm) HGR from Radiolysis	Gtherm (cfm) HGR from Thermolysis	Gcorr (cfm) HGR from Corrosion	(Grad)% Percent HGR from Radiolysis	(Gtherm)% Percent HGR from Thermolysis	(Gcorr)% Percent HGR from Corrosion	Gmod (cfm) Total HGR from Model	Gmod (L/Day) Total HGR from Model	Sr90 in Waste (uCi/g)	Cs137 in Waste (uCi/g)	Density (g/ml)	Waste Volume (kL)	Waste Volume (ft3)	H2O (wt%)	Power Load (watt)
C-101 liquid	not exist	not exist	not exist	not exist	not exist	not exist	not exist	not exist	1.29E+01	1.09E+02	1.17	0	0	74%	0.00E+01
C-101 solid	4.80E-05	1.14E-05	6.18E-04	7.1%	1.7%	91.2%	6.77E-04	28	5.33E+02	8.20E+01	1.54	333	11764	28%	2.03E+03
241-C-102	5.93E-04	2.35E-05	7.99E-04	41.9%	1.7%	56.5%	1.41E-03	58	2.04E+03	1.10E+02	1.80	1196	42244	44%	3.06E+04
C-102 liquid	not exist	not exist	not exist	not exist	not exist	not exist	not exist	not exist	1.29E+01	1.09E+02	1.17	0	0	75%	0.00E+01
C-102 solid	5.93E-04	2.35E-05	7.99E-04	41.9%	1.7%	56.5%	1.41E-03	58	2.04E+03	1.10E+02	1.80	1196	42244	44%	3.06E+04
241-C-103	1.74E-03	3.70E-05	7.31E-04	69.4%	1.5%	29.1%	2.51E-03	103	2.02E+03	1.05E+02	1.23	750	26469	67%	1.29E+04
C-103 liquid	3.92E-05	1.66E-05	7.06E-05	31.0%	13.1%	55.9%	1.26E-04	5	1.29E+01	1.09E+02	1.08	299	10561	86%	1.94E+02
C-103 solid	1.70E-03	2.04E-05	6.60E-04	71.4%	0.9%	27.7%	2.38E-03	98	3.10E+03	1.03E+02	1.34	450	15908	57%	1.28E+04
241-C-104	2.08E-04	1.02E-04	7.97E-04	18.8%	9.2%	72.0%	1.11E-03	45	3.31E+02	5.43E+01	1.70	1117	39436	52%	4.70E+03
C-104 liquid	not exist	not exist	not exist	not exist	not exist	not exist	not exist	not exist	1.29E+01	1.09E+02	1.17	0	0	81%	0.00E+01
C-104 solid	2.08E-04	1.02E-04	7.97E-04	18.8%	9.2%	72.0%	1.11E-03	45	3.31E+02	5.43E+01	1.70	1117	39436	52%	4.70E+03
241-C-105	9.26E-05	2.67E-06	6.57E-04	12.3%	0.4%	87.3%	7.52E-04	31	5.24E+02	1.79E+02	1.44	496	17516	37%	3.11E+03
C-105 liquid	not exist	not exist	not exist	not exist	not exist	not exist	not exist	not exist	3.55E-00	3.08E+02	1.23	0	0	67%	0.00E+01
C-105 solid	1.18E-04	2.67E-06	6.57E-04	15.1%	0.3%	84.5%	7.77E-04	32	7.37E+02	1.26E+02	1.55	496	17516	25%	4.25E+03
241-C-106	4.11E-05	3.78E-07	5.50E-04	6.9%	0.1%	93.0%	5.91E-04	24	8.00E+01	1.20E+02	1.16	189	6684	59%	2.43E+02
C-106 liquid	1.02E-05	3.43E-07	3.45E-05	22.6%	0.8%	76.6%	4.50E-05	2	8.29E-01	3.18E+01	1.09	159	5615	69%	2.70E+01
C-106 solid	3.09E-05	3.54E-08	5.15E-04	5.7%	0.0%	94.3%	5.46E-04	22	3.72E+02	4.45E+02	1.55	30	1069	26%	2.16E+02
241-C-107	5.12E-04	1.54E-04	7.96E-04	35.0%	10.5%	54.4%	1.46E-03	60	1.23E+03	2.24E+01	1.40	973	34356	54%	1.13E+04
C-107 liquid	not exist	not exist	not exist	not exist	not exist	not exist	not exist	not exist	1.29E+01	1.09E+02	1.17	0	0	79%	0.00E+01
C-107 solid	5.12E-04	1.54E-04	7.96E-04	35.0%	10.5%	54.4%	1.46E-03	60	1.23E+03	2.24E+01	1.40	973	34356	54%	1.13E+04
241-C-108	1.36E-05	4.52E-06	5.84E-04	2.3%	0.8%	97.0%	6.02E-04	25	2.70E+01	2.59E+02	1.40	250	8823	43%	4.91E+02
C-108 liquid	not exist	not exist	not exist	not exist	not exist	not exist	not exist	not exist	1.29E+01	1.09E+02	1.17	0	0	75%	0.00E+01
C-108 solid	1.36E-05	4.52E-06	5.84E-04	2.3%	0.8%	97.0%	6.02E-04	25	2.70E+01	2.59E+02	1.40	250	8823	43%	4.91E+02
241-C-109	7.49E-05	4.52E-06	5.86E-04	11.3%	0.7%	88.1%	6.65E-04	27	7.22E+02	7.79E+02	1.23	250	8823	46%	2.61E+03
C-109 liquid	5.20E-07	4.28E-07	3.42E-06	11.9%	9.8%	78.3%	4.36E-06	0	1.29E+01	1.09E+02	1.17	15	15	75%	1.06E+01
C-109 solid	7.43E-05	4.09E-06	5.82E-04	11.3%	0.6%	88.1%	6.61E-04	27	7.66E+02	8.20E+02	1.23	235	8288	44%	2.60E+03
241-C-110	3.04E-06	7.42E-06	6.71E-04	0.4%	1.1%	98.5%	6.82E-04	28	4.78E-00	1.92E+01	1.45	674	23795	58%	1.20E+02
C-110 liquid	1.13E-07	5.69E-08	8.42E-07	11.2%	5.6%	83.2%	1.01E-06	0	1.29E+01	1.09E+02	1.17	4	4	75%	2.66E+00
C-110 solid	2.93E-06	7.37E-06	6.71E-04	0.4%	1.1%	98.5%	6.81E-04	28	4.75E-00	1.88E+01	1.45	670	23662	58%	1.17E+02
241-C-111	1.18E-04	1.75E-06	5.75E-04	16.9%	0.3%	82.8%	6.95E-04	28	4.16E+03	4.32E+01	1.30	216	7620	24%	7.86E+03
C-111 liquid	not exist	not exist	not exist	not exist	not exist	not exist	not exist	not exist	1.29E+01	1.09E+02	1.17	0	0	75%	0.00E+01
C-111 solid	1.18E-04	1.75E-06	5.75E-04	16.9%	0.3%	82.8%	6.95E-04	28	4.16E+03	4.32E+01	1.30	216	7620	24%	7.86E+03
241-C-112	2.88E-04	1.14E-05	6.21E-04	31.3%	1.2%	67.4%	9.21E-04	38	1.93E+03	3.81E+02	1.65	394	13903	44%	9.55E+03
C-112 liquid	not exist	not exist	not exist	not exist	not exist	not exist	not exist	not exist	1.29E+01	1.09E+02	1.17	0	0	75%	0.00E+01
C-112 solid	2.88E-04	1.14E-05	6.21E-04	31.3%	1.2%	67.4%	9.21E-04	38	1.93E+03	3.81E+02	1.65	394	13903	44%	9.55E+03
241-C-201	2.21E-08	4.96E-08	4.29E-05	0.1%	0.1%	99.8%	4.30E-05	2	1.24E+01	2.75E-00	1.33	8	267	44%	9.68E-01
C-201 liquid	not exist	not exist	not exist	not exist	not exist	not exist	not exist	not exist	1.29E+01	1.09E+02	1.17	0	0	75%	0.00E+01
C-201 solid	2.21E-08	4.96E-08	4.29E-05	0.1%	0.1%	99.8%	4.30E-05	2	1.24E+01	2.75E-00	1.33	8	267	44%	9.68E-01
241-C-202	2.98E-07	3.56E-09	3.97E-05	0.7%	0.0%	99.2%	4.00E-05	2	2.57E+03	1.61E+01	1.50	4	134	6%	9.79E+01
C-202 liquid	not exist	not exist	not exist	not exist	not exist	not exist	not exist	not exist	1.29E+01	1.09E+02	1.17	0	0	75%	0.00E+01
C-202 solid	2.98E-07	3.56E-09	3.97E-05	0.7%	0.0%	99.2%	4.00E-05	2	2.57E+03	1.61E+01	1.50	4	134	6%	9.79E+01
241-C-203	5.95E-06	8.54E-08	5.21E-05	10.2%	0.1%	89.6%	5.82E-05	2	2.04E+03	2.70E-00	1.16	19	668	39%	3.01E+02
C-203 liquid	not exist	not exist	not exist	not exist	not exist	not exist	not exist	not exist	1.29E+01	1.09E+02	1.17	0	0	75%	0.00E+01
C-203 solid	5.95E-06	8.54E-08	5.21E-05	10.2%	0.1%	89.6%	5.82E-05	2	2.04E+03	2.70E-00	1.16	19	668	39%	3.01E+02
241-C-204	3.34E-08	7.70E-08	4.59E-05	0.1%	0.2%	99.8%	4.60E-05	2	1.43E+01	2.70E-00	1.16	11	401	44%	1.42E-00
C-204 liquid	not exist	not exist	not exist	not exist	not exist	not exist	not exist	not exist	1.29E+01	1.09E+02	1.17	0	0	75%	0.00E+01
C-204 solid	3.34E-08	7.70E-08	4.59E-05	0.1%	0.2%	99.8%	4.60E-05	2	1.43E+01	2.70E-00	1.16	11	401	44%	1.42E-00
241-S-101	6.22E-04	1.80E-03	9.15E-04	18.6%	53.9%	27.4%	3.33E-03	137	1.57E+02	1.49E+02	1.64	1616	57082	40%	4.65E+03
S-101 liquid	1.78E-05	6.57E-05	1.05E-05	18.9%	69.9%	11.2%	9.40E-05	4	4.00E-00	2.83E+02	1.36	45	1604	63%	8.42E+01

Tank Name	Grad (cfm) HGR from Radiolysis	Gtherm (cfm) HGR from Thermolysis	Gcorr (cfm) HGR from Corrosion	(Grad)% Percent HGR from Radiolysis	(Gtherm)% Percent HGR from Thermolysis	(Gcorr)% Percent HGR from Corrosion	Gmod (cfm) Total HGR from Model	Gmod (L/Day) Total HGR from Model	Sr-90 in Waste (uCi/g)	Cs137 in Waste (uCi/g)	Density (g/ml)	Waste Volume (kl.)	Waste Volume (ft3)	H2O (wt%)	Power Load (watt)
S-101 solid	6.04E-04	1.73E-03	9.05E-04	18.6%	53.4%	27.9%	3.24E-03	133	1.61E+02	1.45E+02	1.65	1571	55478	39%	4.56E+03
241-S-102	4.45E-04	1.11E-03	9.80E-04	17.6%	43.8%	38.7%	2.53E-03	104	1.38E+02	1.38E+02	1.67	1946	68713	28%	5.12E+03
S-102 liquid	not exist	not exist	not exist	not exist	not exist	not exist	not exist	not exist	8.00E-00	3.01E+02	1.39	0	0	51%	0.00E+01
S-102 solid	4.45E-04	1.11E-03	9.80E-04	17.6%	43.8%	38.7%	2.53E-03	104	1.38E+02	1.38E+02	1.67	1946	68713	28%	5.12E+03
241-S-103	8.87E-05	1.58E-04	7.25E-04	9.1%	16.3%	74.6%	9.72E-04	40	2.93E+01	1.74E+02	1.59	874	30881	32%	1.42E+03
S-103 liquid	not exist	not exist	not exist	not exist	not exist	not exist	not exist	not exist	8.00E-00	3.01E+02	1.39	0	0	50%	0.00E+01
S-103 solid	8.87E-05	1.58E-04	7.25E-04	9.1%	16.3%	74.6%	9.72E-04	40	2.93E+01	1.74E+02	1.59	874	30881	32%	1.42E+03
241-S-104	2.11E-04	1.40E-04	7.96E-04	18.4%	12.2%	69.4%	1.15E-03	47	3.00E+02	6.05E+01	1.64	1113	39303	38%	4.18E+03
S-104 liquid	2.01E-07	5.07E-07	8.71E-07	12.7%	32.1%	55.1%	1.58E-06	0	1.29E+01	1.09E+02	1.17	4	134	56%	2.66E+00
S-104 solid	2.11E-04	1.39E-04	7.95E-04	18.4%	12.2%	69.4%	1.15E-03	47	3.00E+02	6.04E+01	1.64	1109	39169	38%	4.17E+03
241-S-105	4.18E-05	4.90E-05	9.09E-04	4.2%	4.9%	90.9%	1.00E-03	41	4.82E+01	1.58E+02	1.63	1726	60959	32%	3.00E+03
S-105 liquid	not exist	not exist	not exist	not exist	not exist	not exist	not exist	not exist	8.00E-00	3.01E+02	1.39	0	0	51%	0.00E+01
S-105 solid	4.18E-05	4.90E-05	9.09E-04	4.2%	4.9%	90.9%	1.00E-03	41	4.82E+01	1.58E+02	1.63	1726	60959	32%	3.00E+03
241-S-106	8.97E-05	1.93E-04	8.83E-04	7.7%	16.5%	75.8%	1.17E-03	48	1.64E+01	1.15E+02	1.72	1613	56949	30%	1.81E+03
S-106 liquid	not exist	not exist	not exist	not exist	not exist	not exist	not exist	not exist	8.00E-00	3.01E+02	1.39	0	0	51%	0.00E+01
S-106 solid	8.97E-05	1.93E-04	8.83E-04	7.7%	16.5%	75.8%	1.17E-03	48	1.64E+01	1.15E+02	1.72	1613	56949	30%	1.81E+03
241-S-107	1.18E-04	1.29E-04	8.60E-04	10.7%	11.6%	77.7%	1.11E-03	45	1.61E+02	8.82E+01	1.43	1423	50264	35%	3.04E+03
S-107 liquid	2.87E-06	7.64E-06	1.21E-05	12.7%	33.8%	53.5%	2.26E-05	1	1.29E+01	1.09E+02	1.17	53	1872	68%	3.72E+01
S-107 solid	1.15E-04	1.21E-04	8.48E-04	10.6%	11.2%	78.2%	1.08E-03	44	1.66E+02	8.76E+01	1.44	1370	48393	34%	3.00E+03
241-S-108	7.23E-06	1.53E-05	9.06E-04	0.8%	1.6%	97.6%	9.29E-04	38	2.33E+01	1.34E+02	1.65	1703	60157	32%	2.21E+03
S-108 liquid	not exist	not exist	not exist	not exist	not exist	not exist	not exist	not exist	8.00E-00	3.01E+02	1.39	0	0	51%	0.00E+01
S-108 solid	7.23E-06	1.53E-05	9.06E-04	0.8%	1.6%	97.6%	9.29E-04	38	2.33E+01	1.34E+02	1.65	1703	60157	32%	2.21E+03
241-S-109	5.83E-05	7.66E-05	9.52E-04	5.4%	7.0%	87.6%	1.09E-03	45	8.94E+01	1.57E+02	1.31	1919	67777	10%	3.36E+03
S-109 liquid	not exist	not exist	not exist	not exist	not exist	not exist	not exist	not exist	8.00E-00	3.01E+02	1.39	0	0	52%	0.00E+01
S-109 solid	5.83E-05	7.66E-05	9.52E-04	5.4%	7.0%	87.6%	1.09E-03	45	8.94E+01	1.57E+02	1.31	1919	67777	10%	3.36E+03
241-S-110	1.65E-04	4.87E-04	8.67E-04	10.8%	32.1%	57.1%	1.52E-03	62	1.61E+02	9.91E+01	1.70	1476	52136	26%	3.88E+03
S-110 liquid	not exist	not exist	not exist	not exist	not exist	not exist	not exist	not exist	7.11E-01	2.79E+02	1.43	0	0	50%	0.00E+01
S-110 solid	1.65E-04	4.87E-04	8.67E-04	10.8%	32.1%	57.1%	1.52E-03	62	1.61E+02	9.91E+01	1.70	1476	52136	26%	3.88E+03
241-S-111	1.57E-04	5.81E-05	9.89E-04	13.0%	4.8%	82.2%	1.20E-03	49	2.34E+02	1.26E+02	1.58	2044	72188	34%	6.99E+03
S-111 liquid	1.99E-05	1.63E-05	9.46E-05	15.2%	12.5%	72.3%	1.31E-04	5	2.29E-01	1.92E+02	1.39	420	14839	53%	5.29E+02
S-111 solid	1.37E-04	4.17E-05	8.94E-04	12.8%	3.9%	83.4%	1.07E-03	44	2.85E+02	1.12E+02	1.63	1624	57350	30%	6.46E+03
241-S-112	2.54E-04	3.25E-04	9.67E-04	16.4%	21.0%	62.6%	1.55E-03	63	9.27E+01	1.52E+02	1.63	1980	69916	32%	4.32E+03
S-112 liquid	not exist	not exist	not exist	not exist	not exist	not exist	not exist	not exist	8.00E-00	3.01E+02	1.39	0	0	51%	0.00E+01
S-112 solid	2.54E-04	3.25E-04	9.67E-04	16.4%	21.0%	62.6%	1.55E-03	63	9.27E+01	1.52E+02	1.63	1980	69916	32%	4.32E+03
241-SX-101	1.09E-04	2.61E-04	9.56E-04	8.2%	19.7%	72.1%	1.33E-03	54	1.00E+02	1.13E+02	1.91	1696	59890	31%	4.59E+03
SX-101 liquid	not exist	not exist	not exist	not exist	not exist	not exist	not exist	not exist	8.00E-00	3.01E+02	1.50	0	0	49%	0.00E+01
SX-101 solid	1.09E-04	2.61E-04	9.56E-04	8.2%	19.7%	72.1%	1.33E-03	54	1.00E+02	1.13E+02	1.91	1696	59890	31%	4.59E+03
241-SX-102	3.34E-04	1.86E-03	9.98E-04	10.5%	58.2%	31.3%	3.19E-03	131	8.87E+01	2.05E+02	1.66	1946	68713	41%	5.02E+03
SX-102 liquid	9.03E-05	4.89E-04	1.18E-04	13.0%	70.1%	16.9%	6.97E-04	29	1.80E-02	3.36E+02	1.45	507	17913	48%	1.17E+03
SX-102 solid	2.44E-04	1.37E-03	8.80E-04	9.8%	54.9%	35.3%	2.49E-03	102	1.15E+02	1.66E+02	1.73	1438	50799	39%	3.86E+03
241-SX-103	9.52E-04	6.15E-03	1.10E-03	11.6%	75.0%	13.4%	8.19E-03	336	2.43E+02	1.46E+02	1.77	2400	84754	31%	9.86E+03
SX-103 liquid	not exist	not exist	not exist	not exist	not exist	not exist	not exist	not exist	8.49E+02	3.24E+02	1.47	0	0	47%	0.00E+01
SX-103 solid	9.52E-04	6.15E-03	1.10E-03	11.6%	75.0%	13.4%	8.19E-03	336	2.43E+02	1.46E+02	1.77	2400	84754	31%	9.86E+03
241-SX-104	7.84E-04	2.88E-03	9.43E-04	17.0%	62.5%	20.5%	4.60E-03	189	1.62E+02	1.29E+02	1.65	1768	62430	35%	4.95E+03
SX-104 liquid	not exist	not exist	not exist	not exist	not exist	not exist	not exist	not exist	8.00E-00	3.01E+02	1.39	0	0	51%	0.00E+01
SX-104 solid	7.84E-04	2.88E-03	9.43E-04	17.0%	62.5%	20.5%	4.60E-03	189	1.62E+02	1.29E+02	1.65	1768	62430	35%	4.95E+03
241-SX-105	8.70E-04	1.03E-02	1.11E-03	7.1%	83.8%	9.1%	1.22E-02	501	1.11E+02	1.45E+02	1.64	2411	85155	35%	5.66E+03
SX-105 liquid	not exist	not exist	not exist	not exist	not exist	not exist	not exist	not exist	1.21E-01	2.89E+02	1.47	0	0	43%	0.00E+01

Tank Name	Grad (cfm) HGR from Radiolysis	Gtherm (cfm) HGR from Thermolysis	Gcorr (cfm) HGR from Corrosion	(Grad)% Percent HGR from Radiolysis	(Gtherm)% Percent HGR from Thermolysis	(Gcorr)% Percent HGR from Corrosion	Gmod (cfm) Total HGR from Model	Union (L/Day) Total HGR from Model	Sr90 in Waste (uCi/g)	Cs137 in Waste (uCi/g)	Density (g/ml)	Waste Volume (kL)	Waste Volume (ft3)	H2O (wt%)	Power Load (watt)
SX-105 solid	8.70E-04	1.03E-02	1.11E-03	7.1%	83.8%	9.1%	1.22E-02	501	1.11E+02	1.45E+02	1.64	2411	85155	35%	5.66E+03
241-SX-106	1.77E-04	4.88E-04	8.97E-04	11.5%	30.4%	58.2%	1.54E-03	63	3.23E-00	2.04E+02	1.57	1601	56547	42%	2.47E+03
SX-106 liquid	5.84E-05	1.11E-04	8.60E-05	22.9%	43.4%	33.7%	2.55E-04	10	2.67E-01	2.95E+02	1.42	379	13368	46%	7.50E+02
SX-106 solid	1.18E-04	3.58E-04	8.11E-04	9.2%	27.8%	63.0%	1.29E-03	53	4.04E-00	1.79E+02	1.61	1223	43179	40%	1.72E+03
241-SX-107	1.11E-03	6.56E-04	6.63E-04	45.6%	27.1%	27.3%	2.42E-03	99	2.04E+03	1.10E+02	1.46	394	13903	44%	8.16E+03
SX-107 liquid	not exist	not exist	not exist	not exist	not exist	not exist	not exist	not exist	1.29E+01	1.09E+02	1.17	0	0	75%	0.00E+01
SX-107 solid	1.11E-03	6.56E-04	6.63E-04	45.6%	27.1%	27.3%	2.42E-03	99	2.04E+03	1.10E+02	1.46	394	13903	44%	8.16E+03
241-SX-108	5.22E-05	4.39E-05	6.63E-04	6.9%	5.8%	87.3%	7.59E-04	31	2.04E+03	1.10E+02	1.46	329	11630	2%	6.82E+03
SX-108 liquid	not exist	not exist	not exist	not exist	not exist	not exist	not exist	not exist	1.29E+01	1.09E+02	1.17	0	0	75%	0.00E+01
SX-108 solid	5.22E-05	4.39E-05	6.63E-04	6.9%	5.8%	87.3%	7.59E-04	31	2.04E+03	1.10E+02	1.46	329	11630	2%	6.82E+03
241-SX-109	7.60E-04	1.77E-03	8.04E-04	22.8%	53.1%	24.1%	3.33E-03	137	4.94E+02	1.48E+02	1.64	946	33421	32%	6.21E+03
SX-109 liquid	not exist	not exist	not exist	not exist	not exist	not exist	not exist	not exist	8.00E-00	3.01E+02	1.39	0	0	51%	0.00E+01
SX-109 solid	7.60E-04	1.77E-03	8.04E-04	22.8%	53.1%	24.1%	3.33E-03	137	4.94E+02	1.48E+02	1.64	946	33421	32%	6.21E+03
241-SX-110	1.17E-04	3.66E-04	6.33E-04	10.4%	32.8%	56.7%	1.12E-03	46	2.89E+02	7.75E+01	1.77	235	8288	44%	9.54E+02
SX-110 liquid	not exist	not exist	not exist	not exist	not exist	not exist	not exist	not exist	1.29E+01	1.09E+02	1.17	0	0	75%	0.00E+01
SX-110 solid	1.17E-04	3.66E-04	6.33E-04	10.4%	32.8%	56.7%	1.12E-03	46	2.89E+02	7.75E+01	1.77	235	8288	44%	9.54E+02
241-SX-111	4.22E-04	2.83E-03	6.92E-04	10.7%	71.7%	17.6%	3.94E-03	161	2.89E+02	7.75E+01	1.77	462	16309	44%	1.88E+03
SX-111 liquid	not exist	not exist	not exist	not exist	not exist	not exist	not exist	not exist	1.29E+01	1.09E+02	1.17	0	0	75%	0.00E+01
SX-111 solid	4.22E-04	2.83E-03	6.92E-04	10.7%	71.7%	17.6%	3.94E-03	161	2.89E+02	7.75E+01	1.77	462	16309	44%	1.88E+03
241-SX-112	1.63E-04	3.80E-04	6.70E-04	13.4%	31.3%	55.3%	1.21E-03	50	2.89E+02	7.75E+01	1.77	409	14438	44%	1.66E+03
SX-112 liquid	not exist	not exist	not exist	not exist	not exist	not exist	not exist	not exist	1.29E+01	1.09E+02	1.17	0	0	75%	0.00E+01
SX-112 solid	1.63E-04	3.80E-04	6.70E-04	13.4%	31.3%	55.3%	1.21E-03	50	2.89E+02	7.75E+01	1.77	409	14438	44%	1.66E+03
241-SX-113	1.54E-05	3.64E-06	5.59E-04	2.7%	0.6%	96.7%	5.78E-04	24	2.04E+03	1.10E+02	1.19	685	24196	44%	1.15E+04
SX-113 liquid	not exist	not exist	not exist	not exist	not exist	not exist	not exist	not exist	1.29E+01	1.09E+02	1.17	0	0	75%	0.00E+01
SX-113 solid	1.54E-05	3.64E-06	5.59E-04	2.7%	0.6%	96.7%	5.78E-04	24	2.04E+03	1.10E+02	1.19	685	24196	44%	1.15E+04
241-SX-114	1.82E-03	1.27E-03	7.50E-04	47.3%	33.2%	19.5%	3.84E-03	157	1.29E+01	1.09E+02	1.17	0	0	75%	0.00E+01
SX-114 liquid	not exist	not exist	not exist	not exist	not exist	not exist	not exist	not exist	1.29E+01	1.09E+02	1.17	0	0	75%	0.00E+01
SX-114 solid	1.82E-03	1.27E-03	7.50E-04	47.3%	33.2%	19.5%	3.84E-03	157	1.29E+01	1.09E+02	1.17	0	0	75%	0.00E+01
241-SX-115	7.78E-05	1.27E-06	5.42E-04	12.5%	0.2%	87.3%	6.21E-04	25	4.86E+03	2.07E+02	1.73	45	1604	44%	2.63E+03
SX-115 liquid	not exist	not exist	not exist	not exist	not exist	not exist	not exist	not exist	1.29E+01	1.09E+02	1.17	0	0	75%	0.00E+01
SX-115 solid	7.78E-05	1.27E-06	5.42E-04	12.5%	0.2%	87.3%	6.21E-04	25	4.86E+03	2.07E+02	1.73	45	1604	44%	2.63E+03
241-T-101	1.07E-04	2.45E-05	6.04E-04	14.6%	3.3%	82.1%	7.36E-04	30	5.20E+02	1.38E+02	1.56	386	13636	35%	2.48E+03
T-101 liquid	4.90E-07	3.38E-07	8.37E-07	29.5%	20.3%	50.2%	1.67E-06	0	4.00E-00	2.83E+02	1.40	4	134	55%	7.22E+00
T-101 solid	1.07E-04	2.45E-05	6.04E-04	14.6%	3.3%	82.1%	7.36E-04	30	5.20E+02	1.38E+02	1.56	386	13636	35%	2.48E+03
241-T-102	4.17E-06	2.16E-07	5.46E-04	0.8%	0.0%	99.2%	5.51E-04	23	1.66E+02	3.95E+01	1.53	121	4278	53%	2.40E+02
T-102 liquid	4.40E-07	9.19E-08	1.09E-05	3.9%	0.8%	95.3%	1.14E-05	0	1.09E-00	5.69E+01	1.14	49	1738	75%	1.55E+01
T-102 solid	3.73E-06	1.24E-07	5.35E-04	0.7%	0.0%	99.3%	5.39E-04	22	2.38E+02	3.19E+02	1.79	72	2540	44%	2.24E+02
241-T-103	4.32E-05	7.78E-07	5.37E-04	7.4%	0.1%	92.4%	5.81E-04	24	1.80E+03	1.10E+02	1.42	102	3609	47%	1.81E+03
T-103 liquid	4.11E-07	1.44E-07	3.32E-06	10.6%	3.7%	85.7%	3.88E-06	0	1.29E+01	1.09E+02	1.17	15	535	72%	1.06E+03
T-103 solid	4.28E-05	6.34E-07	5.37E-04	7.4%	0.1%	92.5%	5.77E-04	24	2.04E+03	1.10E+02	1.46	87	3075	44%	1.80E+03
241-T-104	1.05E-06	1.15E-05	7.87E-04	0.1%	1.4%	98.4%	7.99E-04	33	3.15E-00	1.83E-01	1.27	1234	43580	64%	3.44E+01
T-104 liquid	not exist	not exist	not exist	not exist	not exist	not exist	not exist	not exist	1.29E+01	1.09E+02	1.17	0	0	84%	0.00E+01
T-104 solid	1.05E-06	1.15E-05	7.87E-04	0.1%	1.4%	98.4%	7.99E-04	33	3.15E-00	1.83E-01	1.27	1234	43580	64%	3.44E+01
241-T-105	2.90E-05	1.14E-06	5.97E-04	4.6%	0.2%	95.2%	6.27E-04	26	2.81E+02	3.23E+01	1.45	371	13101	54%	1.09E+03
T-105 liquid	not exist	not exist	not exist	not exist	not exist	not exist	not exist	not exist	1.29E+01	1.09E+02	1.18	0	0	80%	0.00E+01
T-105 solid	2.90E-05	1.14E-06	5.97E-04	4.6%	0.2%	95.2%	6.27E-04	26	2.81E+02	3.23E+01	1.45	371	13101	54%	1.09E+03
241-T-106	4.55E-07	2.79E-07	5.32E-04	0.1%	0.1%	99.9%	5.33E-04	22	2.62E+01	2.40E+01	1.46	79	2807	21%	3.36E+01
T-106 liquid	2.07E-07	7.47E-08	1.66E-06	10.7%	3.8%	85.5%	1.94E-06	0	1.29E+01	1.09E+02	1.17	8	267	75%	5.32E+00
T-106 solid	2.48E-07	2.05E-07	5.31E-04	0.0%	0.0%	99.9%	5.31E-04	22	2.73E+01	1.70E+01	1.49	72	2540	17%	2.83E+01

Tank Name	Grad (cfm) HGR from Radiolysis	Gtherm (cfm) HGR from Thermolysis	Gcorr (cfm) HGR from Corrosion	(Grad)% Percent HGR from Radiolysis	(Gtherm)% Percent HGR from Thermolysis	(Gcorr)% Percent HGR from Corrosion	Gmod Total HGR from Model	Gmod Total HGR from Model	Sr-90 in Waste (uCi/g)	Cs137 in Waste (uCi/g)	Density (g/ml)	Waste Volume (kL)	Waste Volume (ft3)	H2O (wt%)	Power Load (watt)
241-T-107	1.51E-05	4.84E-06	6.61E-04	2.2%	0.7%	97.1%	6.81E-04	28	1.06E+02	1.21E+01	1.51	655	23127	45%	7.58E+02
T-107 liquid	not exist	not exist	not exist	not exist	not exist	not exist	not exist	not exist	1.29E+01	1.09E+02	1.17	0	0	84%	0.00E+01
T-107 solid	1.51E-05	4.84E-06	6.61E-04	2.2%	0.7%	97.1%	6.81E-04	28	1.06E+02	1.21E+01	1.51	655	23127	45%	7.58E+02
241-T-108	4.12E-05	7.99E-06	5.52E-04	6.9%	1.3%	91.8%	6.01E-04	25	5.66E+02	3.81E+00	1.58	167	5882	37%	10.00E+02
T-108 liquid	not exist	not exist	not exist	not exist	not exist	not exist	not exist	not exist	4.00E+00	2.83E+02	1.40	0	0	55%	0.00E+01
T-108 solid	4.12E-05	7.99E-06	5.52E-04	6.9%	1.3%	91.8%	6.01E-04	25	5.66E+02	3.81E+00	1.58	167	5882	37%	10.00E+02
241-T-109	1.71E-05	1.15E-05	5.63E-04	2.9%	1.9%	95.2%	5.92E-04	24	4.10E+01	1.58E+02	1.55	220	7754	42%	3.47E+02
T-109 liquid	not exist	not exist	not exist	not exist	not exist	not exist	not exist	not exist	8.00E+00	3.01E+02	1.39	0	0	51%	0.00E+01
T-109 solid	1.71E-05	1.15E-05	5.63E-04	2.9%	1.9%	95.2%	5.92E-04	24	4.10E+01	1.58E+02	1.55	220	7754	42%	3.47E+02
241-T-110	2.93E-05	1.43E-05	8.37E-04	3.3%	1.6%	95.1%	8.80E-04	36	3.24E+01	5.25E+01	1.26	1465	51735	75%	8.57E+02
T-110 liquid	not exist	not exist	not exist	not exist	not exist	not exist	not exist	not exist	1.29E+01	1.09E+02	1.17	0	0	87%	0.00E+01
T-110 solid	2.93E-05	1.43E-05	8.37E-04	3.3%	1.6%	95.1%	8.80E-04	36	3.24E+01	5.25E+01	1.26	1465	51735	75%	8.57E+02
241-T-111	2.42E-06	1.57E-05	8.85E-04	0.3%	1.7%	98.0%	9.04E-04	37	5.16E+00	1.58E+01	1.28	1688	59622	71%	7.62E+01
T-111 liquid	not exist	not exist	not exist	not exist	not exist	not exist	not exist	not exist	1.29E+01	1.09E+02	1.17	0	0	75%	0.00E+01
T-111 solid	2.42E-06	1.57E-05	8.85E-04	0.3%	1.7%	98.0%	9.04E-04	37	5.16E+00	1.58E+01	1.28	1688	59622	71%	7.62E+01
241-T-112	2.12E-06	2.37E-07	5.71E-04	0.4%	0.0%	99.6%	5.74E-04	24	1.91E+01	1.05E+01	1.26	254	8957	77%	5.67E+01
T-112 liquid	7.03E-07	2.38E-08	5.83E-06	10.7%	0.4%	88.9%	6.55E-06	0	1.29E+01	1.09E+02	1.10	26	936	85%	1.75E+01
T-112 solid	1.42E-06	2.14E-07	5.66E-04	0.2%	0.0%	99.7%	5.67E-04	23	1.97E+01	6.09E+01	1.28	227	8021	77%	3.92E+01
241-T-201	1.09E-07	9.38E-07	1.27E-04	0.1%	0.7%	99.2%	1.28E-04	5	5.59E+01	3.52E+00	1.27	110	3877	70%	2.83E+00
T-201 liquid	1.04E-07	3.91E-08	3.11E-06	3.2%	1.2%	95.6%	3.25E-06	0	1.29E+01	1.09E+02	1.17	4	134	91%	2.66E+00
T-201 solid	5.01E-09	8.99E-07	1.24E-04	0.0%	0.7%	99.3%	1.24E-04	5	1.53E+01	4.95E+02	1.27	106	3743	69%	1.69E+01
241-T-202	6.28E-10	8.35E-07	1.02E-04	0.0%	0.8%	99.2%	1.03E-04	4	2.70E+03	3.05E+02	1.24	79	2807	76%	1.59E+02
T-202 liquid	not exist	not exist	not exist	not exist	not exist	not exist	not exist	not exist	1.29E+01	1.09E+02	1.17	0	0	75%	0.00E+01
T-202 solid	6.28E-10	8.35E-07	1.02E-04	0.0%	0.8%	99.2%	1.03E-04	4	2.70E+03	3.05E+02	1.24	79	2807	76%	1.59E+02
241-T-203	6.36E-10	1.35E-06	1.45E-04	0.0%	0.9%	99.1%	1.46E-04	6	2.79E+03	1.96E+02	1.23	132	4679	76%	1.81E+02
T-203 liquid	not exist	not exist	not exist	not exist	not exist	not exist	not exist	not exist	1.29E+01	1.09E+02	1.17	0	0	85%	0.00E+01
T-203 solid	6.36E-10	1.35E-06	1.45E-04	0.0%	0.9%	99.1%	1.46E-04	6	2.79E+03	1.96E+02	1.23	132	4679	76%	1.81E+02
241-T-204	5.15E-10	1.76E-06	1.55E-04	0.0%	1.1%	98.9%	1.57E-04	6	4.99E+03	8.40E+03	1.21	144	5080	76%	1.27E+02
T-204 liquid	not exist	not exist	not exist	not exist	not exist	not exist	not exist	not exist	1.29E+01	1.09E+02	1.17	0	0	75%	0.00E+01
T-204 solid	5.15E-10	1.76E-06	1.55E-04	0.0%	1.1%	98.9%	1.57E-04	6	4.99E+03	8.40E+03	1.21	144	5080	76%	1.27E+02
241-TX-101	2.05E-04	9.19E-06	6.03E-04	25.1%	1.1%	73.8%	8.17E-04	33	1.77E+03	8.20E+01	1.74	329	11630	45%	7.00E+03
TX-101 liquid	3.99E-07	3.57E-07	2.56E-06	12.0%	10.8%	77.2%	3.32E-06	0	1.29E+01	1.09E+02	1.17	11	401	75%	7.98E+00
TX-101 solid	2.05E-04	8.83E-06	6.00E-04	25.2%	1.1%	73.7%	8.14E-04	33	1.81E+03	8.14E+01	1.76	318	11229	44%	7.00E+03
241-TX-102	2.21E-05	4.49E-05	7.14E-04	2.8%	5.7%	91.4%	7.81E-04	32	4.10E+01	1.11E+02	1.70	821	29009	32%	1.12E+03
TX-102 liquid	not exist	not exist	not exist	not exist	not exist	not exist	not exist	not exist	8.00E+00	3.01E+02	1.39	0	0	51%	0.00E+01
TX-102 solid	2.21E-05	4.49E-05	7.14E-04	2.8%	5.7%	91.4%	7.81E-04	32	4.10E+01	1.11E+02	1.70	821	29009	32%	1.12E+03
241-TX-103	2.20E-05	2.29E-05	6.54E-04	3.1%	3.3%	93.6%	6.99E-04	29	4.10E+01	1.58E+02	1.70	594	20988	32%	1.03E+03
TX-103 liquid	not exist	not exist	not exist	not exist	not exist	not exist	not exist	not exist	8.00E+00	3.01E+02	1.39	0	0	51%	0.00E+01
TX-103 solid	2.20E-05	2.29E-05	6.54E-04	3.1%	3.3%	93.6%	6.99E-04	29	4.10E+01	1.58E+02	1.70	594	20988	32%	1.03E+03
241-TX-104	4.43E-05	1.28E-06	5.74E-04	7.1%	0.2%	92.6%	6.20E-04	25	4.53E+02	1.47E+02	1.72	246	8689	46%	1.58E+03
TX-104 liquid	1.19E-06	9.40E-08	4.19E-06	21.8%	1.7%	76.5%	5.48E-06	0	4.00E+00	2.83E+02	1.45	19	668	52%	3.74E+01
TX-104 solid	4.31E-05	1.19E-06	5.70E-04	7.0%	0.2%	92.8%	6.14E-04	25	4.84E+02	1.38E+02	1.74	227	8021	46%	1.54E+03
241-TX-105	2.78E-05	1.03E-04	1.05E-03	2.4%	8.7%	88.9%	1.18E-03	48	4.10E+01	1.11E+02	1.70	2305	81412	32%	3.14E+03
TX-105 liquid	not exist	not exist	not exist	not exist	not exist	not exist	not exist	not exist	8.00E+00	3.01E+02	1.39	0	0	51%	0.00E+01
TX-105 solid	2.78E-05	1.03E-04	1.05E-03	2.4%	8.7%	88.9%	1.18E-03	48	4.10E+01	1.11E+02	1.70	2305	81412	32%	3.14E+03
241-TX-106	4.39E-05	8.23E-05	8.16E-04	4.7%	8.7%	86.6%	9.42E-04	39	4.10E+01	1.11E+02	1.70	1291	45586	32%	1.76E+03
TX-106 liquid	not exist	not exist	not exist	not exist	not exist	not exist	not exist	not exist	8.00E+00	3.01E+02	1.39	0	0	51%	0.00E+01
TX-106 solid	4.39E-05	8.23E-05	8.16E-04	4.7%	8.7%	86.6%	9.42E-04	39	4.10E+01	1.11E+02	1.70	1291	45586	32%	1.76E+03
241-TX-107	2.26E-05	7.30E-06	5.53E-04	3.9%	1.3%	94.9%	5.82E-04	24	3.90E+02	1.08E+02	1.71	136	4813	23%	7.25E+02

Tank Name	Grad (cfm) HGR from Radiolysis	Gtherm (cfm) HGR from Thermolysis	Gcorr (cfm) HGR from Corrosion	(Grad)% Percent HGR from Radiolysis	(Gtherm)% Percent HGR from Thermolysis	(Gcorr)% Percent HGR from Corrosion	Gmod (cfm) Total HGR from Model	Gmod (L/Day) Total HGR from Model	Sr90 in Waste (uCi/g)	Cs137 in Waste (uCi/g)	Density (g/ml)	Waste Volume (kL)	Waste Volume (ft3)	H2O (wt%)	Power Load (watt)
TX-107 liquid	5.49E-07	3.68E-07	8.43E-07	31.2%	20.9%	47.9%	1.76E-06	0	8.00E-00	3.01E+02	1.39	4	134	51%	7.76E+00
TX-107 solid	2.21E-05	6.93E-06	5.52E-04	3.8%	1.2%	95.0%	5.81E-04	24	3.99E+02	1.03E+02	1.72	132	4679	22%	7.17E+02
241-TX-108	9.81E-06	6.10E-06	6.28E-04	1.5%	0.9%	97.5%	6.44E-04	26	1.01E+02	1.07E+02	1.69	507	17913	32%	1.02E+03
TX-108 liquid	not exist	not exist	not exist	not exist	not exist	not exist	not exist	not exist	8.00E-00	3.01E+02	1.39	0	0	51%	0.00E+01
TX-108 solid	9.81E-06	6.10E-06	6.28E-04	1.5%	0.9%	97.5%	6.44E-04	26	1.01E+02	1.07E+02	1.69	507	17913	32%	1.02E+03
241-TX-109	2.34E-05	5.18E-05	8.57E-04	2.5%	5.6%	91.9%	9.33E-04	38	5.43E+01	6.14E+00	1.40	1454	51334	44%	7.98E+02
TX-109 liquid	not exist	not exist	not exist	not exist	not exist	not exist	not exist	not exist	1.29E+01	1.09E+02	1.17	0	0	75%	0.00E+01
TX-109 solid	2.34E-05	5.18E-05	8.57E-04	2.5%	5.6%	91.9%	9.33E-04	38	5.43E+01	6.14E+00	1.40	1454	51334	44%	7.98E+02
241-TX-110	3.86E-05	4.73E-05	9.18E-04	3.9%	4.7%	91.4%	1.00E-03	41	1.42E+02	1.04E+02	1.68	1749	61761	32%	4.24E+03
TX-110 liquid	not exist	not exist	not exist	not exist	not exist	not exist	not exist	not exist	8.00E-00	3.01E+02	1.39	0	0	51%	0.00E+01
TX-110 solid	3.86E-05	4.73E-05	9.18E-04	3.9%	4.7%	91.4%	1.00E-03	41	1.42E+02	1.04E+02	1.68	1749	61761	32%	4.24E+03
241-TX-111	3.56E-05	2.83E-05	8.34E-04	4.0%	3.2%	92.9%	8.98E-04	37	1.89E+02	1.01E+02	1.67	1401	49462	32%	4.07E+03
TX-111 liquid	not exist	not exist	not exist	not exist	not exist	not exist	not exist	not exist	8.00E-00	3.01E+02	1.39	0	0	51%	0.00E+01
TX-111 solid	3.56E-05	2.83E-05	8.34E-04	4.0%	3.2%	92.9%	8.98E-04	37	1.89E+02	1.01E+02	1.67	1401	49462	32%	4.07E+03
241-TX-112	3.44E-05	4.59E-05	1.06E-03	3.0%	4.0%	93.0%	1.14E-03	47	4.10E+01	1.07E+02	1.70	2457	86760	32%	3.26E+03
TX-112 liquid	not exist	not exist	not exist	not exist	not exist	not exist	not exist	not exist	8.00E-00	3.01E+02	1.39	0	0	51%	0.00E+01
TX-112 solid	3.44E-05	4.59E-05	1.06E-03	3.0%	4.0%	93.0%	1.14E-03	47	4.10E+01	1.07E+02	1.70	2457	86760	32%	3.26E+03
241-TX-113	9.09E-05	3.73E-05	1.03E-03	7.9%	3.2%	88.9%	1.16E-03	47	3.70E+02	8.38E+01	1.61	2298	81145	35%	1.06E+04
TX-113 liquid	not exist	not exist	not exist	not exist	not exist	not exist	not exist	not exist	4.00E-00	2.83E+02	1.40	0	0	55%	0.00E+01
TX-113 solid	9.09E-05	3.73E-05	1.03E-03	7.9%	3.2%	88.9%	1.16E-03	47	3.70E+02	8.38E+01	1.61	2298	81145	35%	1.06E+04
241-TX-114	1.88E-05	2.43E-05	9.66E-04	1.9%	2.4%	95.7%	1.01E-03	41	5.03E+01	9.87E+01	1.70	2025	71520	32%	2.77E+03
TX-114 liquid	not exist	not exist	not exist	not exist	not exist	not exist	not exist	not exist	8.00E-00	3.01E+02	1.39	0	0	51%	0.00E+01
TX-114 solid	1.88E-05	2.43E-05	9.66E-04	1.9%	2.4%	95.7%	1.01E-03	41	5.03E+01	9.87E+01	1.70	2025	71520	32%	2.77E+03
241-TX-115	2.22E-05	2.15E-05	9.93E-04	2.1%	2.1%	95.8%	1.04E-03	42	4.10E+01	1.58E+02	1.70	2150	75931	32%	3.73E+03
TX-115 liquid	not exist	not exist	not exist	not exist	not exist	not exist	not exist	not exist	8.00E-00	3.01E+02	1.39	0	0	51%	0.00E+01
TX-115 solid	2.22E-05	2.15E-05	9.93E-04	2.1%	2.1%	95.8%	1.04E-03	42	4.10E+01	1.58E+02	1.70	2150	75931	32%	3.73E+03
241-TX-116	5.23E-05	3.78E-05	1.05E-03	4.6%	3.3%	92.1%	1.14E-03	47	1.98E+02	2.81E+01	1.69	2389	84353	32%	5.90E+03
TX-116 liquid	not exist	not exist	not exist	not exist	not exist	not exist	not exist	not exist	8.00E-00	3.01E+02	1.39	0	0	51%	0.00E+01
TX-116 solid	5.23E-05	3.78E-05	1.05E-03	4.6%	3.3%	92.1%	1.14E-03	47	1.98E+02	2.81E+01	1.69	2389	84353	32%	5.90E+03
241-TX-117	1.99E-05	1.93E-05	1.05E-03	1.8%	1.8%	96.4%	1.09E-03	45	1.08E+02	7.74E+01	1.71	2370	83685	32%	4.41E+03
TX-117 liquid	not exist	not exist	not exist	not exist	not exist	not exist	not exist	not exist	8.00E-00	3.01E+02	1.39	0	0	51%	0.00E+01
TX-117 solid	1.99E-05	1.93E-05	1.05E-03	1.8%	1.8%	96.4%	1.09E-03	45	1.08E+02	7.74E+01	1.71	2370	83685	32%	4.41E+03
241-TX-118	7.88E-05	4.66E-05	7.74E-04	8.8%	5.2%	86.1%	8.99E-04	37	2.15E+02	1.11E+02	1.70	1136	40105	47%	3.79E+03
TX-118 liquid	not exist	not exist	not exist	not exist	not exist	not exist	not exist	not exist	8.00E-00	3.01E+02	1.39	0	0	51%	0.00E+01
TX-118 solid	7.88E-05	4.66E-05	7.74E-04	8.8%	5.2%	86.1%	8.99E-04	37	2.15E+02	1.11E+02	1.70	1136	40105	47%	3.79E+03
241-TY-101	3.10E-06	5.76E-06	6.16E-04	0.5%	0.9%	98.6%	6.25E-04	26	2.62E+01	6.00E+01	1.64	447	15774	35%	3.37E+02
TY-101 liquid	not exist	not exist	not exist	not exist	not exist	not exist	not exist	not exist	4.00E-00	2.83E+02	1.40	0	0	55%	0.00E+01
TY-101 solid	3.10E-06	5.76E-06	6.16E-04	0.5%	0.9%	98.6%	6.25E-04	26	2.62E+01	6.00E+01	1.64	447	15774	35%	3.37E+02
241-TY-102	1.58E-05	1.03E-05	5.68E-04	2.7%	1.7%	95.6%	5.94E-04	24	4.10E+01	1.58E+02	1.72	242	8556	32%	4.25E+02
TY-102 liquid	not exist	not exist	not exist	not exist	not exist	not exist	not exist	not exist	8.00E-00	3.01E+02	1.39	0	0	51%	0.00E+01
TY-102 solid	1.58E-05	1.03E-05	5.68E-04	2.7%	1.7%	95.6%	5.94E-04	24	4.10E+01	1.58E+02	1.72	242	8556	32%	4.25E+02
241-TY-103	1.24E-05	4.23E-06	6.54E-04	1.8%	0.6%	97.5%	6.71E-04	27	9.06E+01	1.47E+01	1.70	613	21656	44%	7.04E+02
TY-103 liquid	not exist	not exist	not exist	not exist	not exist	not exist	not exist	not exist	1.29E+01	1.30E+00	1.23	0	0	75%	0.00E+01
TY-103 solid	1.24E-05	4.23E-06	6.54E-04	1.8%	0.6%	97.5%	6.71E-04	27	9.06E+01	1.47E+01	1.70	613	21656	44%	7.04E+02
241-TY-104	9.31E-05	1.69E-06	5.55E-04	14.3%	0.3%	85.4%	6.50E-04	27	1.94E+03	1.10E+02	1.44	174	6149	53%	3.38E+03
TY-104 liquid	3.18E-07	1.26E-07	2.50E-06	10.8%	4.3%	84.9%	2.95E-06	0	1.29E+01	1.09E+02	1.17	11	401	75%	7.98E+00
TY-104 solid	9.27E-05	1.56E-06	5.52E-04	14.3%	0.2%	85.4%	6.47E-04	27	2.04E+03	1.10E+02	1.46	163	5748	52%	3.37E+03
241-TY-105	3.68E-05	1.45E-05	7.17E-04	4.8%	1.9%	93.3%	7.68E-04	31	1.88E+02	7.86E+00	1.53	874	30881	44%	1.73E+03
TY-105 liquid	not exist	not exist	not exist	not exist	not exist	not exist	not exist	not exist	1.29E+01	1.09E+02	1.17	0	0	75%	0.00E+01

Tank Name	Grad (cfm) HGR from Radiolysis	Gtherm (cfm) HGR from Thermolysis	Gcorr (cfm) HGR from Corrosion	(Grad)% Percent HGR from Radiolysis	(Gtherm)% Percent HGR from Thermolysis	(Gcorr)% Percent HGR from Corrosion	Gmod (cfm) Total HGR from Model	Gmod (L/Day) Total HGR from Model	Sr90 in Waste (uCi/g)	Cs137 in Waste (uCi/g)	Density (g/ml)	Waste Volume (kL)	Waste Volume (ft3)	H2O (wt%)	Power Load (watt)
TY-105 solid	3.68E-05	1.45E-05	7.17E-04	4.8%	1.9%	93.3%	7.68E-04	31	1.88E+02	7.86E-00	1.53	874	30881	44%	1.73E+03
241-TY-106	1.63E-06	4.20E-07	5.33E-04	0.3%	0.1%	99.6%	5.33E-04	22	1.12E+02	1.81E+01	1.37	79	2807	35%	9.06E+01
TY-106 liquid	not exist	not exist	not exist	not exist	not exist	not exist	not exist	not exist	1.29E+01	1.09E+02	1.17	0	0	75%	0.00E+01
TY-106 solid	1.63E-06	4.20E-07	5.33E-04	0.3%	0.1%	99.6%	5.33E-04	22	1.12E+02	1.81E+01	1.37	79	2807	35%	9.06E+01
241-U-101	2.87E-05	7.65E-07	5.41E-04	5.0%	0.1%	94.8%	5.71E-04	23	1.84E+03	1.10E+02	1.43	95	3342	34%	1.73E+03
U-101 liquid	3.36E-07	1.67E-07	2.52E-06	11.1%	5.5%	83.3%	3.02E-06	0	1.29E+01	1.09E+02	1.17	11	401	76%	7.98E-00
U-101 solid	2.84E-05	5.97E-07	5.39E-04	5.0%	0.1%	94.9%	5.68E-04	23	2.04E+03	1.10E+02	1.46	83	2941	30%	1.73E+03
241-U-102	3.13E-04	4.38E-04	8.50E-04	19.5%	27.4%	53.1%	1.60E-03	66	7.13E+01	1.56E+02	1.68	1420	50131	37%	2.89E+03
U-102 liquid	1.71E-05	2.29E-05	1.54E-05	30.9%	41.3%	27.8%	5.54E-05	2	6.78E-00	2.61E+02	1.38	68	2406	48%	1.20E+02
U-102 solid	2.96E-04	4.15E-04	8.35E-04	19.1%	26.9%	54.0%	1.55E-03	63	7.40E+01	1.52E+02	1.69	1351	47724	36%	2.77E+03
241-U-103	3.32E-04	6.16E-04	9.33E-04	17.7%	32.8%	49.6%	1.88E-03	77	2.30E+01	2.11E+02	1.66	1772	62563	40%	3.37E+03
U-103 liquid	1.62E-05	1.83E-05	1.11E-05	35.6%	40.0%	24.4%	4.57E-05	2	8.28E-00	3.90E+02	1.41	49	1738	50%	1.32E+02
U-103 solid	3.16E-04	5.98E-04	9.21E-04	17.2%	32.6%	50.2%	1.84E-03	75	2.33E+01	2.06E+02	1.66	1722	60825	40%	3.24E+03
241-U-104	2.98E-04	9.53E-05	6.35E-04	29.0%	9.3%	61.7%	1.03E-03	42	8.25E+02	1.26E+02	1.65	462	16309	35%	4.65E+03
U-104 liquid	not exist	not exist	not exist	not exist	not exist	not exist	not exist	not exist	4.00E-00	2.83E+02	1.40	0	0	55%	0.00E+01
U-104 solid	2.98E-04	9.53E-05	6.35E-04	29.0%	9.3%	61.7%	1.03E-03	42	8.25E+02	1.26E+02	1.65	462	16309	35%	4.65E+03
241-U-105	3.35E-04	5.07E-04	8.90E-04	19.4%	29.3%	51.4%	1.73E-03	71	9.43E-00	2.95E+02	1.63	1582	55879	32%	3.74E+03
U-105 liquid	9.83E-05	7.98E-05	3.18E-05	46.8%	38.0%	15.1%	2.10E-04	9	1.96E+01	5.96E+02	1.46	140	4946	63%	6.02E+02
U-105 solid	2.37E-04	4.27E-04	8.59E-04	15.6%	28.0%	56.4%	1.52E-03	62	8.55E-00	2.69E+02	1.64	1442	50933	29%	3.14E+03
241-U-106	5.24E-04	5.65E-04	7.22E-04	28.9%	31.2%	39.9%	1.81E-03	74	7.81E+01	1.74E+02	1.60	856	30212	41%	1.84E+03
U-106 liquid	3.83E-05	3.78E-05	1.28E-05	43.1%	42.5%	14.4%	8.89E-05	4	8.00E-00	3.01E+02	1.35	57	2005	49%	1.13E+02
U-106 solid	4.85E-04	5.28E-04	7.09E-04	28.2%	30.6%	41.2%	1.72E-03	71	8.22E+01	1.67E+02	1.62	799	28207	40%	1.73E+03
241-U-107	3.77E-05	6.98E-05	8.74E-04	3.8%	7.1%	89.1%	9.82E-04	40	2.90E-00	9.33E+01	1.67	1544	54542	29%	1.19E+03
U-107 liquid	1.13E-05	8.23E-06	2.81E-05	23.7%	17.3%	59.0%	4.70E-05	2	2.94E+01	2.69E+02	1.41	125	4412	50%	2.24E+02
U-107 solid	2.65E-05	6.15E-05	8.46E-04	2.8%	6.6%	90.6%	9.34E-04	38	3.09E-00	8.04E+01	1.70	1420	50131	27%	9.64E+02
241-U-108	2.57E-04	3.34E-04	9.29E-04	16.9%	22.0%	61.1%	1.52E-03	62	1.02E+02	1.55E+02	1.72	1772	62563	36%	4.29E+03
U-108 liquid	1.58E-05	1.92E-05	2.05E-05	28.5%	34.5%	37.0%	5.54E-05	2	8.00E-00	3.09E+02	1.39	91	3208	50%	1.91E+02
U-108 solid	2.41E-04	3.15E-04	9.09E-04	16.5%	21.5%	62.0%	1.46E-03	60	1.06E+02	1.48E+02	1.73	1681	59355	36%	4.10E+03
241-U-109	7.81E-05	1.52E-04	9.24E-04	6.8%	13.2%	80.1%	1.15E-03	47	9.29E-00	1.34E+02	1.66	1760	62162	27%	2.04E+03
U-109 liquid	9.71E-06	1.03E-05	1.62E-05	26.8%	28.4%	44.7%	3.62E-05	1	7.11E-01	2.79E+02	1.47	72	2540	51%	1.39E+02
U-109 solid	6.84E-05	1.42E-04	9.08E-04	6.1%	12.7%	81.2%	1.12E-03	46	9.61E-00	1.29E+02	1.67	1688	59622	26%	1.90E+03
241-U-110	3.21E-04	1.13E-04	6.87E-04	31.5%	1.1%	67.4%	1.02E-03	42	2.04E+03	1.10E+02	1.46	704	24865	34%	1.46E+04
U-110 liquid	not exist	not exist	not exist	not exist	not exist	not exist	not exist	not exist	1.29E+01	1.09E+02	1.17	0	0	75%	0.00E+01
U-110 solid	3.21E-04	1.13E-04	6.87E-04	31.5%	1.1%	67.4%	1.02E-03	42	2.04E+03	1.10E+02	1.46	704	24865	34%	1.46E+04
241-U-111	1.72E-04	1.59E-04	8.08E-04	15.1%	13.9%	70.9%	1.14E-03	47	1.48E+02	1.22E+02	1.63	1245	43981	32%	3.19E+03
U-111 liquid	not exist	not exist	not exist	not exist	not exist	not exist	not exist	not exist	8.00E-00	3.01E+02	1.39	0	0	51%	0.00E+01
U-111 solid	1.72E-04	1.59E-04	8.08E-04	15.1%	13.9%	70.9%	1.14E-03	47	1.48E+02	1.22E+02	1.63	1245	43981	32%	3.19E+03
241-U-112	7.76E-06	1.30E-06	5.60E-04	1.4%	0.2%	98.4%	5.69E-04	23	1.55E+02	6.67E+01	1.63	185	6550	29%	5.28E+02
U-112 liquid	4.39E-07	2.00E-07	3.35E-06	11.0%	5.0%	84.0%	3.99E-06	0	1.29E+01	1.09E+02	1.17	15	535	75%	1.06E+01
U-112 solid	7.33E-06	1.10E-06	5.57E-04	1.3%	0.2%	98.5%	5.65E-04	23	2.27E+02	6.41E+01	1.67	170	6016	26%	5.18E+02
241-U-201	6.66E-07	1.28E-07	5.24E-05	1.3%	0.2%	98.5%	5.32E-05	2	1.65E+02	5.54E+01	1.53	19	668	34%	3.94E+01
U-201 liquid	1.06E-07	4.10E-08	3.13E-06	3.2%	1.3%	95.5%	3.27E-06	0	1.29E+01	1.09E+02	1.17	4	134	70%	2.66E-00
U-201 solid	5.61E-07	8.71E-08	4.93E-05	1.1%	0.2%	98.7%	4.99E-05	2	1.92E+02	4.57E+01	1.62	15	535	27%	3.68E+01
241-U-202	6.94E-07	1.33E-07	5.24E-05	1.3%	0.3%	98.4%	5.32E-05	2	1.65E+02	5.54E+01	1.53	19	668	36%	3.94E+01
U-202 liquid	1.06E-07	4.13E-08	3.13E-06	3.2%	1.3%	95.5%	3.27E-06	0	1.29E+01	1.09E+02	1.17	4	134	73%	2.66E-00
U-202 solid	5.88E-07	9.20E-08	4.93E-05	1.2%	0.2%	98.6%	5.00E-05	2	1.92E+02	4.57E+01	1.62	15	535	29%	3.68E+01
241-U-203	5.17E-07	9.92E-08	4.60E-05	1.1%	0.2%	98.7%	4.66E-05	2	1.45E+02	6.25E+01	1.47	11	401	48%	2.10E+01
U-203 liquid	1.04E-07	3.83E-08	3.12E-06	3.2%	1.2%	95.6%	3.26E-06	0	1.29E+01	1.09E+02	1.17	4	134	70%	2.66E-00
U-203 solid	4.13E-07	6.09E-08	4.29E-05	1.0%	0.1%	98.9%	4.34E-05	2	1.92E+02	4.57E+01	1.62	8	267	40%	1.84E+01

Tank Name	Grad (cfm) HGR from Radiolysis	Gtherm (cfm) HGR from Thermolysis	Gcorr (cfm) HGR from Corrosion	(Grad)% Percent HGR from Radiolysis	(Gtherm)% Percent HGR from Thermolysis	(Gcorr)% Percent HGR from Corrosion	Gmod (cfm) Total HGR from Model	Gmod (L/Day) Total HGR from Model	Sr-90 in Waste (uCi/g)	Cs-137 in Waste (uCi/g)	Density (g/ml)	Waste Volume (kL)	Waste Volume (ft3)	H2O (wt%)	il
241-U-204	1.05E-07	6.35E-08	4.60E-05	0.2%	0.1%	99.6%	4.62E-05	2	3.98E-00	3.54E+01	1.26	11	401	45%	2.78
U-204 liquid	1.04E-07	3.79E-08	3.12E-06	3.2%	1.2%	95.7%	3.26E-06	0	1.29E+01	1.09E+02	1.17	4	134	87%	2.66
U-204 solid	1.44E-09	2.56E-08	4.29E-05	0.0%	0.1%	99.9%	4.29E-05	2	6.00E-03	2.60E-00	1.31	8	267	26%	2.2

APPENDIX B

POSTULATED BUMP SCENARIOS DEEMED NOT PLAUSIBLE

This **page** intentionally left blank

APPENDIX B

POSTULATED BUMP SCENARIOS DEEMED NOT PLAUSIBLE

B.1 STEAM BUMP BY INTERSTITIAL SLUDGE SUPERHEAT

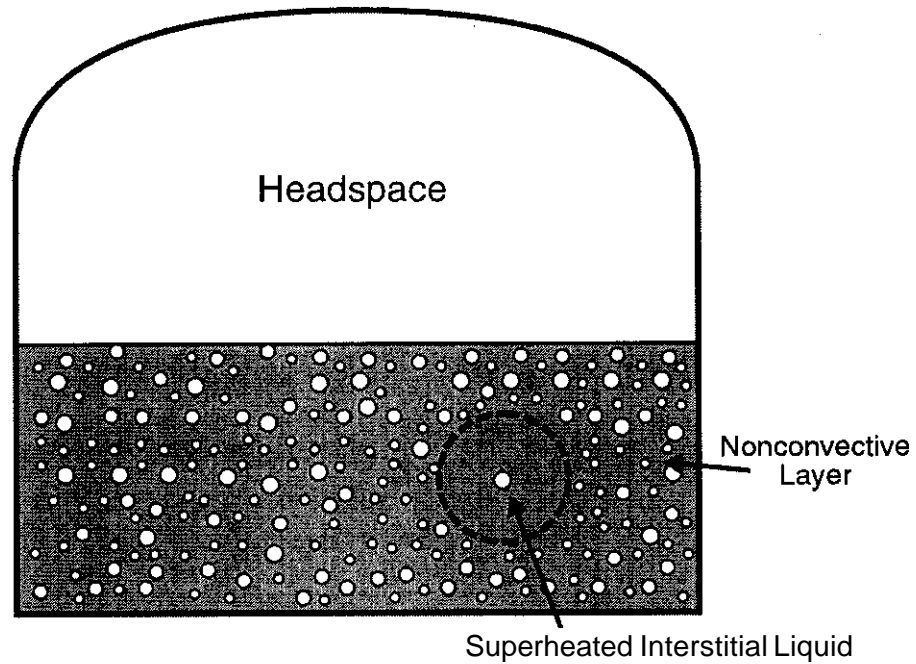
In Section 4.0, we demonstrated the importance of a deep supernatant layer as a necessary condition for a tank bump. Here we examine the potential for a steam bump within a non-convective layer during dryout (see Figure B-I). Steam bumps are known to occur in pure water that is rapidly brought to boiling in a vessel with smooth walls. In this case, boiling is started with large liquid water superheats. The few bubbles that form at large superheats grow very rapidly at a rate controlled largely by heat conduction in the surrounding liquid just outside the bubbles. The process is rather unstable and could result in the ejection of liquid from the vessel (i.e., "bumping"). To prevent the occurrence of bumping, the water is usually seeded with solid particles or gas bubbles that act as nucleation sites and promote boiling at low superheats. In this case, numerous slowly growing bubbles are formed and a more uniform (smooth) boiling activity is realized. Thus, steam bumps in boiling water derive mainly from high liquid superheats. As we shall see below, significant liquid superheating is precluded in sludge by the presence of the solid phase particulate and pre-existing gas bubbles that serve as vapor-bubble nuclei.

In the analysis that follows, it is assumed that the non-convective layer evaporation process is one of bubble production by volumetric (decay) heating. This picture is believed to be conservative because water loss from the overheated layer is likely a dryout phenomenon in which an evaporation front propagates up from the bottom toward the surface of the layer. In this regard, it should be recognized that the effective upward heat flux in the sludge is very low ($I \approx 100 \text{ W m}^{-2}$, see Section 3.6) and about two-to-four orders of magnitude less than typical nucleate boiling heat fluxes (10^4 to 10^6 W m^{-2}).

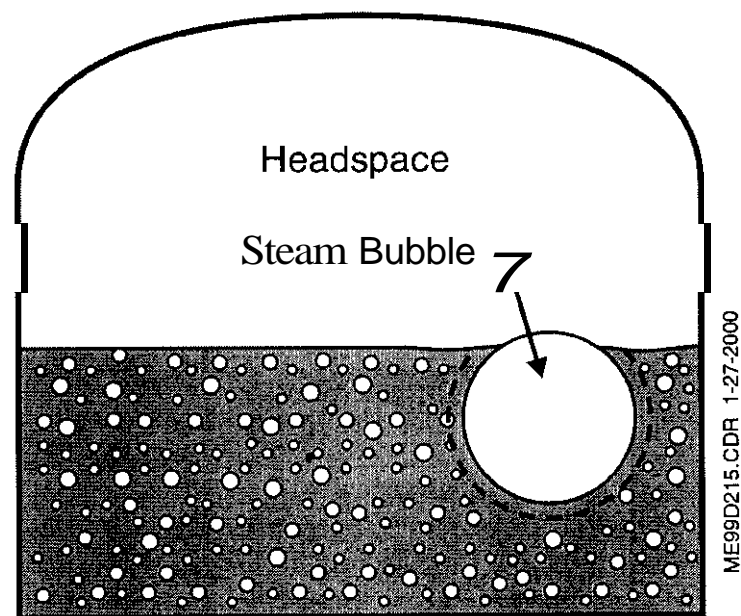
Bubble growth occurs when the internal pressure (vapor pressure plus partial pressure of any additional gas) is large enough to overcome the external bubble pressure due to surface tension and yield stress ($2\sigma/R + 2/\sqrt{3} \tau_0$, where R is the bubble radius, σ is the surface tension, and τ_0 is the yield stress in the Bingham model of the non-convective layer). The bubble is then unstable and grows at a rate governed by the inertia of the surrounding liquid and conduction heat transfer from the surrounding liquid to the bubble "surface". The initial period of inertially-limited growth is important only in cases involving very high liquid superheats and/or low (sub-atmospheric) ambient pressures. This gives rise to a "waiting time" before a period of thermally-dominated bubble growth. After the waiting time, which is practically non-existent for the conditions of interest here, bubbles grow by the thermally-limited process and the bubble radius after time t is (see, e.g., Scriven [1959]):

$$R = Ja (\pi \alpha_l t)^{1/2} \quad (\text{B-1})$$

Figure B-1. Steam Bump Due to Interstitial Superheat in Non-Convective Layer (Hypothetical).



(a) Sludge with region of interstitial liquid heated above its boiling point



(b) Rapid bubble growth following nucleation of bubble in superheated region

with the Jakob number, Ja, defined as

$$Ja = \frac{\rho_\ell c_{p,\ell} (T - T_{bp})}{\rho_g h_{\ell g}} \quad (B-2)$$

In equations (B-1) and (B-2) T_{bp} , ρ_ℓ , $c_{p,\ell}$, α_ℓ , and $h_{\ell g}$ are, respectively, the boiling point, density, specific heat, thermal diffusivity, and latent heat of evaporation of the liquid (interstitial water), T is the instantaneous temperature of the volumetrically heated waste, and ρ_g is the density of the vapor in the bubble. In writing equation (B-1) it is assumed that the bubble displaces both the precipitate particles and the liquid as it grows, so that the bubble only contains water vapor. If, instead, the precipitate particles are locked in place so that the bubble must push the surrounding liquid through channels in a stationary precipitate matrix, then a different bubble growth equation is required (see Epstein [1994]). For the double-shell tanks of interest, bubbles growing between stationary particles is not possible (Gauglitz et al. 1996; and Stewart et al. 1996a).

As the liquid temperature T rises above the liquid boiling point owing to volumetric decay, heating new bubbles will form from the nuclei present in the liquid if the rate of energy input is higher than that removed by the bubbles nucleated previously at lower superheats. Thus, at any particular time there will be a distribution of bubble sizes within the waste. We will ignore this complication and assume that all the bubble nuclei in the system are activated as soon as the waste is heated to its boiling temperature T_{bp} . Subject to this assumption, the distribution of bubble sizes is a uniform one and given by R in equation (B-1).

By considering an energy balance for the boiling waste, we may write

$$Q = \rho_\ell c_{p,\ell} \frac{dT}{dt} + N h_{\ell g} \rho_g 4\pi R^2 \frac{dR}{dt} \quad (B-3)$$

where N is the number of active nuclei (precipitate + gas bubbles) per unit volume of non-convective layer and Q is the volumetric decay heating rate (in $W m^{-3}$). Equation (B-3) simply states that the rate of energy input is equal to the rate of increase in liquid waste sensible heat plus the heat removed volumetrically by the growing bubbles. For small temperature increases, equation (B-3) may be integrated from $T = T_{bp}$ and $R = 0$ at $t = 0$ to get

$$T - T_{bp} = \frac{Q t}{\rho_\ell c_{p,\ell}} - \frac{h_{\ell g} N \rho_g}{\rho_\ell c_{p,\ell}} \frac{4}{3} \pi R^3 \quad (B-4)$$

Eliminating R between equations (B-1) and (B-4) gives

$$T - T_{bp} = \frac{Q t}{\rho_\ell c_{p,\ell}} - \frac{4\pi h_{\ell g} N \rho_g}{3\rho_\ell c_{p,\ell}} \left(\frac{\rho_\ell c_{p,\ell}}{\rho_g h_{\ell g}} \right)^3 (\pi \alpha_\ell t)^{\frac{3}{2}} (T - T_{bp})^3 \quad (B-5)$$

Equation (B-5) is an implicit relationship between the instantaneous liquid superheat ($T - T_{bp}$) and time (t). A careful examination of equation (B-5) reveals the important behavior that $T - T_{bp}$ achieves a maximum value. This value can be determined by differentiating equation (B-5) with respect to time and setting the derivatives equal to zero. To facilitate this mathematical operation, it is convenient to introduce the following dimensionless variables:

$$\tau = \left(\frac{16 \pi^5 Q^4 \alpha_\ell^3 N^2}{9 \rho_g^4 h_{\ell g}^4} \right)^{\frac{1}{7}} t \quad (B-6)$$

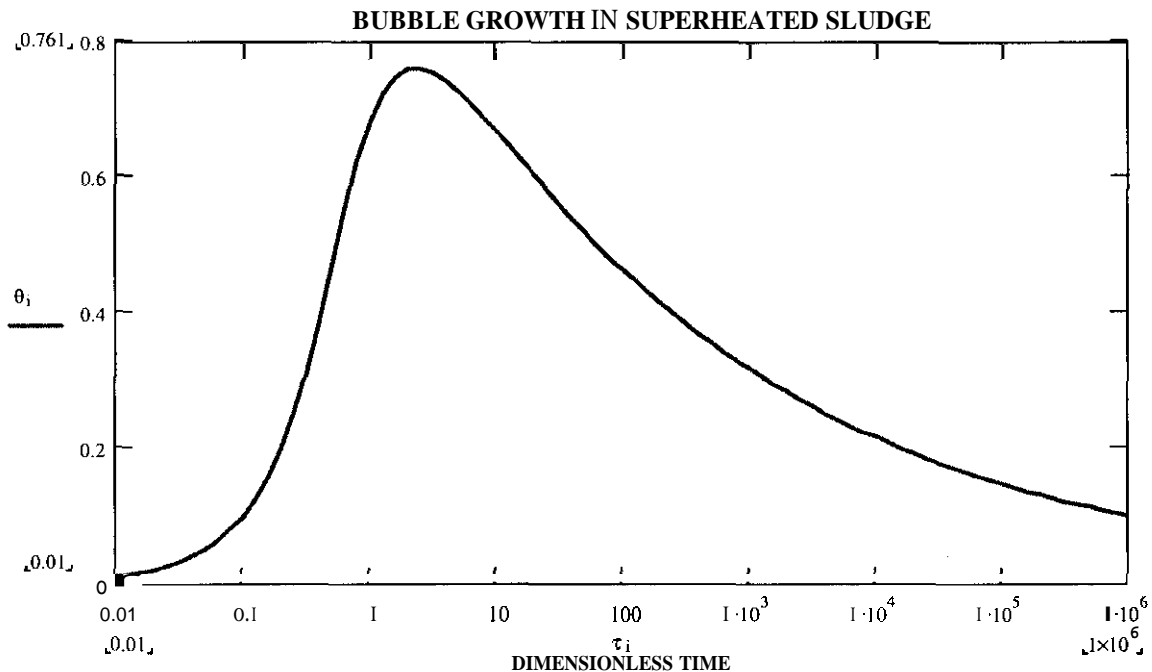
$$\theta = \left(\frac{16 \pi^5 k_\ell^3 N^2}{9 Q^3} \right)^{\frac{1}{7}} \left(\frac{\rho_\ell c_{p,\ell}}{\rho_g h_{\ell g}} \right)^{\frac{4}{7}} (T - T_{bp}) \quad (B-7)$$

Then, equation (B-5) reduces to the compact and universal form

$$\theta = \tau - \tau^{\frac{3}{2}} \theta^3 \quad (B-8)$$

For any chosen value of dimensionless time τ , the dimensionless superheat is readily seen to be the solution of a cubic equation. Equation (B-8) is plotted in Figure B-2.

Figure B-2. Dimensionless Liquid Superheat Versus Dimensionless Time.



To obtain the peak superheat value θ_{\max} , we seek the condition $d\theta/d\tau=0$. From equation (B-8), we find that this condition is satisfied at all points $(\epsilon_{\max}, \tau_{\max})$ that lie along the curve

$$\frac{3}{2} \theta_{\max}^3 \tau_{\max}^{\frac{1}{2}} = 1.0 \quad (\text{B-9})$$

Finally, solving equations (B-8) and (B-9) gives the maximum dimensionless superheat

$$\theta_{\max} = \left(\frac{4}{27} \right)^{\frac{1}{7}} = 0.761 \quad (\text{B-IO})$$

which occurs at the dimensionless time

$$\tau_{\max} = (324)^{\frac{1}{7}} = 2.28 \quad (\text{B-11})$$

Using equations (B-6) and (B-7) to convert back to physical variables, we find that the liquid superheat attains its peak value after an elapsed time

$$t_{\max} = \left(\frac{182 \rho_g^4 h_{\ell g}^4}{\pi^5 Q^4 \alpha_{\ell}^3 N^2} \right)^{\frac{1}{7}} \quad (\text{B-12})$$

and the peak liquid superheat is

$$T_{\max} - T_{bp} = \left(\frac{Q^3}{12 \pi^5 k_{\ell}^3 N^2} \right)^{\frac{1}{7}} \left(\frac{\rho_g h_{\ell g}}{\rho_{\ell} c_{p,\ell}} \right)^{\frac{4}{7}} \quad (\text{B-13})$$

We note from equation (B-13) that the maximum liquid superheat increases with increasing decay power Q and decreases with increasing bubble nucleation site density N . All the parameters in equation (B-13) are known, except for the nucleation site density N . The potential number density of nucleation sites in waste can be bounded from above by assuming that each precipitate particle of radius r_p is an active site. This results in the estimate

$$N = \frac{\epsilon_s}{\left(\frac{4}{3} \right) \pi r_p^3} \quad (\text{B-14})$$

where ϵ_s is the volume fraction occupied by the solid precipitate ($\epsilon_s = 0.5$) and r_p is the effective (average) radius of the precipitate particles ($r_p \approx 1.0 \mu\text{m}$). Equation (B-14) results in $N \approx 10^{17}/\text{m}^3$, an estimate which is probably unrealistically high. The value of N for pre-existing gas bubbles is obtained from the relation

$$N = \frac{\alpha}{\left(\frac{4}{3} \pi r_b^3\right)} \quad (\text{B-15})$$

where α is the volume fraction occupied by the gas bubbles (α ; 0.2) and r_b is the average bubble radius (r_b ; 1.0 mm). Equation (B-15) yields N ; $5 \times 10^7/\text{m}^3$ for the number density of pre-existing gas-bubbles. Coincidentally, this value of N falls within the range of values for ordinary water (no precipitate particles) containing natural impurities (dust, etc.), namely 10^6 to $10^{11}/\text{m}^3$ (Richter 1981; Abdollahian et al. 1982; Ardon 1978; and Rivard and Travis 1980).

Some indication of the validity of equation (B-13) can be given by considering the Lipkis et al. (1956) experimental study of boiling in a volumetrically-heated aqueous KOH solution pool. In order to prevent bumpiness, a sheet of teflon™ with embedded aluminum chips was placed on the bottom of the test vessel. The aluminum/KOH reaction produced very many tiny hydrogen bubbles which acted as vapor-bubble nuclei. The volumetric power applied to the pool was nominally $1.5 \times 10^7 \text{ W m}^{-3}$. The corresponding measured superheat was $\Delta T = 0.5^\circ\text{C}$. Substituting these measured values into equation (B-13), together with the water physical properties $h_{lg} = 2.3 \times 10^6 \text{ J kg}^{-1}$, $k_l = 0.68 \text{ W m}^{-1} \text{ K}^{-1}$, $c_{p,l} = 4200 \text{ J kg}^{-1} \text{ K}^{-1}$, $\rho_g = 0.6 \text{ kg m}^{-3}$, and $\rho_l = 960 \text{ kg m}^{-3}$, and solving for N gives

$$N = 2.3 \times 10^9 / \text{m}^3 \quad (\text{B-16})$$

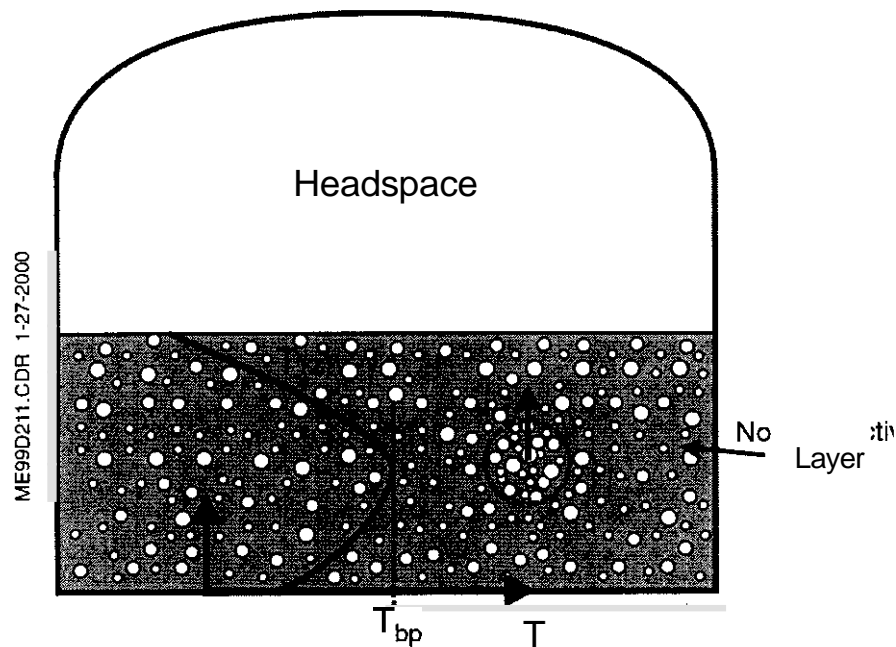
This is an encouraging result because it falls in the middle of the expected range of site densities 10^6 to $10^{11}/\text{m}^3$.

Inserting our previous estimate N ; $5 \times 10^7/\text{m}^3$ for 1.0 mm pre-existing gas bubbles together with the decay heat rate $Q = 200 \text{ W m}^{-3}$ into equation (B-13) gives a maximum waste-liquid superheat of only $T_{\max} - T_{bp} = 1.2 \times 10^{-2}^\circ\text{C}$. Even if one adopts the lower end of the site density range for gas bubble, namely $N = 4 \times 10^5/\text{m}^3$ for $r_b = 5 \text{ mm}$, the liquid superheat in boiling waste is still small and equal to $T_{\max} - T_{bp} = 4.8 \times 10^{-2}^\circ\text{C}$. Laboratory experience with boiling liquids indicate that these superheats are far too small to produce bumpy boiling action. For example, smooth volumetric boiling activity was achieved in the experiments of Lipkis et al. (1956) with measured water superheats as high as 0.5°C . We conclude by stating that the volume-heating rate in the non-convective layer is too low to produce a steam bump.

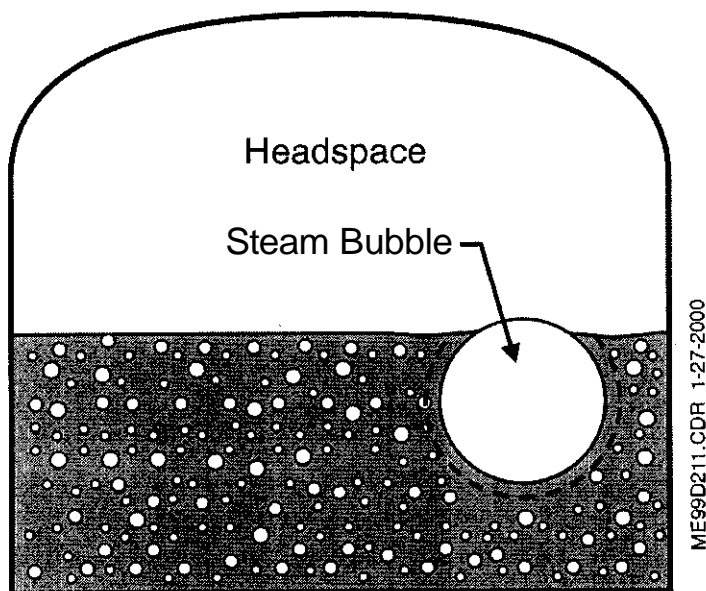
B.2 STEAM BUMP BY LOCAL CONVECTION IN SLUDGE (FUMARoles)

Tank bumps have been postulated to occur via a buoyant displacement within a hot, otherwise non-convective layer (see Figure B-3). The mechanism that might cause a buoyant displacement within the non-convective layer is as follows. Generally, the waste material near the mid-plane of the non-convective layer retains more gas than the overlying layer that extends to the surface. A Taylor instability develops in which the central waste material is presumed buoyant enough with respect to the overlying layer to rise and mix with the overlying layer. During an overheated condition, the temperature of the sludge near the mid-plane of the non-convective

Figure B-3. Steam Bump Due to Local Convection in Non-Convective Layer (Hypothetical, "Fumarole").



(a) Hot sludge parcel begins to rise and superheat.



(b) Steam bubble growth within hot sludge parcel

layer is close to the boiling point of the interstitial liquid. As the initially, centrally located hot sludge rises through the non-convective layer, it experiences a reduction in hydrostatic pressure and its interstitial liquid may boil and produce steam. We emphasize that this mechanism differs from the rollover mechanism for steam production in that an overlying convective layer is not required - the buoyant displacement is postulated to occur within the non-convective layer itself. However, in the absence of a convective layer, it is difficult to envision significant waste release from the tank.

In order to rigorously apply the Taylor instability theory to Hanford sludge, it is necessary to take into account the viscoplastic nature of the sludge material. Construction of the equations and their solution for this case would be very difficult and no analysis of this problem is available. Here, we content ourselves with an analysis that considers the waste material to be a viscous Newtonian material. That is, the waste gel is assumed to be shocked into a liquefied state. The same waste rheology was assumed by Meyer et al. (1997) in their Taylor-instability model of buoyant displacements in DSTs. We are concerned with the waste tank situation in which a central horizontal waste layer of thickness h and low density lies below a relatively thick, dense layer that extends to the surface of the waste. The lower layer is less dense than the upper layer owing to a higher degree of gas retention in the lower layer. The two layers are assumed to have the same kinematic viscosity.

An approximate dispersion relation for the problem described above has been derived by Plesset and Whipple (1974) and is

$$h = \nu k^2 \left[1 + \frac{g k \Delta \rho / \rho}{[1 + \coth(kh)] (\nu k^2)^2} \right]^{1/2} \quad (\text{B-17})$$

where ν and ρ are the kinematic viscosity and the density of the waste material, respectively, $\Delta \rho$ is the density difference between the upper and lower layers, g is the gravitational constant, k is the wave number, and n is the growth rate of the unstable waves that develop at the boundary that separates the two layers. The wave number is related to the disturbance wavelength by the definition

$$k = \frac{2\pi}{\lambda} \quad (\text{B-18})$$

and the characteristic time for the waves to grow to an amplitude of the order of the wavelength is

$$\tau \equiv \frac{1}{n} \quad (\text{B-19})$$

A typical in situ measurement in DSTs shows a void fraction increment in the lower layer over the upper layer of 10% (Stewart et al. 1996b). The void fraction in a hypothetical tank without a supernate layer could be much higher than 10%. Assuming 30% for the void fraction,

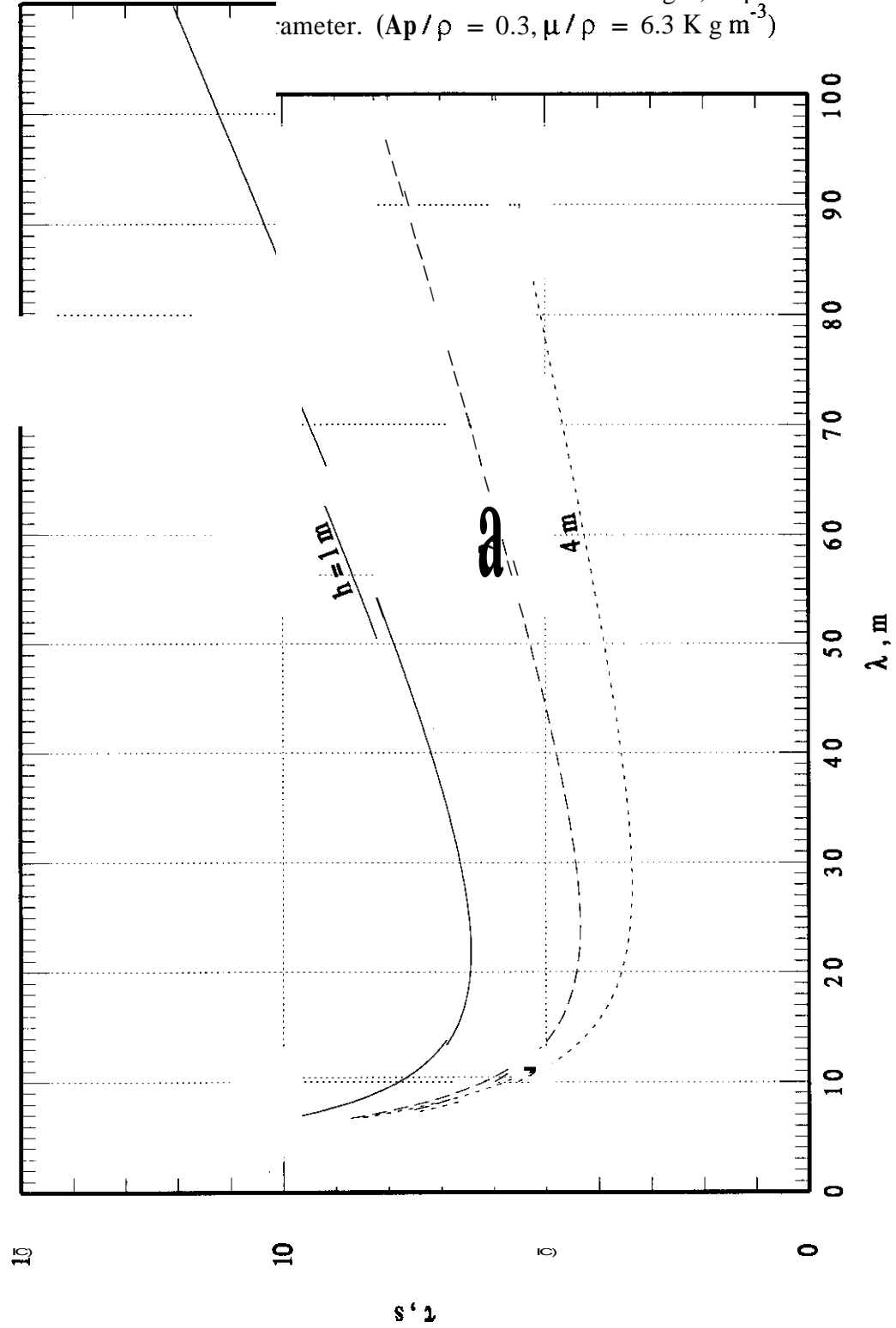
$\Delta\rho/\rho$; 0.3. The waste viscosity μ is assigned the value 10^4 Pa•s which is the peak measured value at the bottom of undisturbed DST waste, that is first-pass ball rheometer measurements reported by Stewart et al. (1996b) and Stewart (1998). The waste material density is approximately ρ ; 1600 kg m^{-3} so that $v = 6.25\text{ m}^2\text{ s}^{-1}$. Figure B-4 shows the characteristic time for the buoyant displacement to develop as a function of the wavelength of the disturbance that caused the instability for several relevant values of the thickness h of the central layer. The minimums in the curves correspond to the most unstable disturbance wavelengths. These waves cannot materialize within the Hanford waste tanks because they exceed the lateral dimensions of the tanks (~ 20 m). However, smaller wavelengths are also unstable and may occur with lower probability. The most probable wavelength coincides with the tank diameter. Despite the high viscosity assigned to the material, seven orders of magnitude larger than the viscosity of water, these waves will develop and reach the surface of the waste less than about 10 s.

Obviously, the Taylor instability has the potential of producing significant quantities of steam by transporting massive quantities of waste material from the hot mid-plane region to the surface in a relatively short period of time compared with, say, bubble rise times in the assumed Newtonian waste layer. When the sludge temperature is low and not conducive to steam production, the Taylor instability should still be operative and result in very efficient and dangerous gas release events. However, this has not been observed in waste tanks that lack a convective layer (e.g., SSTs). Field measurements indicate gas release times of at least 1.0 hour in duration. The release efficiencies are less than 10% with most of the releases in the 0.1 to 1.0% range. The actual small, lethargic releases are consistent with a mechanism of gas percolation to the surface through bubble inter-connectivity. Apparently, the strength of the material, which enables it to accumulate gas, stabilizes the waste layer against an internal buoyant displacement. If the Taylor stability analysis were performed for the viscoplastic case (a difficult analysis), one would most likely find a cutoff wavelength that exceeds the tank diameter.

B.3 REFERENCES

- Abdollahian, D., J. Healzer, E. Janssen, and C. Amos, 1982, *Critical Flow Data Review and Analysis*, EPRI NP-2192, Electric Power Research Institute, Palo Alto, California.
- Ardon, K. H., 1978, "A Two-Fluid Model for Critical Vapor-Liquid Flow," *Int. J. Multiphase Flow*, Vol. 4, pp. 323-333.
- Epstein, M., 1994, "A Similarity Solution for Combined Hydrodynamic and Heat Transfer Controlled Growth in a Porous Medium," *J. Heat Transfer*, Vol. 116, pp. 516-518.
- Gauglitz, P. A., S. D. Rassat, P. R. Brecht, J. H. Konynenbelt, S. M. Tingey, and D. P. Mendoza, 1996, *Mechanisms of Gas Bubble Retention and Release: Results for Hanford Waste Tanks 241-S-102 and 241-SY-103 and Single-Shell Tank Simulants*, PNNL-11298, Pacific Northwest National Laboratory, Richland, Washington.
- Lipkis, R. P., C. Liu, and N. Zuber, 1956, "Measurement and Prediction of Density Transients in a Volume-Heated Boiling System," *Chem. Engng. Progress Symposium*, Series 52, pp. 105-113.

Figure B-4. Wave Growth Time Versus Disturbance Wave Length; Depth of Less-Dense Parameter. ($A\rho/\rho = 0.3, \mu/\rho = 6.3 \text{ K g m}^{-3}$)



- Meyer, P. A., M. E. Brewster, S. A. Bryan, G. Chen, L. R. Pederson, C. W. Stewart, and G. Terrones, 1997, *Gas Retention and Release Behavior in Hanford Double-Shell Waste Tanks*, PNNL-11536, Rev. 1, Pacific Northwest National Laboratory, Richland, Washington.
- Plesset, M. S., and C. G. Whipple, 1974, "Viscous Effects in Rayleigh-Taylor Instability," *Physics of Fluids*, Vol. 17, pp. 1-7.
- Richter, H. J., 1981, *Separated Two-Phase Flow Model: Application to Critical Two-Phase Flow*, EPRI NP-1800, Electric Power Research Institute, Palo Alto, California.
- Rivard, W. C., and J. R. Travis, 1980, "A Nonequilibrium Vapor Production Model for Critical Flow," *Nuclear Sci. and Engng.*, Vol. 74, pp. 40-48.
- Scriven, L. A., 1959, "On the Dynamics of Phase Growth," *Chem. Eng. Sci.*, Vol. 10, pp. 1-13.
- Stewart, C. W., M. E. Brewster, P. A. Gauglitz, L. A. Mahoney, P. A. Meyer, K. P. Recknagle, and H. C. Reid, 1996a, *Gas Retention and Release Behavior in Hanford Single-Shell Waste Tanks*, PNNL-11391, Pacific Northwest National Laboratory, Richland, Washington.
- Stewart, C. W., J. M. Alzheimer, M. E. Brewster, G. Chen, R. E. Mendoza, H. C. Reid, C. L. Shepard, and G. Terrones, 1996b, *In Situ Rheology and Gas Volume in Hanford Double-Shell Waste Tanks*, PNNL-11296, Pacific Northwest National Laboratory, Richland, Washington.
- Stewart, C. W., 1998, *Presentations*, Presented at Stage II Experts' Panel Elicitation Workshop 1, Richland, Washington.

This **page** intentionally left blank.

APPENDIX C

RISE DISTANCE TO YIELDING OF VOID-BEARING PARCEL

This **page** intentionally left **blank**.

APPENDIX C

RISE DISTANCE TO YIELDING OF VOID-BEARING PARCEL

In this appendix the assumption that the buoyant displacement parcel becomes fluid after rising only a short distance z is examined. Meyer et al. (1997) presented a model that describes the energy requirements to yield the gas-retaining material and transform it into a liquid state. According to the model, the material within the buoyant parcel will yield and start to flow when the available buoyant energy,

$$E_b = \int_0^z g [\rho_\ell V(z) - \rho_s V_s] dz \quad (C-1)$$

equals or exceeds the energy required to yield the parcel,

$$E_y = V_0 \varepsilon_y \tau_y (1 - \alpha_0) \quad (C-2)$$

In the above equations ρ_ℓ is the density of the convective layer, g is the gravitational constant, ε_y is the strain at failure (≤ 1.0), τ_y is the yield stress of the non-convective layer material, α_0 is the initial void fraction within the non-convective layer which should be nearly equal to the neutral buoyancy void fraction (α_{NB}), V_0 and $V(z)$ are, respectively, the initial volume of the parcel and the volume of the parcel at elevation z above the mid-plane of the non-convective layer, and ρ_s and V_s are, respectively, the density and volume of the void-free material within the non-convective layer.

The ratio of the two energies given by equations (C-1) and (C-2) is

$$\frac{E_b}{E_y} = \frac{\int_0^z g [\rho_\ell V(z) - \rho_s V_s] dz}{V_0 \varepsilon_y \tau_y (1 - \alpha_0)} \quad (C-3)$$

Meyer et al. (1997) compared equation (C-3) with scaled experimental results (Stewart et al. 1996) and concluded that most of the buoyant parcel will yield when $E_b / E_y \gtrsim 5.0$. They concluded that for current tank conditions the buoyant parcel must rise several meters before the buoyant parcel yields and flows. It should be recognized, however, that the increase in buoyant energy of the parcel at the current, relatively low waste temperatures is due mainly to bubble growth via hydrostatic pressure reduction with distance z . As the temperature of the non-convective layer increases and approaches the boiling point of the layer, bubble expansion by evaporation becomes increasingly important and the Meyer et al. (1997) criterion must be modified to account for this.

Assuming that the steam/non-condensable gas mixture that fills the void is always in equilibrium with the interstitial liquid at temperature T_{NC} (see equation (4-12) with $P_v = P_{eq}$), we have

$$\frac{V_b(z)}{V_b(0)} = \frac{P_{hs} + \rho_\ell g H - P_{eq}(T_{NCL})}{P_{hs} + \rho_\ell g (H - z) - P_{eq}(T_{NCL})} \quad (C-4)$$

where $V_b(0)$ is the initial void volume in the buoyant parcel before its ascent (i.e., at $z = 0$), $V_b(z)$ is the void volume at elevation z , and H is the distance from the mid-plane of the non-convective layer to the surface of the waste. The equilibrium assumption underlying equation (C-4) is justified because it gives results in good agreement with the non-equilibrium model when the temperature is low (see Figure 4-3) and when the temperature is high because the rise distances to yielding are small and the rise velocities through these distances are low. Note that in the low-temperature limit $P_{eq}(T_{NCL}) \ll P_{hs}$ and equation (C-4) reduces to the void expansion equation used by Meyer et al. (1997).

The total volume of the parcel at elevation z is

$$V(z) = V_s + V_b(z) \quad (C-5)$$

The density of the void-free material is related to ρ_ℓ and the neutral buoyancy void fraction α_{NB} by

$$\rho_s = \frac{\rho_\ell}{1 - \alpha_{NB}} \quad (C-6)$$

The volume of the void-free material and the initial void volume in the buoyant parcel may be expressed as

$$V_s = V_0 (1 - \alpha_0) \quad (C-7)$$

$$V_b(0) = \alpha_0 V_0 \quad (C-8)$$

Combining equations (C-1) and (C-5) to equation (C-8) gives

$$E_b = g \rho_\ell \alpha_0 V_0 \frac{\overline{V_b(z)}}{V_b(0)} \quad (C-9)$$

$$\text{where } k = \frac{\alpha_{NB} (1 - \alpha_0)}{\alpha_0 (1 - \alpha_{NB})} \quad (C-10)$$

Substituting equation (C-4) into equation (C-9) and carrying out the indicated integration yields

$$E_b = -g \rho_\ell \alpha_0 V_0 H \left[\frac{1+\gamma}{\gamma} \ln \left(1 - \frac{\gamma}{1+\gamma} \frac{z}{H} \right) + k \frac{z}{H} \right] \quad (C-11)$$

$$\text{where } \gamma = \frac{\rho_\ell g H}{P_{hs} - P_{eq}(T_{NCL})} \quad (C-12)$$

Dividing equation (C-11) by equation (C-2) leads to the criterion for the yielding of the parcel:

$$\frac{E_b \varepsilon_y \tau_y (1 - \alpha_0)}{E_y g \rho_\ell \alpha_0 H} = - \frac{1+\gamma}{\gamma} \ln \left(1 - \frac{\gamma}{1+\gamma} \frac{z}{H} \right) - k \frac{z}{H} \quad (C-13)$$

which is an implicit expression for the rise distance z where failure of the parcel occurs. If the initial void fraction α_0 is equal to the neutral buoyancy void fraction, then $k = 1$ in equation (C-13).

Before solving equation (C-13), it is important to point out that the equation becomes invalid as T_{NCL} approaches the boiling point T_{bp} of the non-convective layer at the mid-plane static pressure, as defined by the equation

$$P_{eq}(T_{bp}) = P_{hs} + \rho_\ell g H = P_{NCL} \quad (C-14)$$

This is because as T_{bp} is approached equation (C-4) predicts more vapor production than is thermodynamically possible by converting the available sensible energy in the buoyant parcel to steam. Indeed the minimum rise distance z_{min} to yielding the parcel may be determined by replacing equation (C-4) with a void growth or "flashing" expression that accounts for the finite thermal energy stored in the void-free non-convective layer material.

If the sensible heat available in the buoyant parcel is adiabatically delivered to the surfaces of the bubbles, the mass m_v of steam produced as the parcel rises to elevation z is

$$m_v(z) = m_v(0) + \frac{m_s c_s [T_{NCL} - T(z)]}{h_{fv}} \quad (C-15)$$

where $m_v(0)$ is the initial mass of steam in the parcel, c_s and m_s are, respectively, the specific heat and mass of the void-free material, h_{fv} is the latent heat of evaporation of the parcel's interstitial liquid, and $T(z)$ is the temperature of the parcel at elevation z . Using the ideal gas law, $m_v(z)$ and $m_v(0)$ can be expressed as

$$m_v(z) = \frac{P(z) V_b(z)}{R T(z)} \quad (C-16)$$

$$m_v(0) = \frac{P_{NCL} V_b(0)}{R T_{NCL}} \quad (C-17)$$

where R is the ideal gas constant for water, $P(z)$ is the static pressure at elevation z , and P_{NCL} is the pressure in the non-convective layer (see equation (C-14)). Also, m , is given by

$$m_s = \rho_s V_s = \rho_s V_0 (1 - \alpha_0) \quad (C-18)$$

where again ρ_s is the density of the void-free non-convective material.

Substituting equations (C-16) to (C-18) into equation (C-15) results in

$$V_b(z) = \frac{T(z)}{T_{NCL}} \frac{P_{NCL}}{P(z)} V_b(0) + \frac{R T(z) \rho_s V_0 (1 - \alpha_0) c_s}{h_{fv} P(z)} [T_{NCL} - T(z)] \quad (C-19)$$

It will be seen below that the parcel rises only a short distance before it yields; consequently it is permissible to exploit the following approximations in equation (C-19):

$$T(z) \cong T_{NCL} \quad (C-20)$$

$$P(z) \cong P_{NCL} \quad (C-21)$$

except, of course, for the temperature difference term $T_{NCL} - T(z)$. This term may be approximated by the linearized form of the Clausius-Clapeyron equation

$$T_{NCL} - T(z) = \frac{T_{NCL}^2 R}{h_{fv}} \left[\frac{P_{NCL} - P(z)}{P_{NCL}} \right] = \frac{T_{NCL}^2 R}{h_{fv}} \left[1 - \frac{P_{hs} + \rho_\ell g (H - z)}{P_{hs} + \rho_\ell H} \right] \quad (C-22)$$

Combining equations (C-19) to (C-22) gives the desired expression for the void volume enhancement in the rising and "flashing" buoyant parcel:

$$\frac{V_b(z)}{V_b(0)} = 1 + \frac{J \rho_\ell g z}{P_{NCL}} \quad (C-23)$$

$$\text{where } J = \frac{R^2 T_{NCL}^3 \rho_s (1 - \alpha_0) c_s}{h_{fv}^2 P_{NCL} \alpha_0} \quad (C-24)$$

Inserting equation (C-23) into equation (C-9) yields

$$E_b = g \rho_\ell \alpha_0 V_0 \left[\frac{J \rho_\ell g z^2}{2 P_{NCL}} + (1 - k) z \right] \quad (C-25)$$

Forming the ratio E_b / E , and solving the result for z in the practical limit $\mathbf{k} = \mathbf{I}$ gives the following expression for the minimum rise distance to yielding of the buoyant parcel:

$$z_{\min} = \left[\frac{2 E_b P_{\text{NCL}} \varepsilon_y \tau_y (1 - \alpha_0)}{E_y g^2 \rho_\ell^2 \alpha_0 J} \right]^{1/2} \quad (\text{C-26})$$

The solution to equation (C-13) for parameter values that correspond to conditions in tank 241-AZ-102 is presented in Figure C-1. The parameter values used in the calculations are listed in Table C-1. At low non-convective layer temperatures the parcel maintains a yield stress during its first 2 meters of travel. However, the vertical distance required to turn the parcel into a fluid decreases rapidly as its boiling point is approached. For all practical purposes, the boiling *or* near-boiling parcel can be assumed to liquefy as soon as it begins to move ($z_{\min} = 13 \text{ cm}$).

Figure C-1. Rise Distance to Yielding of Void-Bearing Parcel Versus Temperature of Non-Convective Layer; Input Parameters Pertain to Tank 241-AZ-102.

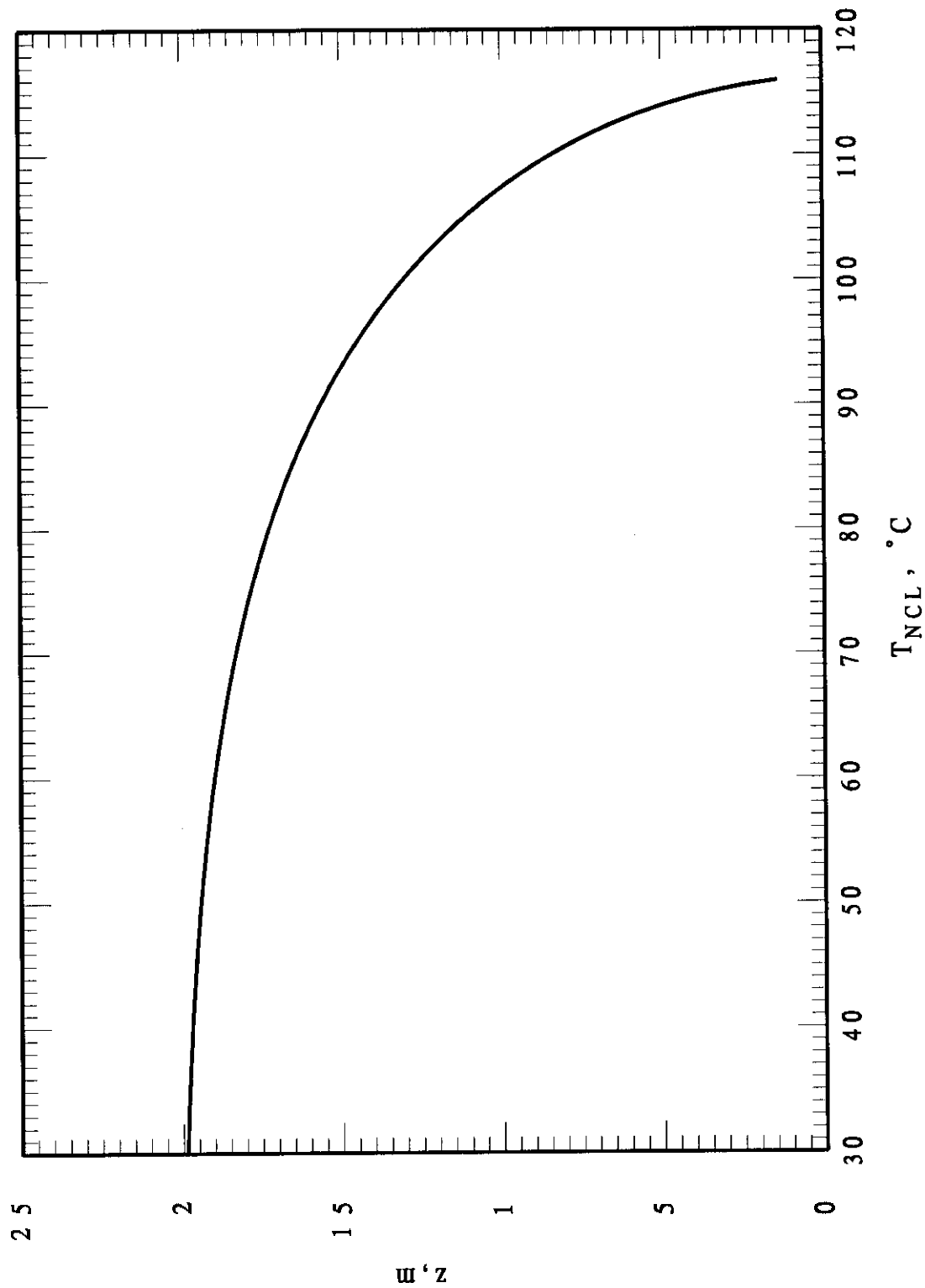


Table C-1. Parameter Values for the Buoyant Parcel Yielding Criterion (Tank 241-AZ-102).

$\alpha_0 = \alpha_{NB} = 0.262$	Initial void fraction.
$H = 1.44 \text{ m}$	Depth to mid-plane of non-convective layer.
$\rho_l = 1100 \text{ kg m}^{-3}$	Density of supernatant.
$\rho_s = 1490 \text{ kg m}^{-3}$	Density of void-free non-convective layer material.
$c_s = 4200 \text{ kg m}^{-3}$	Specific heat of void-free non-convective layer material.
$\tau_v = 100 \text{ Pa}$	Yield strength of non-convective layer material.
$E'' = 1.0$	Strain of non-convective layer material at yielding.
$E_h / E_v = 5.0$	Buoyant-to-yield energy ratio.
$h_{fv} = 2.2 \times 10^6 \text{ J kg}^{-1}$	Latent heat of evaporation of interstitial water.

C.1 REFERENCES

- Meyer, P. A., M. E. Brewster, S. A. Bryan, G. Chen, L. R. Pederson, C. W. Stewart, and G. Terrones, 1997, *Gas Retention and Release Behavior in Hanford Double-Shell Waste Tanks*, PNNL-11536, Rev. 1, Pacific Northwest National Laboratory, Richland, Washington.
- Stewart, C. W., M. E. Brewster, P. A. Gauglitz, L. A. Mahoney, P. A. Meyer, K. P. Recknagle, and H. C. Reid, 1996, *Gas Retention and Release Behavior in Hanford Single-Shell Waste Tanks*, PNNL-11391, Pacific Northwest National Laboratory, Richland, Washington.

This **page** intentionally left **blank**.

APPENDIX D

BUBBLE GROWTH MODEL AND INPUT

This **page** intentionally left **blank**.

APPENDIX D

BUBBLE GROWTH MODEL AND INPUT

D.1 GASCAVGRTH.FOR: Calculations ~~for~~ Chapter 4 Figures

```

C GAS CAVITY GROWTH IN HOT WATER
C M EPSTEIN / G HAUSER
C 9-FEB-2000
C CORRECTIONS MADE 20-APR-2000
C
      IMPLICIT REAL*8 (A-H,O-Z)
      DATA PI /3.14159D0/
      CHARACTER*3 BTYPE
      DIMENSION TLA(6), DOA(6)
      DATA TLA /90.D0, 95.D0, 99.D0, 99.D0, 99.D0, 99.D0/
      DATA DOA /5.D-3, 5.D-3, 5.D-3, 1.D-3, 5.D-3, 1.D-2/

C
C INPUT
C
      RHOL=1100.D0
      G=9.8D0
      TL=100.D0
      DIFF=9.2D-5
      D0=5.D-3
      UB=0.2D0
      U=1.D0
      PHS=1.0136D5
      H=5.D0
      BTYPE='WET'
      STEPS=10000.D0

C
C WRITE BACK INPUT
C
C
      A=72.55D0
      B=-7.2067D3
      C=-7.1385D0
      D=4.046D-6
      E=2.D0

C
C FIRST DO CASES FOR TLA AND DOA ARRAYS DEFINED ABOVE; TOTAL OF SIX CASES
C WITH VARYING TL AND DO PLOTS ARE H VS V AND VEQ
C
      DO I=1,6
        TL=TLA(I)
        T=TL+273.16D0
        D0=DOA(I)

C
        IF (I.EQ.3)
          & OPEN(UNIT=2, FILE='GASCAVGRTH1.STORY', STATUS='NEW')
        WRITE(2,*) 'RHOL=', RHOL
        WRITE(2,*) 'G=', G

```

```

WRITE(2,*) 'D=',D
WRITE(2,*) 'U=',U
WRITE(2,*) 'PHS=',PHS
WRITE(2,*) 'D0=',D0
WRITE(2,*) 'BTYP=','BTYP
WRITE(2,*) 'STEPS=',STEPS
CLOSE(UNIT=2)
IF (I.EQ.6)
& OPEN(UNIT=2,FILE='GASCAVGRTH2.STORY',STATUS='NEW')
WRITE(2,*) 'RHOL=',RHOL
WRITE(2,*) 'G=',G
WRITE(2,*) 'D=',D
WRITE(2,*) 'U=',U
WRITE(2,*) 'PHS=',PHS
WRITE(2,*) 'TL=',TL
WRITE(2,*) 'BTYP=','BTYP
WRITE(2,*) 'STEPS=',STEPS
CLOSE(UNIT=2)
DO J=1,100
  H=FLOAT(J)/10.DO
  TERM1=C*LOG(T)
  TERM2=D*T**E
  PEQ=EXP(A+B/T+TERM1+TERM2)
  V0=4.E0/3.D0*PI*(D0/2.D0)**3
  B1=PEQ/(RHOL*G)*SQRT(24.D0*DIFF*UB/(U**2*V0))
  B2=(PHS+RHOL*G*H)/PEQ
  YF=RHOL*G*H/PEQ
C
C INITIAL CONDITIONS
C
  Y=0.D0
  IF (BTYP.EQ.'WET') THEN
    BT=1.DO
  END IF
  IF (BTYP.EQ.'DRY') THEN
    BT=0.DO
  END IF
  X=BT
  DY=YF/STEPS
C
C INTEGRATION
C
  IF (I.EQ.1)
& OPEN(UNIT=1,FILE='GASCAVGRTH1.OUT',STATUS='NEW')
  IF (I.EQ.2)
& OPEN(UNIT=1,FILE='GASCAVGRTH2.OUT',STATUS='NEW')
  IF (I.EQ.3)
& OPEN(UNIT=1,FILE='GASCAVGRTH3.OUT',STATUS='NEW')
  IF (I.EQ.4)
& OPEN(UNIT=1,FILE='GASCAVGRTH4.OUT',STATUS='NEW')
  IF (I.EQ.5)
& OPEN(UNIT=1,FILE='GASCAVGRTH5.OUT',STATUS='NEW')
  IF (I.EQ.6)
& OPEN(UNIT=1,FILE='GASCAVGRTH6.OUT',STATUS='NEW')
  DO WHILE(Y.LT.YF)
    Y=Y+DY
    V=(B2-BT)/(B2-Y-X)

```

RPP-6213 REV I

```

      DXDY=(B1*SQRT(V)*(B2-Y)*LOG(1.D0+(1.D0-X)/(B2-Y)) -
&      (X*V*V)/(B2-BT))/(V+X*V*V/(B2-BT))
C      WRITE(1,*) Y,V,X,DXDY
      X=X+DXDY*DY
      END DO
      IF (BTTYPE.EQ.'WET'.AND.PEQ.LT.PHS) THEN
        VEQ=(B2-1.D0)/(B2-Y-1.D0)
      ELSE
        VEQ=0.D0
      END IF
C      WRITE(*,*) H,V
      WRITE(1,*) H,V,VEQ
      END DO
      CLOSE(UNIT=1)
    END DO

C
C NOW DO ONE MORE CASE FOR D0=5 MM (5.E-3 M) H=5 M; U=1 M/S; AND UB=.2 M/S
C PLOTS WILL BE TL VS V AND VEQ
C
      D0=5.D-3
      H=5.D0
      U=1.D0
      UB=.2D0
C
      OPEN(UNIT=1,FILE='GASCAVGRTH.OUT',STATUS='NEW')
      DO J=8000,11000
        TL=FLOAT(J)/100.D0
        T=TL+273.16D0
        TERM1=C*LOG(T)
        TERM2=D*T**E
        PEQ=EXP(A+B/T+TERM1+TERM2)
        V0=4.E0/3.D0*PI*(D0/2.D0)**3
        B1=PEQ/(RHOL*G)*SQRT(24.D0*DIFF*UB/(U**2*V0))
        B2=(PHS+RHOL*G*R)/PEQ
        YF=RHOL*G*H/PEQ
C
C INITIAL CONDITIONS
C
      Y=O.E0
      IF (BTTYPE.EQ.'WET') THEN
        BT=1.D0
      END IF
      IF (BTTYPE.EQ.'DRY') THEN
        BT=0.D0
      END IF
      X=BT
      DY=YF/STEPS
C
C INTEGRATION
C
      DO WHILE(Y.LT.YF)
        Y=Y+DY
        V=(B2-BT)/(B2-Y-X)
        DXDY=(B1*SQRT(V)*(B2-Y)*LOG(1.D0+(1.D0-X)/(B2-Y)) -
&      (X*V*V)/(B2-BT))/(V+X*V*V/(B2-BT))
        X=X+DXDY*DY
      END DO

```



```

      IF (BTYPE.EQ.'WET'.AND.PEQ.LT.PHS) THEN
        VEQ=(B2-1.D0)/(B2-Y-1.D0)
      ELSE
        VEQ=0.D0
      END IF
      WRITE(1,*) TL,V,VEQ
    END DO
  CLOSE(UNIT=1)
  STOP
END

```

D.2 GASCAVGRTH.GCL: Plot Script for Chapter 4 Figures

```

INPUT FILE 1 IS GASCAVGRTH1.OUT
INPUT FILE 2 IS GASCAVGRTH2.OUT
INPUT FILE 3 IS GASCAVGRTH3.OUT
INPUT FILE 4 IS GASCAVGRTH4.OUT
INPUT FILE 5 IS GASCAVGRTH5.OUT
INPUT FILE 6 IS GASCAVGRTH6.OUT
NUMBER OF COLUMNS IN IS 3
COLUMN 1 LABEL IS H
COLUMN 2 LABEL IS V
COLUMN 3 LABEL IS VEQ

X AXIS TICS IS 10
Y AXIS TICS IS 10
FRAME

TEXT STYLE IS ROMAN+SOLID
NOTAG
SWITCH CHARACTER IS ^
INSTRUCTION CHARACTER IS #
LINE CONTINUATION CHARACTER IS $
ROTATE Y AXIS MARKERS 0 DEGREES
STORY CHARACTER SIZE IS .18
PLACE STORY AT GOOD LOCATION

PAGE
BEGIN STORY
d#D.3;#o#U.3;#=5 mm
U=1.0 m/s
U#D.3;#b#U.3;#=0.2m/s
P#D.3;#hs#U.3;#=0.1MPa
END STORY
Y AXIS LABEL IS V#D.3;#b#U.3;#(H)/V#D.3;#b#U.3;#(0)
X AXIS LABEL IS H,m
X AXIS SCALE IS FROM 0 BY 1 TO 10
! Y AXIS SCALE IS FROM 0 BY 50 TO 200
PLOT H VS V FROM FILE 1 USING THICK LINE
! CURVE LABEL IS #U.5;#90^g^C<CENTERED>
PLOT H VS V FROM FILE 2 USING THICK LINE
! CURVE LABEL IS #U.5;#95^g^C<CENTERED>
PLOT H VS V FROM FILE 3 USING THICK LINE CURVE LABEL IS
#U.3;#99^g^C<CENTERED>.8
PLOT H VS VEQ FROM FILE 1 USING THICK DASHED LINE CURVE LABEL IS
#U.3;#90^g^C<CENTERED>.8

```

RPP-6213 REV 1

```

PLOT H VS VEQ FROM FILE 2 USING THICK DASHED LINE CURVE LABEL IS
#U.3;#95^g^C<CENTERED>.8
PLOT H VS VEQ FROM FILE 3 USING THICK DASHED LINE CURVE LABEL IS
#U.3;#T#D.3;#^=#U.3;#=99^g^C<CENTERED>.8
! CAPTION IS Fig.4-3 Bubble expansion ratio versus depth of supernatant
pool; pool temperature$
! T#D.3;#^=#U.3;# as a parameter. Dashed curves refer to zero mass transfer
resistance.
DISPLAY

PAGE
BEGIN STORY
T#D.3;#^=#U.3;#=99^g^C
U=1.0 m/s
U#D.3;#b#U.3;#=0.2m/s
P#D.3;#hs#U.3;#=0.1MPa
END STORY
PLOT H VS V FROM FILE 4 USING THICK LINE CURVE LABEL IS
#U.3;#d#D.3;#o#U.3;#=1mm<CENTERED>.8
PLOT H VS V FROM FILE 5 USING THICK LINE CURVE LABEL IS
#U.3;#5mm<CENTERED>.8
PLOT H VS V FROM FILE 6 USING THICK LINE CURVE LABEL IS
#U.3;#10mm<CENTERED>.8
PLOT H VS VEQ FROM FILE 4 USING THICK DASHED LINE
! CAPTION IS Fig.4-4 Bubble expansion ratio versus depth of supernatant
pool; initial bubble$
! diameter as a parameter. Dashed curve refers to zero mass transfer
resistance.
DISPLAY

PAGE
BEGIN STORY
d#D.3;#o#U.3;#=5mm
H=5.0m
U=1.0 m/s
U#D.3;#b#U.3;#=0.2m/s
P#D.3;#hs#U.3;#=0.1MPa
END STORY
INPUT FILE 1 IS GASCAVGRTH.OUT
NUMBER OF COLUMNS IS 3
COLUMN 1 LABEL IS TL
COLUMN 2 LABEL IS V
COLUMN 3 LABEL IS VEQ
X AXIS SCALE IS FROM 80 BY 5 TO 110
X AXIS TICS IS 5
X AXIS LABEL IS Temperature, ^g^C
Y AXIS SCALE IS FROM 0 BY 100 TO 800
PLOT TL VS MIN(800,V) FROM FILE 1 USING THICK LINE
! CAPTION IS Fig.4-5 Bubble expansion ratio versus convective layer
temperature (<100^g^C) or$
! buoyant parcel temperature T#D.3;#nc#U.3;# during buoyant displacement.
Dashed curve refers to$
! zero mass transfer resistance.
DISPLAY

NO STORY
NO CAPTION

```

X AXIS LABEL IS •
Y AXIS LABEL IS •
X WINDOW IS FROM 0 TO 99.99
PLOT TL VS MIN(800,VEQ) FROM FILE 1 USING THICK DASHED LINE
X AXIS SCALE IS SAME
Y AXIS SCALE IS SAME
DISPLAY

APPENDIX E

CLUSTER ENTRAINMENT MODEL AND INPUT

This **page** intentionally left blank.

APPENDIX E

CLUSTER ENTRAINMENT MODEL AND INPUT

E.1 TANK_BUMP.FOR: Chapter 5 Calculations

```

C TANK BUMP COMPUTER PROGRAM
C M EPSTEIN / G HAUSER
C 6-MAR-2000
C ALL VARIABLES ARE IN SI UNITS
C
      IMPLICIT REAL*8 (A-H,O-Z)
      REAL*8 ML,MLEN,MLEN0,M,K,MAER,MUG,JG,MDOTV
      LOGICAL NOT_ESCAPING,DONE
C
C INPUT
C
      OPEN(UNIT=1,FILE='TANK_BUMP.INP',STATUS='OLD')
      READ(1,*) UB          !BUBBLE VELOCITY
      READ(1,*) GRAV        !GRAVITATIONAL CONSTANT
      READ(1,*) DIF         !BUBBLE GAS H2/WATER VAPOR DIFFUSION COEFFICIENT
      READ(1,*) TL1        !INITIAL TEMPERATURE OF NONCONVECTIVE LAYER
C                          (STARTING VALUE)
      READ(1,*) TL2        !INITIAL TEMPERATURE OF NONCONVECTIVE LAYER
C                          (ENDING VALUE)
      READ(1,*) DTL        !TEMPERATURE OF NONCONVECTIVE LAYER (INCREMENT)
C NOTE IF DTL = 0.0 THEN ONLY TL1 CASE WILL BE RUN AND DETAILED OUTPUT SAVED
      READ(1,*) HO         !INITIAL DEPTH OF CONVECTIVE LAYER
      READ(1,*) PHSO       !INITIAL HEAD SPACE PRESSURE
      READ(1,*) VHSO       !INITIAL HEAD SPACE VOLUME
      READ(1,*) HOUT       !INITIAL HEIGHT OF OUTLET PIPE ABOVE SURFACE
C                          !OF CONVECTIVE LAYER
      READ(1,*) VBCO       !INITIAL VOLUME OF BUBBLE CLUSTER
      READ(1,*) DBO        !INITIAL DIAMETER OF REPRESENTATIVE BUBBLE
      READ(1,*) VL         !VOLUME OF CONVECTIVE LAYER
      READ(1,*) RHOL       !DENSITY OF CONVECTIVE LAYER
      READ(1,*) R          !IDEAL GAS CONSTANT
      READ(1,*) M          !MOLECULAR WEIGHT OF HEADSPACE GAS
      READ(1,*) GAMA       !SPECIFIC HEAT RATIO OF HEADSPACE GAS
      READ(1,*) K          !OVERALL LOSS COEFFICIENT FOR RISER PIPE
      READ(1,*) HRISER     !VERTICAL HEIGHT OF RISER PIPE
      READ(1,*) ARISER     !FLOW AREA IN RISER
      READ(1,*) MUG        !VISCOSITY OF BUBBLE GAS (VAPOR)
      READ(1,*) RHOG       !DENSITY OF BUBBLE GAS (VAPOR)
      READ(1,*) SIG        !SURFACE TENSION OF LIQUID WASTE
      READ(1,*) ALPHA      !VOID FRACTION OF BUBBLE CLUSTER
      READ(1,*) PHEPA      !HEPA FILTER FAILURE PRESSURE
      READ(1,*) IRELEASE   !=1 ALL AEROSOL RELEASED
C                          !=0 RELEASE DURING DEPRESSUIZATION
      READ(1,*) MLENO      !INITIAL MASS OF LIQUID IN BUBBLE CLUSTER
      READ(1,*) CL         !SPECIFIC HEAT OF LIQUID
      READ(1,*) HVL        !LIQUID HEAT OF EVAPORIZATION
      READ(1,*) TCL        !TEMPERATURE OF CONVECTIVE LAYER
      READ(1,*) MV         !MOLECULAR WEIGHT OF LIQUID

```

RPP-6213 REV 1

```

      READ(1,*) EO          !ENTRAINMENT COEFFICIENT
C
      READ(1,*) DTAU        !INTEGRATION TIME STEP
      READ(1,*) DPR         !PRINTOUT TIME STEP
      READ(1,*) TAUEND      !FORCED END OF PROBLEM TIME (FOR DEBUGGING)
      TLI=TL1
      IF (DTL.GT.0.D0)
&    OPEN(UNIT=4,FILE='TANK_BUMP.HISTORY',STATUS='UNKNOWN')
      DONE=.FALSE.
      DO WHILE (.NOT.DONE)
        IF (DTL.EQ.0.D0) DONE=.TRUE.
C
        PI=ACOS(0.D0)*2.D0
C
C
C
C CALCULATE INITIAL VOLUME OF REPRESENTATIVE BUBBLE
      VB0=PI/6.D0*DB0**3
C
C CALCULATE VAPOR PRESSURE AT BUBBLE SURFACE
      TL=TL1
      PEQ=1.102D11*EXP(-5185.D0/TL)
C
C INITIAL CONDITIONS AT TIME TAU=0)
      TAU=0.D0
      VBBAR=1.D0
      E=PEQ
      MLEN=MLEN0
      ZBC=0.D0
      H=H0
      ML=0.D0
      PR=DPR
C
      IF (DTL.EQ.0.0) THEN
        OPEN(UNIT=3,FILE='TANK_BUMP.OUT',STATUS='UNKNOWN')
        OPEN(UNIT=7,FILE='TANK_BUMP.PRN',STATUS='NEW',
&          CARRIAGECONTROL='LIST',RECL=200)
      END IF
C
      DO WHILE(ZBC.LT.H.AND.TAU.LT.TAUEND)
C
C CALCULATE VAPOR PRESSURE AT BUBBLE SURFACE
      PEQ=1.102D11*EXP(-5185.D0/TL)
C
C CALCULATE VOLUME OF BUBBLE CLUSTER
      VBC=VBC0*VBBAR
C
C CALCULATE BUBBLE CLUSTER RISE VELOCITY
      U=0.76D0*(GRAV**3*VBC)**(1.D0/6.D0)
C
C DEPTH OF CONVECTIVE LAYER
      H=H0*((VL+VBC)/(VL+VBC0))
C
C HEADSPACE PRESSURE
      PHS=(VHS0**GAMA*PHS0)/(VHS0+VBC0-VBC)**GAMA
C

```

RPP-6213REV 1

```

C DIFFERENTIAL EQUATION FOR VERTICAL LOCATION OF CENTER OF BUBBLE CLUSTER
  DZBCDT=U
C
C NORMALIZED BUBBLE VOLUME
  VBBAR=(E+PHS+RHOL*GRAV*H-PEQ)/(PHS+RHOL*GRAV*(H-ZBC))
C
C CALCULATE PRESSURE IN NONCONVECTIVE LAYER
  PNC=PHS+RHOL*GRAV*(H-ZBC)
C
C DIFFERENTIAL EQUATION FOR E
  DEDT=SQRT(24.D0*DIF/VB0*UB*VBBAR)*PNC*
    & LOG(1.D0+(PEQ-E/VBBAR)/(PNC-PEQ))
C
C BUBBLE CLUSTER SURFACE AREA
  ABC=4.83D0*(VBC+MLN/RHOL)**(2.D0/3.D0)
C
C VAPOR GENERATION RATE
  MDOTV=MV*VBC0/(R*TL)*DEDT
C
C DIFFERENTIAL EQUATION FOR LIQUID MASS IN BUBBLE CLUSTER
  DMLENDT=RHOL*ABC*E0*U-MDOTV
C
C DIFFERENTIAL EQUATION FOR TEMPERATURE OF LIQUID IN BUBBLE CLUSTER
  DTLDT=-((TL-TCL)*RHOL*E0*U*ABC)/(MLN-MDOTV*HVL/(MLN*CL))
C
C BUBBLE PRESSURE
  PV=E/VBBAR
C
C LIQUID ESCAPE THROUGH RISER
  DP=PHS-PHS0+RHOL*GRAV*(H-H0-HOUT-HRISER)
  NOT_ESCAPING=(DP.LE.0.D0.OR.H.LE.H0+HOUT)
  IF (NOT-ESCAPING) THEN
    DMLDT=0.D0
  ELSE
    DMLDT=SQRT((2.D0*DP*RHOL)/K)*ARISER
  END IF
C
C OUTPUT
  IF (TAU.GE.PR.AND.DTL.EQ.0.0) THEN
    WRITE(7,100) TAU,DMLENDT,DEDT,MDOTV,U,ABC,DTLDT,TL,
      & MLN,VBC
    100 FORMAT(10(1PG13.5))
    WRITE(3,*) ' '
    WRITE(3,*) TAU,ZBC,E,VBC,U,H,PHS,VBBAR,PV,DZBCDT,DEDT,
      & PEQ-PV,DEDT/SQRT(24.D0*DIF/VB0*U*VBBAR),
      & ML,DP,MLN,TL,
      & -5185.D0/LOG((PHS+RHOL*GRAV*(H-ZBC))/1.102D11)
    PR=PR+DPR
  END IF
C
C INTEGRATE
  ZBC=ZBC+DZBCDT*DTAU
  E=E+DEDT*DTAU
  ML=ML+DMLDT*DTAU
  MLN=MLN+DMLENDT*DTAU
  TL=TL+DTLDT*DTAU
  TAU=TAU+DTAU

```



```

      END DO
      IF (DTL.EQ.0.0) THEN
        WRITE(7,100) TAU,DMLENDT,DEDT,MDOTV,U,ABC,DTLDT,TL,
&          MLEN,VBC
        WRITE(3,*) ' '
        WRITE(3,*) TAU,ZBC,E,VBC,U,H,PHS,VBBAR,PV,DZBCDT,DEDT,
&          PEQ-PV,DEDT/SQRT(24.D0*DIF/VB0*U*VBBAR),
&          ML,DP,MLEN,TL,
&          -5185.D0/LOG((PHS+RHOL*GRAV*(H-ZBC))/1.102D11)
      END IF
      IF (PHS.GT.PHEPA) THEN
C
C INITIAL HEADSPACE DENSITY
      RHOHS0=(PHS0*M)/(R*TL)
C
C FINAL HEADSPACE DENSITY
      RHOHS=RHOHS0*PHS/PHS0
C
C AEROSOL GENERATION EFFICIENCY
      JG=ALPHA*U
      EFF=7.13D-4*((MUG**4*RHOG**2*(RHOL-RHOG)**3)/
&          (SIG**9*GRAV**5))**(1.D0/8.D0)*JG**3
C
C AEROSOL RELEASED (MASS)
      IF (IRELEASE.EQ.1)FACTOR=1.D0
      IF (IRELEASE.EQ.0)
&          FACTOR=(1.D0-(PHS0/PHS)**(2.D0-1.D0/GAMA))
      MAER=EFF*RHOHS*VBC*FACTOR
    ELSE
      MAER=0.D0
    END IF
    IF (DTL.EQ.0.0) THEN
      OPEN(UNIT=2,FILE='TANK_BUMP.STORY',STATUS='UNKNOWN')
      WRITE(2,*) ' MASS AEROSOL RELEASED=',MAER,' Kg'
    END IF
    IF (DTL.GT.0.0) THEN
      WRITE(4,*) ' '
      WRITE(4,*) TLI,VBBAR,MAER,U,ML,PHS
      WRITE(*,*) TLI,VBBAR
      TLI=TLI+DTL
      IF (TLI.GT.TL2) DONE=.TRUE.
    END IF
  END DO
  CLOSE(UNIT=1)
  CLOSE(UNIT=2)
  CLOSE(UNIT=3)
  CLOSE(UNIT=4)
  STOP
END

```

E.2 TANK_BUMP.INP: Chapter 5 Input

```

0.2      !UB; BUBBLE VELOCITY
9.8D0     !GRAV; GRAVITATIONAL CONSTANT
9.2D-5    !DIF; BUBBLE GAS H2/WATER VAPOR DIFFUSION COEFFICIENT
373.0     !TL1; INITIAL TEMPERATURE OF NONCONVECTIVE LAYER (STARTING VALUE)

```

RPP-6213 REV 1

```

373.0      !TL2; INITIAL TEMPERATURE OF NONCONVECTIVE LAYER (ENDING VALUE)
0.0        !DTL; TEMPERATURE OF NONCONVECTIVE LAYER (INCREMENT)
8.D0       !H0; INITIAL DEPTH OF CONVECTIVE LAYER
1.0119D5   !PHS0; INITIAL HEAD SPACE PRESSURE
1800.D0    !VHS0; INITIAL HEAD SPACE VOLUME
4.D0       !HOUT; INITIAL HEIGHT OF OUTLET PIPE ABOVE SURFACE OF CONVECTIVE
LAYER
32.D0      !VBC0; INITIAL VOLUME OF BUBBLE CLUSTER
5.D-3      !DB0; INITIAL DIAMETER OF REPRESENTATIVE BUBBLE
3200.D0    !VL; VOLUME OF CONVECTIVE LAYER
1210.D0    !RHOL; DENSITY OF CONVECTIVE LAYER
8314.D0    !R; IDEAL GAS CONSTANT
29.D0      !M; MOLECULAR WEIGHT OF HEADSPACE GAS
1.4D0      !GAMA; SPECIFIC HEAT RATIO OF HEADSPACE GAS
2.D0       !K; OVERALL LOSS COEFFICIENT FOR RISER PIPE
4.D0       !HRISER; VERTICAL HEIGHT OF RISER PIPE
0.2D0      !ARISER; FLOW AREA IN RISER
1.2D-5     !MUG; VISCOSITY OF BUBBLE GAS (VAPOR)
0.6D0      !RHOG; DENSITY OF BUBBLE GAS (VAPOR)
0.059      !SIG; SURFACE TENSION OF LIQUID WASTE
0.66666D0  !ALPHA; VOID FRACTION OF BUBBLE CLUSTER
1.D5       !PHEPA; HEPA FILTER FAILURE PRESSURE 1.356D5
1          !IRELEASE; =1 RELEASE ALL AEROSOL; =0 ONLY DURING DEPRESS
4.D4       !MLEN0; INITIAL MASS OF LIQUID IN BUBBLE CLUSTER
4200.D0    !CL; SPECIFIC HEAT OF LIQUID
2.2D6      !HVL; LIQUID HEAT OF EVAPORIZATION
373.D0     !TCL; TEMPERATURE OF CONVECTIVE LAYER
18.D0      !MV; MOLECULAR WEIGHT OF LIQUID
0.1D0      !EO; ENTRAINMENT COEFFICIENT

1.D-5      !INTEGRATION TIME STEP
0.001D0    !PRINT OUT TIME STEP
100.D0     !FORCED END OF PROBLEM

```

E.3 TANK_BUMP.GCL: Chapter 5 Plots

```

INPUT FILE 1 IS TANK_BUMP.OUT
NUMBER OF COLUMNS IN FILE 1 IS 18
COLUMN 1 LABEL IN FILE 1 IS TAU
COLUMN 2 LABEL IN FILE 1 IS ZBC
COLUMN 3 LABEL IN FILE 1 IS E
COLUMN 4 LABEL IN FILE 1 IS VBC
COLUMN 5 LABEL IN FILE 1 IS U
COLUMN 6 LABEL IN FILE 1 IS H
COLUMN 7 LABEL IN FILE 1 IS PHS
COLUMN 8 LABEL IN FILE 1 IS VBBar
COLUMN 9 LABEL IN FILE 1 IS PV
COLUMN 10 LABEL IN FILE 1 IS DZBCDT
COLUMN 11 LABEL IN FILE 1 IS DEDT
COLUMN 12 LABEL IN FILE 1 IS DIFF
COLUMN 13 LABEL IN FILE 1 IS DIFF2
COLUMN 14 LABEL IN FILE 1 IS ML
COLUMN 15 LABEL IN FILE 1 IS DP
COLUMN 16 LABEL IN FILE 1 IS MLEN
COLUMN 17 LABEL IN FILE 1 IS TL
COLUMN 18 LABEL IN FILE 1 IS TEQ

```

RPP-6213 REV 1

```
|      TEXT STYLE IS ROMAN+SOLID
      BEGIN STORY
      INCLUDE FILE IS TANK_BUMP.INP
      INCLUDE FILE IS TANK_BUMP.STORY
      END STORY
      STORY CHARACTER SIZE IS .08
      PLACE STORY AT GOOD LOCATION

!HARD COPY OFF

      PAGE
      X AXIS LABEL IS Time, sec
      Y AXIS LABEL IS ZBC, Vertical location of bubble cluster, m
      X AXIS TICS IS 10
      Y AXIS TICS IS 10
      FRAME
      PLOT TAU VS ZBC FROM FILE 1 USING LINE
      DISPLAY

|      PAGE
      NO STORY
      !      Y AXIS LABEL IS Bubble pressure * volume
      !      PLOT TAU VS E FROM FILE 1 USING LINE
      !      DISPLAY

      PAGE
      Y AXIS LABEL IS VBC, Volume of bubble cluster, m**3
      PLOT TAU VS VBC FROM FILE 1 USING LINE
      DISPLAY

      PAGE
      Y AXIS LABEL IS U, Bubble cluster rise velocity, m/sec
      PLOT TAU VS U FROM FILE 1 USING LINE
      DISPLAY

      PAGE
      Y AXIS LABEL IS H, Depth of convective layer, m
      PLOT TAU VS H FROM FILE 1 USING LINE
      DISPLAY

      PAGE
      Y AXIS LABEL IS PHS, Headspace pressure, Pa
      PLOT TAU VS PHS FROM FILE 1 USING LINE
      DISPLAY

      PAGE
      Y AXIS LABEL IS VBBAR, Normalized bubble volume
      PLOT TAU VS VBBAR FROM FILE 1 USING LINE
      DISPLAY

      PAGE
      Y AXIS LABEL IS PV, Bubble pressure, Pa
      PLOT TAU VS PV FROM FILE 1 USING LINE
      DISPLAY
```

RPP-6213 REV 1

```
! PAGE
! Y AXIS LABEL IS DZBCDT, m/sec
! PLOT TAU VS DZBCDT FROM FILE 1 USING LINE
! DISPLAY
```

```
! PAGE
! Y AXIS LABEL IS DEDT
! PLOT TAU VS DEDT FROM FILE 1 USING LINE
! DISPLAY
```

```
! PAGE
! Y AXIS LABEL IS PEQ-E/VBBAR
! PLOT TAU VS DIFF FROM FILE 1 USING LINE
! PLOT TAU VS DIFF2 FROM FILE 1 USING DASHED LINE
! DISPLAY
```

```
PAGE
Y AXIS LABEL IS ML, Mass of liquid escaping through riser, Kg
PLOT TAU VS ML FROM FILE 1 USING LINE
DISPLAY
```

```
PAGE
Y AXIS LABEL IS MLEN, Mass of liquid in bubble, Kg
PLOT TAU VS MLEN FROM FILE 1 USING LINE
DISPLAY
```

```
BEGIN STORY
d#D.3;#o#U.3;#=5 mm

!P#D.3;#hs#U.3;#=0.1 MPa

U#D.3;#b#U.3;#=0.2 m/s

M#D.3;#^=#U.3;#(0)=4000 Kg

V#D.3;#b#U.3;#(0)=32 m#U.3;#3
END STORY
STORY CHARACTER SIZE IS .2
PLACE STORY AT GOOD LOCATION
```

```
TEXT STYLE IS ROMAN+SOLID
ROTATE Y AXIS MARKERS 0 DEGREES
SWITCH CHARACTER IS ^
INSTRUCTION CHARACTER IS #
Y AXIS SCALE IS FROM 370 BY 5 TO 395
X AXIS TICS IS 5
Y AXIS TICS IS 5
NOTAG
```

```
!HARD COPY ON
PAGE
Y AXIS LABEL IS Temperature, K
PLOT TAU VS TL FROM FILE 1 USING THICK LINE CURVE LABEL IS
#U.5;#T#D.3;#^=#<CENTERED>.3
PLOT TAU VS TEQ FROM FILE 1 USING THICKDASHED LINE CURVE LABEL IS
#U.5;#T#D.3;#bp<CENTERED>.3
```

CAPTION IS Fig.4-6 Temperature history of buoyant parcel compared with its boiling temperature.

DISPLAY

! PAGE
! Y AXIS LABEL IS DP
! PLOT TAU VS DP FROM FILE 1 USING LINE
! DISPLAY

APPENDIX F

HADCRT CHANGES AND INPUT

This page intentionally left blank.

APPENDIX F

HADCRT CHANGES AND INPUT

F.1 BUMP.FOR: Addition to HADCRT for Chapter 8

```

C*****
C
C   HADCRT: CREATED FOR THE PROJECT HANFORD MANAGEMENT COMPANY (PHMC)
C
C   WITH A LIMITED USE AND OWNERSHIP LICENSE GRANTED BY:
C
C   FAUSKE & ASSOCIATES, INC. (FAI)
C   16W070 W. 83RD ST.
C   BURR RIDGE IL 60521 USA
C   PHONE USA 630-323-8750
C   RESPONSIBLE MANAGER AND AUTHOR:
C   MARTIN PLYS
C   OTHER AUTHORS: SUNG JIN LEE, BORO MALINOVIC, JIM BURELBACH,
C   MICHAEL MCCARTNEY
C
C   THIS CODE IS COPYRIGHTED 1999 BY FAUSKE & ASSOCIATES, INC.
C
C   NO PARTS OF THIS CODE MAY BE USED OR DISSEMINATED, IN WHOLE
C   OR IN PART, AND NO PARTS MAY BE EXTRACTED, CHANGED, AND USED
C   TO CREATE A NEW PROGRAM (DERIVATIVE WORK), WITHOUT EXPLICIT
C   LICENSE AUTHORIZATION FROM FAUSKE & ASSOCIATES, INC.
C
C   PHMC IS GRANTED THE RIGHT TO USE THIS PROGRAM, SUBJECT TO
C   RESTRICTIONS IN ITS LICENSE WITH FAI
C   THIS INCLUDES THE RIGHT TO MODIFY AND DISSEMINATE CODING
C   FOUND IN THE FILES: DCRT.FOR AND DCRT.CML
C   FILES INCLUDED WITH THIS CODE, TO WHICH THE COPYRIGHT
C   AND LICENSE APPLIES, AND WHICH MAY NOT BE DISSEMINATED OR
C   CHANGED OR USED FOR A DERIVATIVE WORK ARE:
C   AMAZON.FOR, AMIO.FOR, AMOD.FOR, AND ALL FILES
C   WITH EXTENSIONS *.CML AND *.CMG NOT NAMED ABOVE
C   LICENSE SIGNED BY:
C   SHERYL K. DAWSON, FLUOR DANIEL NORTHWEST, 3-16-99
C   HANS K. FAUSKE, FAUSKE & ASSOCIATES, INC., 3-15-99
C
C*****

      SUBROUTINE BUMP (ICALL)
      IMPLICIT REAL (A-H, K-Z)

C=====
C
C   TANK BUMP CALCULATION ROUTINE
C
C   INCLUDES:
C     BUBBLE GROWTH PHASE
C     AEROSOL RELEASE & MIXING CUP PHASE
C     BLOWDOWN (NO ACTION)
C   ICALL = 1: NORMAL CALL FROM RATES

```


RPP-6213 REV 1

```

C          2: FROM INTEGRATE, ASSIGN VOLUME UPDATE
C
C=====
C      INCLUDE 'PARAMS.CMG'
C      INCLUDE 'CNTRL.CML'
C      INCLUDE 'GASN.CML'
C      INCLUDE 'GASP.CML'
C      INCLUDE 'BUMP.CML'
C      INCLUDE 'REGIN.CML'
C      INCLUDE 'STATE1.CML'
C      INCLUDE 'STATE2.CML'
C      INCLUDE 'RATES1.CML'
C      INCLUDE 'RATES2.CML'
C      INCLUDE 'JUNCS.CML'
C      INCLUDE 'TIMEIN.CML'
C      INCLUDE 'STATE.CMG'
C      DIMENSION WENT(INGAS)
C      DIMENSION TMX0(10),DTMX0(10),TMN0(10),DTMN0(10)
C      DIMENSION TPMX0(10),DTPMX0(10),TPMN0(10),DTPMN0(10)
C      DIMENSION TPRN0(10),DTPRN0(10)
C      DATA IFIRST /1/
C      DATA PI /3.14159E0/, RGAS /8314.E0/, GRAV /9.81E0/
C-----
C      INITIALIZE ANYTHING NEEDED ON FIRST PASS
C      IWASTE= GAS INDEX OF 'WASTE' FOR ENTRAINMENT
C-----
C      IF (IFIRST.EQ. 1) THEN
C          IFIRST= 0
C
C      PHASE OF CALCULATIONS:
C      CONVENTION: TIME = 0 IS START OF FIRST BUBBLE RISE
C
C      IBRISE= 1: BUBBLE RISE
C              0: AFTER RELEASE
C      CHANGE WHEN TIMER EXPIRES: TBNEXT IS TIME OF NEXT BUMP
C      NBUMP= NUMBER OF BUMPS, UP TO INPUT VALUE OF NBMAX
C
C          IBRISE= 1
C          TBNEXT= 1.E6
C          NBUMP= 1.E0
C
C      POINTERS
C
C          IWASTE= IGNAM'WASTE      ',GAS,INGAS)
C          IH2O=   IGNAM'STEAM      ',GAS,INGAS)
C          IH2 =   IGNAM'HYDROGEN   ',GAS,INGAS)
C          IO2 =   IGNAM('OXYGEN    ',GAS,INGAS)
C          IC2 =   IGNAM('CARBON_DIO',GAS,INGAS)
C          ICO =   IGNAM('CARBON_MON',GAS,INGAS)
C          IN2 =   IGNAM'NITROGEN   ',GAS,INGAS)
C          IH2OTR= IGNAM('STEATRAC  ',GAS,INGAS)
C          IWASTR= IGNAM('WASTTRAC  ',GAS,INGAS)
C
C      ZERO OUT VECTORS OF ENTRAINED MATERIAL AND SPECIAL STATE VARS
C
C      DO 120 II=1, INXSP
C          XSP(II)= 0.E0

```

```

120  CONTINUE
C
C  ASSIGNMENT OF SPECIAL VECTOR:
C  1  ZBUB  BUBBLE CLUSTER AVG HEIGHT, STARTS AT ZERO
C  2  VRAT  RATIO OF BUBBLE VOLUME V/V0, STARTS AT 1.E0
C  3  PBUB  STEAM PRESSURE IN BUBBLE
C  4  VHS   HEADSPACE VOLUME
C  5  ZW    (FOR PLOTS) WATER LEVEL
C  6  GAMMA (FOR PLOTS) GAMMA
C  7  WOUT  (FOR PLOTS) OUTFLOW
C  8  TBC   BUBBLE CLUSTER LIQUID TEMPERATURE
C  9  MLBC  BUBBLE CLUSTER LIQUID MASS
C 10  FROUDE NUMBER
C      AND EQUILIBRIUM PRESSURE
C      AND SAVE INITIAL GAS VOLUME
C
      VB0= 4.E0/3.E0 * PI * DB0**3
      TCL= TSUPR
      VOLHSO = VOLR (IRBUMP)
      VBC= VBCO
      HCL= ZWO
      PEQ= SPV(TWASTE, IH2O)
      XSP(1)= 0.E0
      XSP(2)= 1.E0
      XSP(3)= PEQ
      XSP(4)= VOLHSO
      XSP(5)= ZWO
      XSP(6)= GAMM(IRBUMP)
      XSP(8)= TWASTE
      XSP(9)= MLBCO
      XSP(10)= 0.E0
C
C  SAVE INPUT TIMESTEP CONTROL INFORMATION:
C  USER PROVIDES THROUGH TIMEIN.CML:
C  TIDTMAX(10), DTMAX1(10)      MAX TIMESTEP CONTROL LOOKUPS
C  TIDTMIN(10), DTMIN1(10)     MIN TIMESTEP CONTROL LOOKUPS
C  THESE ARE SAVED RESPECTIVELY AS:
C  TMX0(10),   DTMX0(10),
C  TMN0(10),   DTMN0(10)
C
C  INPUTS AND SAVED VALUES ARE BASED ON THE FOLLOWING RULE:
C  ENTRIES 1-5 APPLY DURING BUBBLE RISE
C  ENTRIES 6-10 APPLY BETWEEN BUBBLE RISE EVENTS
C  THEREFORE 5 ENTRIES MUST BE MADE FOR BUBBLE RISE,
C      SO THAT INPUTS 6-X ARE READ
C  TIME LOOKUP VALUES TIDTMAX() AND TIDTMIN() ARE RELATIVE
C      TO THE START OF EACH PHASE
C
C  SAME APPLIES TO PLOTS, SAVED AS TPMX0() ETC
C  SAME APPLIES TO PRINT, SAVED AS TPRN0(), DTPRN0()
C
      DO 130 II=1,10
      TMX0(II)= TIDTMAX(II)
      DTMX0(II)= DTMAX1(II)
      TMN0(II)= TIDTMIN(II)
      DTMN0(II)= DTMIN1(II)
      TPMX0(II)= TIPLTMAX(II)

```

```

      DTPMX0(II) = PLTMAX1(II)
      TPMN0(II) = TIPLTMIN(II)
      DTPMN0(II) = PLTMIN1(II)
      TPRN0(II) = TIDTPRIN(II)
      DTPRN0(II) = DTPRIN1(II)
130    CONTINUE
C
      ENDIF
C
-----
C    ADJUST VOLUME AFTER INTEGRATION
C-----
      IF (ICALL .EQ. 2 .AND. IBRISE .EQ. 1) THEN
        VOLR(IRBUMP) = XSP(4)
        RETURN
      ENDIF
C-----
C    INITIALIZATION EACH PASS: ONLY CASE ICALL = 1 REMAINS
C-----
      RZBUB = 0.E0
      RVRAT = 0.E0
      RPBUB = 0.E0
      RVHS = 0.E0
      QENTR = 0.E0
      WENTW = 0.E0
      RTBC = 0.E0
      RMLBC = 0.E0
C
      DO 250 II=1,INGAS
        WENT(II) = 0.E0
250    CONTINUE
      DO 260 II=1,INXSP
        RXSP(II) = 0.E0
260    CONTINUE
C-----
C
C    INTEGRATE BUBBLE RISE AND GET PV WORK
C    1 ZBUB BUBBLE CLUSTER AVG HEIGHT, STARTS AT ZERO
C    2 VRAT RATIO OF BUBBLE VOLUME V/V0, STARTS AT 1.E0
C    3 PBUB STEAM PRESSURE IN BUBBLE
C    4 VHS HEADSPACE VOLUME
C    8 TBC BUBBLE CLUSTER TEMPERATURE, STARTS AT TWASTE
C    9 MLBC MASS OF LIQUID IN BUBBLE CLUSTER
C
C    SAVE THESE FOR REFERENCE:
C    5 HCL WATER LEVEL
C    6 GAMM() GAMMA
C    7 WOUT OUTFLOW
C    10 FROUDE NUMBER
C-----
C
C    RENAME SPECIAL VARIABLES FOR SCRUTABILITY
C
      ZBUB = XSP(1)
      VRAT = XSP(2)
      PBUB = XSP(3)

```

RPP-6213 REV 1

```

VHS= XSP(4)
TBC= XSP(8)
MLBC= XSP(9)

C
C
C   DECIDE ON PHASE OF PROBLEM:
C   NEED AUXILIARY RELATIONS IF DURING RISE PHASE
C
  IF (IBRISE.EQ. 1) THEN
    VBC= VBCO * VRAT
    HCL= ZWO * (VLIQ + VBC)/(VLIQ + VBCO)
  ENDIF

C
C   TRANSITION BETWEEN PHASES:  END OF BUMP
C   ADD AEROSOL, MIX BUBBLE AND HEADSPACE,
C   NEW PRESSURE & TEMPERATURE
C
  IF (IBRISE.EQ. 1 .AND. ZBUB.GE. HCL) THEN
    IR= IRBUMP
    IBRISE = 0
    TENEXT= TIME + TINTB
    XSP(5)= HCL
    XSP(6)= GAMM(IR)
    XSP(10)= 0.E0

C   ENTRAINED WASTE
    UBUB= 0.76 * SQRT(GRAV) * VBC**(1.E0/6.E0)
    USUP= 0.666630 * UBUB
    EGROUP= (MUGR(IR)**4 * RHOG(IR)**2 * (RHOLIQ-RHOG(IR))**3)
&      / (SURWAS**9 * GRAV**5)
    ENT= FBENT * 7.13E-4 * EGROUP**0.125 * USUP**3
    MAER= ENT*RHOG(IR)*VBC

C   STEAM AND WASTE ENTHALPIES; USE WASTE AT HEADSPACE TEMP
    WENT(IWASTE)= 1.E0
    HWASTE= HGSRC(2,PR(IRBUMP),TBC,WENT,0.E0)
    WENT(IWASTE)= 0.E0
    WENT(IH2O)= 1.E0
    HSTM= HGSRC(1,PR(IR),TBC,WENT,0.E0)
    WENT(IH2O)= 0.E0

C   MIXING CUP VALUES
    RHOSTM= PR(IR)*MWG(IH2O)/RGAS/TWASTE
    MG(IH2O,IR)= MG(IH2O,IR) + VBC*RHOSTM
    MA(IWASTE,IR)= MA(IWASTE,IR) + MAER
    UG(IR)= UG(IR) + MAER*HWASTE + HSTM*VBC*RHOSTM
    VOLR(IR)= VOLHSO + VBCO
    XSP(4)= VOLHSO + VBCO
    TGES= TGR(IRBUMP)
    PGES= PR(IRBUMP)
    CALL GAST(1,IREG,IGAS,MWG,MG,MA,MFG,NFG,MGT,NGT,MAT,
@      FWG)
    CALL PTREG1
  I (VOLR(IR),TGES,PGES,MG,UG(IR),IR,TIME,
  I  MFG,NFG,MGT(IR),NGT(IR),MA,ML,UL(IR),
  O  TGR(IR),PR(IR),PPG,RHOG(IR),DPDT(IR),MCE(IR),DPDMG,
  O  UGI,HGI,TLR(IR),UAG(IR),DPDV(IR),
  O  CPGR(IR),GAMM(IR),HLSAT,RHOL,IPTRREG)

C
C   TIMESTEP CONTROL FOR PERIOD BETWEEN BUMPS,
C   SAVED IN PLACES 6-10

```

```

C
DO 332 II=1,5
TIDTMAX(II)= TIME + TMX0(II+5)
DTMAX1(II)= DTMX0(II+5)
TIDTMIN(II)= TIME + TMN0(II+5)
DTMIN1(II)= DTMN0(II+5)
TIPLTMAX(II)= TIME + TPMX0(II+5)
PLTMAX1(II)= DTPMX0(II+5)
TIPLTMIN(II)= TIME + TPMN0(II+5)
PLTMIN1(II)= DTPMN0(II+5)
TIDTPRIN(II)= TIME + TPRN0(II+5)
DTPRIN1(II)= DTPRNO(II+5)
332 CONTINUE
C
ENDIF
C
C TRANSITION BETWEEN PHASES: NEXT BUMP
C RE-INITIALIZE THE XSP VECTOR
C
IF (IBRISE.EQ. 0 .AND.
& TIME+DELT/2.E0 .GE. TBNEXT .AND.
& NBUMP .LT. NBMAX) THEN
C
IBRISE= 1
NBUMP= NBUMP + 1
C
PEQ= SPV(TWASTE, IH2O)
XSP(1)= 0.E0
XSP(2)= 1.E0
XSP(3)= PEQ
XSP(4)= VOLHSO
XSP(5)= ZWO
XSP(6)= GAMM(IRBUMP)
XSP(8)= TWASTE
XSP(9)= MLBCO
XSP(10)= 0.E0
C
VBC= VBCO
HCL= ZWO
ZBUB= XSP(1)
VRAT= XSP(2)
PBUB= XSP(3)
VHS= XSP(4)
TBC= XSP(8)
MLBC= XSP(9)
C
C TIMESTEP CONTROL FOR BUBBLE RISE,
C SAVED IN PLACES 1-10
C
DO 432 II=1,5
TIDTMAX(II)= TIME + TMX0(II)
DTMAX1(II)= DTMX0(II)
TIDTMIN(II)= TIME + TMN0(II)
DTMIN1(II)= DTMN0(II)
TIPLTMAX(II)= TIME + TPMX0(II)
PLTMAX1(II)= DTPMX0(II)
TIPLTMIN(II)= TIME + TPMN0(II)

```

```

      PLTMIN1(II) = DTPMNO(II)
      TIDTPRIN(II) = TIME + TPRNO(II)
      DTPRIN1(II) = DTPRNO(II)
432      CONTINUE
C
      ENDIF
C
      IF (IBRISE.EQ. 1) THEN
C
      BUBBLE RISE PHASE
C
C      FLOW OUT OF HEADSPACE, LAST TIMESTEP VALUE, NEEDED FOR DP/DT,
C      SO SUM OVER JUNCTIONS CONNECTED TO IRBUMP, NOTING:
C      /JUNCS/INJR(IR)      - NUMBER OF JUNCTIONS CONNECTED TO COMPARTMENT-IR
C      /JUNCS/IJPTR(IL,IR) - 'IL'TH JUNCTION INDEX CONNECTED TO COMPARTMENT-IR
C
      IR = IRBUMP
      WOUT = 0.E0
      DO 1100 IL=1, INJR(IR)
        IJ = IJPTR(IL, IR)
        IF (IR.EQ. IR1(IJ)) THEN
          SENSE = 1.E0
        ELSE
          SENSE = -1.E0
        ENDIF
        WOUT = WOUT + WJN(IJ)*SENSE
      1100 CONTINUE
C
      BUBBLE RISE RATES OF CHANGE:
      BUBBLE CLUSTER VELOCITY, CHANGE OF V RATIO, CHANGE OF PEQ
C
      LOCALLY INTEGRATE VRAT AND PBUB EQUATIONS, DUE TO STIFFNESS,
      KEEPING OTHER VARIABLES AT BEGINNING-OF-TIMESTEP VALUES
C
      PEQ = SPV(TBC, IH2O)
C
      INLOC = 50
      DTLOC = DELT/FLOAT(INLOC)
      VR1 = VRAT
      PB1 = PBUB
C
      DO 2100 II=1, INLOC
        VBC = VR1*VBC0
        RZBUB = 0.76 * SQRT(GRAV) * VBC**(1.E0/6.E0)
        DENOM = PR(IR) + RHOLIQ*GRAV*(HCL - ZBUB) - PEQ
        A12 = 1.E0 - (1.E0 - VRAT)/DENOM
      &      ( PR(IR)*GAMM(IR)*VBC0/(VHS+VBC0)
      &      + RHOLIQ*GRAV*ZW0*VBC0/(VBC0 + VLIQ) )
        A22 = -VRAT/DENOM
        DET = PBUB*A22 - VRAT*A12
        PMIX = PR(IR) + RHOLIQ*GRAV*(HCL - ZBUB)
        PDRAT = (PEQ-PBUB)/(PMIX-PEQ)
        B1 = SQRT(24.E0*DIFFB*RZBUB*VRAT/VB0)*PMIX*LOG(1.E0 + PDRAT)
        B2 = RHOLIQ*GRAV*RZBUB*VRAT/DENOM
      &      - (1.E0-VRAT)/DENOM * PR(IR)*WOUT*GAMM(IR)/MGT(IR)
        RVRAT = (B1*A22 - VRAT*B2) / DET

```

```

RPBUB= -(B1*A12 - PBUB*B2) / DET
VR1= VR1 + RVRAT*DTLOC
PB1= PB1 + RPBUB*DTLOC
2100 CONTINUE
RVRAT= (VR1 - VRAT) / DELT
RPBUB= (PB1 - PBUB) / DELT
C
RVHS= -RVRAT*VBC0
C
C BUBBLE CLUSTER SURFACE AREA AND ENTRAINMENT RATE
C CALCULATE VAPOR GENERATION RATE FIRST
C
WVAP= MWG(IH2O)*VBC0/RGAS/TBC*(PBUB*RVRAT+RPBUB*VRAT)
ABC= 4.83D0*(VBC + MLBC/RHOLIQ)**(2.D0/3.D0)
RMLBC= ENTB*RHOLIQ*ABC*RZBUB - WVAP
C
C TEMPERATURE AS A FUNCTION OF Z
C
RTBC= -(TBC - TCL)*RMLBC/MLBC -
@ WVAP*SHFG(TCL/TCR(IH2O), IH2O)/MLBC/4200.E0
XSP(5)= HCL
XSP(6)= GAMM(IR)
XSP(7)= WOUT
XSP(10)= 0.0345 * (VBC0*RVRAT)**2.E0 /
& (GRAV * (VBC0*VRAT + MLBC0/RHOLIQ))**1.6E0
C
ENDIF
C
C DUMMY LOCATIONS FOR PHASE BETWEEN & AFTER BUMPS,
C IN CASE OF FURTHER DEVELOPMENT, OR DEBUG
C
IF (IBRISE.EQ. 0) THEN
IDUM=1
ENDIF
IF (TIME.GT. TBUMP) THEN
IDUM=1
ENDIF
C
C-----
C INCREMENT RATES OF CHANGE - ENTRAIN INTO THE AEROSOL BIN
C-----
3000 CONTINUE
C
ENTRAINMENT
C
DO 3020 II=1, INGAS
RMG(II, IRBUMP)= RMG(II, IRBUMP) + WENT(II)
3020 CONTINUE
RMA(IWASTE, IRBUMP)= WENTW
C
HEADSPACE
C
RUG(IRBUMP)= RUG(IRBUMP) + QENTR - PR(IRBUMP)*RVHS
C
SPECIAL VECTOR
C
RXSP(1)= RZBUB

```

RPP-6213 REV 1

```

RXSP(2) = RVRAT
RXSP(3) = RPBUB
RXSP(4) = RVHS
RXSP(8) = RTBC
RXSP(9) = RMLBC

C
RETURN
END

SUBROUTINE BUMPIN
IMPLICIT REAL (A-H, K-Z)
C-----
C   DCRT INPUT ROUTINE
C-----
INCLUDE 'PARAMS.CMG'
INCLUDE 'CNTRL.CML'
INCLUDE 'GASN.CML'
INCLUDE 'BUMP.CML'

C
LOGICAL LTOK, TOKENL
CHARACTER*10 WORD, NAME(INGAS)
CHARACTER*80 LINE
CHARACTER*20 PWORD(30)
CHARACTER*1 STAR
C   DIMENSION WGAST(INGAS), IPGAST(INGAS), MATRIX(10,10)
DATA STAR / '*' /
DATA TOK / 273.15E0 /

C
2 FORMAT(' ', A10, 1P, 5(1E10.3, 3X))
4 FORMAT(' ', A10, ' = ', I2)
5 FORMAT(A80)
6 FORMAT(' !', A80)
8 FORMAT(' ')
DATA PI / 3.14159E0 /
C-----
C   1.0 INITIALIZE VARIABLES
C-----
C
C --- SET DEFAULT VALUES OF ALL DCRT PARAMETERS
C
C   TANK
C
IRBUMP = 1
TWASTE = 383.E0
ZW0 = 8.E0
VLIQ = 3200.E0
RHOLIQ = 1210.E0
MLBC0 = 40.E3
NBMAX = 10

C
C   MODEL
C
DB0 = 0.005
VBC0 = 10.E0
DIFFB = 9.2E-5
TBUMP = 1.E6

```


RPP-6213 REV I

```

      ENTB= 0.1E0
      TSUPR= 373.E0
      TINTB= 100.E0
C
      WRITE (*,61)
      WRITE(ILUNIT,61)
61  FORMAT(/,'      Tank Bump Simulation Input Group ',/)
C-----
C      2.0  SEARCH FOR MAJOR KEYWODS - IN ANY ORDER
C-----
C
5000  CONTINUE
C
C --- GET A LINE, LOOK FOR A KEYWORD
C
      READ (INUNIT,5,END=666) LINE
      LTOK= TOKENL(0,0,6,0,0,LINE,PWORD,INTOK)
      IF (INTOK .LT. 1) GOTO 5000
      WORD= PWORD(1)
      IF (WORD .EQ. STAR) GOTO 5000
C
C --- IDENTIFY A MAJOR KEYWORD
C
C-----
C --- TIMING KEYWORD GROUP
C-----
      IF (WORD .EQ. 'TANK') THEN
200  CONTINUE
      READ (INUNIT,5,END=666) LINE
      LTOK= TOKENL(0,0,6,0,0,LINE,PWORD,INTOK)
      IF (INTOK .LT. 1) GOTO 200
      WORD= PWORD(1)
      IF (WORD .EQ. STAR) GOTO 200
      IF (WORD .EQ. 'END') GOTO 5000
C
C
C      GET HERE IF A KEYWORD IN THE GROUP EXPECTED
C
      IF (WORD .EQ. 'IRBUMP') THEN
          IF (INTOK .LT. 2) GOTO 777
          IRBUMP= INTNUM(PWORD(2))
          WRITE (*,4) WORD,IRBUMP
          WRITE(ILUNIT,4) WORD,IRBUMP
          GOTO 200
      ENDIF
C
      IF (WORD .EQ. 'HEIGHT-CL') THEN
          IF (INTOK .LT. 2) GOTO 777
          ZW0= RELNUM(PWORD(2))
          WRITE (*,2) WORD,ZW0
          WRITE(ILUNIT,2) WORD,ZW0
          GOTO 200
      ENDIF
C
      IF (WORD .EQ. 'T_WASTE') THEN
          IF (INTOK .LT. 2) GOTO 777
          TWASTE= RELNUM(PWORD(2))
          WRITE (*,2) WORD,TWASTE

```

RPP-6213 REV 1

```

        WRITE(ILUNIT,2) WORD,TWASTE
        GOTO 200
    ENDIF
C
    IF (WORD.EQ. 'T_SUPER') THEN
        IF (INTOK.LT. 2) GOTO 777
        TSUPR= RELNUM(PWORD(2))
        WRITE (*,2) WORD,TSUPR
        WRITE(ILUNIT,2) WORD,TSUPR
        GOTO 200
    ENDIF
C
    IF (WORD.EQ. 'VOLUME-CL') THEN
        IF (INTOK.LT. 2) GOTO 777
        VLIQ= RELNUM(PWORD(2))
        WRITE (*,2) WORD,VLIQ
        WRITE(ILUNIT,2) WORD,VLIQ
        GOTO 200
    ENDIF
C
    IF (WORD.EQ. 'GAS-VOL') THEN
        IF (INTOK.LT. 2) GOTO 777
        VBC0= RELNUM(PWORD(2))
        WRITE (*,2) WORD,VBC0
        WRITE(ILUNIT,2) WORD,VBC0
        GOTO 200
    ENDIF
C
    IF (WORD.EQ. 'MASS-LIQ') THEN
        IF (INTOK.LT. 2) GOTO 777
        MLBC0= RELNUM(PWORD(2))
        WRITE (*,2) WORD,MLBC0
        WRITE(ILUNIT,2) WORD,MLBC0
        GOTO 200
    ENDIF
C
    IF (WORD.EQ. 'NBMAX') THEN
        IF (INTOK.LT. 2) GOTO 777
        NBMAX= RELNUM(PWORD(2))
        WRITE (*,2) WORD,NBMAX
        WRITE(ILUNIT,2) WORD,NBMAX
        GOTO 200
    ENDIF
C
C
C
C --- FALL THROUGH HERE IF A COMMENT PRESENT NOT STARTING WITH STAR
        WRITE (*,6) LINE
        WRITE(ILUNIT,6) LINE
        GOTO 200
    ENDIF
C-----
C    MODEL PARAMETER KEYWORD GROUP
C-----
    IF (WORD.EQ. 'MODEL') THEN
300    CONTINUE
        READ (INUNIT,5,END=222) LINE

```

```

LTOK=TOKENL(0,0,6,0,0,LINE,PWORD,INTOK)
IF (INTOK.LT. 1) GOTO 300
WORD= PWORD(1)
IF (WORD.EQ. STAR) GOTO 300
IF (WORD.EQ. 'END')GOTO 5000
C
IF (WORD.EQ. 'BUB_DIAM') THEN
  IF (INTOK.LT. 2) GOTO 777
  DB0= RELNUM(PWORD(2))
  WRITE (*,2) WORD,DB0
  WRITE(ILUNIT,2) WORD,DB0
  GOTO 300
ENDIF
C
IF (WORD.EQ. 'DIFFB')THEN
  IF (INTOK.LT. 2) GOTO 777
  DIFFB= RELNUM(PWORD(2))
  WRITE (*,2) WORD,DIFFB
  WRITE(ILUNIT,2) WORD,DIFFB
  GOTO 300
ENDIF
C
IF (WORD.EQ. 'FBENT')THEN
  IF (INTOK.LT. 2) GOTO 777
  FBENT= RELNUM(PWORD(2))
  WRITE (*,2) WORD,FBENT
  WRITE(ILUNIT,2) WORD,FBENT
  GOTO 300
ENDIF
C
IF (WORD.EQ. 'ENTB')THEN
  IF (INTOK.LT. 2) GOTO 777
  ENTB= RELNUM(PWORD(2))
  WRITE (*,2) WORD,ENTB
  WRITE(ILUNIT,2) WORD,ENTB
  GOTO 300
ENDIF
C
IF (WORD.EQ. 'TBUMP')THEN
  IF (INTOK.LT. 2) GOTO 777
  TBUMP= RELNUM(PWORD(2))
  WRITE (*,2) WORD,TBUMP
  WRITE(ILUNIT,2) WORD, TBUMP
  GOTO 300
ENDIF
C
IF (WORD.EQ. 'TINTB')THEN
  IF (INTOK.LT. 2) GOTO 777
  TINTB= RELNUM(PWORD(2))
  WRITE (*,2) WORD,TINTB
  WRITE(ILUNIT,2) WORD, TINTB
  GOTO 300
ENDIF
C
IF (WORD.EQ. 'TENDB')THEN
  IF (INTOK.LT. 2) GOTO 777
  TENDB= RELNUM(PWORD(2))

```

RPP-6213 REV 1

```

        WRITE (*,2) WORD,TENDB
        WRITE(ILUNIT,2) WORD, TENDB
        GOTO 300
    ENDIF
C
C
C --- MUST BE A COMMENT, GET ANOTHER PARAMETER
        WRITE (*,6) LINE
        WRITE(ILUNIT,6) LINE
        GOTO 300
C --- END OF ACTIVE MODEL PARAMETERS KEYWORD GROUP
    ENDIF
C
C
C-----
C    WASTE PROPERTY PARAMETER KEYWORD GROUP
C-----
    IF (WORD.EQ. 'WASTE')THEN
400    CONTINUE
        READ (INUNIT,5,END=222) LINE
        LTOK=TOKENL(0,0,6,0,0,LINE,PWORD,INTOK)
        IF (INTOK.LT. 1) GOTO 400
        WORD= PWORD(1)
        IF (WORD.EQ. STAR) GOTO 400
        IF (WORD.EQ. 'END') GOTO 5000
C
        IF (WORD.EQ. 'DENSITY-CL')THEN
            IF (INTOK.LT. 2) GOTO 771
            RHOLIQ= RELNUM(PWORD(2))
            WRITE (*,2) WORD,RHOLIQ
            WRITE(ILUNIT,2) WORD,RHOLIQ
            GOTO 400
        ENDIF
C
C
        IF (WORD.EQ. 'SURT_CL') THEN
            IF (INTOK.LT. 2) GOTO 777
            SURWAS= RELNUM(PWORD(2))
            WRITE (*,2) WORD,SURWAS
            WRITE(ILUNIT,2) WORD,SURWAS
            GOTO 400
        ENDIF
C
C
C --- MUST BE A COMMENT, GET ANOTHER PARAMETER
        WRITE (*,6) LINE
        WRITE(ILUNIT,6) LINE
        GOTO 400
C --- END OF WASTE PROPERTY KEYWORD GROUP
    ENDIF
C
C-----
C --- NORMAL TERMINATION:  'END' FOUND AS A MAJOR KEYWORD
C-----
    IF (WORD.EQ. 'END') THEN
        WRITE (*,667)
        WRITE(ILUNIT,667)

```

```

        RETURN
    ENDIF
667  FORMAT(' DCRT inputs completed',/)
C-----
C --- GET HERE IF A COMMENT LINE (NONBLANK, NONSTAR, NONKEYWORD)
C-----
        GOTO 5000
C-----
C    BOTTOM OF LOOP SEARCHING FOR MAJOR KEYWORDS
C-----
C --- ERROR HANDLING
C
666  CONTINUE
      WRITE (*,668)
      WRITE(ILUNIT,668)
668  FORMAT(' UNEXPECTED END OF FILE DURING DCRT-TANK INPUT')
      WRITE (*,6) LINE
      WRITE(ILUNIT,6) LINE
      STOP
C
777  CONTINUE
      WRITE (*,778)
      WRITE(ILUNIT,778)
778  FORMAT(' NOT ENOUGH TOKENS READING TANK INPUT')
      WRITE (*,6) LINE
      WRITE(ILUNIT,6) LINE
      STOP
C
222  CONTINUE
      WRITE (*,223)
      WRITE(ILUNIT,223)
223  FORMAT(' UNEXPECTED END OF FILE READING DCRT MODEL PARAMETERS')
      WRITE (*,6) LINE
      WRITE(ILUNIT,6) LINE
      STOP
C
555  CONTINUE
      WRITE (*,558)
      WRITE(ILUNIT,558)
558  FORMAT(' UNEXPECTED END OF FILE DURING DCRT FUEL INPUT')
      WRITE (*,6) LINE
      WRITE (ILUNIT,6) LINE
      STOP
C
      END

```

F.2 BUMP.CML: Addition to HADCRT for Chapter 8

```

COMMON /BUMP1/
&    IRBUMP, ZWO,    TWASTE, RHOLIQ, VLIQ,    FBENT,
&    DBO,    VBCO,    DIFFB, TBUMP,    SURWAS, ENTB,
&    MLBCO. NBMAX, TINTB, TSUPR

```

F.3 Differences in AMIO.FOR: Addition to HADCRT for Chapter 8

BeyondCompare Version 2.00

Copyright (C) Stepping Stone Software 1987. All rights reserved.
Portions Copyright (C) Microsoft Corp 1984, 1985, 1986. All rights reserved.

```
#####00116#####amio.for
# 117 C --- BUMP KEYWORD GROUP
# =====
# 117 C --- DCRT KEYWORD GROUP
#####00001#####..\code11\amio.for
```

```
#####00001#####amio.for
# 119 IF (WORD.EQ. 'BUMP')THEN
# 120 CALL BUMPIN
# =====
# 119 IF (WORD.EQ. 'DCRT') THEN
# 120 CALL DCRTIN
#####00076#####..\code11\amio.for
```

```
#####00076#####amio.for
# 197 IBUMP= 0
# =====
# deleted
#####00255#####..\code11\amio.for
```

```
#####00255#####amio.for
# 453 IF (WORD.EQ. 'IBUMP')THEN
# 454 IF (INTOK.LT. 2) GOTO 777
# 455 IBUMP= INTNUM(PWORD(2))
# 456 WRITE(ILUNIT,4) WORD,IBUMP
# 457 GOTO 300
# 458 ENDIF
# 459 C
# =====
# deleted
#####04432#####..\code11\amio.for
```

F.4 Differences in AMOD.FOR: Addition to HADCRT for Chapter 8

BeyondCompare Version 2.00

Copyright (C) Stepping Stone Software 1987. All rights reserved.
Portions Copyright (C) Microsoft Corp 1984, 1985, 1986. All rights reserved.

```
#####00591#####amod.for
# 592 IF (IBUMP.EQ. 1) CALL BUMP (1)
# =====
# deleted
#####00891#####..\code11\amod.for
```

```
#####00891#####amod.for
# 1484 C! FOR BUMP ROUTINE, GAS VOLUME
# 1485          CALL BUMP(2)
# 1486 C
# =====
# deleted
#####04186#####..\code11\amod.for
```

F.5 Differences in CNTRL.CML: Addition to HADCRT for Chapter 8

BeyondCompare Version 2.00

Copyright (C) Stepping Stone Software 1987. All rights reserved.
 Portions Copyright (C) Microsoft Corp 1984, 1985, 1986. All rights reserved.

```
#####00006#####cntrl.cml
#      7      &          ISLAY, RSTRTF,  IRMAX, IDCRT, IBUMP
# =====
#      7      &          ISLAY, RSTRTF,  IRMAX, IDCRT
#####00000#####..\code11\cntrl.cml
```

F.6 AZ102.DAT: Input to HADCRT for Chapter 8

```
*****
*   TANK BUMP PV test
*
*****
*
*-----
CONTROL      ! Major keyword group
*-----
  TITLE      ! Keyword; next line is title, title can be any length*  -
*****
      AZ 102 TANK BUMP
*****

*END TITLE ! Anything after END is a comment
*.....
TIMING      ! Keyword
  TSTART      0.      !  START TIME, >0 FOR RESTART RUN
  TLAST 50000.      !  END TIME
  DTMIN      !  MIN TIMESTEP (Seconds)
    0.0 0.001
    1.0 0.001
    2.0 0.001
    3.0 0.001
    4.0 0.01
    0.0 0.01
    1.0 0.01
    10.0 0.1
```

```

100.  1.0
1000. 1.0
DTMAX      ! MAX TIMESTEP (Seconds)
0.0  0.005
1.0  0.005
2.0  0.005
3.0  0.005
4.0  0.01
0.0  0.1
1.0  0.1
10.0 1.0
100. 10.0
1000. 100.0
DTPRIN     ! PRINT INTERVAL (Seconds)
0.0  0.25
1.0  0.25
2.0  0.25
3.0  0.25
4.0  0.25
0.0  0.25
1.0  2.0
10.0 100.0
100. 1000.0
1000. 10000.0
PLTMIN     ! MIN PLOT INTERVAL (Seconds)
0.0  0.01
1.0  0.01
2.0  0.01
3.0  0.01
4.0  0.01
0.0  0.01
1.0  0.1
10.0 1.0
100. 10.0
1000. 100.0
PLTMAX     ! MAX INTERVAL WITHOUT PLOT (Seconds)
0.0  0.1
1.0  0.1
2.0  0.1
3.0  0.1
4.0  0.1
0.0  0.1
1.0  1.0
10.0 10.0
100. 100.0
1000. 1000.0
DTRST     ! RESTART INTERVAL (Seconds)
0.0  100000.
*
FTPCH      0.003      ! FRACTIONAL CHANGE IN T AND P
FAECH      0.003      ! FRACTIONAL CHANGE IN aerosol mass
FPPLCH     0.03       ! FRACTIONAL CHANGE FOR PLOTTING
END TIMING ! TIMING is a comment.
*
* .....
PLOT      ! Keyword for plotting section
* Plotting syntax:

```



```

•
* PRESSURE n rlist - Pressure, Pa
* GAS-T n rlist - Gas Temperature, K
* HS-TI n hlist - Heat Sink Temperature - Inner Surface, K
• HS-TO n hlist - Heat Sink Temperature - Outer Surface, K
* HS-TA n hlist - Heat Sink Temperature - Average, K
* AEROSOL n rlist - Aerosol Mass (Total), kg
* GAS-W n jlist - Mass Flowrate, kg/s
* GAS-WX n jlist - Countercurrent Mass Flowrate, kg/s
* SPECIAL-X n xlist - Special model state variable
• SPECIAL-R n xlist - Special model rate variable
* GAS-X GASNAME n rlist - Gas Mole Fraction
* GAS-RH GASNAME n rlist - Gas Relative Humidity
* GAS-MASS GASNAME n rlist - Gas Mass (Species), kg
• AER-MASS GASNAME n rlist - Aerosol Mass (Species), kg
* MASS GASNAME n rlist - Total Mass (Species), kg
* LIQ-MASS GASNAME n rlist - Deposited Mass (Species), kg

• Pressure, Gas Temperature, and total aerosol mass require a region
* list
*
* Heat Sink Temperatures need a heat sink number list
*
* Flowrates need a junction number list
*
* Gas concentration, relative humidity, individual species gas mass,
* individual species aerosol mass, total (gas+aerosol) individual
• species mass, and individual species deposited liquid mass require
• a region and gas name
*
* BUMP special state & rate variables are:
* 1= Bubble height
* 2= volume ratio
• 3= Vapor pressure
* 4= Headspace volume
*

PRESSURE          3  1 2 3 4      ! Pressure in 1, 2, 3
GAS-T             3  1 2 3 4      ! Temps in regions 1.2.3
GAS-X NITROGEN    3  1 2 3 4      ! N2 concentration in
GAS-X OXYGEN      3  1 2 3 4      ! O2 concentration in
GAS-X STEAM       3  1 2 3 4      ! H2O concentration in
GAS-W             5  1 2 3 4 5     ! Uni-directional mass flowrate
GAS-WX            5  1 2 3 4 5     ! Counter-current mass flowrate
AEROSOL           4  1 2 3 4      ! Mass of total aerosol
AER-MASS WASTE    4  1 2 3 4      ! Mass of WASTE aerosol
AER-MASS STEAM    4  1 2 3 4      ! Mass of STEAM aerosol
LIQ-MASS WASTE    4  1 2 3 4      ! Mass of deposited WASTE
LIQ-MASS STEAM    4  1 2 3 4      ! Mass of deposited/condensed STEAM
SPECIAL-X         6  1 2 3 4 5 6
SPECIAL-X         2  8 9
SPECIAL-R         4  1 2 3 4
SPECIAL-R         2  8 9
* END PLOT ! PLOT is a comment
*
* .....
ACTIVE MODELS ! Keyword; MODELS is a comment; 1 = on, 0 = off
  IJUNC 1 ! Junction flow model

```

RPP-6213 REV 1

```

ICCFLW  1      | Counter-current flow model
IHSINK  1      ! Heat sinks
ICNDS   0      ! Condensation
IASSED  1      ! Aerosol Sedimentation
IALEAK  1      Aerosol Leakage
IFOG    1      Fog formation
ISRC    1      ! User-defined sources
ISENS   0      sensitivity runs
IBUMP   1      ! BUMP Runs
END ACTIVE MODELS ! ACTIVE MODELS is a comment
*
* .....
MODEL PARAMETERS
  AGAMMA  2.5    ! Shape factor for nonsphericity for coagulation
  ACHI    1.0    ! Shape factor for nonsphericity for stokes' law
  AFEO    1.0    ! Collision efficiency: 1.0 Fuchs, 0.33 Prupacher-Klett
END MODEL PARAMETERS
*
*
C-----
C      SOURCE GROUP:  GROUPS REPEATED FOR INPUT # OF REGIONS
C      END OF GROUP DESIGNATED BY 'REGION' OR 'END' KEYWORDS
C      ENTER: TIME, TEMP, FLOWRATES, POWER
*
* STEAM SOURCE FROM VAPORIZATION
* BASED ON 40 KW / 2.2E6 = 0.022 KG/S
* HEAT SOURCE IS POWER - STEAM - OVERBURDEN = ABOUT 10 KW
*
* SOURCES          1          !-- KEYWORD AND # SOURCE GROUPS
* REGION 1 GASES 1          !-- REGION #, # GASES; <0 MEANS AEROSOL
* STEAM              !-- Gas
* 0.0  100.0  0.022E0  1.E4    ! TIME, TEMP (C), KG/S, WATTS
* 1.E3  100.0  0.022E0  1.E4
* 1.E5  100.0  0.022E0  1.E4
*   END REGION              ! END OF SOURCE IN THIS REGION
*   END SOURCE              ! END ALL SOURCES
*
*
END CONTROL      ! End of CONTROL keyword group
*
* -----
VOLUMES      4      ! total number of control volumes
* -----
* No more than 5 columns (regions) at a time
* units:
* VOLUME m^3, SED-AREA m^2, ELEVATION m, TEMP-GAS K, PRESSURE Pa
*
*
*           SLUICE      PUMP
*           HEADSPACE  PIT 1      PIT 2      Atmosphere
REGIONS      1          2          3          4
VOLUME      1800.      40.0      20.0      1.E9
SED-AREA     411.      0.1       0.0       0.00
ELEVATION     0.0       5.0       5.0       8.0
TEMP-GAS     100.0     75.0     75.0     25.01
PRESSURE     1.0119E5   1.013E5   1.013E5   1.013E5
END REGIONS  ! REGIONS is a comment
*

```

RPP-6213REV 1

•
 * Gas composition of each region; specify mole fraction of each gas
 * No more than five columns at a time

* **30% H2 in air using 1% H2O, 20% O2, 79% N2 Initially
 *

GASES	1	2	3	4
STEAM	0.95	0.01	0.01	0.01
OXYGEN	0.01	0.20	0.20	0.20
NITROGEN	0.04	0.79	0.79	0.79

* END GASES ! GASES is a comment

•
 * Aerosol concentration of each region (kg/m³)
 * No more than five columns at a time

AEROSOLS	1	2	3	4
WASTE	0.000	0.0	0.0	0.0

* END AEROSOLS ! AEROSOLS is a comment

* END VOLUMES ! VOLUMES is a comment

*
 HEAT-SINKS 1 ! Total number of heat sinks
 *
 * No more than 5 columns at a time,

* Syntax:

* IGEOM 1 for plane, 0 or 2 for cylinder
 * RHO Density (kg/m³)
 * KHS Thermal Conductivity (W/m/K)
 * CPHS Specific Heat (J/kg/K)
 * QV Volumetric Heat Generation (W/m³)
 * XRI Inner Radius (m)
 * XRO Outer Radius (m); for plane wall, thickness = XRO-XRI
 * AHS One-sided heat sink area (m²)
 * TIINIT Initial inside surface temperature (C)
 * TOINIT Initial outside surface temperature (C)
 * IMSLAB Number of slabs; 3 is minimum
 * IREGI Region index for inner surface or 0 (insulated)
 * or -1 for constant temperature
 * TIHS Region surface temperature when IREGI = -1 (C)
 * IREGO Region index for outer surface or 0 (insulated)
 * or -1 for constant temperature
 * TOHS Region surface temperature when IREGO = -1 (C)
 * XLHS Characteristic length for natural convection (m)
 * EHSI Emissivity of inner surface
 * EHSO Emissivity of outer surface

* SINKS 1

IGEOM	1
RHO	1200.00
KHS	0.6
CPHS	1.E10
QV	0.0

RPP-6213 REV 1

```

XRI          0.0
XRO          1.0
AHS          1000.
TIINIT       100.00
TOINIT       100.00
IMSLAB       10
IREGI        1
TIHS         100.0
IREGO        0
TOHS         100.0
XLHS         10.0
EHSI         1.0
EHSO         1.0

```

* END

END HEAT-SINKS ! HEAT-SINKS is a comment

*-----

JUNCTIONS 6 ! # Junctions

*-----

- * 1) TANK TO ENV - INLET
- 2) TANK TO ENV - OUTLET
- * 3) TANK TO PIT1
- * 4) TANK TO PIT2
- * 5) PIT1 TO ENV
- * 6) PIT2 TO ENV

*

•

* Syntax:

- * IJTYP Junction Type: 1 = Normal, 2 = HEPA, 3 = Cover
- * IR1 Upstream Region
- * IR2 Downstream Region
- * AJN Area (m^2)
- * ABYP Bypass area for HEPA junction (m^2)
- * PHEPA HEPA Filter Failure Pressure (Pa)
- * ACOV Cover Area (m^2)
- * MCOV Cover Weight (kg)
- * Z1JN Elevation wrt floor of IR1 opening (m)
- * Z2JN " IR2 "
- * CJN Loss coefficient multiplies $0.5 \cdot \rho \cdot v^2$
- IHORIZ Orientation: 1 = horizontal, 0 = vertical
- * XWJN Characteristic width, m
- * XHJN Characteristic height, m
- * XLJN Characteristic length, m
- * DFJN Decontamination Factor
- N90 No. of 90 bends

* PATHS	1	2	3	4
IJTYP	1	1	1	1
IR1	1	1	1	1
IR2	4	4	2	3
IHORIZ	1	1	1	1
XWJN	0.20	0.50	0.010	0.010
XHJN	0.20	0.50	0.010	0.010
XLJN	100.0	100.0	1.0	1.0
AJN	0.030	0.200	0.053	0.00133
Z1JN	4.0	8.0	5.0	5.0

RPP-6213 REV 1

Z2JN	0.0	0.0	1.0	1.0
CJN	4.0	4.0	2.0	2.0
DFJN	1.0	1.0	1.0	1.0
N90	0	0	0	0
ABYP	0	0	0	0
PHEPA	0	0	0	0
ACOV	0	0	0	0
MCOV	0	0	0	0

* END PATHS ! PATHS is a comment.

* PATHS 5 6

IJTYP	3	3
IR1	2	3
IR2	4	4
IHORIZ	1	1
XWJN	0.01	0.01
XHJN	0.01	0.01
XLJN	0.3	0.3
AJN	0.32	0.08
Z1JN	0.6	0.6
Z2JN	0.0	0.0
CJN	2.0	2.0
DFJN	1.0	1.0
N90	0	0
DP1	0	0
DP2	0	0
ABYP	0	0
PHEPA	0	0
ACOV	5.00	9.50
MCOV	6.8E3	16.6E3

* END PATHS ! PATHS is a comment.

END JUNCTIONS ! JUNCTIONS is a comment.

•

BUMP! Input Section for "DCRT.For" Model

TANK

IRBUMP	1	! BUMP region index
HEIGHT-CL	7.0	! Conv layer height
T_WASTE	388.0	! Non-Conv Waste temp, K
T_SUPER	373.0	! Supernatant Temp.
VOLUME-CL	2859.	! Conv layer volume, m ³
GAS-VOL	8.0	! Volume of released gas, m ³
MASS-LIQ	34.E3	! Mass of liquid in cluster
NBMAX	12.E0	! Number of total bumps

END TANK

*

WASTE

DENSITY-CL	1100.	! Conv layer density, kg/m ³
SURT_CL	0.059	! Conv layer surface tension, N/m

END

*

MODEL

BUB_DIAM	0.005	! Bubble diameter, m
----------	-------	----------------------

RPP-6213 REV I

DIFFB	9.23-5	! Diffusion coefficient
FBENT	1.0	! Multiplier on Ishii release model
ENTB	0.1E0	! Entrainment mult for Ricou-Spalding
TINTB	1800.E0	! Time between bumps
TBUMP	200.	! Development use only

END MODEL

*
*

END DCRT

This page intentionally **left** blank.

APPENDIX G

SPREADSHEETS FOR BUMP CRITERIA

This page intentionally left blank.

APPENDIX G

SPREADSHEETS FOR BUMP CRITERIA

Time to Bump Conditions for Non-AZ/AY DSTs That Don't Make the Initial Screening Criteria: Current Waste Temperatures											
Pedigreed Database Heat Loads, Hu et al. (2000) Inventories											
DSTs	RhoCL (kg/m3)	RhoNCL (kg/m3)	T (K)	VCL (m³)	VNCL (m³)	CCL (J/kg)	CNCL (J/kg)	Q (W)	k (W/m-K)	dsoil, m	Rtank,
SY101	1390	1610	323	2286	2214	30W	3300	16100	1	4	11
AN103	1490	1710	314	2074	1552	30w	3300	18700	1	4	11
AN104	14W	1590	317	2286	17W	30W	33W	19700	1	4	11
AN105	1420	1580	313	2411	1851	30w	33w	13400	1	4	11
AW101	14W	1630	314	31M	1158	3000	3300	15200	1	4	11
AN102	1410	1500	320	3676	337	3000	33W	11500	1	4	11
AN107	1370	1560	308	3017	935	3000	33W	13700	1	4	11
DSTs	q, K/s	K, l/s	Tf	t (s)	t(yr)	t (d)	t(hr)	Note: #NUM! Means that the time is infinite and the waste reaches steady-state before boiling.			
SY101	7.56E-07	6.57946E-09	377	1.75E+08	5.55751432	2028	48683.83				
AN103	1.04E-06	7.77169E-09	377	1.15E+08	3.6553639	1334	32020.99				
AN104	1.06E-06	7.56508E-09	377	1.03E+08	3.27769143	1196	2871258				
AN105	6.73E-07	7.03312E-09	377	3.57E+08	11.3347143	4137	99292.1				
AW101	7.89E-07	7.27271E-09	377	2.04E+08	6.46834152	2361	56662.67				
AN102	6.68807	8.13782E-09	377	INUM!	XNUM!	XNUM!	XNUM!				
AN107	7.96E-07	8.13987E-09	377	2.81E+08	8.9195704	3256	78135.44				
Hu et al. (2000) Heat Loads and Inventories											
DSTs	RhoCL (kg/m3)	RhoNCL (kg/m3)	T (K)	VCL (m³)	VNCL (m³)	CCL (J/kg)	CNCL (J/kg)	Q (W)	k (W/m-K)	dsoil, m	Rtank,
SY101	1390	1610	323	2286	2214	30W	33w	10600	1	4	11
AN103	1490	1710	314	2014	1552	30W	3300	12100	1	4	11
AN104	1400	1590	317	2286	1700	30W	3303	13700	1	4	11
AN105	1420	1580	313	2411	1851	30W	3300	9340	1	4	11
AW101	1400	1630	314	3104	1158	3003	3303	10300	1	4	11
AN102	1410	1500	320	3676	337	3000	33w	9340	1	4	11
AN107	1370	1560	308	3017	935	3000	33w	11700	1	4	11
DSTs	q, K/s	K, l/s	Tf	t (s)	t(yr)	t (d)	t(hr)	Note: #NUM! Means that the time is infinite and the waste reaches steady-state before boiling.			
SY101	4.98E-07	6.57946E-09	377	XNUM!	XNUM!	#NUM!	INUM!				
AN103	6.71E-07	7.77169E-09	377	INUM!	INUM!	XNUM!	#NUM!				
AN104	7.40E-07	7.56508E-09	377	2.86E+08	9.07466052	3312	79494				
AN105	4.69E-07	7.03312E-09	377	INUM!	XNUM!	XNUM!	INUM!				
AW101	5.35E-07	7.27271E-09	377	#NUM!	XNUM!	INUM!	INUM!				
AN102	5.42E-07	8.13782E-09	377	XNUM!	#NUM!	XNUM!	XNUM!				
AN107	6.80E-07	8.13987E-09	377	INUM!	INUM!	INUM!	XNUM!				

**Time to Bump Conditions for Non-AWAY DSTs That Don't Make the Initial Screening Criteria:
LCO Waste Temperatures**

Pedigreed Database Heat Loads, Hu et al. (2000) Inventories

DSTs	RhoCL (kg/m3)	RhoNCL (kg/m3)	T (K)	VCL (m ³)	VNCL (m ³)	CCL (J/kg)	CNCL (J/kg)	Q (W)	k (W/m-K)	dsoil, m	Rtank
SY101	1390	1610	364	2286	2214	3000	3300	16100	1	4	11
AN103	1490	1710	364	2074	1552	30W	33w	18700	1	4	11
AN104	14M	1590	364	2286	1700	3000	33W	19700	1	4	11
AN105	1420	1580	364	2411	1851	3000	3300	13400	1	4	11
AW101	1400	1630	364	3104	1158	3wo	3300	15200	1	4	11
AN102	1410	1500	364	3676	337	3000	33W	11500	1	4	11
AN107	1370	1560	364	3017	935	3000	33M	13700	1	4	11

DSTs	q, K/s	K, 1/s	Tf	t (s)	t(yr)	t (d)	t(hr)	Note: #NUM! Means that the time is infinite and the waste reaches steady-state before boiling.
SY101	7.56E-07	6.57946E-09	377	63833563	2.02414901	739	17731.5453	
AN103	1.04E-06	7.77169E-09	377	33670277	1.06767747	390	9352.85461	
AN104	1.06E-06	7.56508E-09	377	30225878	0.9584563	350	8396.0772	
AN105	6.73E-07	7.03312E-09	377	1.7E+08	5.39160547	1968	47230.4639	
AW101	7.89E-07	7.27271E-09	377	73231063	2.32214178	848	20341.962	
AN102	6.68E-07	8.13782E-09	377	#NUM!	#NUM!	#NUM!	#NUM!	
AN107	7.96E-07	8.13987E-09	377	1.21E+08	3.82788195	1397	33532.2459	

Hu et al. (2000) Heat Loads and Inventories

DSTs	RhoCL (kg/m3)	RhoNCL (kg/m3)	T (K)	VCL (m ³)	VNCL (m ³)	CCL (J/kg)	CNCL (J/kg)	Q (W)	k (W/m-K)	dsoil, m	Rtank
SY101	1390	1610	364	2286	2214	3000	33w	10600	1	4	11
AN103	1490	1710	364	2074	1552	3wo	33w	12100	1	4	11
AN104	1400	1590	364	2286	1700	3wo	33w	13700	1	4	11
AN105	1420	1580	364	2411	1851	3wo	3300	9340	1	4	11
AW101	1400	1630	364	3104	1158	3000	33M	10300	1	4	11
AN102	1410	15W	364	3676	337	3wo	3300	9340	1	4	11
AN107	1370	1560	364	3017	935	3000	33w	11700	1	4	11

DSTs	q, K/s	K, 1/s	Tf	t (s)	t(yr)	t (d)	t(hr)	Note: #NUM! Or negative values means that the time is infinite and the waste reaches steady-state before boiling.
SY101	4.98E-07	6.57946E-09	377	-3.6E+08	-11.400936	4161.3415	-99872.195	
AN103	6.71E-07	7.77169E-09	377	XNUM!	#NUM!	XNUM!	XNUM!	
AN104	7.40E-07	7.56508E-09	377	1.3E+08	4.11872159	1503	36080	
AN105	4.69E-07	7.03312E-09	377	-1.16E+08	-3.6707453	-1339.822	-32155.729	
AW101	5.35E-07	7.27271E-09	377	-2.14E+08	-6.7723401	-2471.9041	-59325.699	
AN102	5.42E-07	8.13782E-09	377	-1E+08	-3.172447	-1157.9432	-27790.636	
AN107	6.80E-07	8.13987E-09	377	XNUM!	#NUM!	#NUM!	#NUM!	

The 241-AZ-101 transient temperature rise calculation is shown in the table below as an example for a 60,000 W total heat load. Results of parametric calculations for the total heat load are shown on the next page

Transient Temperature Rise Calculation for AZ-101: Hu and Barker Inventory and Parametric Heat Loads, LCO Conditions										
	CL Density (kg/m ³)	NCL Density (kg/m ³)	Volume CL (m ³)	Volume NCL (m ³)	Specific Heat CL (J/kg)	specific Heat NCL (J/kg)				
	1190	1670	3021	178	3300	3000				
	Air Temp., K	Soil Temp., K	Heat Transfer Area, m ²	Heat Transfer Coeff.	Q (W)	Soil Conductivity, (W/m-K)	Soil Overburden, m	Tank Radius, m		DIFF
	265	267	411	6.46406	60000	1	4	11		-5.01E-06
	NCL Temp., K	CL Temp., K	CL Heat Load, W	NCL Heat Load, W	HX Through Soil Overburden, W	Exchange Heat Transfer	Downward HX, W	NCL Heatup Rate, K/s	CL Heatup Rate, K/s	
Time	Days	TNCL	TCL	QCL	ONCL	UPLOSS	QEX	DNLOSS	DTNCL	DTCL
0										
100000	1.16	375.38	364.36	24000.0	36000.0	61564	20314.5	3302.2	3.79E-06	3.81E-06
200000	2.31	375.76	364.76	24000.0	36000.0	6105.5	29311.1	3316.4	3.78E-06	3.80E-06
300000	3.47	376.14	365.14	24000.0	36000.0	8234.6	29305.5	3330.5	3.77E-06	3.80E-06
400000	4.63	376.52	365.52	24000.0	36000.0	6273.6	29296.3	3344.6	3.76E-06	3.80E-06
500000	5.79	376.69	365.90	24000.0	36000.0	6312.6	29290.1	3356.7	3.76E-06	3.79E-06
600000	6.04	377.27	366.26	24000.0	36000.0	6351.6	29281.2	3372.7	3.75E-06	3.79E-06
700000	8.10	377.64	366.66	24000.0	36000.0	8390.5	29271.6	3386.6	3.75E-06	3.78E-06
800000	9.26	376.02	367.04	24000.0	36000.0	6420.4	29262.2	3400.6	3.74E-06	3.78E-06
900000	10.42	378.39	367.42	24000.0	36000.0	6466.2	29252.3	3414.7	3.74E-06	3.77E-06
1000000	11.57	376.77	367.79	24000.0	36000.0	6507.0	29242.3	3426.7	3.73E-06	3.77E-06
1100000	12.73	379.14	366.17	24000.0	36000.0	8545.7	20232.2	3442.7	3.73E-06	3.77E-06
1200000	13.89	370.51	366.55	24000.0	36000.0	8584.4	20222.1	3456.6	3.72E-06	3.76E-06
1300000	15.05	370.66	366.92	24000.0	36000.0	6623.1	20211.9	3470.5	3.72E-06	3.76E-06
1400000	16.20	360.26	360.30	24000.0	36000.0	6661.7	20201.7	3484.4	3.72E-06	3.75E-06
1500000	17.36	360.63	369.67	24000.0	36000.0	6700.3	29191.5	3498.3	3.71E-06	3.75E-06
1600000	16.52	361.00	370.05	24000.0	36000.0	6736.6	29161.3	3512.2	3.71E-06	3.75E-06
1700000	19.66	381.37	370.42	24000.0	36000.0	6777.3	29171.1	3526.0	3.70E-06	3.74E-06
1800000	20.63	361.74	370.60	24000.0	36000.0	6815.8	29160.6	3539.6	3.70E-06	3.74E-06
1900000	21.00	382.11	371.17	24000.0	36000.0	6654.2	29150.6	3553.7	3.70E-06	3.73E-06
2000000	23.15	362.46	371.55	24000.0	36000.0	8892.5	29140.5	3567.5	3.69E-06	3.73E-06
2100000	24.31	382.85	371.02	24000.0	36000.0	8930.8	29130.3	3561.3	3.69E-06	3.73E-06
2300000	26.62	363.59	372.66	24000.0	36000.0	0007.4	20109.9	3606.8	3.68E-06	3.72E-06

Parametric Summary for AZ-101					
Heat Transfer Coefficient, W/m ² /K	6.48	7.66	10.00	8.51	11.17
Total Heat Load, W	60000	70000	90000	77300	100000
NCL Heatup Rate, K/s	3.81E-06	4.59E-06	6.16E-06	5.17E-06	6.95E-06
NCL Heatup Rate, Wday	0.329	0.397	0.532	0.446	0.600
CL Heatup Rate, K/s	3.81E-06	4.59E-06	6.16E-06	5.17E-06	6.95E-06
CL Heatup Rate, K/day	0.329	0.397	0.532	0.446	0.600

Regression Output for Parametric Summary of AZ-101			
Regression Statistics		=mx + b	Coefficients
Multiple R	1	b	-0.077255452
R Square	1	m	0.006773681
Adjusted R Square	-1.66666667		
Standard Error	1.15302E-07		
Observations	1		

The transient temperature rise calculation for **Tank 241-AZ-102** is shown in the table below as an example for a 100,000 W total heat load. Results of parametric calculations for the total heat load are shown on the next page.

Transient Temperature Rise Calculation for AZ-102: Hu and Barker Inventory and Parametric Heat Loads, LCO Conditions										
CL Density (kg/m ³)	NCL Density (kg/m ³)	Volume CL (m ³)	Volume NCL (m ³)	Specific Heat CL (J/kg)	Specific Heat NCL (J/kg)					
1100	1490	3131	394	3300	3000					
Air Temp., K	Soli Temp., K	Heat Transfer Area, m ²	Heat Transfer Coeff.	O(W)	Soil Conductivity, (W/m·K)	Soil Overburden, m	Tank Radius, m			
285	267	411	9.91469	100000	1	4	11			
										2.25E-06
		NCL Temp., K	CL Temp., K	CL Heat Load, W	NCL Heat Load, W	HX Through Soil Overburden, W	Exchange Heat Transfer	Downward HX, W	NCL Heatup Rate, K/s	CL Heatup Rate, K/s
Time	Days	TNCL	TCL	QCL	QNCL	UPLOSS	QEX	DNLOSS	DTNCL	DTCL
100000	1.16	375.67	364.67	40000.0	60000.0	8166.6	44825.3	3313.2	6.73E-06	6.74E-06
200000	2.31	376.35	365.35	40000.0	60000.0	8255.9	44622.0	3338.4	6.72E-06	6.74E-06
300000	3.47	377.02	366.02	40000.0	60000.0	8325.1	44616.2	3363.5	6.71E-06	6.73E-06
400000	4.63	377.69	366.70	40000.0	60000.0	8394.3	44606.7	3366.6	6.70E-06	6.72E-06
500000	5.79	378.36	367.37	40000.0	60000.0	8463.3	44799.6	3413.6	6.69E-06	6.72E-06
600000	6.94	379.03	368.04	40000.0	60000.0	8532.3	44790.0	3436.6	6.68E-06	6.71E-06
700000	8.10	379.70	368.71	40000.0	60000.0	8601.3	44779.5	3463.6	6.68E-06	6.70E-06
800000	9.26	380.37	369.38	40000.0	60000.0	8670.2	44766.5	3488.5	6.67E-06	6.70E-06
900000	10.42	381.03	370.05	40000.0	60000.0	8739.0	44767.2	3513.5	6.66E-06	6.69E-06
1000000	11.57	381.70	370.72	40000.0	60000.0	8807.7	44745.5	3536.3	6.65E-06	6.68E-06
1100000	12.73	382.37	371.39	40000.0	60000.0	8876.3	44733.7	3563.2	6.65E-06	6.67E-06
1200000	13.89	383.03	372.06	40000.0	60000.0	8944.9	44721.6	3586.0	6.64E-06	6.67E-06
1300000	15.05	383.69	372.72	40000.0	60000.0	9013.4	44709.7	3612.6	6.63E-06	6.66E-06
1400000	16.20	384.36	373.39	40000.0	60000.0	9081.8	44697.6	3637.6	6.62E-06	6.65E-06
1500000	17.36	385.02	374.05	40000.0	60000.0	9150.2	44685.5	3662.3	6.62E-06	6.65E-06
1600000	18.52	385.66	374.72	40000.0	60000.0	9216.5	44673.3	3667.1	6.61E-06	6.64E-06
1700000	19.66	386.34	375.36	40000.0	60000.0	9266.7	44661.1	3711.6	6.60E-06	6.63E-06
1800000	20.83	387.00	376.04	40000.0	60000.0	9354.9	44648.9	3736.4	6.59E-06	6.62E-06
1900000	21.99	387.66	376.71	40000.0	60000.0	9422.9	44636.7	3761.1	6.59E-06	6.62E-06
2000000	23.15	388.32	377.37	40000.0	60000.0	9490.9	44624.5	3765.7	6.58E-06	6.61E-06
2100000	24.31	388.98	378.03	40000.0	60000.0	9558.8	44612.3	3610.3	6.57E-06	6.60E-06
2300000	26.62	390.29	379.35	40000.0	60000.0	9694.5	44587.9	3659.4	6.56E-06	6.59E-06

Q (kW)	30	63	80	100
Heat Transfer Coefficient, W/m²/K	2.7023	6.1025	7.85414	9.91489
Heat Load, W	30000	63000	80000	100000
NCL Heatup Rate, K/s	1.42E-06	3.93E-06	5.23E-06	6.75E-06
NCL Heatup Rate, Wday	1.22E-01	3.40E-01	4.51 E-01	5.83E-01
CL Heatup Rate, K/s	1.42E-06	3.93E-06	5.23E-06	6.75E-06
CL Heatup Rate, Wday	1.22E-01	3.40E-01	4.51 E-01	5.83E-01

Regression Output for AZ-102			
Regression Statistics		$y=mx+b$	Coefficients
Multiple R	1	b	-0.075064523
R Square	1	m	0.006581936
Adjusted R Square	-2		
Standard Error	2.71961E-06		
Observations	1		

CHECKLIST FOR AB DOCUMENT CALCULATION TECHNICAL PEER REVIEW

Document and Section Reviewed:

RPP-6213, Rev. 1, App G, & its use
in Chapter 6.

Scope of Review:

Yes No NA

- ☒ ☐ ☐ Previous reviews are complete and cover the analysis, up to the scope of this review, with no gaps.
- ☒ ☐ ☐ Problem is completely defined.
- ☒ ☐ ☐ Accident scenarios are developed in a clear and logical manner.
- ☒ ☐ ☐ Necessary assumptions are explicitly stated and supported.
- ☒ ☐ ☐ Computer codes and data files are documented.
- ☒ ☐ ☐ Data used in calculations are explicitly stated.
- ☒ ☐ ☐ Bases for calculations, including assumptions and data, are consistent with the supported authorization basis document (e.g., the Tank Farms Final Safety Analysis Report).
- ☒ ☐ ☐ Data were checked for consistency with original source information as applicable.
- ☒ ☐ ☐ Mathematical derivations were checked including dimensional consistency of results.
- ☒ ☐ ☐ Models are appropriate and were used within their established range of validity, or adequate justification was provided for use outside their established range of validity.
- ☒ ☐ ☐ Spreadsheet results and all hand calculations were verified.
- ☒ ☐ ☐ Software input is correct and consistent with the document reviewed.
- ☒ ☐ ☐ Software output is consistent with the input and with the results reported in the document reviewed.
- ☒ ☐ ☐ Limits/criteria/guidelines applied to the analysis results are appropriate and referenced. Limits/criteria/guidelines were checked against references.
- ☒ ☐ ☐ Safety margins are consistent with good engineering practices.
- ☒ ☐ ☐ Conclusions are consistent with analytical results and applicable limits.
- ☒ ☐ ☐ Results and conclusions address all points required in the purpose.
- ☒ ☐ ☐ **Concurrence** MARTIN G. PLYS

Reviewer (Printed Name and Signature)

Date

2/22/01

This **page** intentionally left blank.

APPENDIX H

RESERVED FOR FUTURE USE

This page intentionally left blank.

APPENDIX I

QUALITY ASSURANCE DOCUMENTS

This page intentionally left blank.

APPENDIX I
QUALITY ASSURANCE DOCUMENTS

Included here are:

1. Calculation Note Cover Sheet
2. Authorship and Reviewer Table
3. Calculation Note Methodology Checklist

FAUSKE & ASSOCIATES, INC.

CALCULATION NOTE COVER SHEET

SECTION TO BE COMPLETED BY AUTHOR(S):

Calc-Note Number <u>FAU/00-14</u>		Revision Number <u>0</u>	Page <u>1-2</u>
Title <u>Hanford Waste Tank Bump Accident and Consequence Analysis</u>			
Project <u>Nuclear Safety & Licensing</u>		Project No. or Shop Order <u>CHG01B</u>	
Purpose: Re-evaluate Hanford waste tank bump accident			
Results Summary: Physical models, criteria, frequency, and consequences are provided.			
References of Resulting Reports, Letters, or Memoranda (Optional)			
Author(s): Name (Print or Type)	Signature	Completion Date	
<u>Michael Epstein</u>	<u>Michael Epstein</u>	<u>5/31/00</u>	
<u>Boro Malinovic</u>	<u>Boro Malinovic</u>	<u>5/31/00</u>	
<u>Martin G. Plys</u>	<u>M. G. Plys</u>	<u>5/31/00</u>	
<u>George Hauser</u>	<u>George Hauser</u>	<u>5/31/00</u>	

SECTION TO BE COMPLETED BY VERIFIER(S):

Verifier(s): Name (Print or Type)	Signature	Completion Date
<u>Martin G. Plys</u>	<u>M. G. Plys</u>	<u>5/31/00</u>
<u>Boro Malinovic</u>	<u>Boro Malinovic</u>	<u>5/31/00</u>
Method of Verification: Design Review _____, Independent Review or Alternate Calculations <u>X</u> , Testing _____		
Other (specify) _____		

SECTION TO BE COMPLETED BY MANAGER:

Responsible Manager: Name (Print or Type)	Signature	Approval Date
<u>Martin G. Plys</u>	<u>M. G. Plys</u>	<u>5/31/00</u>

Section	Author(s)	Reviewer(s)
3	B. Malinovic	M. G. Plys
4	M. Epstein	M. G. Plys
5	M. Epstein	M. G. Plys
6	B. Malinovic	M. G. Plys
7	B. Malinovic	M. G. Plys
8	M. G. Plys	B. Malinovic
9.1	M. Epstein	M. G. Plys
9.2	B. Malinovic	M. G. Plys
App. A	M. G. Plys	B. Malinovic
App. B	M. Epstein	M. G. Plys
App. C	M. Epstein	M. G. Plys
App. D	G. M. Hauser	M. G. Plys
App. E	G. M. Hauser	M. G. Plys
App. F	M. G. Plys	B. Malinovic
App. I	N/A	N/A
App. J	N/A	N/A

CALC NOTE NUMBER FAI/00-14 REV. 0 PAGE 1-4

CALCULATION NOTE METHODOLOGY CHECKLIST

CHECKLIST TO BE COMPLETED BY AUTHOR(S)

(CIRCLE APPROPRIATE RESPONSE)

1. Is the subject and/or the purpose of the design analysis clearly stated? YES • NO
2. Are the required inputs and their sources provided? YES • NO • N/A
3. Are the assumptions clearly identified and justified? YES • NO • N/A
4. Are the methods and units clearly identified? YES • NO • N/A
5. Have the limits of applicability been identified? YES • NO • N/A
(Is the analysis for a 3 or 4 loop plant or for a single application.)
6. Are the results of literature searches, if conducted, or other background data provided? YES • NO • N/A
7. Are all the pages sequentially numbered and identified by the calculation note number?.. YES • NO
8. Is the project or shop order clearly identified? YES • NO
9. Has the required computer calculation information been provided? YES • NO • N/A
10. Were the computer codes used under configuration control? YES • NO • N/A
11. Were the computer code(s) used applicable for modeling the physical and/or computational problems identified? YES • NO • N/A
(Is the correct computer code being used for the intended purpose.)
12. Are the results and conclusions clearly stated? YES • NO
13. Are Open Items properly identified YES • NO • N/A
14. Were approved Design Control practices followed without exception? YES • NO • N/A
(Approved Design Control practices refers to guidance documents within NSD that state how the work is to be performed, such as how to perform a LOCA analysis.)
15. Have all related contract requirements been met? YES • NO • N/A

NOTE: If NO to any of the above, Page Number containing justification: _____

APPENDIX J

CHECKLIST FOR TECHNICAL PEER REVIEW

This page intentionally left blank.

APPENDIX J

CHECKLIST FOR TECHNICAL PEER REVIEW


Document Reviewed: RPP-6213

Scope of Review: The review consisted participation in a series of several meeting in which FAI presented their work and a review of the subject report. Items identified as NA below were not included in this review.

Yes No NA

- ☐ ☐ ☒ Previous reviews are complete and cover the analysis, up to the scope of this review, with no gaps.
- ☒ ☐ ☐ Problem is completely defined.
- ☒ ☐ ☐ Accident scenarios are developed in a clear and logical manner.
- ☒ ☐ ☐ Necessary assumptions **are** explicitly stated and supported.
- ☒ ☐ ☐ Computer codes and data files are documented.
- ☒ ☐ ☐ Data used in calculations are explicitly stated.
- ☐ ☐ ☒ Data were checked **for** consistency with original source information **as** applicable.
- ☐ ☐ ☒ Mathematical derivations were checked including dimensional consistency of results.
- ☒ ¹☐ ☐ Models are appropriate and were used within their established range of validity or adequate justification was provided for use outside their established range of validity.
- ☐ ☐ ☒ Spreadsheet results and all hand calculations were verified.
- ☐ ☐ ☒ Software input is correct and consistent with the document reviewed.
- ☐ ☐ ☒ Software output is consistent with the input and with the results reported in the document reviewed.
- ☒ ☐ ☐ Limits/criteria/guidelines applied to the analysis results are appropriate and referenced. Limits/criteria/guidelines were checked against references.
- ☐ ☐ ☒ Safety margins are consistent with good engineering practices.
- ☒ ☐ ☐ Conclusions are consistent with analytical results and applicable limits.
- ☒ ☐ ☐ Results and conclusions address all points in the purpose.
- ☐ ☐ ☒ The document was prepared in accordance with HNF-2353, Section 4.3, Attachment B, "Calculation Note Format and Preparation Instructions".

☒ ☐ ☐ **Concurrence**



 Reviewer (Donald M Ogden) Date 5/3 1/00

¹ Reviews conducted by John Marvin, Inc (JMI) identified some areas of concern relative to the applicability of the models. A consensus was not reached. The JMI RCR comments document areas of disagreement

CHECKLIST FOR TECHNICAL PEER REVIEW

Document Reviewed: *RPP6213, HANFORD WASTE TANK BUMP ACCIDENT AND CONSEQUENCE ANALYSIS.*

Scope of Review: *TECHNICAL BASIS FOR MODELS FOR STEAM BUMP CRITERIA AND INITIATION.*

Yes No NA

- | | | | |
|-------------------------------------|-------------------------------------|-------------------------------------|---|
| <input checked="" type="checkbox"/> | <input type="checkbox"/> | <input type="checkbox"/> | Previous reviews are complete and cover the analysis, up to the scope of this review, with no gaps. |
| <input checked="" type="checkbox"/> | <input type="checkbox"/> | <input type="checkbox"/> | Problem is completely defined. |
| <input checked="" type="checkbox"/> | <input type="checkbox"/> | <input type="checkbox"/> | Accident scenarios are developed in a clear and logical manner. |
| <input checked="" type="checkbox"/> | <input type="checkbox"/> | <input type="checkbox"/> | Necessary assumptions are explicitly stated and supported. |
| <input type="checkbox"/> | <input type="checkbox"/> | <input checked="" type="checkbox"/> | Computer codes and data files are documented. |
| <input checked="" type="checkbox"/> | <input type="checkbox"/> | <input type="checkbox"/> | Data used in calculations are explicitly stated. |
| <input checked="" type="checkbox"/> | <input type="checkbox"/> | <input type="checkbox"/> | Data were checked for consistency with original source information as applicable. |
| <input checked="" type="checkbox"/> | <input type="checkbox"/> | <input type="checkbox"/> | Mathematical derivations were checked including dimensional consistency of results. |
| <input checked="" type="checkbox"/> | <input type="checkbox"/> | <input type="checkbox"/> | Models are appropriate and were used within their established range of validity or adequate justification was provided for use outside their established range of validity. |
| <input type="checkbox"/> | <input type="checkbox"/> | <input checked="" type="checkbox"/> | Spreadsheet results and all hand calculations were verified. |
| <input type="checkbox"/> | <input type="checkbox"/> | <input checked="" type="checkbox"/> | Software input is correct and consistent with the document reviewed. |
| <input type="checkbox"/> | <input type="checkbox"/> | <input checked="" type="checkbox"/> | Software output is consistent with the input and with the results reported in the document reviewed. |
| <input type="checkbox"/> | <input checked="" type="checkbox"/> | <input checked="" type="checkbox"/> | Limits/criteria/guidelines applied to the analysis results are appropriate and referenced. Limits/criteria/guidelines were checked against references. |
| <input type="checkbox"/> | <input type="checkbox"/> | <input checked="" type="checkbox"/> | Safety margins are consistent with good engineering practices. |
| <input checked="" type="checkbox"/> | <input type="checkbox"/> | <input type="checkbox"/> | Conclusions are consistent with analytical results and applicable limits. |
| <input checked="" type="checkbox"/> | <input type="checkbox"/> | <input type="checkbox"/> | Results and conclusions address all points in the purpose. |
| <input type="checkbox"/> | <input type="checkbox"/> | <input type="checkbox"/> | The document was prepared in accordance with HNF-2353, Section 4.3, Attachment B, "Calculation Note Format and Preparation Instructions". |

☒ ☐ ☐ **Concurrence**

Reviewer (Printed Name and Signature)



CW STEWART (PNNL)

Date

5/18/00

CHECKLIST FOR TECHNICAL PEER REVIEW

Document Reviewed: FRI/00-14, HANFORD WASTE TANK BUMPScope of Review: ACCIDENT AND CONSEQUENCE ANALYSIS
SECTION 8.4, ... RADIOLOGICAL AND TOXIC
CHEMICAL CONSEQUENCES

Yes No NA

- | | | | |
|-------------------------------------|--------------------------|-------------------------------------|---|
| <input checked="" type="checkbox"/> | <input type="checkbox"/> | <input type="checkbox"/> | Previous reviews are complete and cover the analysis, up to the scope of this review, with no gaps. |
| <input checked="" type="checkbox"/> | <input type="checkbox"/> | <input type="checkbox"/> | Problem is completely defined. |
| <input checked="" type="checkbox"/> | <input type="checkbox"/> | <input type="checkbox"/> | Accident scenarios are developed in a clear and logical manner. |
| <input checked="" type="checkbox"/> | <input type="checkbox"/> | <input type="checkbox"/> | Necessary assumptions are explicitly stated and supported, |
| <input type="checkbox"/> | <input type="checkbox"/> | <input checked="" type="checkbox"/> | Computer codes and data files are documented. |
| <input checked="" type="checkbox"/> | <input type="checkbox"/> | <input type="checkbox"/> | Data used in calculations are explicitly stated. |
| <input checked="" type="checkbox"/> | <input type="checkbox"/> | <input type="checkbox"/> | Data were checked for consistency with original source information as applicable. |
| <input checked="" type="checkbox"/> | <input type="checkbox"/> | <input type="checkbox"/> | Mathematical derivations were checked including dimensional consistency of results. |
| <input checked="" type="checkbox"/> | <input type="checkbox"/> | <input type="checkbox"/> | Models are appropriate and were used within their established range of validity or adequate justification was provided for use outside their established range of validity. |
| <input checked="" type="checkbox"/> | <input type="checkbox"/> | <input type="checkbox"/> | Spreadsheet results and all hand calculations were verified. |
| <input type="checkbox"/> | <input type="checkbox"/> | <input checked="" type="checkbox"/> | Software input is correct and consistent with the document reviewed. |
| <input type="checkbox"/> | <input type="checkbox"/> | <input checked="" type="checkbox"/> | Software output is consistent with the input and with the results reported in the document reviewed. |
| <input checked="" type="checkbox"/> | <input type="checkbox"/> | <input type="checkbox"/> | Limits/criteria/guidelines applied to the analysis results are appropriate and referenced. Limits/criteria/guidelines were checked against references. |
| <input checked="" type="checkbox"/> | <input type="checkbox"/> | <input type="checkbox"/> | Safety margins are consistent with good engineering practices. |
| <input checked="" type="checkbox"/> | <input type="checkbox"/> | <input type="checkbox"/> | Conclusions are consistent with analytical results and applicable limits. |
| <input checked="" type="checkbox"/> | <input type="checkbox"/> | <input type="checkbox"/> | Results and conclusions address all points in the purpose. |
| <input checked="" type="checkbox"/> | <input type="checkbox"/> | <input type="checkbox"/> | The document was prepared in accordance with HNF-2353, Section 4.3, Attachment B, "Calculation Note Format and Preparation Instructions". |
| <input checked="" type="checkbox"/> | <input type="checkbox"/> | <input type="checkbox"/> | Concurrence |

T B MCCALL  6/7/00
Reviewer (Printed Name and Signature) Date

CHECKLIST FOR AB DOCUMENT ~~CALCULATION~~ TECHNICAL PEER REVIEW
(from **• • F-2353, DI 4.2, Rev. 2** dated December **21, 2000**)

Document and Section Reviewed: **RPP-6213, Hanford ~~Waste Tank Bump Accident and~~ Consequence Analysis, Rev. 1.**

Scope of Review: Review only **included** changes made **as** part of Revision **1** of the document

Yes No NA

- | | | | |
|-------------------------------------|--------------------------|-------------------------------------|--|
| <input checked="" type="checkbox"/> | <input type="checkbox"/> | <input type="checkbox"/> | Previous reviews are complete and cover the analysis, up to the scope of this review, with no gaps. |
| <input checked="" type="checkbox"/> | <input type="checkbox"/> | <input type="checkbox"/> | Problem is completely defined. |
| <input checked="" type="checkbox"/> | <input type="checkbox"/> | <input type="checkbox"/> | Accident scenarios are developed in a clear and logical manner. |
| <input checked="" type="checkbox"/> | <input type="checkbox"/> | <input type="checkbox"/> | Necessary assumptions are explicitly stated and supported. |
| <input type="checkbox"/> | <input type="checkbox"/> | <input checked="" type="checkbox"/> | Computer codes and data files are documented. |
| <input checked="" type="checkbox"/> | <input type="checkbox"/> | <input type="checkbox"/> | Data used in calculations are explicitly stated. |
| <input checked="" type="checkbox"/> | <input type="checkbox"/> | <input type="checkbox"/> | Bases for calculations, including assumptions and data, are consistent with the supported authorization basis document (e.g., the Tank Farms Final Safety Analysis Report). |
| <input checked="" type="checkbox"/> | <input type="checkbox"/> | <input type="checkbox"/> | Data were checked for consistency with original source information as applicable. |
| <input checked="" type="checkbox"/> | <input type="checkbox"/> | <input type="checkbox"/> | Mathematical derivations were checked including dimensional consistency of results. |
| <input checked="" type="checkbox"/> | <input type="checkbox"/> | <input type="checkbox"/> | Models are appropriate and were used within their established range of validity, or adequate justification was provided for use outside their established range of validity. |
| <input checked="" type="checkbox"/> | <input type="checkbox"/> | <input type="checkbox"/> | Spreadsheet results and all hand calculations were verified. |
| <input type="checkbox"/> | <input type="checkbox"/> | <input checked="" type="checkbox"/> | Software input is correct and consistent with the document reviewed. |
| <input type="checkbox"/> | <input type="checkbox"/> | <input checked="" type="checkbox"/> | Software output is consistent with the input and with the results reported in the document reviewed. |
| <input type="checkbox"/> | <input type="checkbox"/> | <input checked="" type="checkbox"/> | Limit criteria guidelines applied to the analysis results are appropriate and referenced. Limit criteria guidelines were checked against references. |
| <input type="checkbox"/> | <input type="checkbox"/> | <input checked="" type="checkbox"/> | Safety margins are consistent with good engineering practices. |
| <input checked="" type="checkbox"/> | <input type="checkbox"/> | <input type="checkbox"/> | Conclusions are consistent with analytical results and applicable limits. |
| <input checked="" type="checkbox"/> | <input type="checkbox"/> | <input type="checkbox"/> | Results and conclusions address all points required in the purpose. |
| <input checked="" type="checkbox"/> | <input type="checkbox"/> | <input type="checkbox"/> | Concurrence |


2/23/01
 Reviewer (Printed Name and Signature) Date

APPENDIX K

**DECAY HEAT LOAD FOR TANK 241-AZ-101 BASED ON THE BEST BASIS
INVENTORY AND DECAYED TO JANUARY 31,2001**

This page intentionally left **blank**

APPENDIX K

DECAY HEAT LOAD FOR TANK 241-AZ-101 BASED ON THE BEST BASIS INVENTORY AND DECAYED TO JANUARY 31,2001

The decay heat load in Tank 241-AZ-101 is assessed by using the best basis inventory (BBI) as described in Memo, "Heat Load Estimates for Tanks 241-AZ-101, 241-AZ-102, and 241-AY-102," a copy of which is included in this appendix.

The isotopes are decayed from the BBI data date of January 1, 1994, to January 31,2001, using the spreadsheet described in this appendix.

Nuclide half-lives are from *Chart of the Nuclides*, Thirteenth Edition, 1963, General Electric Company, San Jose, California.

The waste inventory is decayed according to the following equation from *DOE Fundamental Handbook, Nuclear Physics and Reactor Theory*, DOE-HDBK-1019/1-93, January 1993.

$$\text{Present inventory} = \text{Past inventory} * (e^{-\lambda t})$$

Where $\lambda = 0.693/\text{half-life}$

References

Chart of the Nuclides, Thirteenth Edition, 1963, General Electric Company, San Jose, California.

DOE Fundamental Handbook, Nuclear Physics and Reactor Theory, DOE-HDBK-1019/1-93, January 1993, Washington, D.C.

Calculation of Heat Load (Q) from CHG Letter 7KN00-00-JGF-062 (for Tank 241-AZ-101)

Radionuclide	Waste Inventory - 111194	Decay Heat (W/Ci)	Heat Load (W)
Sr-90	5.65E+06	0.00669	37,799
cs-137	7.05E+06	0.00472	33,276
Am-241	2.66E+04	0.0328	872
		Sum	71,947

Updated calculation of Heat Load (Q) for Tank 241-AZ-101

Radionuclide	Waste Inventory - 1/31/01	Decay Heat (W/Ci)	Heat Load (W)
Sr-90	4.77E+06	0.00669	31,930
Cs-137	5.99E+06	0.00472	28,279
Am-241	2.63E+04	0.0328	863
		Sum	61,072

	Half-life(yr)
Sr-90 =	29.1
Cs-137 =	30.17
Am-241 =	432.7

Decay time (1/1/94 to 1/31/01) = 7.083 yr

	A	B	C	D
1				
2	Calculation of Heat Load (Q) from CHG Letter 7KN00-00-JGF-062 (for Tank 241-AZ-101)			
3	Radionuclide	Waste Inventory - 1/1/94	Decay Heat (W/CI)	Heat Load (W)
4	Sr-90	5650000	0.00669	=B4*C4
5	Cs-137	7050000	0.00472	=B5*C5
6	Am-241	26600	0.0328	=B6*C6
7			Sum	=SUM(D4:D6)
8				
9	Updated calculation of Heat Load (Q) for Tank 241-AZ-101			
10	Radionuclide	Waste Inventory -1/31/01	Decay Heat (W/CI)	Heat Load (W)
11	Sr-90	=B4*EXP(-(0.6931/C17)*\$C\$2)	0.00669	=B11*C11
12	Cs-137	=B5*EXP(-(0.6931/C18)*\$C\$2)	0.00472	=B12*C12
13	Am-241	=B6*EXP(-(0.6931/C19)*\$C\$2)	0.0328	=B13*C13
14			Sum	=SUM(D11:D13)
15				
16			Half-life (yr)	
17		Sr-90 =	29.1	
18		Cs-137 =	30.17	
19		Am-241 =	432.7	
20				
21		ecay time (1/1/94 to 1/31/01) =	=7+(1/12)	yr



INTEROFFICE MEMO

From: Data Development and Interpretation 7KN00-00-JGF-062
 Phone: 373-5589
 Date: December 20, 2000
 Subject: HEAT LOAD ESTIMATES FOR TANK 241-AZ-101, 241-AZ-102 AND 241-AY-102

To: J. M. Grigsby RI-44

Copies: J.G. Field *JGF*
 K.W. Kirch
 J. H. Rasmussen
 L. M. Sasaki
 A. M. Templeton
 A. E. Young
 LB

References: (1) Tank Characterization Database at <http://twins.pnl.gov:8001/TCD/main.html>, CH2M HILL Hanford Group Inc., Richland, Washington, dated 2000.
 (2) HNF-SD-WM-OCD-015. 2000, "Tank Farm Waste Transfer Compatibility Program", Rev. 3A, K. D. Fowler, CH2M HILL Hanford Group Inc., Richland, Washington. dated 2000.

This memo documents the heat load for tanks 241-AZ-101, 241-AZ-102 and 241-AY-102. The heat loads have been calculated from the most current best basis inventory (BBI) values and are documented in Reference 1. The BBI radionuclide concentrations documented in the BBI are decayed to January 1, 1994.

Tank 241-AZ-101

The tank heat load estimate from the BBI for tank 241-AZ-101 is 72,000 W (246,000 Btu/Hr), as shown in Table 1.

Table 1. Heat Load Estimate Based on Best Basis Inventory

Radionuclide	Waste Inventory (Ci)	Decay Heat (W/Ci)	Heat Load (W)
⁹⁰ Sr	5.65E+06	0.00669	37,800
¹³⁷ Cs	7.05E+06	0.00472	33,300
²⁴¹ Am	2.66E+04	0.00328	900
Total		<i>6.8E-05</i>	<i>72,000</i> <i>stat</i>

J. M. Grigsby
Page 2
December 13, 2000

7KN00-00-JGF-062

Tank 241-AZ-102

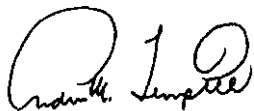
The tank heat load based on the BBI (Reference 1) for tank 241-AZ-102 is **46.100 W (157,000 Btu/hr)** as shown in Table 2.

Table 2. Heat Load Estimate Based on the Best-Basis Radionuclide Inventory

Radionuclide	Waste Inventory (Ci)	Decay Heat Generation Rate (W/Ci)	Heat Load (W)
Strontium-90	3.64E+06	0.00669	24,400
Total	-		46,100

Radionuclide	Waste Inventory (Ci)	Decay Heat Generation Rate (W/Ci)	Heat Load (W)
Strontium-90	7.34+06	0.00669	49,100
Cesium-137	2.91+05	10.00472	1,370
Total			50,500

All three heat loads are less than the **1,172,000 W (4,000,000 Btu/hr)** operating specification limit for this tank (Reference 2). If I can be of any further assistance with these results, please call me at **373-5589**.



Andrew M. Templeton, Scientist I
Data Development and Interpretation

dmn

CHECKLIST FOR AB DOCUMENT CALCULATION TECHNICAL PEER REVIEW

Document and Section Reviewed: *RPP-6213, Appendix K, "Decay Heat Load for Tank 241-A2-101 BASED ON TBEI DECAYED TO JANUARY 31, 2004"*
 Scope of Review: *CHECKED INPUTS TO SPREADSHEET AND OUTPUTS.*

Yes No NA

- | | | | |
|-------------------------------------|--------------------------|-------------------------------------|--|
| <input type="checkbox"/> | <input type="checkbox"/> | <input checked="" type="checkbox"/> | Previous reviews are complete and cover the analysis, up to the scope of this review, with no gaps. |
| <input checked="" type="checkbox"/> | <input type="checkbox"/> | <input type="checkbox"/> | Problem is completely defined. |
| <input type="checkbox"/> | <input type="checkbox"/> | <input checked="" type="checkbox"/> | Accident scenarios are developed in a clear and logical manner. |
| <input type="checkbox"/> | <input type="checkbox"/> | <input type="checkbox"/> | Necessary assumptions are explicitly stated and supported. |
| <input type="checkbox"/> | <input type="checkbox"/> | <input checked="" type="checkbox"/> | Computer codes and data files are documented. |
| <input checked="" type="checkbox"/> | <input type="checkbox"/> | <input type="checkbox"/> | Data used in calculations are explicitly stated. |
| <input type="checkbox"/> | <input type="checkbox"/> | <input checked="" type="checkbox"/> | Bases for calculations, including assumptions and data, are consistent with the supported authorization basis document (e.g., the Tank Farms Final Safety Analysis Report). |
| <input checked="" type="checkbox"/> | <input type="checkbox"/> | <input type="checkbox"/> | Data were checked for consistency with original source information as applicable. |
| <input checked="" type="checkbox"/> | <input type="checkbox"/> | <input type="checkbox"/> | Mathematical derivations were checked including dimensional consistency of results. |
| <input checked="" type="checkbox"/> | <input type="checkbox"/> | <input type="checkbox"/> | Models are appropriate and were used within their established range of validity, or adequate justification was provided for use outside their established range of validity. |
| <input checked="" type="checkbox"/> | <input type="checkbox"/> | <input type="checkbox"/> | Spreadsheet results and all hand calculations were verified. |
| <input checked="" type="checkbox"/> | <input type="checkbox"/> | <input type="checkbox"/> | Software input is correct and consistent with the document reviewed. |
| <input checked="" type="checkbox"/> | <input type="checkbox"/> | <input type="checkbox"/> | Software output is consistent with the input and with the results reported in the document reviewed. |
| <input type="checkbox"/> | <input type="checkbox"/> | <input checked="" type="checkbox"/> | Limit criteria guidelines applied to the analysis results are appropriate and referenced. Limit criteria guidelines were checked against references. |
| <input type="checkbox"/> | <input type="checkbox"/> | <input checked="" type="checkbox"/> | Safety margins are consistent with good engineering practices. |
| <input type="checkbox"/> | <input type="checkbox"/> | <input checked="" type="checkbox"/> | Conclusions are consistent with analytical results and applicable limits. |
| <input type="checkbox"/> | <input type="checkbox"/> | <input checked="" type="checkbox"/> | Results and conclusions address all points required in the purpose. |
| <input checked="" type="checkbox"/> | <input type="checkbox"/> | <input type="checkbox"/> | Concurrence |

Reviewer (Printed Name and Signature)

J. M. GREGG

Date

2/13/01

APPENDIX L

**THERMOCOUPLE ACCURACY
(MEMO 7KN00-TCO-001)**

This **page** intentionally left blank.

APPENDIX L

THERMOCOUPLE ACCURACY
(MEMO 7KN00-01-TCO-001)**CH2MHILL**
Hanford Group, Inc.

INTEROFFICE MEMO

From: DST Cognizant Engineering
 Phone: 376-3563
 Date: February 14, 2001
 Subject: THERMOCOUPLE ACCURACY

7KN00-01-TCO-001

To: J. E. Meacham R1-49

Copies: J.M. Grigsby R1-44
 G.W. Ryan B4-47
 C.C. Scaief III R3-83
 W.D. Winkelman S5-05

- References:
- 1) WHC-SD-WM-TI-483, 1991, "Temperature Measurement ~~Error~~ Analysis," Revision 0, Westinghouse Hanford Company, Richland, Washington.
 - 2) WHC-SD-WM-ER-134, 1992, "Engineering Evaluation of Thermocouples in FeCN Watch list Tanks," Revision 0-A, Westinghouse Hanford Company, Richland, Washington.

A question was recently raised regarding the accuracy of the thermocouples used to measure temperature in double shell tanks. The thermocouples are located in the tank dome, walls and bottom, and in thermocouple trees or multifunction instrument trees (MIT), which are installed inside the tanks. The thermocouples are typically either type J, K, or E (as defined by the American National Standards Institute) and most have been in service for many years.

Reference 1 documents the uncertainty associated with the measurement of temperature using thermocouples. The discussion addresses the uncertainty that is introduced by the elements of a typical temperature measurement loop, as well as the uncertainty associated with the thermocouple itself. The uncertainty associated with the individual components of the temperature measurement loop are combined, assuming that the uncertainty of each is independent of the others, and an overall system accuracy is determined. The results of the study indicate that the absolute instrument loop accuracy for measuring tank temperature is approximately ± 4 to $\pm 6^\circ\text{F}$, depending upon the quality of the installation and the thermocouple type. This range of loop accuracy is representative of a new installation that has not deteriorated with time, and does not include the effects of repeatability errors.

Reference 2 documents the results of an engineering analysis of thermocouple field measurements and provides an indication of installed accuracy after a period of many years. Although the analysis was performed for single shell tanks, the results should be representative of double shell tank installations. The report evaluates twenty-three thermocouple trees containing a total of 265 thermocouples. The accuracy of the thermocouples was evaluated by comparing the thermocouple temperature reading to the temperature measured at the same elevation in an adjacent liquid observation well (LOW). Of the 265 thermocouples evaluated, approximately 66% were found to provide acceptable readings. Among the thermocouples found to be acceptable, a maximum difference of $\pm 7^\circ\text{F}$ was found between the thermocouple reading and the LOW reading.

J. E. Meacham, et al.

7KN00-01-TCO-001

Page 2

February 14, 2001

Determination of the accuracy of a tank temperature measurement loop should consider the analytically determined accuracy as well as the accuracy several years after installation, to account for normal degradation with time. Based upon the results of Reference 1 and 2, it is recommended that $\pm 10^\circ \text{F}$ be used as the tank temperature measurement accuracy for the purposes of the tank bump analysis. This accuracy can be reasonably achieved utilizing existing equipment. Commitment to a more accurate temperature measurement capability may require additional surveillances to demonstrate that the required accuracy is met or a redesign of the temperature measurement system.

If you have questions or need additional information, please contact me at 376-3563.



T.C. Otter

DST Cognizant Engineering

eob